COMPLEXES OF CATECHOL AND RELATED LIGANDS WITH GROUP VI METALS AND THE PLATINUM METALS

A thesis submitted for the degree of Doctor of Philosophy of the University of London and also for the Diploma of Membership of Imperial College

by

CAROL ANNE PUMPHREY

Department of Chemistry
Imperial College of Science and Technology,
London, SW7 2AZ

September, 1984

CONTENTS

		Page
Abstract		11
Acknowledgements		13
Abbreviations		14
List of Figures		16
List of Tables		20
CHAPTER I:-	CATECHOLATO AND RELATED COMPLEXES	
1.	Introduction	27
1.1	Catechols in nature	27
1.2	Catecholato, semiquinone, and benzoquinone ligands.	28
1.3	Occurrence of catecholato complexes.	31
1.4	Oxidation states in quinone complexes.	32
1.5	Preparation of o-quinone complexes.	33
1.5.1	Catecholato ligands.	33
1.5.2	Semiquinone complexes.	36
1.5.3	Benzoquinone complexes.	39
1.6	X-ray crystallographic studies of o-quinone complexes.	39
1.6.1.	Structures of catecholato complexes.	41
	(a) Tris (catecholato) complexes.	41
	(b) Tetrakis (catecholato) complexes.	41
	(c) Mixed ligand catecholato complexes	42
	(i) Oxo complexes	42
	(ii) Miscellaneous complexes.	44

		Page
1.6.2	The catechol monoanion	45
1.6.3	Structures of semiquinone complexes	45
1.6.4	Mixed semiquinone-catecholato complexes	47
1.6.5	Benzoquinone complex	48
1.6.6	Inter-molecular interactions	48
2.	Preparation of Complexes	56
3.	Infra-red and Raman spectra of quinone complexes.	59
3.1	Spectra of the metal-oxo groups and of the ligands.	59
3.1.1	Metal-oxo vibrations	59
	(a) cis-dioxo groups in cis-$[MO_2X_4]^{n-}$ systems.	60
	(b) trans-dioxo groups in trans-$[MO_2X_4]^{n-}$ systems.	60
	(c) Complexes containing M-O-M units.	61
	(d) Structure and bonding in these complexes.	62
	(e) Ligand bridges.	63
3.1.2	Catechol and o-benzoquinone.	63
3.2	Spectra of catecholato and quinone complexes.	64
3.2.1	Literature work and spectra of known complexes.	64
	(a) The coordinated catecholato dianion.	64
	(b) The coordinated catecholato monoanion.	66
	(c) Benzoquinone complexes.	67
	(d) Semiquinone complexes.	67

			Page
3.2.2		Experimental results.	69
	(a)	Tris (catecholato) complexes	69
	(b)	Reformulation of molybdenum(VI) - catecholato complexes.	75
	(i)	Spectra of $K_2[MoO_2(cat)_2]$ and $(NH_4)_2[Mo_2O_5(cat)_2]$	75
	(ii)	"(pyH)H $[MoO_3(cat)]$"	82
	(iii)	"$K[MoO_2(OH)(cat)]$" and "$(NH_4)[MoO_2(OH)(C_6H_4O_3)]$"	83
	(iv)	Complexes with a catechol molecule of crystallisation.	84
	(c)	$Na_2[W_2O_5(cat)_2]$	84
	(d)	$MoO_2(PSQ)_2$	87
3.3		Ortho-aminophenol complexes.	89
3.3.1		Literature measurements	89
3.3.2		Experimental results	90
	(a)	$MoO_2(C_6H_4ONH_2)$	90
	(b)	$K_2[OsO_2(C_6H_4ONH)_2]$	90
4.		^1H Nuclear Magnetic Resonance Spectroscopy	93
4.1		Spectra of the ligands.	93
4.2		Spectra of catecholato complexes.	94
4.2.1		Literature work	94
4.2.2		Experimental results.	95
	(a)	Oxo-catecholato complexes	95
	(i)	$K_2[OsO_2(cat)_2]$	95
	(ii)	$UO_2(cat)2H_2O$	95
	(iii)	cis-$[MoO_2(cat)_2]^{2-}$ and cis-$[M_2O_5(cat)_2]^{2-}$ complexes.	96

			Page
		(b) Reformulated molybdenum(VI)-catecholato complexes.	98
		(c) Catecholato versus benzoquinone coordination.	100
5.		^{13}C Nuclear Magnetic Resonance Spectroscopy	104
5.1		Spectrum of free catechol	104
5.2		Spectra of quinone complexes	105
	5.2.1	Literature measurements	105
	5.2.2	Experimental results.	105
		(a) $K_3[Rh(cat)_3]$	106
		(b) Oxo-catecholato complexes	108
		(i) $K_2[OsO_2(cat)_2]$	108
		(ii) cis-dioxo molybdenum(VI) and tungsten(VI) complexes.	109
		(iii) cis-$(NH_4)_2[MoO_2(4\text{-nitrocat})_2]$ versus trans-$K_2[OsO_2(4\text{-nitrocat})_2]$	109
		(c) $Pt(PPh_3)_2(cat)$	111
		(d) Spectra of reformulated molybdenum complexes	112
		(e) Benzoquinone versus catecholato coordination	114
		(f) $Mo_2O_5(PSQ)_2$	119
5.3		Cyclohexanediol complexes	119
6.		Electron Paramagnetic Resonance Spectroscopy	124
6.1		Tris(catecholato) complexes	124
	6.1.1	$(Ph_4P)_2[Ir(cat)_3]$	124
	6.1.2	$(Ph_4P)_2[Re(cat)_3]$	124
	6.1.3	$(Ph_4P)_3[Ru(cat)_3]$	125

		Page
6.2	$MoO_2(PSQ)_2$	125
7.	Electrochemistry	128
7.1	Electrochemistry of the ligands	128
7.2	Electrochemistry of quinone - transition metal complexes	130
7.2.1	Literature measurements	130
7.2.2	Experimental data	131
	(a) Tris(catecholato) complexes	132
	(i) $(Ph_4P)_2[Ir(cat)_3]$	132
	(ii) $(Ph_4P)_2[Re(cat)_3]$	133
	(iii) $(Ph_4P)_3[Ru(cat)_3]$	133
	(b) $MoO_2(PSQ)_2$	133
Resume of Chapter I		138
8.	Experimental	139
8.1	Catecholato complexes	139
8.2	Semiquinone complexes	147
8.3	Ortho-aminophenol complexes	148
CHAPTER II:-	COMPLEXES CONTAINING CATECHOLAMINES AS LIGANDS	
1.	Introduction	152
1.1	The catecholamines	152
	(a) Nomenclature and structure	152
	(b) Biochemical function	154
	(c) Interactions of catecholamines with metal ions.	155
	(d) Histochemical location of catecholamines using the electron microscope.	156

Page

1.2	Catecholamine complexes with transition metals.	157
	(a) Complexes with Dopa	158
	(b) Complexes with other catecholamines	160
1.3	New catecholamine complexes	163
	(a) Investigation of catecholamine interactions with osmium(VI) and uranium(VI)	163
	(b) Other metals as potential staining agents.	163
2.	Preparation of complexes	165
2.1	Osmium complexes	165
2.2	Uranyl complexes	165
2.3	Molybdenum and tungsten complexes	166
3.	Infra-red and Raman spectroscopy of catecholamine complexes.	169
3.1	Spectra of the ligands	169
3.2	Spectra of the complexes	170
	(a) Changes in the spectra expected for the three postulated modes of coordination	173
	(b) Osmium(VI) complexes with catecholamines	174
	(c) Uranyl complexes with catecholamines	178
	(d) Molybdenum(VI) and Tungsten(VI) catecholamine complexes	181
	(i) $Na_2[MO_2(catecholamine)_2]$ complexes	181
	(ii) MO_2(dopamine)	183
	(iii) Mo_2O_5(adrenaline)$_2$	185

		Page
4.	^{1}H Nuclear Magnetic Resonance Spectroscopy	196
4.1	Spectra of the ligands	196
4.2	Spectra of the complexes	197
	(a) Osmium(VI)-catecholamine complexes	197
	(b) Molybdenum(VI) and Tungsten(VI) catecholamine complexes	198
5.	^{13}C Nuclear Magnetic Resonance Spectroscopy	204
5.1	Spectra of the ligands	204
	(a) Literature measurements	204
	(b) Experimental data	204
5.2	Spectra of the complexes	206
	(a) Complexes of the type $Na_2[MO_2(catecholamine)_2]$	207
	(b) Spectrum of $Mo_2O_5(adrenaline)_2$	208
6.	Electrochemistry	213
6.1	Literature measurements	213
6.2	Experimental results	214
	(a) $K_2[OsO_2(catecholamine)_2]$ complexes	214
	(b) $UO_2(catecholamine)nH_2O$ complexes	214
	(c) Catecholamine complexes of molybdenum (VI) and tungsten(VI)	214
	(i) $Na_2[MO_2(catecholamine)_2]$	214
	(ii) $Mo_2O_5(adrenaline)_2$	215
	Resumé of Chapter II	217
7.	Experimental	218
7.1	Preparation of Osmium(VI)-catecholamine complexes	218
7.2	Preparation of Uranyl-catecholamine complexes.	221

		Page
7.3	Preparation of Molybdenum(VI) and Tungsten(VI)-catecholamine complexes	222
	(a) Complexes of the type $Na_2[MO_2(cat)_2]$	222
	(b) Molybdenum(VI) and Tungsten(VI) - Dopamine Complexes	224
	(c) Mo_2O_5(adrenaline)$_2$	225

CHAPTER III:- TROPOLONE AND THE TROPOLONATO LIGAND

1.1	Introduction	227
1.2	The tropolonato ligand	228
1.3	Transition metal-tropolonato complexes	233
	(a) Occurrence	233
	(b) Preparation of complexes	234
	(c) Tris (tropolonato) complexes	234
	(d) Tetrakis (tropolonato) complexes	239
	(e) The bridging tropolonato ligand	241
2.	Preparation of complexes	246
3.	Infra-red and Raman spectroscopy	248
3.1	Spectra of the parent tropolone	248
3.2	The tropolonato ion	251
3.3	Tropolonato-transition metal complexes	254
3.3.1	Literature measurements	254
3.3.2	Experimental results	256
	(a) Tris (tropolonato) complexes	256
	(b) Oxo-tropolonato complexes	259
	(i) $MoO_2(trop)_2$	259
	(ii) $W_2O_5(trop)_2$	260
	(iii) $OsO_2(trop)_2$	262
	(c) $[Pt(PPh_3)_2(trop)](BPh_4)$	263

			Page
4.		^{1}H Nuclear Magnetic Resonance Spectroscopy	270
4.1		Spectrum of tropolone	270
4.2		Spectrum of sodium tropolonate	270
4.3		Spectra of tropolonato complexes	270
	4.3.1	Literature measurements	270
	4.3.2	Experimental results	271
5.		^{13}C Nuclear Magnetic Resonance Spectroscopy	276
5.1		Spectrum of the free ligand tropolone	276
5.2		Spectrum of sodium tropolonate	279
5.3		Spectra of tropolonato complexes	279
6.		Electron Paramagnetic Resonance Spectroscopy	285
7.		Electrochemistry	286
8.		Mass Spectroscopy of tropolonato complexes	287
8.1		Literature measurements	287
8.2		Experimental results	288
9.		Crystal structure of $MoO_2(trop)_2$	294
		Resume of Chapter III	301
10.		Experimental	302
10.1		Tris(tropolonato) complexes	302
10.2		Oxo-tropolonato complexes	303
10.3		$[Pt(PPh_3)_2(trop)](BPh_4)$	305
10.4		Other tropolonato complexes	306
		References	307
		Appendix - Instrumentation	325

ABSTRACT

COMPLEXES OF CATECHOL AND RELATED LIGANDS WITH GROUP VI METALS AND THE PLATINUM METALS

The work described in this thesis is principally concerned with the preparation and characterisation of complexes of the 0,0 chelating ligands catechol and tropolone, and of five biological catecholamines, with metals of groups VI and VIII.

With the catecholato di-anion (cat. $C_6H_4O_2^{2-}$) the new complexes $(Ph_4P)_2[Ir(cat)_3]$, $(Ph_4P)_2[Re(cat)_3]$, $(Ph_4P)_3[Ru(cat)_3]$, were characterised. A new 9,10-phenanthrenesemiquinone complex, $MoO_2(PSQ)_2$, was also synthesised. A reinvestigation was undertaken of several molybdenum(VI) catecholato complexes whose formulations in the early literature appeared inaccurate in the light of our subsequent research. It appears that all these complexes can be identified as containing either $[MoO_2(cat)_2]^{2-}$, or $[Mo_2O_5(cat)_2]^{2-}$.

All these catecholato complexes were characterised by infrared spectroscopy, cyclic voltammetry, elemental analyses, and magnetic resonance spectroscopy (^1H and ^{13}C nuclear magnetic resonance, and, where appropriate, electron spin resonance.).

The reactions of the five catecholamines, adrenaline, dopa, dopamine, isoproterenol and noradrenaline with the electron microscope staining agents osmium tetroxide and uranyl acetate were investigated. Each ligand was found to form complexes of the type $[OsO_2(O_2R)_2]^{2-}$ and $UO_2(O_2R) \times H_2O$ (where H_2O_2R is the free catecholamine) analogous to the previously reported catecholato compounds. The reactions of these ligands with the molybdate and tungstate anions were investigated.

Three different modes of coordination were identified:- three of the ligands formed complexes analogous to the Mo(VI) and W(VI) catecholato complexes, $[MO_2(O_2R)_2]^{2-}$, the ligand dopamine coordinated to these metals via its catechol moeity, but in monodeprotonated form; and adrenaline, in acidic conditions, was found to bind via its amine side chain to form Mo_2O_5(adrenaline)$_2$. The possible adaptation of these reactions for staining in electron microscopy was discussed. These new complexes were characterised by infrared spectroscopy, ^1H and ^{13}C nuclear magnetic resonance spectroscopy, cyclic voltammetry, and elemental analyses.

Reactions of the tropolonato anion, $C_7H_5O_2^-$ (trop), were investigated with group VI and VIII metals. The following new complexes were prepared and characterised by infrared spectroscopy, ^1H and ^{13}C nuclear magnetic resonance spectroscopy, electron paramagnetic resonance spectroscopy where appropriate, cyclic voltammetry, mass spectrometry, and elemental analyses:- $Ir(trop)_3$, $Os(trop)_3$, $OsO_2(trop)_2$, $MoO_2(trop)_2$, $W_2O_5(trop)_2$, and $[Pt(PPh_3)_2(trop)][BPh_4]$. An X-ray crystallographic study of $MoO_2(trop)_2$ is reported.

Finally, some studies with o-aminophenol and cyclohexane-1,2-diol as ligands are briefly reported.

Acknowledgements

I would like to thank Dr.Bill Griffith for his patient supervision during my period of study. My thanks also go to everybody who gave me help and advice during this time, especially Jane, Sue and Dick for recording N.M.R. spectra - Bob, Doug and Nigel for help running E.P.R. spectra, and Nick for recording the Raman spectra.

My especial thanks go to my mother who bravely typed this thesis, and to her boss, Mr.D.S. Potter, without whom she would not have been able to do it.

Thanks to Steve for putting up with me and giving me encouragement when I needed it.

Last, but certainly not least, my thanks to all members of the tea-room, who made this time so enjoyable.

Abbreviations

I.R. = infra-red

The intensities of absorptions in I.R. and Raman spectra are described as vs = very strong, s = strong, m = medium, w = weak, br = broad. The values are given in wavenumbers (cm^{-1}).

N.M.R. = Nuclear magnetic resonance

The resonances are described as s = singlet, d = doublet, t = triplet, q = quartet, m = multiplet. The values are given as δ in parts per million (p.p.m.) recorded to higher frequency of T.M.S. (δ = o).

E.P.R. = electron paramagnetic resonance

acac = acetylacetonato ligand

t-Bu = tertiary butyl

C.V. = cyclic voltammogram

cat^{2-} = catecholato dianion

cat H^- = catechol monoanion

3,5-DTBcat $^-$ = dianion of 3,5-di-t-butylcatechol

$3,5\text{-DTBSQ}^-$ = 3,5-di-t-butylsemiquinone

BQ = benzoquinone

SQ = semiquinone

9,10-PQ = 9,10-phenanthrenequinone

$9,10\text{-PSQ}^-$ 9,10-phenanthrenesemiquinone

$9,10\text{-phencat}^{2-}$ = the catecholato form of 9,10-phenanthrenequinone

4-nitrocat^{2-} = the dianion of 4-nitrocatechol

py = pyridine

pyH^+	=	the pyridinium cation.
bipy	=	bipyridyl
Ph	=	phenyl
$trop^-$	=	the tropolonato ligand
T.M.S.	=	tetramethylsilane
saloph	=	N,N'- (1,2-phenylene) bis (salicylidenimine) dianion
salen	=	N,N'-ethylene bis (salicylidenimine) dianion.
D.M.S.O.	=	dimethyl sulphoxide
D.M.F.	=	dimethyl formamide
T.H.F.	=	tetrahydrofuran.

LIST OF FIGURES

Figure		Page
1.1	The catecholato ligand	28
1.2	The o-quinone ligands	29
1.3(a)	4-t-butylcatechol	30
(b)	3,5-di-t-butylcatechol	30
(c)	4-nitrocatechol	30
(d)	pyrogallol	30
1.4(a)	3,5-di-t-butyl-o-benzoquinone	31
(b)	9,10-phenanthrenequinone	31
(c)	tetrachloro-o-benzoquinone	31
1.5	Bond lengths for $K_3[Cr(cat)_3]$	41
1.6	$Na_4[Ce(cat)_4]$ vs $Na_4[U(cat)_4]$	42
1.7	Structure of $(NH_4)_2[Mo_2O_5(cat)_2]$	43
1.8	Stretching vibrations of the cis-dioxo group	60
1.9	Stretching vibrations of the trans-dioxo group	61
1.10	Stretch vibrations of a μ-oxo bridged system	61
1.11	Infra-red spectrum of catechol	72
1.12	·hydrogen bonded catechol	63
1.13	Infra-red spectrum of $(Ph_4P)_2[Ir(cat)_3]$	74
1.14	Infra-red and Raman absorptions of ν(cis-MO_2)	77
1.15	Infra-red spectrum of $K_2[MoO_2(cat)_2]$ vs $(NH_4)_2[Mo_2O_5(cat)_2]$	81
1.16	Catechol as an A_2B_2 system	93
1.17	^1H N.M.R. spectrum of $K_2[OsO_2(cat)_2]$	102

Figure		Page
1.18	^{1}H N.M.R. spectrum of $K_2[MoO_2(cat)_2]$	102
1.19	^{13}C N.M.R. spectrum of catechol	107
1.20	Labeling of carbon nuclei of catechol	113
1.21	^{13}C N.M.R. spectrum of $K_3[Rh(cat)_3]$	107
1.22	^{13}C N.M.R. spectrum of $K_2[OsO_2(cat)_2]$	113
1.23	Labeling of carbon nuclei of 4-nitrocatechol	109
1.24	$K_2[OsO_2(4\text{-nitrocat})_2]$	111
1.25	^{13}C N.M.R. spectrum of $K_2[MoO_2(cat)_2]$ $C_6H_4(OH)_2$	113
1.26	Labeling of carbon nuclei of $C_6Cl_4O_2$	115
1.27	^{13}C N.M.R. spectra of $C_6Cl_4O_2$ and $Mo(O_2C_6Cl_4)_3$	116
1.28	3,5-di-t-butyl-o-benzoquinone	117
1.29	Part of E.P.R. spectrum of $MoO_2(PSQ)_2$	127
1.30	Cyclic voltammogram of $(Ph_4P)_2[Re(cat)_3]$	136
2.1	Structures of the catecholamines	153
2.2	Structure of hydrochloride salts of some catecholamines	152
2.3	The adrenaline Zwitterion	154
2.4	$Cu(O,N\text{-Dopa})_2$	159
2.5	Binding through the amine site of the catecholamine	160
2.6	$Cu(dopamine)_2$	162
2.7	Infra-red spectrum of $Na_2[MoO_2(noradrenaline)_2]$	189
2.8	Raman spectrum of $Na_2[MoO_2(noradrenaline)_2]$	191
2.9	Infra-red spectrum of $MoO_2(dopamine)_2$	193
2.10	Postulated structure of $MoO_2(dopamine)_2$	184
2.11	Infra-red spectrum of $Mo_2O_5(adrenaline)_2$	195

Figure		Page
2.12	Postulated structure of $Mo_2O_5(adrenaline)_2$	187
2.13	ABC protons of catecholamines	196
2.14	^1H N.M.R. spectrum of $K_2[OsO_2(isoproterenol)_2]$ compared to $K_2[MoO_2(isoproterenol)_2]$	200
2.15	ABX protons of coordinated catecholamines	197
2.16	^{13}C N.M.R. spectrum of Dopa	209
2.17	Labeling of carbon nuclei of Dopa	205
2.18	^{13}C N.M.R. spectrum of $Na_2[MoO_2(Dopa)_2]$	209
2.19	Labeling of carbon nuclei of adrenaline	208
2.20	Carbon nuclei labeling for noradrenaline and isoproterenol	211
2.21	Cyclic voltammogram showing reduction of $Na_2[WO_2(isoproterenol)_2]$	216
3.1	The tropolone dimer	227
3.2	Canonical forms of tropolone	228
3.3	Tropolone hydrochloride	229
3.4	Modes of delocalisation of the tropolonato ligand	230
3.5	Definition of the twist angle	236
3.6	Bond lengths of $Sc(trop)_3$	237
3.7	Non-hydrogen bonded tropolone	248
3.8	Infra-red spectrum of sodium troplonate	253
3.9	Infra-red spectrum of $Ir(trop)_3$	258
3.10	Infra-red and Raman spectra of $MoO_2(trop)_2$	265
3.11	Postulated Structure of $W_2O_5(trop)_2$	261

Figure		Page
3.12	Infra-red and Raman spectra of $OsO_2(trop)_2$	267
3.13	Postulated structure of $OsO_2(trop)_2$	263
3.14	^1H N.M.R. spectrum of tropolone	274
3.15	^1H N.M.R. spectrum of sodium tropolonate	274
3.16	^1H N.M.R. spectrum of $Ir(trop)_3$	275
3.17	^1H N.M.R. spectrum of $MoO_2(trop)_2$	275
3.18	Labeling of carbon nuclei of tropolone	276
3.19	Resonance structures of tropolone	277
3.20	Off-resonance coherent decoupled spectrum of tropolone	283
3.21	^{13}C N.M.R. spectrum of sodium tropolonate	283
3.22	^{13}C N.M.R. spectrum of $Ir(trop)_3$	284
3.23	^{13}C N.M.R. spectrum of $MoO_2(trop)_2$	284
3.24	Mass spectrum of $Ir(trop)_3$	293
3.25	Structure of $MoO_2(trop)_2$ found by X-ray crystallography	298

LIST OF TABLES

Table		Page
1.1	Chelate ring bond lengths for tris (catecholato) complexes.	50
1.2	Chelate ring bond lengths for tetrakis (catecholato) complexes.	51
1.3	Chelate ring bond lengths for oxo-catecholato complexes.	52
1.4	Chelate ring bond lengths for mixed ligand catecholato complexes.	53
1.5	Chelate ring bond lengths for semi-quinone complexes.	54
1.6	Chelate ring bond lengths for mixed semiquinone-catecholato complexes.	55
1.7	Major peaks of the infra-red and Raman spectra of catechol.	71
1.8	Major peaks of the infra-red spectra of new tris (catecholato) complexes.	73
1.9	Major peaks of the infra-red spectra of $K_2[MoO_2(cat)_2]$ and $(NH_4)_2[Mo_2O_5(cat)_2]$	80
1.10	Major peaks of the infra-red spectra of "(pyH)H[MoO_3(cat)]" and $Na_2[W_2O_5(cat)_2]$.	85
1.11	Major peaks of the infra-red spectra of "K[MoO_2(OH)(cat)]" and "(NH_4)[MoO_2(OH)($C_6H_4O_3$)]"	86
1.12	Major peaks of the infra-red spectra of 9,10-phenanthrenequinone, $MoO_2(PSQ)_2$ and $Mo_2O_5(PSQ)_2$.	88

Table		Page
1.13	Major peaks of the infra-red spectra of the new o-aminophenol complexes.	92
1.14	^{1}H N.M.R. resonances of catechol and some catecholato complexes.	101
1.15	^{1}H N.M.R. resonances of 3,5-di-t-butyl catechol, 3,5-di-t-butyl-o-benzoquinone, and $[MoO(3,5\text{-}DTBcat)_2]_2$.	103
1.16	^{13}C N.M.R. resonances for catechol and some catecholato complexes.	121
1.17	^{13}C N.M.R. resonances of 4-nitrocatechol and its complexes with cis-dioxo-molybdenum(VI) and trans-dioxo-osmium(VI).	122
1.18	^{13}C N.M.R. resonances of 3,5-di-t-butyl-o-benzoquinone and $[MoO(3,5\text{-}DTBcat)_2]_2$.	122
1.19	^{13}C N.M.R. resonances of tetrachloro-o-benzoquinone and $[Mo(O_2C_6Cl_4)_3]_2$.	123
1.20	^{13}C N.M.R. resonances of 1,2-cyclohexanediol and $OsO_2(py)_2$(cyclohexanediol).	123
1.21	Electrochemical data.	137
2.1	Major peaks of the infra-red spectra of dopamine hydrochloride and adrenaline.	171
2.2	Major peaks of the infra-red spectra of noradrenaline hydrochloride, isoproterenol hydrochloride and Dopa.	172

Table		Page
2.3	Major peaks of the infra-red spectra of complexes of the type $K_2[OsO_2(cat)_2]$	176
	(a) cat. = Dopa, isoproterenol, noradrenaline	176
	(b) cat. = dopamine, adrenaline.	177
2.4	Major peaks of the infra-red spectra of complexes of the type $UO_2(cat).nH_2O$	179
	(a) cat. = Dopa, isoproterenol, noradrenaline	179
	(b) cat. = dopamine, adrenaline.	180
2.5	Major peaks of the infra-red spectra of complexes of the type $Na_2[MoO_2(cat)_2]$.	188
2.6	Major peaks of the infra-red spectra of complexes of the type $Na_2[WO_2(cat)_2]$	190
2.7	Major peaks of the infra-red spectra of complexes of the type $MO_2(dopamine)_2$ (M = Mo(VI) W(VI))	192
2.8	Major peaks of the infra-red spectrum of $Mo_2O_5(adrenaline)_2$.	194
2.9	^1H N.M.R. resonances of the free catecholamines.	201
2.10	^1H N.M.R. resonances of the aromatic protons of complexes of the type $K_2[OsO_2(cat)_2]$.	202
2.11	^1H N.M.R. resonances of complexes of the type $Na_2[MO_2(cat)_2]$ (M = Mo(VI), W(VI)).	203
2.12(a)	^{13}C N.M.R. resonances of Dopa, $Na_2[MoO_2(Dopa)_2]$ and $Na_2[WO_2(Dopa)_2]$.	210
2.12(b)	^{13}C N.M.R. resonances of noradrenaline hydrochloride, $Na_2[MoO_2(noradrenaline)_2]$ and $Na_2[WO_2(noradrenaline)_2]$.	210

Table		Page
2.12(c)	^{13}C N.M.R. resonances of isoproterenol hydrochloride, $Na_2[MoO_2(isoproterenol)_2]$ and $Na_2[WO_2(isoproterenol)_2]$.	211
2.13	^{13}C N.M.R. resonances of the off-resonance coherent decoupled spectrum of Dopa.	212
3.1	Significant bond lengths and twist angles for tris (tropolonato) complexes.	243
3.2	Significant bond lengths for tetrakis (tropolonato) complexes.	244
3.3	Bond lengths for tropolone and some complexes containing the tropolonato ligand.	245
3.4	Major peaks of the infra-red and Raman spectra of tropolone.	250
3.5	Major peaks of the infra-red spectra of sodium tropolonate.	252
3.6	Major infra-red absorptions of some tris (tropolonato) complexes.	257
3.7	Major infra-red absorptions of the $MoO_2(trop)_2$, $W_2O_5(trop)_2$, and $OsO_2(trop)_2$ complexes.	269
3.8	^{1}H N.M.R. resonances of tropolone, sodium tropolonate, and some tropolonato complexes.	273
3.9	^{13}C N.M.R. resonances of tropolone, sodium tropolonate and tropolonato complexes.	282
3.10	Assignment of major peaks of the mass spectra of $Rh(trop)_3$ and $Ir(trop)_3$.	291
3.11	Assignment of major peaks of the mass spectra of $Ru(trop)_3$ and $Os(trop)_3$.	292

Table		Page
3.12	Bond lengths with standard deviations for $MoO_2(trop)_2$.	299
3.13	Bond angles for $MoO_2(trop)_2$.	300

In memory of my father.

CHAPTER I. CATECHOLATO AND RELATED COMPLEXES

This thesis is principally concerned with complexes of the O,O chelating ligands catechol and substituted catechols (Chapter I), catecholamines (Chapter II), and tropolone (Chapter III). A few complexes of semiquinones, cyclohexane-1,2-diol, and 1,2-aminophenol are also discussed in Chapter I. The metals used are principally those of group VIII (especially the platinum group), molybdenum, tungsten and uranium. A number of known complexes of transition metals, lanthanides and actinides are prepared for comparison purposes.

Within each chapter there is a general introduction (section 1) followed by sections dealing in turn with general preparative methods, vibrational, ^{1}H and ^{13}C N.M.R., and E.P.R. spectroscopy, electrochemistry, and mass spectra of the complexes. The experimental preparations and analytical data are placed in the last section.

1. INTRODUCTION

1.1 Catechols in nature

One of the first references to catechol interacting with transition metals was recorded by Pliny the Younger,[1] who noted that an "infusion of galls" changed colour in the presence of iron. Robert Boyle[2] also reported a reaction of "gallic acid" i.e. catechol, with iron, and the blue colour formed with gallic acid was used as a test for osmium tetroxide, when osmium was first discovered.[3]

Quinones (as the redox series - catechol, o-semiquinone, o-benzoquinone is collectively called) are found widespread throughout the environment, occurring naturally in higher plants, fungi, bacteria and the animal kingdom.[4] Polycyclic quinones are found as atmospheric contaminants over major cities and commonly occuring humic substances contain quinones in their oxidised and reduced forms, as do tannins.[5] Their most important property is their ability to be reversibly reduced or oxidised by transfer of one electron through the series from fully reduced catechol to fully oxidised o-benzoquinone. They therefore play an integral part in many biological electron-transfer processes,[6] particularly in photosynthesis.[7] Their second most important property exploited by nature, is the ability of quinones to chelate transition metals, and this has led to considerable interest in the preparation of transition metal-quinone complexes as model systems.[7] For example, the role of manganese in the catalysis of oxygen evolution in photosystem II is of particular interest.[8,9]

Catechol is a common functional group of the iron sequestering agents - the siderochromes, which are manufactured by microbes. They act as chelating ligands, forming extremely stable octahedral complexes with high-spin ferric ion.[11] Particularly important is enterobactin,[12] which contains three catechol functional groups, all of which coordinate the same ferric ion, with the extremely high formation constant of 10^{52}.[13, 14]

Molybdenum is also found in a number of enzymes that catalyse biological redox reactions,[15] and it appears to undergo oxidation state changes in the process.[16] Of greater interest is the biological function of this metal involving oxygen atom transfer reactions.[17] Some molybdenum-quinone systems have been found to show similar properties.[18]

In Chapter II we shall consider some complexes of catecholamines - naturally occurring substances found in the nervous system, which contain catechol moieties.

1.2 Catecholato, semi-quinone and benzoquinone ligands

The catecholato ligand (Fig 1.1) is the dianion of catechol (1.2-dihydroxy-benzene, $C_6H_4(OH)_2$)

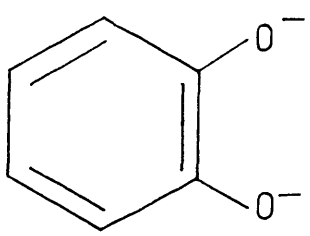
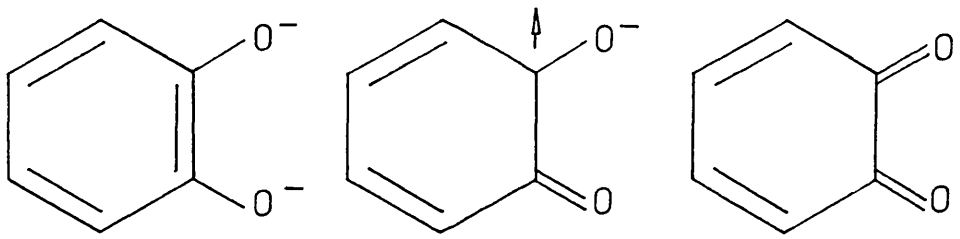


Figure 1.1 The catecholato ligand

It commonly coordinates to metal ions through its cis-oxygen atoms, forming a stable, five-membered chelate[19] ring. It is a terminal member of a redox series of o-quinone ligands[20] (Fig.1.2).



catecholate o-semiquinone o-benzoquinone

Figure 1.2

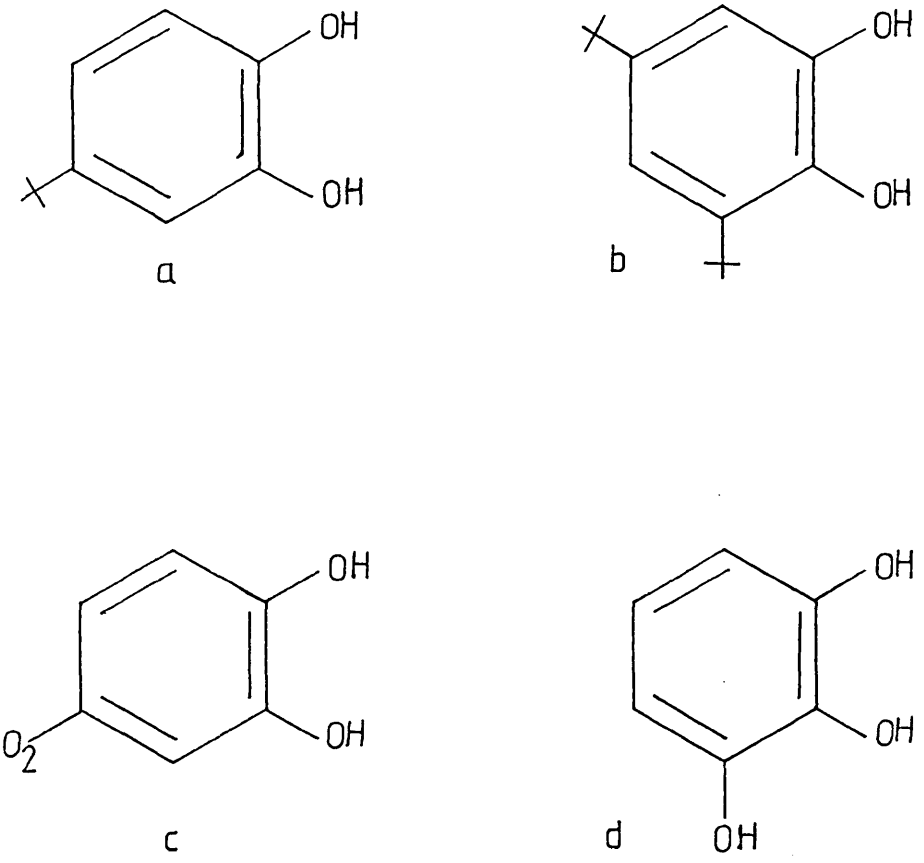
The catecholato ligand can exhibit "non-innocent" behaviour,[21] potentially able to coordinate to metal atoms in any one of these tautomeric forms (collectively called quinones), leading to the interesting possibility of the quinone ligand being able to alter charge at the metal centre via intramolecular transfer of one or two electrons between the metal and the quinone π^* level.[22] Theoretically, there is also the possibility of a fully delocalised chelate ring, as found for 1, 2-dithiolene complexes, but no such species has yet been identified for o-quinone complexes.[23]

This "non-innocent" behaviour also applies for substituted catechols.[24]

The parent compound, catechol, is a weak acid (pKa1 = 9.45, pK_{a2} = 12.89)[25] so at low pH it is a poor ligand.[12] However, its dianion has exceptional chelating ability, being able to displace the very stable vanadyl oxygen from a vanadium (IV) complex in aqueous medium.[26]

In the course of our work, several substituted catechols were also used, in particular, 4-tertiary-butyl catechol (Fig 1.3a) 3,5-di-tertiary-butyl catechol (Fig 1.3b), 4-nitrocatechol (Fig 1.3c), and pyrogallol (Fig 1.3d).

Figure 1.3:-



Most of the complexes we have prepared are of the catecholato type, and we concentrate on these in the introductory review, but some semi-quinone and benzoquinone complexes are also considered. Most of the work in this latter area has been carried out with the ligands 3, 5-di-tertiary-butyl-benzoquinone (Fig 1.4a), 9,10-phenanthrenequinone (Fig 1.4b) and tetrachloro-o-benzoquinone (Fig 1.4c).

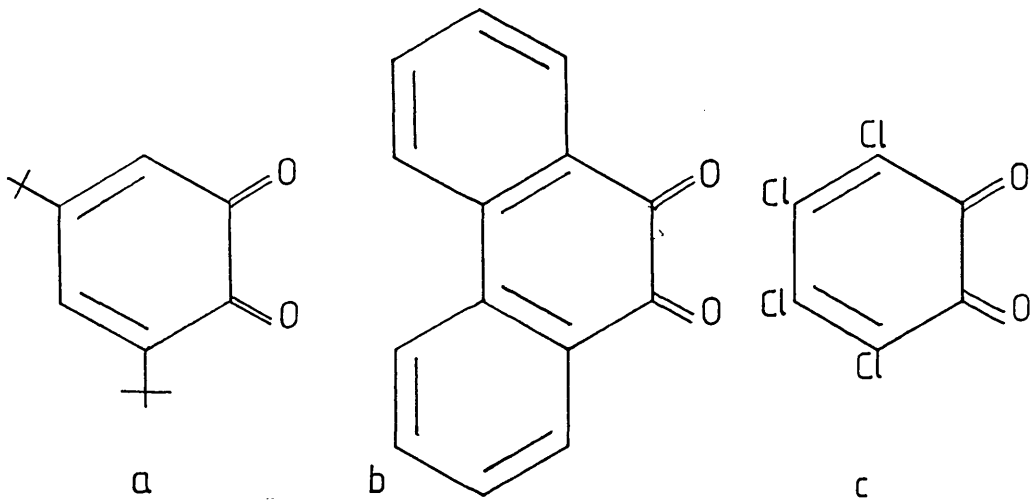


Figure 1.4

Henceforth the abbreviation cat. will denote catecholato complexes; SQ, semiquinone complexes, and BQ will represent complexes with benzoquinone type coordination.

1.3 Occurrence of catecholato complexes

Catecholato complexes are known for almost all the transition metals and also for a number of lanthanides, actinides and main group elements, normally taking the form $[M(cat)_3]^{n-}$. With the exception of rhodium[11] and osmium,[19] which form tris(catecholato) complexes, only mixed ligand complexes have been reported for the platinum group metals, e.g. $M(PPh_3)_2(cat)$, where M = platinum (II),[27,28] palladium (II); and $M(PPh_3)_2XY(cat)$, where M = iridium (III),[29,30,31] ruthenium (III),[32,33] rhodium (III),[30,31] X = Cl, CO, Y = Cl, CO.

There have also been several investigations into the reactions of platinum metal nitrosyl complexes with quinones, resulting in complexes of the type $M(NO)(PPh_3)(cat)$, M = iridium (I);[22,34] $M(NO)(PPh_3)_2(cat)$, M = rhodium and iridium[35,36] and $Ru(PPh_3)_2(NO)Cl(cat)$.[37] For the actinides, $Na_4[Ce(cat)_4]$,[39] $Na_4[Th(cat)_4]$,[39] $Na_4[U(cat)_4]$[40] and $UO_2(cat).\ 2H_2O$[41] are well established.

Catechol complexes of molybdenum have long been known, indeed, the reaction between them has been used for colorimetric estimation of molybdenum.[42] Several complexes reported in the early literature have since been recharacterised, and this has led to considerable doubt about the validity of the other formulations included in these reports.[43,44] The only rhenium complex reported, $H[(OH)_3Re(C_6H_4O_2)\ H_2O]$,[45] also seems to have an unlikely formulation, and we reinvestigate these in our work.

1.4 Oxidation states in quinone complexes

The presence of a non-innocent ligand in a metal complex can lead to considerable difficulty in defining the formal oxidation states[7] of the metal and the ligand.[46] The relative importance of the catecholato or o-benzoquinone form of the ligand in a complex should depend on the basicity of the metal,[47] the oxidising ability of the quinone itself,[36] and, possibly, on the charge of the complex.[48] The weaker oxidants, such as 9,10-phenanthrenequinone, react with difficulty and often form complexes with metals such as zinc (II), coordinating in the o-benzoquinone mode.[35] Addition of such ligands as tetrachloro-o-benzoquinone to nucleophilic Group VIII metal complexes, with d^8 and d^{10} electronic configurations, have been observed to produce catecholato-type coordination.[35,36]

The different forms of the quinone ligands can be interconverted chemically or electrochemically by transfer of charge from ligand-localised electronic levels by interaction with some external species.[48] This leads to the possibility of a series of complexes of a metal in a given oxidation state,[49] with ligands in varying stages of oxidation. This has indeed been observed for chromium (III)-quinone complexes, as described below (p.131).[49]

Where catecholato coordination has been identified (e.g. by X-ray crystallography) it appears that the catecholato ligand has the ability to stabilise metals in relatively high oxidation states,[23] e.g. osmium (VI) in $Os(cat)_3$ and $Os(3,5\text{-}DTBcat)_3$;[19] manganese (IV) in $Na_2[Mn(3,5\text{-}DTBcat)_3]$;[49] and cerium (IV) in $Na_4[Ce(cat)_4]$.[39] This is attributed to "hard acid - hard base" interaction between the higher oxidation state metal ions, and the oxo ions of the catechol ligand. The degree of "hardness" is related to the charge density; large charges and small ionic radii give rise to large electrostatic forces, and the species is described as "hard". The oxo ions of the catecholato dianion are effective as "hard" bases and, therefore, form stable compounds with metals in high oxidation states, which act as "hard" acids.[26,51]

1.5 Preparation of quinone complexes

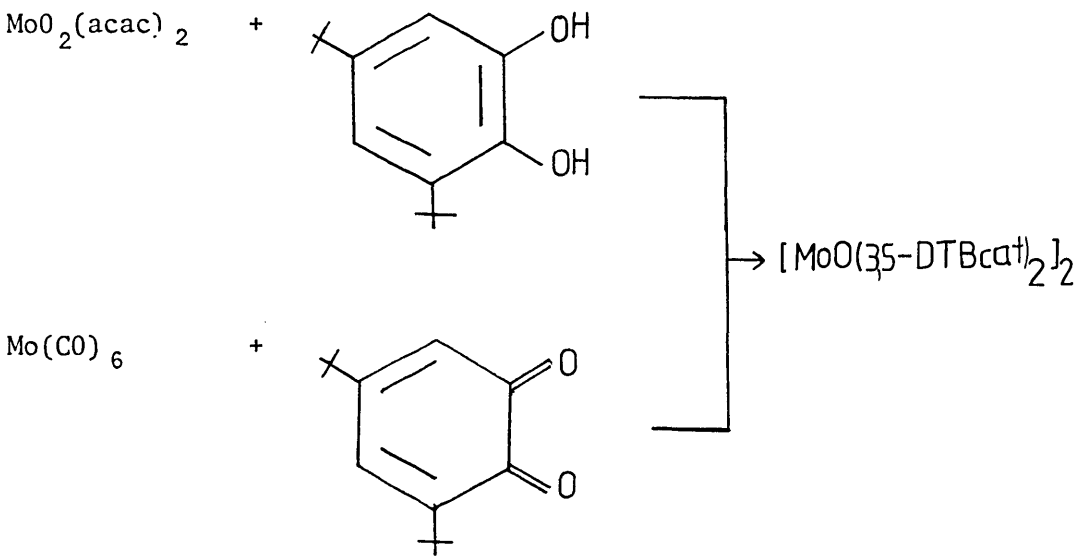
1.5.1 Catecholato complexes

The most common route to catecholato complexes is by reaction of a compound of the given metal (in a relatively high oxidation state) with catechol. Often catechol is used in basic solution to promote formation of the dianion, and under anaerobic conditions to avoid oxidation of the ligand. This usually results in a catecholato complex of the metal in the starting oxidation

state e.g. preparation of the bis (catecholato) dioxo-osmium (VI) complex (equation 1.1).[19]

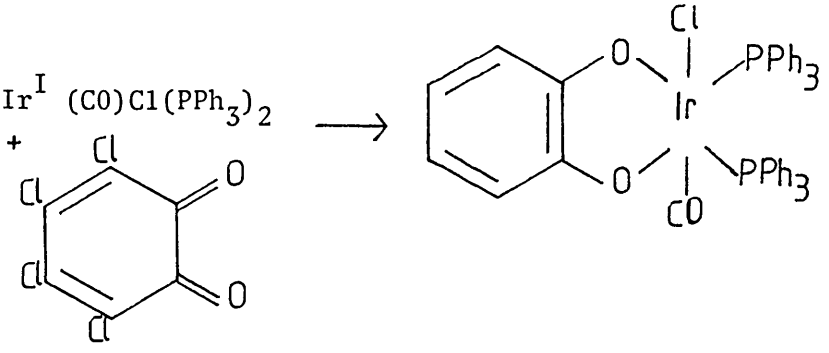
$K_2[OsO_2(OH)_4] + 2\ H_2(cat) \rightarrow K_2[OsO_2(cat)_2] + 4H_2O$ Equation 1.1

Alternatively, a reduced form of the metal may be reacted with the oxidised form of the ligand.[53] This sometimes produces the same complex as was obtained from the first method. This is particularly well illustrated by complexes of molybdenum (VI). Bis (acetylacetonato) cis-dioxo-molybdenum (VI), $MoO_2(acac)_2$, will react with 3,5-di-t-butyl-catechol to give the product bis (bis(3,5-di-t-butyl catechol) oxo-molybdenum (VI), $[MoO(3,5\text{-DTBcat})_2]_2$. Reaction of molybdenum hexacarbonyl with 3,5-di-t-butyl-o-benzoquinone results in the same product (equation 1.2).[17]



Equation 1.2

Several mixed ligand complexes of the platinum group metals are known. They are commonly prepared by oxidative addition of the o-benzoquinone ligand to a complex of the metal in a low oxidation state. Tetrachloro-o-benzoquinone, for example, will react with the square planar complexes, $M(CO)(PPh_3)_2Cl$(M=Rh,Ir,Ru), to yield six-coordinate adducts (equation 1.3).[31]

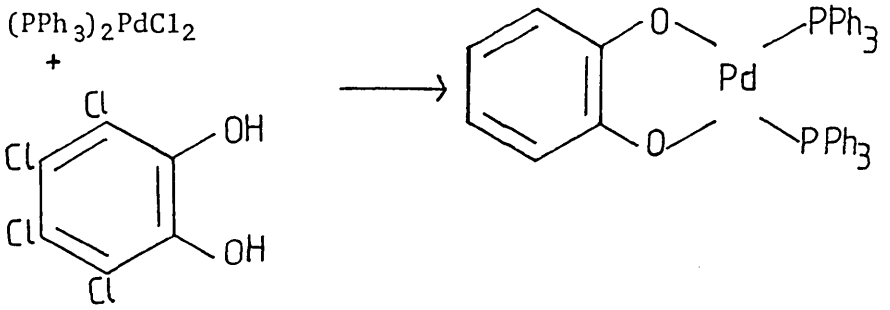


Equation 1.3

This reaction takes place at 25°C.[31] The success of such a thermal addition depends on the oxidation potential of the quinone. Tetrachloro-o-benzoquinone is a strongly oxidising quinone. Under similar conditions the weaker oxidants, such as 9,10-phenanthrenequinone, do not appear to form adducts, but they have been reported to add to $Ir(CO)Cl(Pph_3)_2$ under photochemical conditions.[29,30]

The very reactive[10] complex tetrakis (triphenylphosphine) platinum(o)[30] reacts with tetrachloro-o-benzoquinone[54] and 9,10-phenanthrenequinone[29] under thermal conditions to give $Pt(PPh_3)_2(cat)$. This type of complex has also been prepared by addition of catechol in basic solution to the very reactive dioxygen complex, $Pt(PPh_3)_2(O_2)$.

The analogous palladium complexes have also been reported to form by reaction of $(PPh_3)_2PdCl_2$ with the fully reduced catechol ligand (equation 1.4).[47]

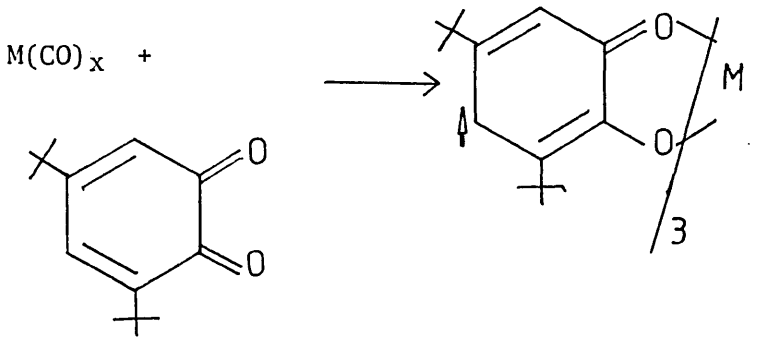


Equation 1.4

1.5.2 Semiquinone complexes

Bis and tris o-semiquinonato complexes of first row transition metals have been synthesised by a number of methods, principally:-

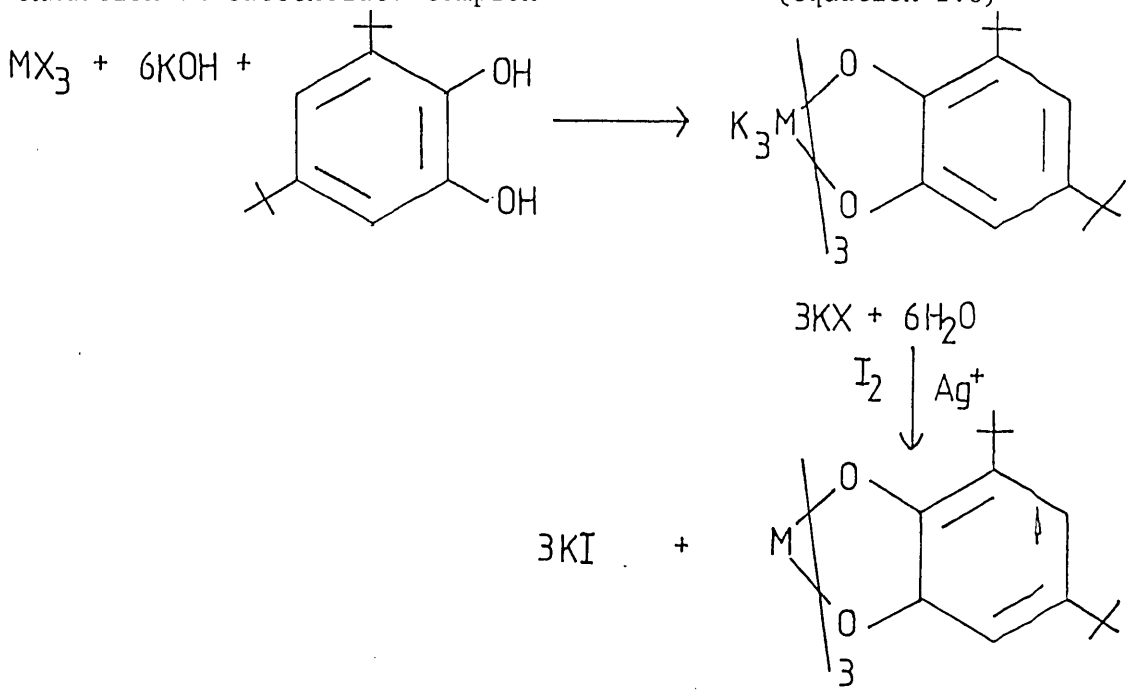
(i) Metal Carbonyl and o-benzoquinone (equation 1.5)[23]



Equation 1.5

Tetrachloro-o-benzoquinone and 9,10-phenanthrenequinone may also be used.[55]

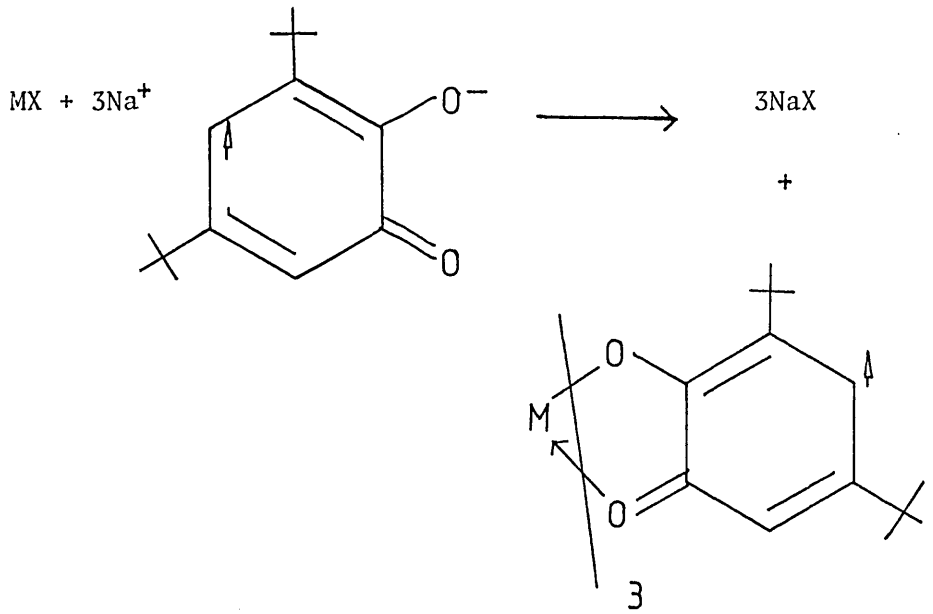
(ii) Oxidation of catecholato complex (equation 1.6)[57]



Equation 1.6

(iii) metal halide and o-semiquinone of sodium or thallium

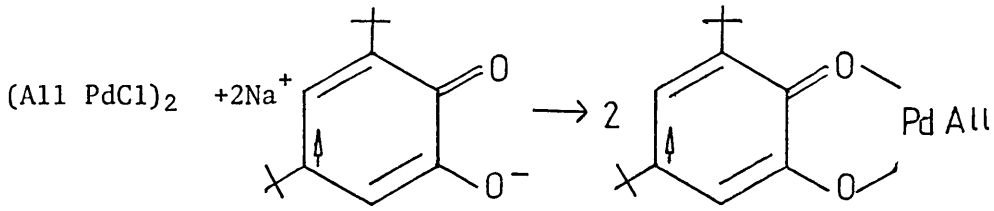
(equation 1.7)



Equation 1.7

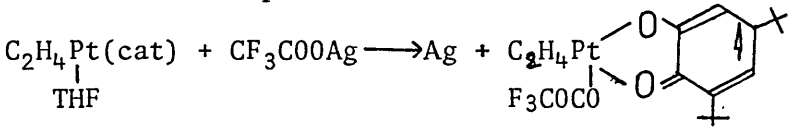
Related bis and tris complexes prepared with second or third row transition metals have been formulated as catecholato complexes, the metal ion having a higher oxidation state e.g. $Cr(O_2C_6Cl_4)_3$ is a tris (semiquinone) chromium (III) complex, compared to the molybdenum (VI) - catecholato complex, $Mo(O_2C_6Cl_4)_3$; $Fe[O_2C_6H_2(tBu)_2]_3$ and $Os[O_2C_6H_2(tBu)_2]_3$- the former is a tris (semiquinone) iron (III) complex, the latter a tris (catecholato) osmium (VI) complex.[23]

Mono o-semiquinonato complexes of copper, silver and palladium with a neutral donor ligand or π-allyl group can be prepared as shown in equation 1.8.[57]



All = π Allyl ligand Equation 1.8

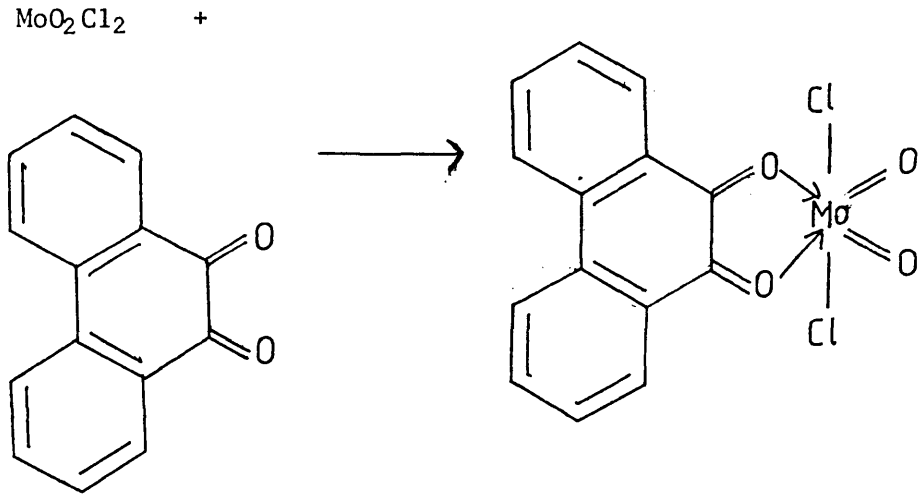
A number of substituted palladium and platinum semiquinone complexes were prepared from $(PPh_3)_2$ Pd(cat) and $(C_2H_4)Pt(cat)(THF)$[58] using various chemical oxidising agents such as $CuCl_2$, in evacuated tubes. An example of these reactions is shown in equation 1.9.



Equation 1.9

1.5.3 O-Benzoquinone complexes

In this mode of coordination, the quinone ligand can only coordinate to the metal as a weak donor, following the anticipated trend that, in the absence of π- acceptor bonding, oxygen donor[4] activity decreases as the ketonic character of the C-O bond increases. Reaction only took place under anhydrous conditions, using 9,10-phenanthrenequinone and a metal halide.[59,60] The molybdenum (VI) complex was formed as shown in equation 1.10[4]



Equation 1.10

1.6 X-ray crystallographic studies of o-quinone complexes

The most definitive method yet found for distinguishing between the bonding modes of the o-quinone ligands is X-ray crystallography. By comparison of the accumulated data from the studies which have been undertaken with other complexes of similar oxidation states, and with the parameters of the free ligands, it is now possible to define the ligand oxidation

state within a complex for which X-ray data may be obtained. The bond lengths most sensitive to the nature of the ligands are those of the M-O, C-O, and C-C bonds.[23,46] The M-O distance is helpful in indicating the oxidation state of the metal, whilst the C-O bond length is most characteristic of the oxidation state of the ligand.[17] Catecholato-type ligands show a C-O bond length, (dc-o) always close to 1.35 Å ,[22,50,64,65] bridging ligands being slightly longer at 1.37 Å.[60] For o-semiquinone complexes dc-o is typically 1.29 Å,[53,62,63,64,65] and the only o-benzoquinone complex which has been characterised X-ray crystallographically has a C-O distance of 1.23 A.[o 17] These bond lengths reflect the greater degree of double bond character found for the C-O bond through the series catecholato-semiquinone-benzoquinone.

Catecholato ligands have C-C bond lengths, dc-c, typical of an aromatic ring, at 1.40 Å;[48,53,65] o-semiquinone complexes show a slight lengthening of dc-c in the chelate ring, to 1.44 Å .[48,53,62,64,65] In the o-benzoquinone complex dc-c of the chelate ring, and the bond opposite it in the quinone ring, both show localised single bond values of 1.530(5) and 1.487(6) Å respectively.[4]

Consistent with the variation in C-O bond lengths within the chelate ring is the associated variation in ligand bite observed between the catecholato and semiquinone complexes.[57,62] The O-M-O bite angle of the semiquinone ligands is typically 2^{o} smaller than that found for the catecholato ligands, for the same metal, (both near 80^{o}).

1.6.1 Structures of catecholato complexes

(a) Tris (catecholato) complexes, $[M(cat)_3]^{n-}$, M = V(III),[26] V(IV),[26] Cr(III),[12] Mn(IV),[50] Fe(III),[12] Os(VI).[67]

The most significant parameters of these complexes are listed in Table 1.1. They all have approximate octahedral geometry. The catecholato ligands all have planar aromatic rings, but some of them have oxygen atoms which slightly deviate from the aromatic plane, possibly due to crystal intermolecular forces. The complex $(Et_3NH)_2$ $[V(cat)_3]$ CH_3CN,[26] however, deviates considerably from rigorous octahedral geometry because of hydrogen-bonding of the triethylammonium cations to two of the catechol oxygen atoms.

A diagram showing typical significant bond lengths and angles is given below (Fig 1.5).[21]

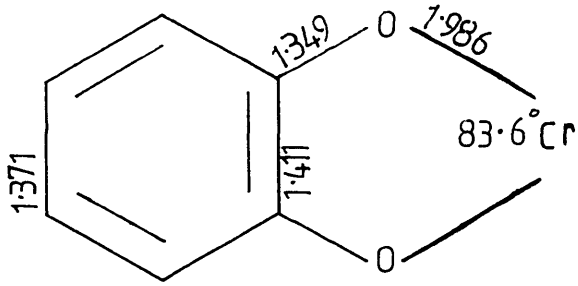


Figure 1.5 Bond lengths for $K_3[Cr(cat)_3]$.

These catecholato complexes have a bit angle (α) near 80^o.

(b) Tetrakis (catecholato) complexes, $[M(cat)_4]^{n-}$, M = Hf(IV),[39] Ce(IV),[39] Th(IV),[40] U(IV)[40]

Structural data for these complexes are listed in Table 1.2. These complexes were all reported as $Na_4[M(cat)_4].2]$ H_2O - the large number of molecules of water of crystallisation forming a hydrogen-bonded network throughout the crystal.

Each complex was found to have dodecahedral coordination geometry, D_{2d} molecular symmetry, with planar ligands. The complex $Na_4[U(cat)_4]21H_2O$ has two different values for the metal-oxygen bond lengths, the difference of 0.027(5)Å being a significant amount. Comparison with the f^o thorium and cerium structures rules out differing ionic radii as the cause, and it was concluded that the lengthening of the M-O bonds was attributable to the ligand field effect arising from the f electrons. The d^o hafnium complex showed a comparable distortion to that found for the uranium (IV) complex, but in this case the cause was concluded to be interligand contacts between the catecholato ligands which are pulled sufficiently close together because of the small ionic radius of hafnium.

Bond lengths and angles are shown below for the uranium (IV)[40] complex versus the cerium (IV)[39] complex, (Fig 1.6).

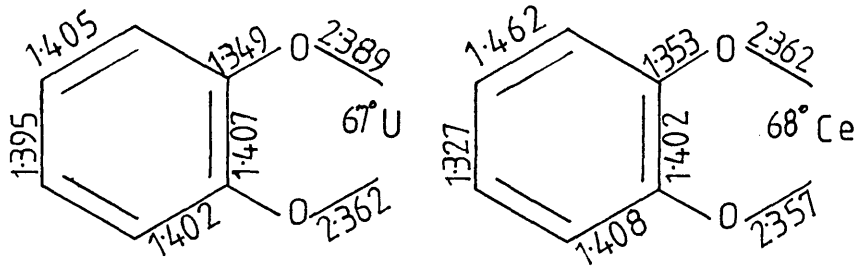


Fig 1.6

(c) Mixed-ligand and catecholato complexes

(i) Oxo-complexes

Structural data for these complexes are listed in Table 1.3. Many complexes of molybdenum with catechol have been reported.[43,44] One of the first to be studied by X-ray crystallography was $K_2[MoO_2(cat)_2]\ 2\ H_2O$.[68] It was found to have the cis-dioxo-molybdenum structure characteristic of molybdenum (VI) complexes.

The coordination geometry was distorted octahedral. The molybdenum to terminal oxygen bond lengths were unusually long (2.10Å) suggesting a possible trans-weakening effect of the catecholato ligands.

The complex $(NH_4)_2[Mo_2O_5(cat_2]$[69,70] previously formulated as $(NH_4)H[MoO_3(cat)]$[43] was found to exist as a dimer of two cis-dioxomolybdenum(VI) centres, formed by sharing of two octahedra through a common face. This is effected by one bridging oxygen atom, and by the sharing of an oxygen atom from each catechol ligand by the two molybdenum centres, as shown in Figure 1.7.

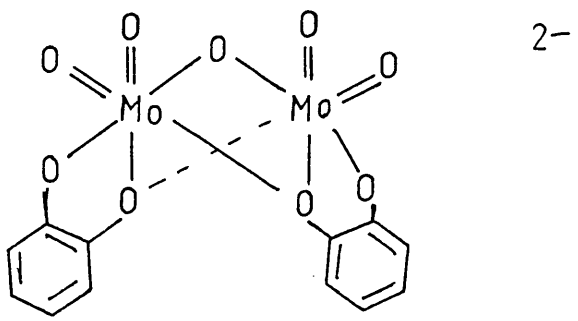


Figure 1.7. Structure of $(NH_4)_2[Mo_2O_5(cat)_2]$.

Again each metal has distorted octahedral coordination. The analogous complex $[(n\text{-}Bu)_4N]_2[Mo_2O_5(3,5\text{-}DTBCat)_2]$ was investigated in a recent study.[18]

The neutral complex $[MoO(3,5\text{-}DTBcat)_2]_2$ formed from molybdenum hexacarbonyl with 3,5-di-t-butyl-o-benzoquinone was found to exist as a centrosymmetric dimer,[17] each molybdenum(VI) centre having one terminal oxo, and two chelating catecholato ligands. Six coordination is achieved by one oxygen atom from each catechol ligand bonding to both molybdenum atoms.

The molybdenum-oxygen bond lengths within the bridge are unsymmetrical with the longest distance occurring within the chelate ring to the catechol oxygen trans to an oxo ligand. Despite the unusual coordination of one oxo ligand to a molybdenum(VI) centre, the compound is stable, and inert to hydrolysis.

The only other oxo-catecholato complex was found with vanadium(IV), $K_2[VO(cat)_2]$ $EtOH.H_2O$.[26] shows approximate square pyramidal coordination, the major deviation from this C_2v symmetry is due to the greater bending of one catechol ring away from the apical terminal oxo ligand.

(ii) Miscellaneous complexes

Structural parameters for these complexes are listed in Table 1.4. The catecholato ligand has been shown to act in a bridging role in the complex $[Mo(O_2C_6Cl_4)_3]_2$,[71] formed from molybdenum hexacarbonyl and tetrachloro-o-benzoquinone. Two catecholato ligands chelate to each of the octahedrally coordinated molybdenum(VI) centres. Two further catecholato ligands bridge the two metal centres, forming a ten-membered ring. The bridging distances show different bond lengths, the M-O distance being shorter for the bridging ligand, and the C-O lengths slightly longer.

Apart from $Os(cat)_3$[67] and $Os(3,5\text{-}DTBcat)_3$,[67] no unsubstituted complexes have been examined, as listed in Table 1.4. Of particular interest is the complex $Ir(NO)(O_2C_6Br_4)(PPh_3)$.[22] Both the quinone and nitrosyl ligands can modulate the charge at the metal centre and have demonstrated the ability to influence their own mode of coordination intramolecularly.

The quinone ligand was found to be coordinated in the catecholato mode, with a linear nitrosyl group, leading to the conclusion that the metal is iridium (I). The unusually short Ir-O bond length *trans* to the nitrosyl ligand can only be reasonably explained by considering the bonding effect of having a strong π acceptor (NO^+) *trans* to a strong π donor. Thus the catecholato ligand may be considered as a strong donor.

1.6.2 The catechol monoanion

The unusual monodeprotonated catechol ligand has been characterised by X-ray crystallography in the complex Fe(saloph)(cat H).[72] (where saloph is the dianion of N,N - (1,2-phenylene) *bis*(salicylidenimine)). It was found to coordinate through the deprotonated oxygen atom only. The geometry was found to be square pyramidal with the coordinated catechol oxygen atom at the apex of the pyramid. The catechol molecule is tilted 15.1^{o} from the perpendicular and the structural parameters are comparable to those of catecholato complexes.

1.6.3 Structures of Semiquinone Complexes

Significant structural parameters for these complexes are listed in Table 1.5.

Originally reported with the catecholato complex $[Mo(O_2C_6Cl_4)_3]_2$ was the chromium complex prepared in the same manner, $Cr(O_2C_6Cl_4)_3$.[73] This complex was subsequently found to be monomeric,[23] with a *tris* chelated octahedral geometry, and bond parameters consistent with semiquinone coordination to a chromium (III) centre. (This complex was originally thought to be a Cr(o) complex[74] with three benzoquinone ligands, until its reformulation.)

The analogous chromium complex prepared from 3,5-di-tert-butyl-benzoquinone and chromium hexacarbonyl was also found to be a tris (semiquinone) chromium (III) complex.[21]

Photochemical reaction of iron pentacarbonyl with 9,10-phenanthrenequinone, resulted in the octahedral tris (9,10-phenanthrene-semiquinone) iron (III) complex, $Fe(PSQ)_3$.[62] The bite angle for these ligands was found to be $79.4(1)^o$ as compared with $81.3(1)^o$ for $K_3[Fe(cat)_3]$.

The tetrameric cobalt (II) complex, $Co_4(3,5\text{-}DTBSQ)_8$,[65] was found to have six ligands which each chelated to one cobalt (II) centre, but also formed a bridging bond to another metal ion. The other two semiquinone ligands of the tetramer did not form any bridging bond.

The complex Mo_2O_5(9,10-phenanthrene-semiquinone)$_2$, $Mo_2O_5(PSQ)_2$,[61] has a very similar structure to those observed for $(NH_4)_2[Mo_2O_5(cat)_2]$[69,70] and $[(tBu)_4N]_2[Mo_2O_5(3,5\text{-}DTBcat)_2]$.[18] The major difference is in the dihedral angle formed between the two quinone ligands of each complex molecule. $Mo_2O_5(PSQ)_2$ has an angle of $19.3(3)^o$, whilst for the 3,5-di-t-butyl catecholato complex it is found to be $50.0(4)^o$.[18] This is explained by the differences in the repulsive interactions of two catecholato ligands as compared to two semiquinone ligands, and partly by steric effects of the bulky tert-butyl groups. The bond lengths and angles of these phenanthrenequinone ligands are typical of semiquinone coordination to a molybdenum (VI) centre. The observed diamagnetism of the complex is explained by antiferromagnetic coupling through space between the semiquinone ligands.[61]

1.6.4 Mixed semiquinone - catecholato complexes

X-ray crystallographic data for these complexes are listed in Table 1.6. The diamagnetic complex consisting of three 9,10-phenanthrenequinone ligands around a molybdenum centre would appear to be a tris (catecholato) molybdenum (VI) complex.[64] However, X-ray studies have shown it to have two catecholato ligands and one semiquinone ligand, coordinated around a molybdenum (V) centre, with trigonal prismatic geometry.[62] Weak antiferromagnetic coupling between the molybdenum (V) ion and the semiquinone results in a magnetic moment which is less than 1.0μB at room temperature. There is some distortion from trigonal prismatic geometry due to the semiquinone ligand being bent at an angle of 60° from its MoO_2 plane. This results in the aromatic region of the ligand lying parallel to a catecholato ligand of an adjacent molecule, due to the relatively strong intermolecular charge-transfer interactions between adjacent molecules related by a crystallographic centre of inversion.

Treatment of the cobalt (II) semiquinone tetramer, $(Co_4(3,5\text{-DTBSQ})_8)$ with bipyridyl results in the cobalt (II) complex, $Co(3,5\text{-DTBSQ})_2$ (3,5-DTBcat)(bipy).[68] The complex was found to form an equilibrium with bis (semiquinone) bipyridyl cobalt(II) complex in solution, by intramolecular transfer of an electron between the metal and the quinone ligands.[23]

The complex $[VO(3,5\text{-DTBSQ})(3,5\text{-DTBcat})]_2$ exists as a centrosymmetric dimer, each metal having distorted octahedral coordination with one terminally bonded oxo ligand at one site.[53] Catecholato ligands bridge adjacent vanadium (V) ions through one oxygen atom; the semiquinone ligands are chelated to the metals, and do not bridge.

1.6.5 Benzoquinone complex

Only one cyrstallographic study has reported a complex of a quinone ligand coordinating in the fully oxidised o-benzoquinone mode. In MoO_2Cl_2(9,10-phenanthrenequinone)[9] the benzoquinone ligand is coordinated at sites trans to the oxo ligands. The chloro ligands are bonded trans to each other as shown in equation 1.10. The 9,10-phenanthrenequinone oxygen atoms are only weakly bound to the metal with Mo-O lengths of 2.306(3)Å , consistent with the strong trans influence of oxo ligands, and the weak donor activity of the ketonic quinone oxygens. The C-O bond lengths, 1.234(4)Å, are slightly longer than those found for the free quinone. The distance between the two carbonyl carbon atoms is 1.530(5)Å; the carbon-carbon bond opposite this also has a longer value of 1.429(4)Å, closer to single bond values.

1.6.6 Intermolecular interactions

Many of these quinone complexes that have been studied by X-ray crystallography have been found to crystallise with a solvent molecule of crystallisation.[23] Some complexes lose their solvent molecules over a relatively short time, causing degradation of the crystal.[62] This behaviour can also lead to erratic chemical analyses.

It is explained by the apparent ability of quinone ligands to form weak interactions with planar molecules. This can lead to difficulty in obtaining crystals sufficiently stable for X-ray crystallographic investigation.[64]

A typical example of this is found with the complex $[Mo(O_2C_6Cl_4)_3]_2$ 3 C_6H_6.[71] Benzene solvate molecules are situated 3.5Å above the ligand planes, located in a sandwich-clathrate structure, resulting in a two-dimensional polymeric array over the whole crystal structure.

Complexes with 9,10-phenanthrenequinone ligands tend to have stacked structures.[63] The central benzene ring of the semiquinone ligand of $Mo_2O_5(PSQ)_2$ [61] overlaps with an outer benzene ring of the ligand of an adjacent complex molecule, forming a chain of molecules with interatomic contacts of 3.4 - 3.5Å.

In the following sections 2 - 7, we describe the experimental results and each section follows the general order:-

1. Spectra of the ligands.
2. Spectra of the complexes.

2.1 Literature work.

2.2 Experimental results.

(a) Tris - catecholato complexes.

(b) Oxo - catecholato complexes.

(c) Other catecholato complexes.

(d) Reformulation of molybdenum(VI) - catecholato complexes.

(e) Benzoquinone versus catecholato coordination.

(f) Semiquinone complexes.

Table 1.1:- Chelate ring bond lengths (Å) for tris (catecholato) complexes studied X-ray crystallographically

Complex	M - O	C - O	C - C[a]	Ref.
Catechol	-	1.372	1.385	75
$K_3[V(cat)_3]$ $1.5H_2O$	2.013(9)	1.345(2)	1.410(4)	26
$(Et_3NH)_2[V(cat)_3]CH_3CN$	1.942(8)	1.338(6)	1.408(6)	26
$Na_2[Mn(3,5\text{-}DBTcat)_3]$ $6CH_3CN$	1.883(6)	1.340(10)	1.399(12)	66
$K_2[Mn(3,5\text{-}DTBcat)_3]$ $6CH_3CN$	1.907(3)	1.362(5)	-	50
$K_3[Cr(cat)_3]1.5H_2O$	1.986(4)	1.349(3)	1.411(4)	12
$K_3[Fe(cat)_3]1.5H_2O$	2.015(6)	1.349(3)	1.409(6)	12
$Os(cat)_3$	1.962(5)	1.32(1)	-	67
$Os(3,5\text{-}DTBcat)_3$	1.958(6)	1.33(1)	-	67

[a]C-C length is average of six C-C bonds of aromatic ring.

Table 1.2:- Chelate ring bond lengths (Å) for tetrakis (catecholato) complexes studied by X-ray crystallography.

Complex	M-O	C-O	C-C	Reference
$Na_4[Hf(cat)_4]21H_2O$	2.220(3) 2.194(3)	1.344(4)	1.414(5)	39
$Na_4[Ce(cat)_4]21H_2O$	2.360(4)	1.353(6)	1.402(7)	39
$Na_4[Th(cat)_4]21H_2O$	2.420(3)	1.345(5)	1.415(6)	40
$Na_4[U(cat)_4]21H_2O$	2.389(4) 2.362(4)	1.349(6)	1.407(7)	40

Table 1.3:- Chelate ring bond lengths (Å) for oxo-catecholato complexes.

Complex	M-O	C-O	C-C	Reference
$K_2[MoO_2(cat)_2]2H_2O$	2.05 2.17	1.39(3)	1.41(3)	68
$(NH_4)_2[Mo_2O_5(cat)_2]2H_2O$	2.17 2.37	1.36(3)	1.41(3)	70
$Ba[Mo_2O_5(cat)_2]5H_2O$ $C_6H_4(OH)_2$	2.18 2.37	1.37(1)	1.41(2)	70
$[(n\text{-}Bu)_4N]_2$ $[Mo_2O_5(3,5\text{-}DTBcat)_2]$	1.977(10)	1.37(2)	1.37(2)	18
$[MoO(3,5\text{-}DTBcat)_2]_2$	1.965(3) 1.233(3)	1.360(6)	1.396(6)	17
$K_2[VO(cat)_2]EtOH.H_2O$	1.956	1.352(6)	1.397(6)	26

Table 1.4:- Chelate ring bond lengths (Å) for mixed-ligand catecholato complexes studied by X-ray crystallography.

Complex	M-O	C-O	C-C	Reference
$[Mo(O_2C_6Cl_4)_3]_2$	1.861(7)	1.37(1)	1.39(1)	71
	1.949(6)	1.33(1)		
K[Fe(salen)(cat)]	1.990(9)	1.321(18)	1.406(20)	76
Fe(saloph)(catH)	1.828(4)	1.352(7)	-	74
$(C_5H_{12}N)_2[(CH_3COO)\{Fe(cat)_2\}_2]$ H_2O	1.94 2.08	-	-	77
$Pd(PPh_3)_2(C_6Cl_4O_2)$	2.033(5)	1.344(9)	1.366(11)	47
$[Rh(\eta\text{-}C_5Me_5)(cat)]2C_6H_4(OH)_2$	2.011(11)	1.387(18)	1.403(21)	78
$Ir(PPh_3)(NO)(C_6Br_4O_2)$	1.959(14)	1.337(25)	1.358(28)	22

Table 1.5:- Chelate ring bond lengths (Å) for semiquinone complexes studied by X-ray crystallography

Complex	M-O	C-O	C-C	Reference
$Cr(O_2C_6Cl_4)_3.CS_2.\frac{1}{2}C_6H_6$	1.949(5)	1.28(1)	1.44(1)	74
$Cr(O_2C_6H_2(C_4H_9)_2)_3$	1.933(5)	1.285(8)	1.433(9)	21
$Fe(C_{14}H_8O_2)$9,10-PQ	2.027(4)	1.283(3)	1.435(6)	62
$Fe(salen)(C_{14}H_8O_2)$	1.995(3)	1.302(5)	1.429(6)	76
$Co_4(O_2C_6H_2(C_4H_9)_2)_8$ $2C_6H_6$	2.050(4)	1.285(7)	1.448(4)	65
$Ni(C_{14}H_8O_2)(py)_2.py$	2.058(7)	1.272(11)	1.442(14)	63
$Mo_2O_5(C_{14}H_8O_2)_2$	2.141(4) 2.495(4)	1.313(8)	1.426(9)	61

Table 1.6:- Chelate ring bond lengths (Å) for mixed semiquinone-catecholato complexes.

Complex	M - O	C - O	C - C	Ref.
$Mo(phencat)_2(PSQ)$	1.952(5)[a]	1.34(1)	1.35(1)	64
	1.979(5)[b]	1.31(1)	1.43(1)	
Co(3,5-DTBcat)(3,5 DTBSQ)(bipy)	1.869(6)[a]	1.358(10)	1.376(12)	48
	1.897(6)[b]	1.297(9)	1.446(11)	
[VO(3,5-DTBcat) (3,5-DTBSQ)]$_2$	1.956(6)[a]	1.355(7)	1.40(1)	53
$C_6H_5OCH_3$	1.981(5)[b]	1.307(8)	1.44(1)	

[a] - bond lengths of catecholato ligands

[b] - bond lengths of semiquinone ligands

phencat = 9,10 phenanthrenequinone bonded in the catecholato mode.

PSQ = 9,10-phenanthrenesemiquinone

bipy = bipyridyl

2. PREPARATION OF COMPLEXES

Examination of the literature revealed that the most common way of preparing catecholato complexes was by reaction of the metal in the appropriate oxidation state, with catechol, in a basic medium, under anaerobic conditions e.g. $K_3[Fe(cat)_3]$,[12] $Na_4[Ce(cat)_4]$.[39] This method was successfully adapted for the preparation of a new rhenium complex by the reaction of $K_2[ReCl_6]$ with catechol. Precipitation of the complex with tetraphenylphosphonium chloride resulted in the new product $(Ph_4P)_2[Re(cat)_3]$.

When using iridium (III) chloride as the starting material, however, under the same conditions, the product was found to be $(Ph_4P)_2[Ir(cat)_3]$, containing iridium in the +4 oxidation state. Attempts to precipitate a complex containing iridium (III) with the trivalent cation, tris (ethylenediamine) cobalt (III), $[Co(en)_3]^{3-}$, instead of tetraphenylphosphonium chloride, gave no product. Using $Na_2[IrCl_6]$ as a starting material also produced the complex $(Ph_4P)_2[Ir(cat)_3]$.

It is well known that the catecholato ligand has the ability to stabilise higher oxidation states of metals,[23,39] indeed seeming to prefer them. In this case, where two common oxidation states of the metal occur, separated only by one unit of charge, it is quite conceivable that catechol would tend to form the complex of the metal in the higher oxidation state.

No catecholato complex of iridium could be isolated from the reaction mixture prepared as described for $[Co(en)_3]$ $[Rh(cat)_3]$.[11] This may be due to the fact that precipitation of the complex was only attempted with $[Co(en)_3]Cl_3$.

The new ruthenium complex $(Ph_4P)_3[Ru(cat)_3]$ was prepared using tris (acetylacetonato) ruthenium (III), $Ru(acac)_3$, as the starting material. (This method has been successfully employed using $VO(acac)_2$ and 3,5-di-t-butylcatechol to give $V(3,5\text{-DBSQ})_3$.[53]) However, this method was not consistently successful.

A new example of a molybdenum semiquinone complex, $MoO_2(PSQ)_2$, was prepared by adaptation of the method reported for $Mo_2O_5(PSQ)_2$,[64] i.e. a solution of molybdenum hexacarbonyl and 9,10-phenanthrenequinone in dichloromethane was irradiated with ultra-violet light. After one hour $Mo_2O_5(PSQ)_2$ was isolated; after several hours $MoO_2(PSQ)_2$was formed.

A number of molybdenum (VI) - catecholato complexes were reported in the early literature, having unusual formulations, based solely on elemental analyses. Later X-ray crystallographic studies have shown that $K_2[MoO_2(cat)_2]$[68] was formulated correctly, but that the complex originally postulated to be "$NH_4.H.[MoO_3(cat)]$"[43] was, in fact, $(NH_4)_2[Mo_2O_5(cat)_2]$.[69] We have prepared several of these complexes as described in the literature and their infrared and nuclear magnetic resonance spectra were compared with those complexes which have been fully characterised by X-ray studies. We find that the complexes reported as "$K[MoO_2(OH)(cat)]$"[44] and "$(NH_4)[MoO_2(OH)(C_6H_4O_3)]$"[44] are, in fact, $K_2[Mo_2O_5(cat)_2]$ and $(NH_4)_2[Mo_2O_5(C_6H_4O_3)_2]$ respectively. Similarly, the complex reported as "$C_5H_5N.H_2[MoO_3(cat)]$"[43] may also be reformulated as $[C_5H_6N]_2\ [Mo_2O_5(cat)_2]$. Several complexes reported as having catechol molecules of crystallisation were also investigated. This formulation is possible, as evidenced by the X-ray crystallographic study of the complex $Ba[Mo_2O_5(cat)_2]5H_2O.C_6H_4(OH)_2$.[70]

Several catecholato and semiquinone complexes have been reported to form by reaction of the metal carbonyl with the appropriate o-benzoquinone ligand. Reaction of catechol with $Os_3(CO)_{12}$ resulted in the complex $[Os_3(CO)_9H_2(OC_6H_3OH)]$[79] in which the catechol ligand was coordinated to one osmium centre via a deprotonated hydroxyl oxygen, and to a second osmium centre through the carbon atom ortho to the coordinating oxygen. This carbon atom has also lost its proton. This suggested the possibility of preparing a number of interesting complexes by reaction of $Os_3(CO)_{12}$ and $Ru_3(CO)_{12}$ with o-benzoquinones. Products containing both carbonyl and quinone ligands were isolated, but could not be fully characterised. This work certainly merits further investigation.

3. INFRA-RED AND RAMAN SPECTRA OF QUINONE COMPLEXES

In this section we report studies of the infra-red spectra of quinone complexes, mainly of the form $[M(cat)_3]^{n-}$, $[MO_2(cat)_2]^{2-}$, and $[M_2O_5(cat)_2]^{2-}$. To aid with characterisation of these complexes a brief discussion is included of the metal-oxo vibrations in cis and trans-dioxo complexes, and in those containing M-O-M bridging units. A summary of the literature work reported for the infrared and Raman spectra of catechol itself is given, and the few data available on given complexes are discussed with particular reference to distinguishing between the three possible modes of coordination of the quinone ligand. We include our own infrared studies on some known quinone complexes to check the conclusions. The bands of the spectra of new complexes are assigned, and a number of molybdenum - catecholato and pyrogallolato complexes reported in the older literature are reformulated.

Due to instrumental difficulties very few Raman data were obtained for any of the areas of work covered in this thesis. However, a few spectra were recorded and they are generally used to confirm assignments of metal-oxo vibrations.

3.1 Spectra of the metal-oxo groups and of the ligands

3.1.1 Metal-oxo vibrations

Since some of the work in this and following sections deals with complexes containing cis or trans MO_2 units, and with binuclear oxo-bridged species, the main features of the infrared and Raman active vibrations of such systems are briefly summarised here.

(a) cis-dioxo groups in cis - $[MO_2X_4]^{n-}$ systems

Three vibrational modes are associated with the MO_2 group, the symmetric stretch, $\nu^s(MO_2)$, the asymmetric stretch, $\nu^{as}(MO_2)$, and the deformation vibration $\delta(MO_2)$.[80,81] The stretching vibrations are shown in fig.1.8.



Fig.1.8 stretching vibrations of the cis-dioxo group

For the C_2V symmetry of this group, all three vibrations are infrared and Raman active, the symmetric stretch being polarised in the Raman, Cis-dioxo-molybdenum (VI) and tungsten (VI) complexes typically have $\nu^s(MO_2)$ near 930 - 950cm^{-1}. $\nu^{as}(MO_2)$ between 880 and 900cm^{-1} and $\delta(MO_2)$ near 380cm^{-1}.

(b) trans-dioxo groups in trans - $[MO_2X_4]^{n-}$ systems

This group has D_{4h} symmetry[80] and the mutual exclusion rule operates, so that $\nu^s(MO_2)$ is strong and polarised in the Raman but inactive in the infrared, whilst $\nu^{as}(MO_2)$ is strong in the infrared but Raman inactive. These vibrations are shown in Fig. 1.9. The deformation mode is infrared active only.

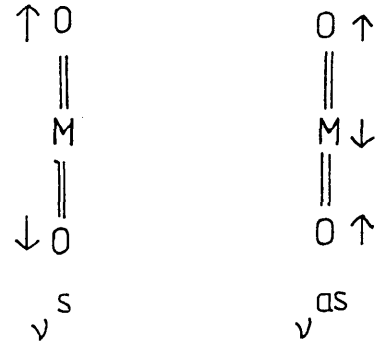


Fig.1.9 stretching vibrations of the trans-dioxo group.

A typical example is found for the osmium (VI) complexes (the so-called "osmyl" species)[82] where $\nu^{s}(MO_2)$ lies between 850 and 900cm^{-1} and $\nu^{as}(MO_2)$ between 790 and 850cm^{-1} with the deformation mode near 330cm^{-1}. The uranyl species containing the trans-UO_2^{2+} unit typically has $\nu^{s}(MO_2)$ between 900 and 800cm^{-1}, and ν^{as} (UO_2) between 960 and 850cm^{-1}.[41]

(c) Complexes containing M-O-M units

Binuclear complexes with one oxygen bridge may be considered as three-body systems, having three fundamental vibrations,[81] whether the bridge is linear or bent. They are the symmetric stretch, $\nu^{s}(M_2O)$, the asymmetric stretch, $\nu^{as}(M_2O)$, and the deformation vibration, $\delta(M_2O)$. The stretching vibrations are shown in Fig.1.10, the deformation often occurs at a frequency too low for observation.

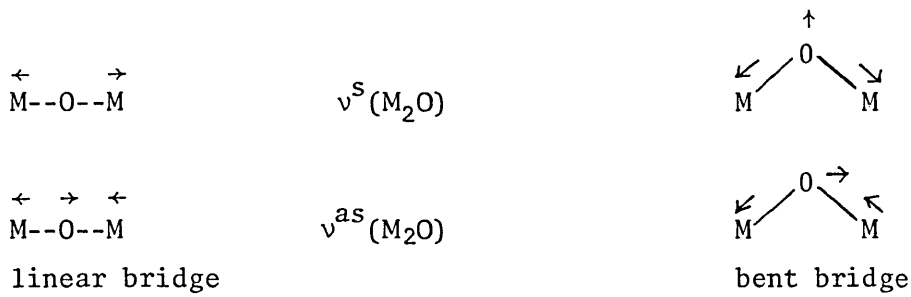


Fig.1.10 stretch vibrations of a μ-oxo bridged system.

For a linear bridge, $\nu^{s}(M_2O)$ is Raman active only, the other two vibrations are only active in the infrared. Bent bridges have all three vibrations active in both the infrared and the Raman. The vibrational frequencies are strongly sensitive to the M-O-M bond angle.[83] Linear systems typically have $\nu^{as}(M_2O)$ between 800 and 850cm^{-1},[87] $\nu^{s}(M_2O)$ near 200 - 300cm^{-1}. The rarer, bent μ-oxo species show $\nu^{as}(M_2O)$ near 750cm^{-1}, and $\nu^{s}(M_2O)$ near 550cm^{-1}.[84]

(d) Structure and bonding in these complexes

Consideration of metal-oxygen π interactions in dioxo complexes (involving overlap of oxygen 2p orbitals with suitably placed metal d orbitals) shows that when the metal has a d^o electronic configuration, the cis configuration is clearly preferable to the trans,[80] the strongly π donating oxo ligands having exclusive use of one t_{2g} orbital each, and share a third. For a trans - configuration, the oxo ligands share two t_{2g} orbitals, and leave one non-bonding. In complexes with d^2 configuration, the non-bonding orbital accommodates the electron pair. For d^o complexes, where three t_{2g} orbitals are involved in bonding with the oxygen, the metal-ligand bond has greater multiple bond character than is the case for trans complexes, and, therefore, higher frequencies are observed for $\nu^{as}(M_2O)$, $\nu^{s}(M_2O)$ and $\delta(M_2O)$.

The force constants for stretching vibrations of the M_2O bridge are approximately half that found for vibrations of the M = O group.[81] This is as expected since 2pπ electron density of the oxo bridge is distributed between two metal atoms rather than one. The degree of M-O π bonding is less in bent systems than for linear complexes,[85] and this leads to the observed lower asymmetric stretch and higher symmetric stretch for bent complexes compared to linear complexes.[84]

(e) Ligand bridges

Complexes in which two cis-dioxo-molybdenum (VI) groups are bridged by a ligand have been reported, e.g. $[MoO_2(npg)(OH_2)]_2$ where npg = neopentyl glycol dianion.[86] The metal to bridging ligand oxygen, M - Olb, bond lengths are longer than those found for μ-oxo bridged complexes, and consequently the infra-red bands lie at lower wavenumbers. The observed range is 620 - 650cm^{-1}. Several quinone complexes have been reported in which ligand bridging occurs to make up six coordination around the molybdenum (VI) centres of the $[Mo_2O_5]^{2+}$ core e.g. $Mo_2O_5(PSQ)_2$.[61]

3.1.2 Catechol and o-benzoquinone

The infrared and Raman spectra of catechol have been reported and the peaks assigned as listed in Table 1.7.[87,88] The catechol infrared spectrum is shown in Figure 1.11.

The absorptions arising from the hydroxyl group stretching vibrations, ν(OH), recorded for the solution spectrum of catechol were reported to give two strong, sharp peaks of approximately equal intensity.[89] These two peaks were assigned to the vibrations of each of the hydroxyl groups of the isomer shown in Figure 1.12.

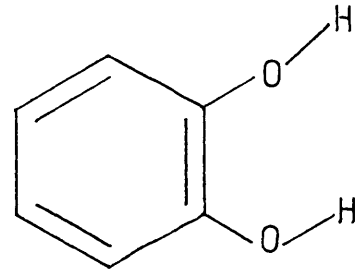


Figure 1.12

This structure, with an intramolecular hydrogen-bond was said to predominate in solution. The spectrum of solid catechol gave rise to broader peaks above 2,500cm^{-1}, but we find that two peaks may still be distinguished. This behaviour was ascribed to the persistence in the solid state of an amount of the intramolecular hydrogen-bonding found in solution. The broadness was caused by considerable associative interaction between different catechol molecules.[90]

Benzoquinones have a characteristically strong peak between 1660 and 1700cm^{-1},[6,91] arising from the carbonyl group stretching frequency.

3.2 Spectra of catecholato and quinone complexes

3.2.1 Literature work and spectra of known complexes

(a) The coordinated catecholato dianion

Infrared studies of $K_3[Cr(cat)_3]$ and $K_3[Fe(cat)_3]$ showed the disappearance of the strong ν(OH) absorptions of free catechol, as expected.[92] The deformation, δ(OH), at 1367cm^{-1} also disappeared.[19,27,84,93] We find that the aromatic peak at 1619cm^{-1} is still observed, but that at 1607cm^{-1} is no longer seen. A new peak is found at 1565cm^{-1} assigned to vibrations of the aromatic ring. The free ligand spectrum exhibits two peaks at 1514 and 1470cm^{-1} of approximately equal intensity. On coordination, these aromatic absorptions show a significant change, resulting in a very strong peak at 1480cm^{-1}, and a peak of moderate intensity at 1440cm^{-1}.

It seems likely that the strong 1480cm^{-1} peak involves some contribution from vibrations of the carbon atoms attached to the oxygen donor atoms. The other major peak of the spectrum occurs at 1250cm^{-1}. Its intensity increased significantly relative to that found for the same peak in the free ligand spectrum, and it is assigned to the stretching vibration of the C-O bond with some contribution from the aromatic ring stretching vibrations, i.e. ν(C - O + C = C).[91] The strong peaks at 1480 and 1250cm^{-1} occur regardless of the catechol derivative used and they are regarded as good qualitative evidence for the presence of a coordinated, fully reduced quinone ligand.[95]

Few Raman data have been reported for catecholato complexes, the work that has been published being mainly concerned with iron complexes as models for biological systems. The strongest absorptions were reported to occur between 1200 and 1600cm^{-1}. Peaks near 1260 or 1280cm^{-1}, 1320, and 1480cm^{-1} appear to be typical of the presence of a catechol ligand.[96,97] The peak near 1260 or 1280cm^{-1} is expected to have a major contribution from the C - O stretching vibration.[98] The peak at 1480cm^{-1} was suggested to be typical of catecholato coordination[96] to the metal, and this absorption was attributed mainly to vibration of the carbon atoms to which the oxygen atoms are attached.[98] Bands at 1572, 1448, 1359, 1322 and 1154cm^{-1} were all assigned[98] to skeletal vibrational modes of the benzene ring.

Although the low frequency region was reported to give only weak peaks, an absorption at 621cm^{-1} may arise from an in-plane deformation mode[98] of the aromatic ring. A peak at 533cm^{-1} may arise from a vibration of the chelate ring.

(b) The coordinated catecholato mono-anion

Several iron complexes have been reported of the type Fe(salen)(catH)[76] and Fe(saloph)(CatH)[72] in which the catechol ligand is monodeprotonated and was found to coordinate to the metal through one oxygen atom only. The infrared spectra of the complexes Fe(salen)(catH),[99], Fe(5-Cl-salen)(catH) and Fe(salen)(DBcatH) were reported to each show a sharp peak near 3,380cm^{-1} due to ν(OH). The complex Fe(salen)(catD), prepared from deuterated catechol, showed a peak at 2520cm^{-1}, arising from ν(OD) (calculated peak at 2460cm^{-1}). The saloph complex, Fe(saloph)(catH), gave rise to a broad band centred at 3200cm^{-1} due to ν(OH), indicating the presence of hydrogen-bonding.

Investigation of the region 1200 - 1600cm^{-1} [96] in the Raman showed that the absorptions near 1300cm^{-1} could be indicative of the ionisation state of the catechol ligand. The catecholato dianion as in $[Fe(cat)_3]^{3-}$, gave peaks near 1260 and 1320cm^{-1}, as described above; monodeprotonated catechol, in Fe(salen)(catH) showed absorptions at 1287 and 1375cm^{-1}.

(c) Benzoquinone complexes

On coordination of a benzoquinone ligand to a metal centre, if the ligand remains in its fully oxidised form, a small shift of the ν(C=O) band would be expected.[91] This was indeed observed for complexes of the type $ZnBr_2(PQ)$, where ν(C=O) shifted by between 9 and 114cm^{-1} to lower frequencies. Concomitant with this decrease in frequency of the carbonyl band, is an increase in intensity of the band at 1595cm^{-1}, arising from vibrations of the aromatic ring.[91,100]

(d) Semiquinone Complexes

The infrared spectra of an o-semiquinonato complex would be expected to exhibit peaks at positions intermediate between those found for the o-benzoquinone and catecholato ligands. An investigation of the spectra of $Fe(DTBSQ)_3$ and $Cr(DTBSQ)_3$ found very strong peaks at 1455 and 1430cm^{-1} respectively, which were assigned to a ν(C-O) stretch, together with a ring vibration mode.[91] It would appear that this strong band together with the absence of any strong band near 1250cm^{-1}, or above 1600cm^{-1}, may be taken as characteristic of a coordinated o-semiquinone ligand.

We observe this behaviour for the complex $Cr(PSQ)_3$. The strong peak at 1675cm^{-1} due to ν(C=O) of the free ligand disappears and no peak is observed near 1250cm^{-1}, although slight changes are observed in this area compared to the free ligand. Two major peaks are seen at 1460 and 1390cm^{-1}.

We find that the semiquinone complex, $Mo_2O_5(PSQ)_2$, has a more complex spectrum. A peak is still observed at 1675cm^{-1}, where ν(C=O) occurs for the starting material for 9,10-phenanthrenequinone, but with diminished intensity. The aromatic peak at 1595cm^{-1} shows enhanced intensity. The two strongest peaks of the spectrum are found at 1460 and 1452cm^{-1}, characteristic of semiquinone coordination. However, a further new peak is found at 1260cm^{-1}. This illustrates that the presence of a strong peak near 1250cm^{-1} is not conclusive evidence of the catecholato mode of coordination, but it must be considered in concert with the pattern of peaks between 1700 and 1600cm^{-1} , and between 1400 and 1500cm^{-1}. In this case, the strong peak at 1260cm^{-1} may be due to overlap of the two peaks observed in the $Cr(PSQ)_3$ spectrum at 1262 and 1245cm^{-1}.

Three strong peaks are observed for $Mo_2O_5(PSQ)_2$, not found for 9,10-phenanthrenequinone or for $Cr(PSQ)_3$, at 957, 950 and 924cm^{-1}. Two of these three peaks are presumably due to $\nu^s(MO_2)$ and $\nu^{as}(MO_2)$. 9,10-phenanthrenequinone shows a peak at 924cm^{-1}, but $Cr(PSQ)_3$ has a peak at 943cm^{-1}. This leads us to tentatively assign the peak at 950cm^{-1} to a ligand vibration, leaving 957cm^{-1} as arising from $\nu^s(MO_2)$ and 924cm^{-1} for $\nu^{as}(MO_2)$. This appears more feasible than assigning the peaks at 957 and 950cm^{-1} to the ν(Mo=O) vibrations, since these would be unusually close together. This assignment, however, is not definite. A peak found at 735cm^{-1} may be tentatively ascribed to the asymmetric stretching vibration of the M-O-M bridge, as described earlier.

The symmetric stretch (expected at lower frequency) could not be identified. Near 750cm^{-1} is the region expected for asymmetric stretching of a bent bridge. In this complex, however, the vibration must be constrained by the bridging bonds formed by the oxygen donor atoms of the semiquinone ligands between the two molybdenum atoms (as described earlier). The number of peaks occurring below 700cm^{-1} precludes any definite identification, but it is likely that some of these arise from the symmetric stretch of the M-O-M bridge, the bridging of the metal atoms by the semiquinone ligands, ν(Mo-Olb)(possibly 643cm^{-1}) and molybdenum-ligand oxygen vibrations.

3.2.2 Experimental Results

(a) Tris-catecholato complexes

As far as possible the peaks of these spectra were assigned by comparison with $K_3[Cr(cat)_3]$ and $K_3[Fe(cat)_3]$,[92] although the spectra were complicated by the presence of absorptions due to the tetraphenylphosphonium cation. The reference reporting peaks due to $K_3[Cr(cat)_3]$ and $K_3[Fe(cat)_3]$[92] assigned the strong peak near 1250cm^{-1} to C-H deformations. If this were the case the great enhancement of intensity observed on coordination would be unlikely to occur. Most other reports in the literature assign these peaks to stretching vibrations of the C-O group, coupled with aromatic stretching vibrations.

The complex $(Ph_4P)_2[Ir(cat)_3]$ gives a complicated spectrum (as listed in Table 1.8, and shown in Figure 1.13). The strong sharp peaks typical of the tetraphenylphosphonium cation often occur with shoulders and sometimes show broadening.

No peaks typical of the ν(OH) vibrations are observed. The region 1770 - 1650cm^{-1} shows no peak that could be assigned to the ν(C=O) of an o-benzoquinone ligand. Between 1500 and 1300cm^{-1} a strong aromatic absorption is found at 1477cm^{-1}. A strong broad absorbance is observed at 1250cm^{-1}, where no such peak is found in the $(Ph_4P)^+$ spectrum. This very large absorbance is typical of catecholato coordination, and, together with the aromatic peak at 1477cm^{-1} is taken as conclusive evidence for the catecholato mode of coordination. The lack of any ν(OH) peaks shows the ligand has coordinated as the dianion, although any weak ν(OH) peaks could be masked by the presence of water of crystallisation absorptions in this region. The broadening of the usually sharp $(Ph_4P)^+$ peaks is due to the very close coincidence of the vibrations of the phenyl rings of the cation, and of the aromatic catechol ring.

This evidence, together with analysis, leads to the formulation $(Ph_4P)_2[Ir(cat)_3]$ for this complex.

A similar interpretation applies to the spectra of the rhenium complex, $(Ph_4P)_2[Re(cat)_3]$ and of the ruthenium complex, $(Ph_4P)_3[Ru(cat)_3]$, as listed in Table 1.8.

Assignment of any metal-oxygen stretching frequencies is very difficult due to the dominance of the very strong $(Ph_4P)^+$ vibrations in the region between 600 and 400cm^{-1}.

Table 1.7:- Major peaks of the infra-red and Raman[87] spectra of catechol(cm^{-1})

Infra-red	Raman	Assignment.
3450 br		
3330 br		ν(OH)
3050 w		ν(CH)
1619 s		
1607	1594	ν(C-C)
1514 vs		
1470 vs		
1367 vs	1329	δ(OH)
1280 s		
1255 s	1263	ν(C-C+C-0)
1242 s		
1185 s		δ(OH) + δ(CH)
1163 m	1144	
1095 s	1099	δ(CH)in plane
1040 s	1036	
957 m		
916 m		
848 m	852	
770 s	774	
754 s		δ(CH)out of plane
740 vs		
630 br	578	
500 br	558	

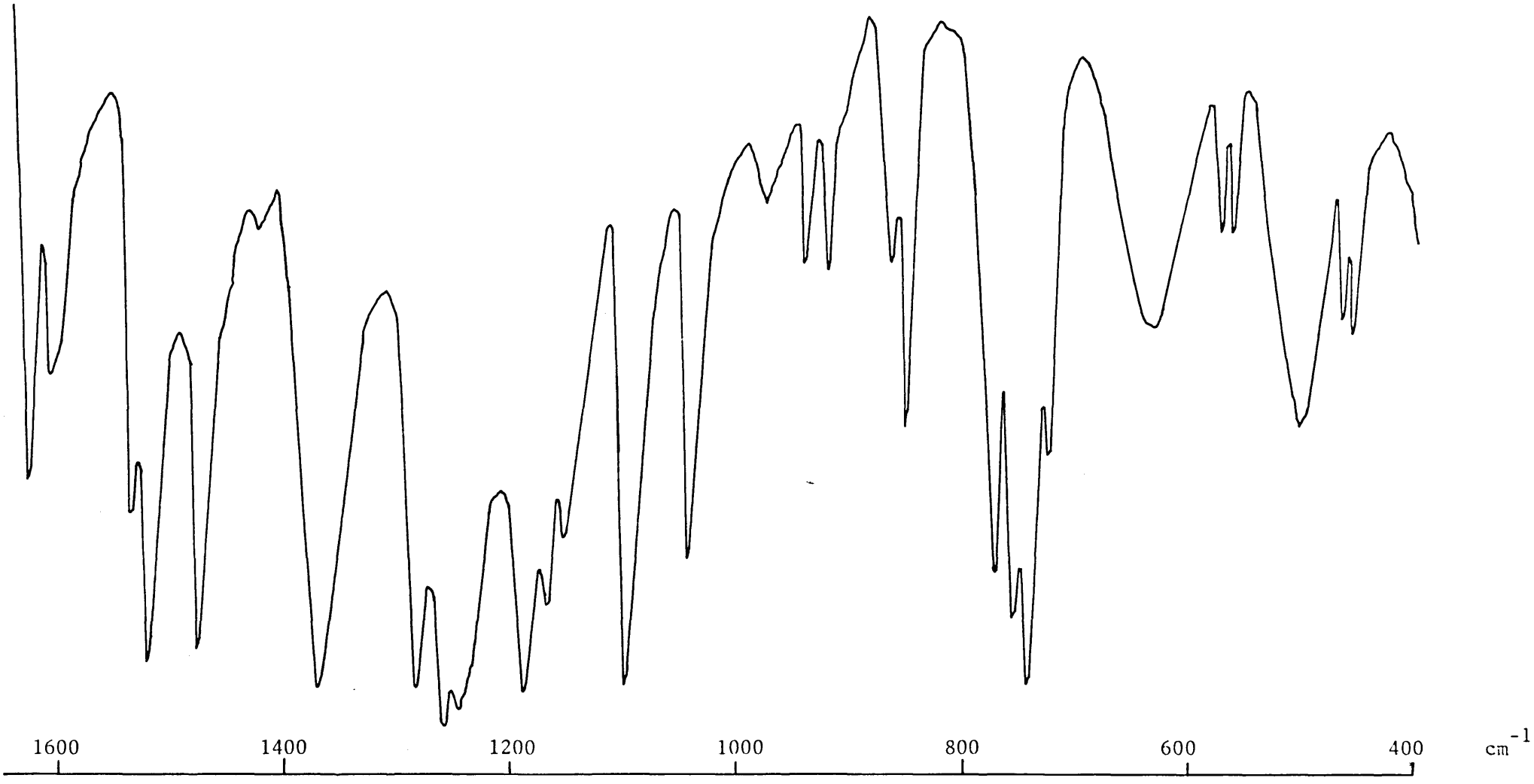


Figure 1.11 - Infra-red spectrum of catechol.

Table 1.8:- Major peaks of the infra-red spectra of new tris(catecholato) complexes (cm^{-1})

$(Ph_4P)_2[Ir(cat)_3]$	$(Ph_4P)_2[Re(cat)_3]$	$(Ph_4P)_3[Ru(cat)_3]$	Assignment
1580 s	1580 s	1583 s	
1477 s	1487 s	1485 vs	ν(C-C)
1437 s	1433 m	1440 s	
1280 m	1276 m	1270 m	
1250 sbr	1253 sbr	1252 sbr	ν(C-O+C-C)
1101 s	1107 s	1110 s	δ(CH)-
1025 m	1028 w	1026 w	in plane
993 m	995 m	995 m	
910 w	908 m		
855 m	855 w	860 w	
758 s	750 s	754 s	δ(CH)out
720 vs	721 vs	720 vs	of plane
685 s	688 s	696 s	$\delta(CH)Ph_4P^+$
526 vs	528 vs	535 vs	

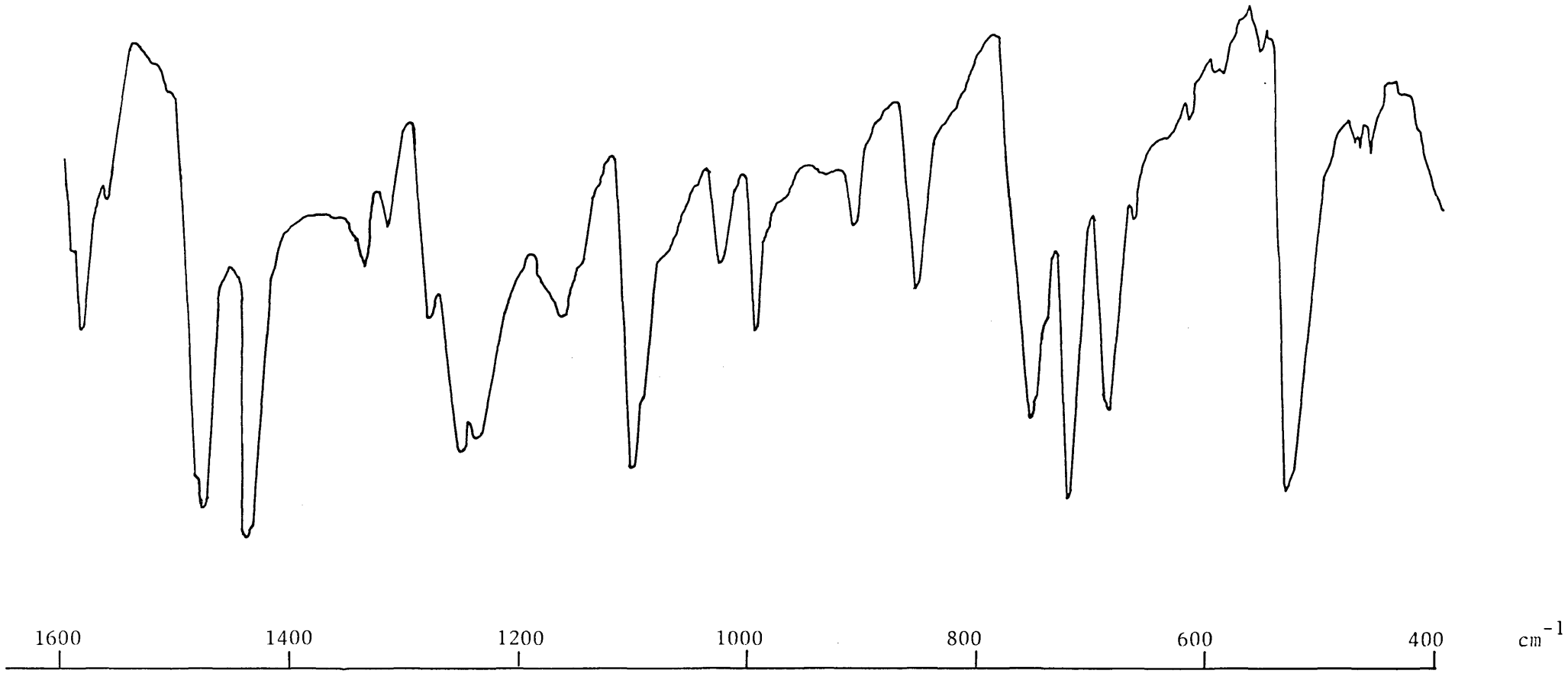


Figure 1.13 - Infra-red spectrum of $(Ph_4P)_2[Ir(cat)_3]$

(b) Reformulation of molybdenum (VI) - catecholato complexes

We have investigated a number of molybdenum (VI)-catecholato complexes which were reported in the early literature and characterised solely by elemental analyses. X-ray crystallographic studies have subsequently confirmed the formulation of $K_2[MoO_2(cat)_2]$[68] but found the complex reported as "$NH_4H[MoO_3(cat)]$"[43] to be $(NH_4)_2[Mo_2O_5(cat)_2]$.[69] These and other molybdenum (VI)-catecholato complexes were prepared as described in the literature, and their infrared spectra studied. On the basis of their analyses and by comparison of their IR spectra with those recorded for species of known structure, we reformulate some of these complexes.

(i) Spectra of $K_2[MoO_2(cat)_2]$ and $(NH_4)_2[Mo_2O_5(cat)_2]$

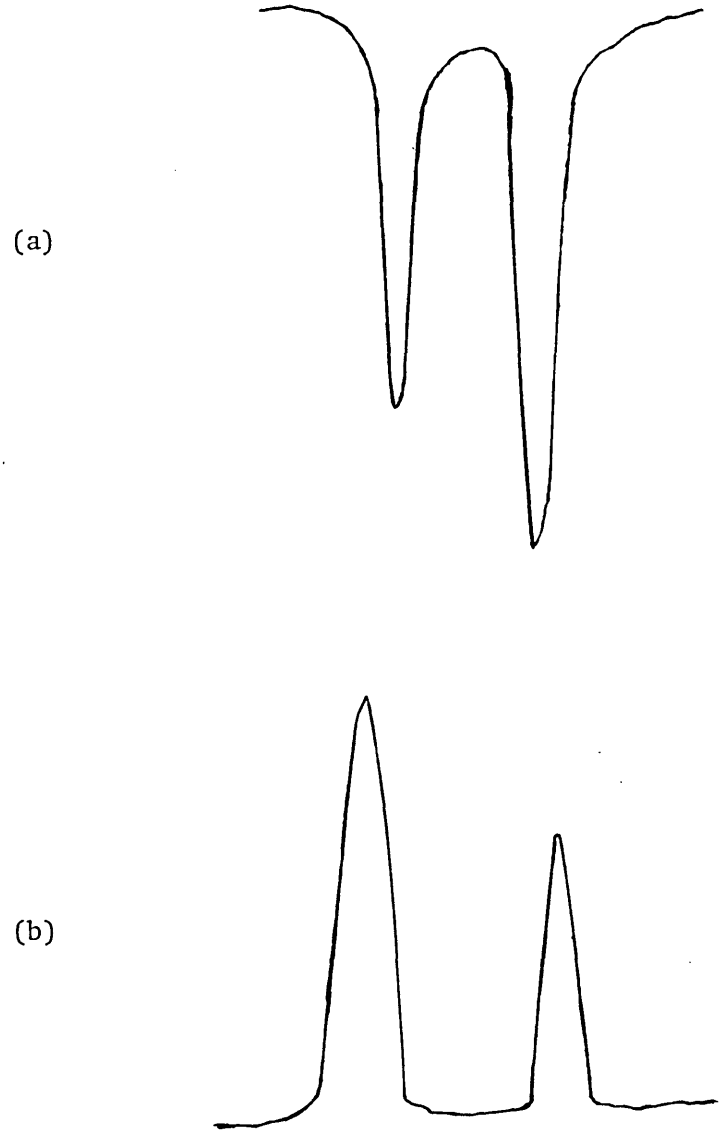
The infrared spectrum of $K_2[MoO_2cat_2]$ shows the ligand vibrations described above typical of catecholato coordination and are listed in Table 1.9. In addition, very strong peaks were observed in the region 920 to 800cm^{-1}, typical of $\nu(MoO_2)$ vibrations, as described earlier. Exact assignment is hampered by the presence of ligand bonds in the same region, but it seems likely that the peak near 890cm^{-1} arises from the symmetric stretch $\nu^s(MO_2)$ and that at 875cm^{-1} from $\nu^{as}(MO_2)$. Peaks found near 640cm^{-1} may be tentatively assigned to molybdenum to ligand-oxygen vibrations, ν(Mo-01).[86]

The complicated Raman spectrum of $K_2[MoO_2(cat)_2]$ shows a doublet 892/900cm^{-1} and a weaker peak at 871cm^{-1}, in a region where no catechol absorptions were observed for the free ligand. These peaks are assigned to $\nu^s(MO_2)$ and $\nu^{as}(MO_2)$ respectively, confirming the assignment of the peaks in the infrared spectrum.

The vibration $\nu^s(MO_2)$ is known to be strong and polarised in the Raman,[80] with $\nu^{as}(MO_2)$ showing a weaker peak. This is the reverse of the situation found in the infrared spectrum as shown in Figure 1.14. This pattern of behaviour is indeed observed in the infrared and Raman spectra of $K_2[MoO_2(cat)_2]$ adding further evidence that these peaks have been correctly assigned.

The observed values of $\nu(MO_2)$ are of quite low frequencies, compared to those found for other cis-dioxo-molybdenum (VI) complexes, indicating a slightly weaker molybdenum to terminal oxygen bond. This is attributed to the weakening effect the catecholato ligand has on the oxo ligands, as shown by the slightly long Mo = O bonds, found in $K_2[MoO_2(cat)_2]$[68] by X-ray crystallography. Catechol is known to be a strong σ donor, but it has also been shown to be a strong π donor. This was particularly well illustrated in the X-ray crystallography study of $Ir(NO)(PPh_3)(C_6Br_4O_2)$[22] described earlier. This means any consideration of the π bonding between molybdenum and the oxo ligands, must also take the catecholato ligand into account.

Figure 1.14 - Infra-red (a) and Raman (b) absorptions of $\nu(\underline{cis}\text{-}MO_2)$.



The d orbitals of the metal centre, which accept the π electron density of the oxo ligands must also accommodate the π electron density donated from the catecholato ligand. This would necessarily weaken the molybdenum to oxo ligand interaction, leading to the lower frequencies observed in the vibrational spectra of this complex.

The remainder of the spectrum shows a large number of peaks arising from the ligand vibrations. Strong peaks at 1264, 1329 and 1482cm^{-1} [96,97] correspond to these reported as typical of the coordinated catecholato dianion, as described above.

The spectrum of $(NH_4)_2[Mo_2O_5(cat)_2]$ shows a different pattern, as listed in Table 1.9. Peaks due to $\nu(MoO_2)$ are found at 920 (symmetric) and 872cm^{-1} (asymmetric). A slight difference is observed in the region 800 - 700cm^{-1}. The three peaks occurring very closely together for $K_2[MoO_2(cat)_2]$, now show a difference in the pattern of their intensities, the peak at 733cm^{-1} showing greatly enhanced intensity. This is tentatively assigned to the $\nu^{as}(M_2O)$ of the bridging bond. The frequency of this vibration is very sensitive to the angle of the bond.[83] For $Mo_2O_5(PSQ)_2$, which has an M-O-M angle of 112.79°,[61] this vibration was found at 735cm^{-1}. No value is available for $(NH_4)_2[Mo_2O_5(cat)_2]$, but the analogous complex $[(n\text{-}Bu)_4N]_2[Mo_2O_5(3,5\text{-}DTBcat)_2]$ has an angle of $\pm$109.4°.[18] Assuming a similar angle for $(NH_4)_2[Mo_2O_5(cat)_2]$, the frequency of $\nu^{as}(M_2O)$ would be expected to be very similar to that for $Mo_2O_5(PSQ)_2$, since the M-O-M angles have similar values. This is further evidence for assigning the peak at 733cm^{-1} to $\nu^{as}(M_2O)$.

Between 600 and 700cm^{-1} instead of the very strong peak at 640cm^{-1} found for $K_2[MoO_2(cat)_2]$ several peaks are observed, sometimes seen as one broad peak in less well-resolved spectra. One of these is due to the stretching vibration of the molybdenum to ligand oxygen bond bridging the two metal centres, ν(Mo-Olb).[86] Although no definitive assignments can be made due to the complexity of peaks found in this region, (both catecholato and metal-oxygen vibrations), the pattern of vibrations is distinctive for each of these two complexes as shown in Figure 1.15, and may be described as follows:-

(1) the region 950 - 800cm^{-1}, including the $\nu(MoO_2)$ vibrations, shows a different pattern for each of these two complexes-

(2) a slightly different pattern of intensities is observed between 800 and 700cm^{-1} (but not always enough to be diagnostic);

(3) between 700 and 600cm^{-1} $K_2[MoO_2(cat)_2]$ shows only one strong peak at 640cm^{-1}, $(NH_4)_2[Mo_2O_5(cat)_2]$ has several peaks in this region due to ν(Mo-Olb).

The complex $(pyH)_2[MoO_2(cat)_2]$ where pyH^+ is the pyridinium cation shows the same pattern as $K_2[MoO_2(cat)_2]$ as expected, but with many extra peaks due to the pyridinium cation.

With these data it was now possible to make tentative assignments of the spectra of some of the earlier reported complexes which have unusual formulae, and on the basis of spectra and analyses, to reformulate them.

Table 1.9:- Major peaks of the infra-red spectra of $K_2[MoO_2(cat)_2]$ and $(NH_4)_2[Mo_2O_5(cat)_2]$ (cm^{-1})

$K_2[MoO_2(cat)_2]$	$(NH_4)_2[Mo_2O_5(cat)_2]$	Assignment
1595 s	1580 m	
1514 s		
1482 s	1485 s	ν(C-C)
1456 s	1445 s	
1329 m	1323 w	
1264 s	1260 s	ν(C-O+C-C)
	1252 s	
1102 s	1100 s	δ(CH) in plane
1038 m		
1020 m	1021 m	
928 s	936 s	
917 w		
890 vs	920 vs	$\nu^{s}(MoO_2)$
	900 vs	
872 vs	872 vs	$\nu^{as}(MoO_2)$
850 s	864 s	
810 s	815 s	δ(CH) out of plane
755 s	755 m	
743 s	745 m	
	733 s	$\nu^{as}(Mo_2O)$
730 w		
635 vs	663 m	
600 m	645 m	
518 m	620 vs	
503 m	514 m	

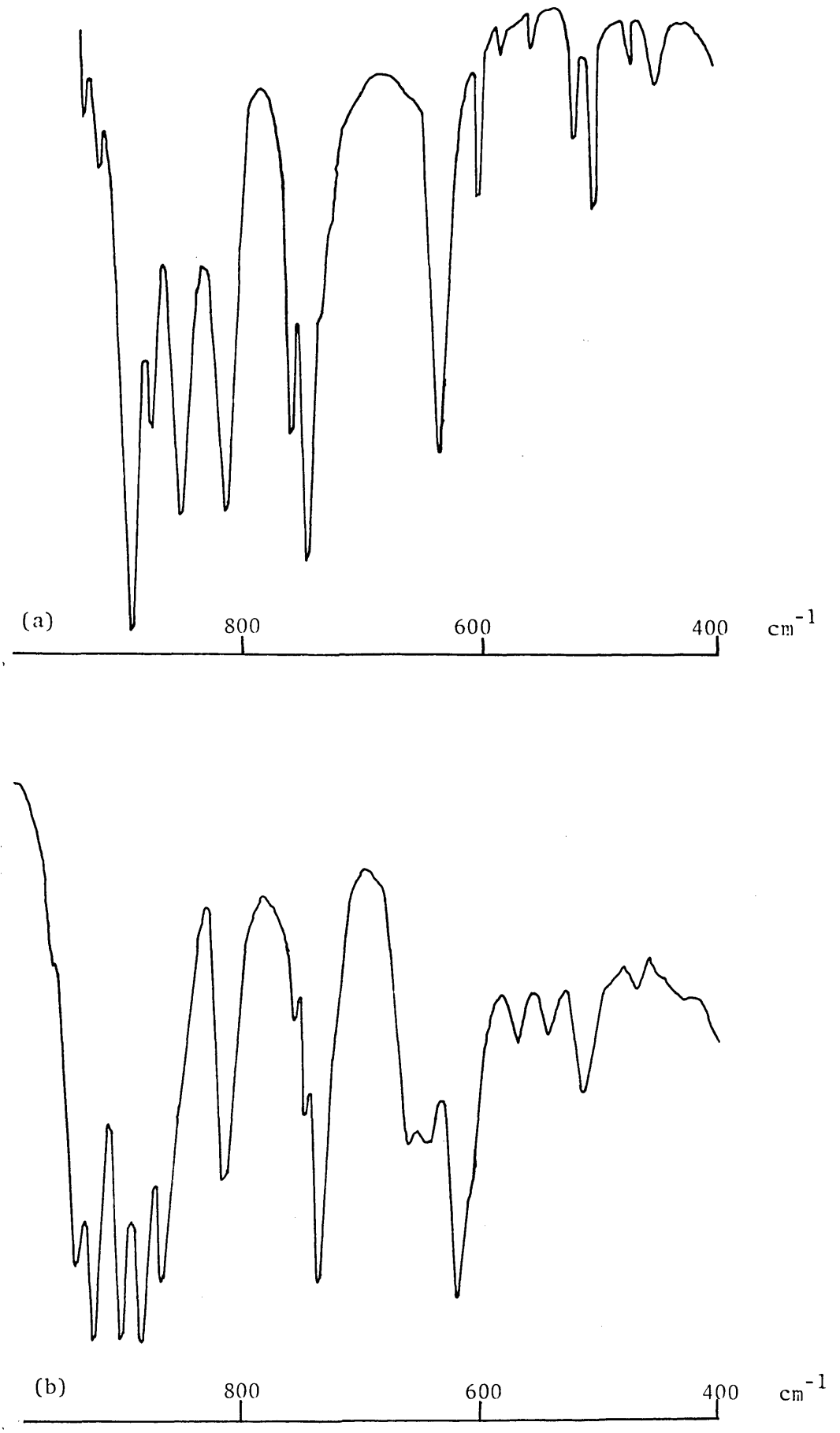


Figure 1.15 - Infra-red spectrum of $K_2[MoO_2(cat)_2]$ (a) versus $(NH_4)_2[Mo_2O_5(cat)_2]$ (b)

(ii) "(pyH)H$[MoO_3(cat)]$"[43]

The complex first reported as "$NH_4H[MoO_3(cat)]$"[43] was later found to be $(NH_4)_2[Mo_2O_5(cat)_2]$.[69] Several other complexes were reported to have this formulation but with different cations. This pyridinium complex was investigated to establish whether the same reformulation would hold for more than one such compound. The absorptions are listed in Table 1.10.

The spectrum of this complex is compared with that of $(pyH)_2[MoO_2(cat)_2]$, both of which will show similar pyridinium cation peaks. A different pattern of peaks is found between 950 and 800cm^{-1}. The peaks at 920,875, and 868cm^{-1} occur in the same pattern as is found for $(NH_4)_2[Mo_2O_5(cat)_2]$(920, 872, 864cm^{-1}). The peaks between 800 and 700cm^{-1} are not particularly useful for identification in this case. Between 600 and 700cm^{-1} a different pattern is observed from that found for $(pyH)_2[MoO_2(cat)_2]$. A strong peak occurs at 682cm^{-1} due to the cation, the other absorptions in this region occur at 669, 646, and 625cm^{-1}, a similar pattern to that found for $(NH_4)_2[Mo_2O_5(cat)_2]$. In the areas considered diagnostic for these complexes, it is apparent that the complex "(pyH)H $[MoO_3(cat)]$" shows a pattern of peaks almost identical to that found for $(NH_4)_2[Mo_2O_5(cat)_2]$, and is therefore reformulated as $(pyH)_2[Mo_2O_5(cat)_2]$.

(iii) "$K[MoO_2(OH)(cat)]$" and "$(NH_4)[MoO_2(OH)(C_6H_4O_3)]$"

The formulation of these two complexes[44] (where $(C_6H_4O_3)^{2-}$ is the dianion of pyrogallol or 1,2,3-trihydroxybenzene), is thought to be highly unlikely as they would be five coordinate complexes of molybdenum (VI), which is very unusual. A study of their infrared spectra, as listed in Table 1.11, shows no evidence of a coordinated hydroxyl group, whose ν(OH) would be expected to be seen. The ligand vibrations are typical of catecholato-type coordination. The region 950 - 800cm^{-1}, has strong peaks at 933, 920, 895 and 870cm^{-1}, in the same pattern as that found for $(NH_4)_2[Mo_2O_5(cat)_2]$. This is also the case for "$(NH_4)[MoO_2(OH)(C_6H_4O_3)]$". Peaks between 800 - 700cm^{-1} are not sufficiently well resolved for any meaningful comparison to be made. Between 700 and 600cm^{-1} three peaks are observed for "$K[MoO_2(OH)(cat)]$". This precludes its reformulation as $K_2[MoO_2(cat)_2]$. The peaks in this region coincide with those found for $(NH_4)_2[Mo_2O_5(cat)_2]$. Similarly "$(NH_4)[MoO_2(OH)(C_6H_4O_2O)]$" in comparison with the spectrum of $(NH_4)_2[MoO_2(C_6H_4O_3)_2]$, precludes its reformulation as this complex. The 600 - 700cm^{-1} region of this spectrum for this pyrogallol complex again shows a pattern identical to that observed for $(NH_4)_2[Mo_2O_5(cat)_2]$.

The infrared data therefore lead to the tentative conclusion that "$K[MoO_2(OH)(cat)]$" and "$(NH_4)[MoO_2(OH)(C_6H_4O_3)]$" may be reformulated as $K_2[Mo_2O_5(cat)_2]$ and $(NH_4)_2[Mo_2O_5(C_6H_4O_3)_2]$ respectively. A calculation of elemental percentages shows that the values found for the originally postulated formulae and those calculated for the formulations here postulated, are very similar, some of them being within experimental error.

(iv) Complexes reported as having a catechol molecule of crystallisation, although elemental analyses suggested the same formulation, show no distinct evidence for this formulation in the infrared, partly because of the presence of water absorptions in the same region as the ν(OH) vibrations of catechol. Such a formulation is indeed possible, as was found in the X-ray crystallographic study of $Ba[Mo_2O_5(cat)_2]C_6H_4(OH)_2$.[70]

(c) $Na_2[W_2O_5(cat)_2]$

Reaction of sodium tungstate and catechol produced a complex analysed to be $Na_2[W_2O_5(cat)_2]$. To confirm this the infrared spectrum (listed in Table 1.10) was compared with those of $K_2[MoO_2(cat)_2]$, and $(NH_4)_2[Mo_2O_5(cat)_2]$. Between 950 and 800cm^{-1} a similar pattern is observed to that found for $(NH_4)_2[Mo_2O_5(cat)_2]$. The region 800 - 700cm^{-1}, however, shows a pattern which matches that of $K_2[MoO_2(cat)_2]$ near 745cm^{-1}. But another peak is found at 770cm^{-1}, a typical value for the asymmetric stretching vibration of the bridge W-O-W. Again between 700 and 600cm^{-1} the pattern is more complicated than that found for $K_2[MoO_2(cat)_2]$. A broad peak is found centred at 647cm^{-1}, and is assigned to the stretching vibration of the tungsten to ligand oxygen bridging bond, ν(W-Olb).[86] The infrared evidence, therefore, supports the formulation $Na_2[W_2O_5(cat)_2]$, in which the catechol ligands both bridge the two metal centres, as well as the bent μ-oxo bond.

Table 1.10:- Major peaks of the infra-red spectra of "(pyH)H[MoO_3(cat)]" and $Na_2[W_2O_5(cat)_2]$ (cm^{-1})

"(pyH)H[MoO_3(cat)]"	$Na_2[W_2O_5(cat)_2]$	Assignment
1572 m	1580 m	
1482 s	1490 s	ν(C-C)
1450 s	1455 s	
1340 m	1338 m	
1276 sh	1277 s	
1255 vs	1264 vs	ν(C-O+C-C)
1224 m	1221 m	
1100 s	1100 m	δ(CH) in plane
1020 m	1017 m	
	955 w	
920 vs	915 sh	$\nu^{s}(MO_2)$
	902 s	
875 vs	864 vs	$\nu^{as}(MO_2)$
868 vs	855 vs	
810 s	814 s	
740 sbr	770 s	$\nu^{as}(M_2O)$
	742 s	
669 sbr	680 m	
646 sh		
625 s	647 s	
605 m	610 s	

Table 1.11:- Major peaks of the infra-red spectra of "$K[MoO_2(OH)(cat)]$" and "$(NH_4)[MoO_2(OH)(C_6H_4O_3)]$ (cm^{-1})

"$K[MoO_2(OH)(cat)]$"	"$(NH_4)[MoO_2(OH)(C_6H_4O_3)]$	Assignment
	1600 s	
1575 m	1583 s	
1515 w		ν(C-C)
1485 s	1496 s	
1445 s	1445 s	
1321 w	1307 m	
1260 s	1247 s	ν(C-O+C-C)
1250 s		
1099 s	1059 m	δ(CH)in plane
1020 m	1031 vs	
933 s	935 s	
920 s	928 s	$\nu^s(MoO_2)$
895 vs	914 s	
870 vs	882 vs	$\nu^{as}(MoO_2)$
815 s	816 s	
743 sh	753 sbr	δ(CH)out of plane
730 sbr	720 s	$\nu^{as}(Mo_2O)$
676 sbr		
650 m	645 sbr	
628 vs	630 s	
510 m	526 m	

(d) $MoO_2(PSQ)_2$

The infrared spectrum of the new complex of molybdenum with 9,10-phenanthrenequinone was compared with that of $Mo_2O_5(PSQ)_2$ and with that of the free ligand (see Table 1.12). The changes observed in the absorptions due to the ligand on complexation were identical to those found on formation of $Mo_2O_5(PSQ)_2$ i.e. the peak at 1674cm^{-1} in the free ligand is still observed, but with diminished intensity; the aromatic peak at 1595cm^{-1} shows enhanced intensity and the peak at 1450cm^{-1} becomes the strongest of the spectrum. Again a large peak was found at 1260cm^{-1}, but not in conjunction with the other characteristic catecholato ligand absorptions near 1490cm^{-1}. Strong absorptions at 958 and 922cm^{-1} may be assigned to the symmetric and asymmetric stretches, respectively of the Mo=O groups. These values are very similar to those found for $Mo_2O_5(PSQ)_2$, as would be expected. The only significant differences between $Mo_2O_5(PSQ)_2$ and $MoO_2(PSQ)_2$ appear around 700cm^{-1}, and between 500 and 600cm^{-1}. This is where vibrations due to the bridging of the molybdenum atoms of $Mo_2O_5(PSQ)_2$ would be expected to occur.

From the identical appearance of ligand absorptions for this complex and for $Mo_2O_5(PSQ)_2$, it is concluded that the ligand again coordinates in o-semiquinone mode. Typical vibrations of the cis-dioxo-molybdenum (VI) core are also observed, but the difference in the spectra in the region typical of Mo-O-Mo bridges (including the bridging ligand-oxygen atoms) suggest this structure is not found in this case. The complex is therefore formulated as $MoO_2(PSQ)_2$.

Table 1.12:- Major peaks of the infra-red spectra of 9,10-phenanthrenequinone, $MoO_2(PSQ)_2$ and $Mo_2O_5(PSQ)_2$. (cm^{-1})

9,10-PQ	$MoO_2(PSQ)_2$	$Mo_2O_5(PSQ)_2$	Assignment
1675 s	1674 s	1675 m	
1595 s	1590 s	1595 s	
	1493 m	1494 m	
		1460 sh	
1452 s	1453 vs	1452 vs	
1385 m	1385 s	1390 s	
1335 w	1340 m	1348 s	
1295 s	1294 s	1297 s	
1284 s	1280 s	1282 m	
	1260 s	1260 s	
1230 s	1224 m	1231 m	
1162 m	1160 m	1168 m	
1121 m	1119 m	1124 m	
	1080 m	1081 m	
	949 s	957 vs	$\nu^{s}(MoO_2)$
962 s	932 sh	950 vs	
	922 s	924 vs	$\nu^{as}(MoO_2)$
	790 w	790 m	
764 s	759 s	762 s	
		735 m	$\nu^{as}(Mo_2O)$
718 s	717 s	719 s	
		700 m	
	695 w	693 m	
	687 m	686 m	
666 m	665 m	672 s	
		643 m	ν(Mo-Olb)
	600 s	600 s	

3.3 Ortho-aminophenol complexes

For the purposes of comparison, some complexes of ortho-aminophenol were prepared and investigated by infrared spectroscopy. The nickel and palladium species have been reported in the literature but the molybdenum and osmium complexes are new.

3.3.1 Literature measurements:-

Infrared spectra of $M(C_6H_4ONH_2)_2$ and $K_2[M(C_6H_4OHN)_2]$, (where M = Ni(II), Pd(II))

The o-aminophenol complexes of palladium (II) and nickel (II) $M(C_6H_4ONH_2)_2$, in which only the hydroxyl proton is lost to form the monoanion, when reacted with potassium amide in liquid ammonia, in the absence of air, resulted in the salts $K_2[M(C_6H_4ONH)_2]$, in which a further proton has been lost, this time from the NH_2 group.[101] These complexes were studied by infrared spectroscopy. Loss of the hydroxyl proton on complexation led to the disappearance of the ν(OH) absorptions from the region 3500 - 3000cm^{-1}. The $\nu(NH_2)$ absorptions were found between 3325 and 3195cm^{-1} in the complex and the NH_2 bending mode, $\delta(NH_2)$ occurs near 1600cm^{-1} for the complexes $M(C_6H_4ONH_2)_2$. The deprotonated species does not exhibit the strong $\nu(NH_2)$ peaks, but weak ν(NH) absorptions were observed near 3270cm^{-1}. The strong peak near 1600cm^{-1} disappears, and only a weak peak was found in this region, ascribed to δ(NH). A number of other bands exhibited by the $M(C_6H_4OHN_2)_2$ complexes also disappeared or showed reduced intensity, and these were probably all associated with the NH_2 bending mode.

3.3.2 Experimental results

$MoO_2(C_6H_4ONH_2)_2$

(a) The major peaks of this spectrum are listed in Table 1.13.

Two strong peaks at 915 and 900cm^{-1} are found in this spectrum which were not observed for the complexes formed with palladium and nickel described above. These peaks are assigned to the symmetric and asymmetric stretching vibrations, respectively, of the cis-dioxo-molybdenum (VI) group.

The remaining absorptions of this spectrum show the same pattern as that described for $Pd(C_6H_4ONH_2)_2$. The region 3,500 to 2,000cm^{-1} shows considerable change from that of the free ligand, the ν(OH) absorptions disappearing, and $\nu(NH_2)$ peaks shifting to slightly lower frequency. A strong peak at 1580cm^{-1} is assigned to $\delta(NH_2)$, and further strong absorptions at 1470 and 1450cm^{-1} are assigned to the aromatic, ν(C-C) vibrations.

The two palladium (II) and the two nickel (II) complexes described in the literature, together with the complex $MoO_2(C_6H_4ONH_2)_2$ all show a strong peak near 1270cm^{-1}, which was not assigned. By analogy with catecholato complexes, it is tentatively ascribed to the stretching vibration of the C-O bond, associated with aromatic stretching vibrations, ν(C-O + C - C).

(b) $K_2[OsO_2(C_6H_4ONH)_2]$

In this case elemental analyses of this new complex led to the formulation shown, in which the ligand has lost two protons, and chelates as the dianion.

The infrared spectrum of this complex listed in Table 1.13 is compared to those of $Pd(C_6H_4ONH_2)_2$ and $K_2[Pd(C_6H_4ONH)_2]$. Above $2000cm^{-1}$, despite the presence of a broad water absorption, the strong peaks which arise from $\nu(NH_2)$ should still be visible if the ligand were present in the monodeprotonated form. No evidence is found for those peaks, however. Near $1600cm^{-1}$, broad absorptions are observed, characteristic of the water deformation vibrations, and it is not clear whether the strong peak due to $\delta(NH_2)$ is present or not. The remainder of the spectrum is very similar to that found for $Pd(C_6H_4ONH_2)_2$.

The exception is the presence of a strong, sharp peak at $820cm^{-1}$. This is characteristic of the asymmetric stretching vibration, $\nu^{as}(OsO_2)$ of the "osmyl" group, indicating the presence of the <u>trans</u>-dioxo osmium (VI) grouping in this complex. This vibration, together with the absence of any $\nu(NH_2)$ absorptions above $2000cm^{-1}$ confirms the postulated structure.

Table 1.13:- Major peaks of the infra-red spectra of the o-aminophenol complexes $MoO_2(C_6H_6NO)_2$ and $K_2[OsO_2(C_6H_5NO)_2]$(cm^{-1})

$MoO_2(C_6H_6NO)_2$	$K_2[OsO_2(C_6H_5NO)_2]$	Assignment
	3400 s.vbr	ν(OH) of H_2O
3210 s		$\nu(NH_2)$
3155 w		
3110 w		
3060 m		ν(CH)
1595 s		$\delta(NH_2)$
1580 m		
1550 m	1565 s	
1470 vs		ν(C-C)
1450 s	1455 s	
	1365 s	
1290 m	1304 w	
1275 s		
1265 vs	1240 s	ν(C-O+C-C)
1200 s		
1115 s	1135 s	
1080 s		δ(CH) in plane
1025 m	1000 m	
	975 m	
915 vs		$\nu^s(MO_2)$
900 vs	830 vs	$\nu^{as}(MO_2)$
870 s		
785 s		
760 m		δ(CH) out of plane
745 vs	740 s	
645 vs	660 m	
500 s	555 m	

4. ^1H NUCLEAR MAGNETIC SPECTROSCOPY

4.1 Spectra of the ligands

Catechol is an A_2B_2 system as shown in Figure 1.16. However, its observed spectrum shows only one peak, at 6.83 p.p.m., arising from the aromatic ring protons, showing that the chemical shift between the H_A and H_B protons is very small[102] (too small to separate the peak into the typical symmetric A_2B_2 pattern).

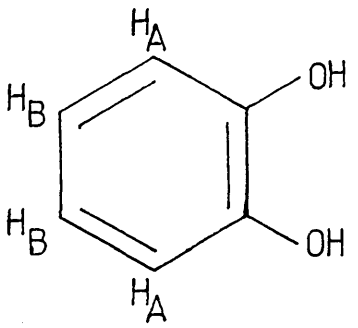


Figure 1.16 Catechol as an A_2B_2 system

When the spectrum is recorded in $CDCl_3$ solutions, a smaller peak is found at 5.20 p.p.m., with an integral half that observed for the aromatic peak. The resonance arises from the two hydroxyl protons. This assignment is confirmed by the fact that no such peak is observed in D_2O solutions, due to rapid exchange of the hydroxyl protons with the solvent.[103]

A comparison of the spectra of 3, 5-di-t-butyl-catechol and 3, 5-di-t-butyl-o-benzoquinone, recorded in $CDCl_3$, shows that they have very similar resonances. The main difference is the absence of any hydroxyl proton resonance from the benzoquinone spectrum. Both compounds show two doublets due to the ring protons.

The benzoquinone peaks have a greater separation than is found for the aromatic proton resonances of the catechol. The tertiary-butyl groups resonate much closer to each other in the benzoquinone spectrum, than is found for 3,5-di-t-butyl-catechol.

4.2 Spectra of catecholato complexes

4.2.1 Literature work

On complexation of catechol to a metal ion, the hydroxyl proton resonance, at δ = 5.20 p.p.m. disappears, due to formation of the catecholato dianion.

The ^{1}H N.M.R. spectra of the tris (catecholato) complexes $Os(cat)_3$[19] and $K_3[Rh(cat)_3]$[11] have been reported. The complex $K_3[Rh(cat)_3]$ showed a complex multiplet, which had been shifted to lower frequency from that observed for the free ligand. This effect was ascribed to the electron-withdrawing metal ion causing decreased electron density in the aromatic ring. This would lead to reduced ring currents, and hence to greater shielding of the ring protons, causing them to resonate at lower frequency. Comparison of the analogous rhodium (III) and gallium (III) - enterobactin complexes[11] (in which the metal coordinates to the three catechol moieties of enterobactin) found that the gallium complex showed the greater shift to lower frequency, consistent with the greater Lewis acidity of gallium, as compared to rhodium. (The positions of these resonances, together with those found experimentally in this work, are listed in Table 1.14.)

The complex $Os(cat)_3$[19] was reported to show two complex multiplets, one of which had shifted to lower frequency, the other was found at approximately the same position as the catechol resonance. The lower frequency multiplet was assigned to the H_A protons, which are apparently more affected by the presence of the metal ion than are the more distant H_B protons.

Similar behaviour was found for $Pt(PPh_3)_2(cat)$;[27] the aromatic ring protons of the catecholato ligand produced a complex multiplet, at least part of which was reported at lower frequency than was the case for free catechol.

4.2.2 Experimental results

(a) oxo-catecholato complexes

i) $K_2[OsO_2(cat)_2]$

The ^1H N.M.R. spectrum of $K_2[OsO_2(cat)_2]$ in D_2O shows two complex multiplets in the region of the spectrum typical of aromatic proton resonances. The lower frequency multiplet lies between 6.87 and 6.60 p.p.m., the higher frequency multiplet between 6.87 and 7.10 p.p.m. (as shown in Figure 1.17). Comparison with the reported spectrum of $K_3[Rh(cat)_3]$ shows the same pattern of resonances, typical of an A_2B_2 spectrum. The lower frequency multiplet would appear to arise from the H_A protons of the ring, by analogy with the $Os(cat)_3$ spectrum, described above.

ii) $UO_2(cat)\ 2H_2O$.

Only very weak solutions of this polymeric complex in d^6 D.M.S.O. could be prepared, so that only a very weak signal could be observed. Although only an approximate value was obtained for the position of the peaks, it was clear that the

observed resonance was an unresolved multiplet, probably in the same pattern as that observed for $K_2[OsO_2(cat)_2]$.

iii) cis-$[MoO_2(cat)_2]^{2-}$ and cis-$[M_2O_5(cat)_2]^{2-}$ complexes (M = Mo, W).

The complex $K_2[MoO_2(cat)_2]$ gives a spectrum which has a single sharp peak, arising from the catecholato ring protons, at 6.72 p.p.m. (see Figure 1.18). This is at slightly lower frequency than was found for free catechol. The binuclear complex, $(NH_4)_2[Mo_2O_5(cat)_2]$ similarly shows a singlet due to the ring protons, but at the still lower frequency of 6.32 p.p.m. The analogous tungsten complex, $Na_2[W_2O_5(cat)_2]$ shows a similar pattern.

It is clear that these bis (catecholato) cis-dioxo complexes give rise to different ^1H N.M.R. spectra from those observed for the other complexes, whether trans-dioxo-catecholato complexes, or tris (catecholato) complexes. The cis-dioxo complexes described here give rise to a spectrum very similar to that found for free catechol, but shifted slightly to lower frequency.

If the case of the 1,2-disubstituted benzenes is considered it was found that the chemical shifts of the phenyl ring protons vary according to the electron withdrawing/donating power of the substituents.[102] Drainage of electron density alters the ring currents of the freely-circulating π electrons of the ring, and hence affects the secondary magnetic field induced in the presence of an applied field. This subsequently alters the shielding of the ring protons, and hence the frequency at which resonance takes place.

In whichever direction the electron density drainage occurs, the ring protons all appear to be affected to the same extent, without any significant difference between the H_A and H_B protons. Electronic effects of the substituent, however, may affect the protons at different positions separately, by inductive and resonance effects, and the resulting spectrum would depend on the variation of this effect on the different protons.

It has been proposed that for uranyl complexes containing a chelated aromatic ligand, two effects must be considered when studying the ^1H N.M.R. spectra. Firstly, drainage of electron density by the metal ion would lead to a shift to lower frequency of the phenyl ring protons, compared to the free ligand. Secondly, the uranyl group has a certain magnetic anisotropy[41] in an applied field and this has been suggested as the possible cause of the observed differences in the chemical shifts of the H_A and H_B protons. The effect of the anisotropic field of the uranyl ion would depend on the position of each proton in relation to this field, and hence the H_A and H_B protons of the catecholato ligand would be affected differently, giving rise to the observed splitting.

If it may be assumed that the "osmyl" group would behave in a similar manner to the uranyl group in setting up a magnetic anisotropic field in the presence of an applied field, then it is indeed feasible to explain the differences between the ^1H N.M.R. spectra of the trans-dioxo and cis-dioxo catecholato complexes as described above.

The complexes $K_2[MoO_2(cat)_2]$ and $Na_2[W_2O_5(cat)_2]$ would be expected to give rise to a spectrum similar to that found for free catechol, but shifted to lower frequency, simply by changes in the ring current effects caused by electron density drainage by the metal ion, as is observed. However, this theory does not explain the spectra arising from the tris (catecholato) complexes, $Os(cat)_3$ and $K_3[Rh(cat)_3]$. The reported spectrum of the latter, was shown to give a complex multiplet, as expected for the trans-dioxo type complexes. However, the spectrometer used was of greater power (180MHz)[11] compared to that used in these experiments (90MHz) and hence greater resolution would be expected. But this does not explain the behaviour observed for $Os(cat)_3$,[19] whose reported spectrum was recorded on a 60MHz spectrometer, and still shows two complex multiplets.

Thus, although the magnetic anisotropy theory may indeed have some effect - resulting in the observed splittings, it clearly does not explain the whole situation, and some other explanation must be found for the spectrum observed for $Os(cat)_3$.

(b) Reformulated molybdenum (VI)-catecholato complexes

We have explained above that the complexes reported as "$K[MoO_2(OH)(cat)]$" and "$(NH_4)[MoO_2(OH)(C_6H_3O_2(OH))]$"[44] in fact probably exist as $K_2[Mo_2O_5(cat)_2]$ and $(NH_4)_2[Mo_2O_5(C_6H_4O_3)_2]$ respectively, while "pyH.H$[MoO_3(cat)]$" is probably $(pyH)_2[Mo_2O_5(cat)_2]$. Little difference would

be expected in the ^1H N.M.R. spectra of the complexes in their original or new formulations, and this technique is thus of little use in the reformulation of these complexes. Furthermore the pyridinium salts of these cis-dioxo-molybdenum(VI) - catecholato complexes have very complicated ^1H N.M.R.-spectra arising from the complex spectrum of the pyridinium cation, so that definite identification of the catecholato resonances is very difficult.

However, it should be possible to confirm the presence of a catechol molecule of crystallisation as in $K_2[MoO_2(cat)_2] . C_6H_4(OH)_2$, and, indeed, this complex shows two resonances in the aromatic region, at 6.59 p.p.m. and 6.79 p.p.m. The higher frequency peak was assigned to the catechol molecule of crystallisation, the lower frequency peak to the coordinated catecholato ligand, in accordance with the shifts noted for free catechol and for $K_2[MoO_2(cat)_2]$. Integration showed that the intensity of the lower frequency peak was approximately twice that of the higher frequency peak in agreement with the ratio of coordinated catechol to free catechol in the complex. No resonance that could be assigned to the hydroxyl protons of the free catechol was found, probably due to rapid exchange of these protons with the D_2O solvent.

(c) Catecholato *versus* benzoquinone coordination:-

Spectrum of $[MoO(3,5\text{-DTBcat})_2]_2$

The ^1H N.M.R. spectrum of this catecholato complex, prepared from the benzoquinone starting material, was examined in relation to those recorded for 3,5-di-t-butyl-catechol and 3,5-di-t-butyl-o-benzoquinone, to investigate the possibility of distinguishing between catecholato and o-benzoquinone coordination using this technique.

The ^1H N.M.R. spectrum of this complex showed two doublets in the aromatic region (as listed in Table 1.15). Four sharp singlets are observed to lower frequency due to the four non-equivalent tertiary-butyl groups of the dimer. The ring proton resonances show a separation similar to that found for the free ligand 3,5-di-t-butyl-catechol. The differences between the catechol and benzoquinone resonances thus may be seen to be not very significant in this case and, on the basis of this evidence, we conclude that this technique is not of great diagnostic value in determining the mode of coordination of a quinone ligand.

Table 1.14:- ^1H N.M.R. Resonances of catechol and some catecholato complexes (p.p.m.)

Substance	phenyl proton resonances	hydroxyl proton resonances	Solvent
Catechol	6.86(s)		D_2O
	6.83(s)	5.20(s)	$CDCl_3$
$K_2[MoO_2(cat)_2]$	6.72(s)	-	D_2O
$K_2[MoO_2(cat)_2]$	[a]6.59(s)	-	D_2O
$C_6H_4(OH)_2$	[b]6.79(s)	-	
$(NH_4)_2[Mo_2O_5(cat)_2]$	6.32(s)	-	D_2O
$Na_2[W_2O_5(cat)_2]$	6.76(s)	-	D_2O
$K_2[OsO_2(cat)_2]$	6.87(m)	-	D_2O
$Os(cat)_3$ [c]	6.40-6.68(m)	-	
$K_3[Rh(cat)_3]$ [d]	6.44-6.69(m)	-	D_2O
$UO_2(cat).nH_2O$	6.73(m,br)	-	d^6DMSO
$(PPh_3)_2Pt(cat)$ [e]	6.42(m)	-	$CDCl_3$

[a]coordinated catechol resonance [b]catechol of crystallisation resonances [c]reference 19 [d]reference 11 [e]reference 27.

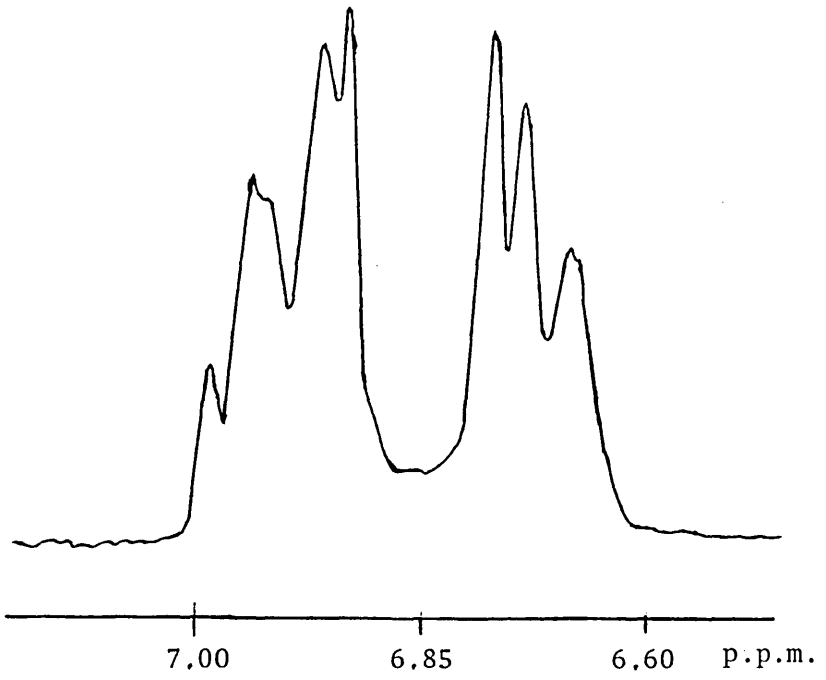


Figure 1.17 - ^1H N.M.R. spectrum of $K_2[OsO_2(cat)_2]$

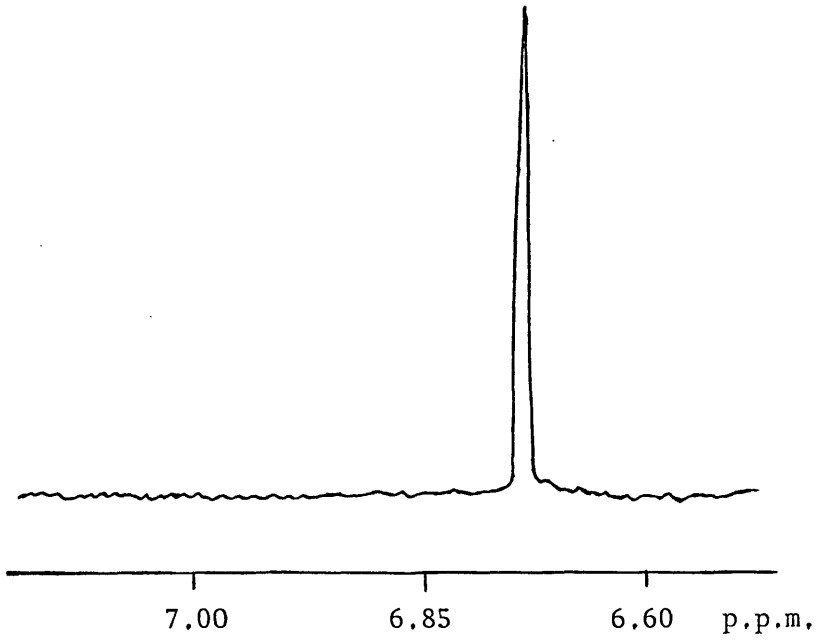


Figure 1.18 - ^1H N.M.R. spectrum of $K_2[MoO_2(cat)_2]$.

Table 1.15:- ^1H N.M.R. Resonances of 3,5-di-t-butyl catechol 3,5-di-t-butyl-o-benzoquinone and $[MoO(3,5\text{-}DTBcat)_2]_2$. (p.p.m.)

Substance	Phenyl ring resonances	Hydroxyl proton resonances	Tertiary butyl resonances
3,5-di-t-butyl catechol	6.76 (d) 6.74 6.60 (d) 6.58	5.12(s)	1.38(s) 1.21(s)
3,5-di-t-butyl o-benzoquinone	6.91 (d) 6.89 6.14 (d) 6.12	-	1.25(s) 1.22(s)
$[MoO(3,5\text{-}DTBcat)_2]_2$	7.08 (d) 7.06 6.83 (d) 6.80	-	1.52(s) 1.27(s) 1.25(s) 0.90(s)

These spectra were recorded in $CDCl_3$ solutions.

5. ^{13}C NUCLEAR MAGNETIC RESONANCE SPECTROSCOPY

5.1 Spectrum of free catechol

The 'H decoupled ^{13}C N.M.R. spectrum of free catechol shows three peaks (as shown in Figure 1.19), one of which is of considerably less intensity than are the other two. When proton decoupling is used, the nuclear Overhauser effect causes enhancement of intensity of those resonances arising from ^{13}C nuclei attached to protons, [105] so that the intensity of each resonance may no longer be proportional to the number of nuclei giving rise to it. However, significant differences in intensities of different resonances may be indicative of the numbers of nuclei causing that resonance. In this case, catechol would be expected to give rise to three resonances, arising from the pairs of equivalent nuclei, C_1 and C_2, C_3 and C_6 and C_4 and C_5 as shown in Figure 1.20.

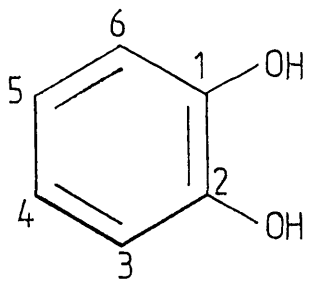


Figure 1.20 Labeling of carbon nuclei of catechol.

The pair C_1 and C_2 have no proton directly attached, so would be expected to give a resonance of significantly less intensity than those arising from the other two pairs. Thus, the smallest peak at 146.6 p.p.m. is assigned to the equivalent nuclei, C_1 and C_2. From previously recorded data, the peak at 123.6 p.p.m. is assigned to the pair C_4 and C_5, and that at 118.9 p.p.m. is due to the C_3 and C_6 equivalent nuclei. [106]

These ^{13}C resonance positions and those recorded for a number of diamagnetic catecholato complexes are listed in Table 1.16.

5.2 Spectra of quinone complexes

5.2.1 Literature measurements

Very little ^{13}C N.M.R. work on quinone complexes of any type, has been reported in the literature. The complexes of the type, $Os(cat)_3$,[19] were said to exhibit a shift in the C_1 and C_2 resonances of catechol and substituted catechols of approximately 25 p.p.m. to higher frequency on coordination. At the same time a slight decrease in frequency for the position of the resonances of the remaining carbons of the aromatic ring was observed.

The interaction of enterobactin with gallium[107] caused a shift in the position of the C_1 and C_2 resonance of the catechol group by 9.30 p.p.m. to higher frequency. At the same time, the remaining aryl carbon resonances of the catechol ring shifted to lower frequency by 3.90 p.p.m. This was suggested to be evidence to support increased electron delocalisation in the chelate.

5.2.2 Experimental results

To a first approximation, the total shielding for a particular nucleus may be considered to be made up of three terms:- the diamagnetic shielding term, the paramagnetic shielding term, and a term arising from contributions from neighbouring-group nuclei.[105,108] The diamagnetic term arises from currents involving electrons on the nucleus under

consideration and its nearest neighbours, the paramagnetic shielding term arises from contributions of higher electronic states to the description of the ground state, and is of greatest importance for ^{13}C N.M.R.

In substituted benzenes, the observed chemical shifts are closely correlated with the electron-withdrawing power of the substituent.[109] This is because the paramagnetic shift is proportional to the π-electron charge densities in the carbon 2pz orbitals and in neighbouring bonds. Consequently, the shift of the C_1/C_2 resonance on coordination of catechol in the complexes studied here, may be considered in terms of the relative bond strengths in the chelate ring and the electron withdrawing power of the metal cemtres, to a first approximation.

(a) $K_3[Rh(cat)_3]$

The isolated solid $[Co(en)_3]$ $[Rh(cat)_3]$ is too insoluble to allow its ^{13}C N.M.R. to be obtained. The spectrum of the reaction mixture was recorded instead, and is shown in Figure 1.21. The reaction takes place in a pH 10 carbonate/bicarbonate buffer,[11] and the solution was kept under nitrogen during measurement of the spectrum, to prevent oxidation of catechol in the basic conditions. Stoichiometric amounts of the starting materials were used so that resonances due to the free catechol would not dominate the spectrum.

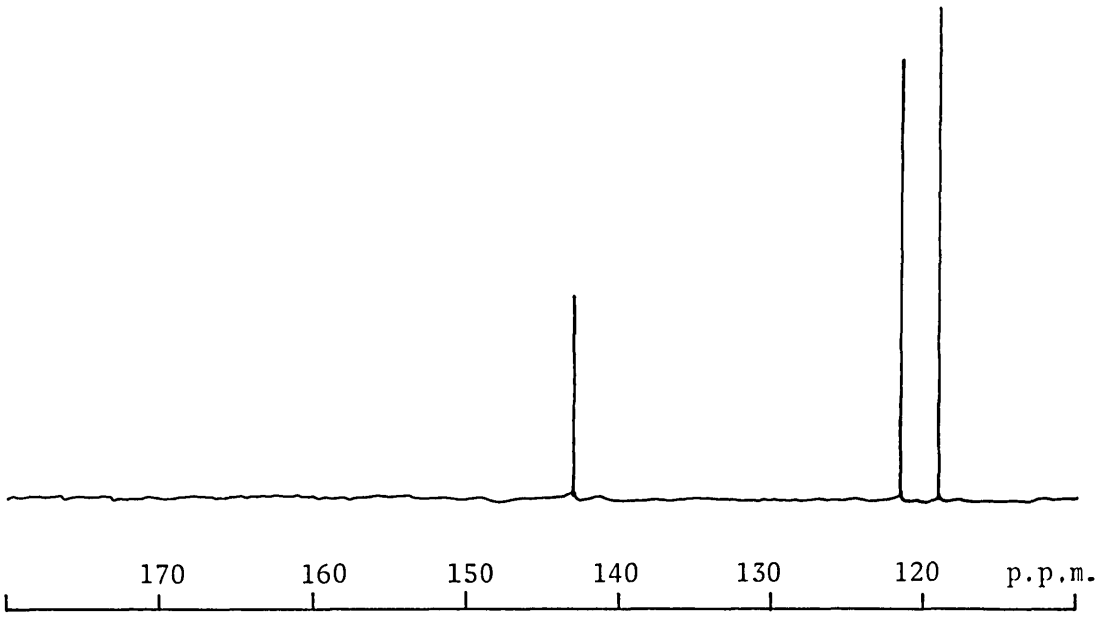


Figure 1.19 - ^{13}C N.M.R. spectrum of catechol.

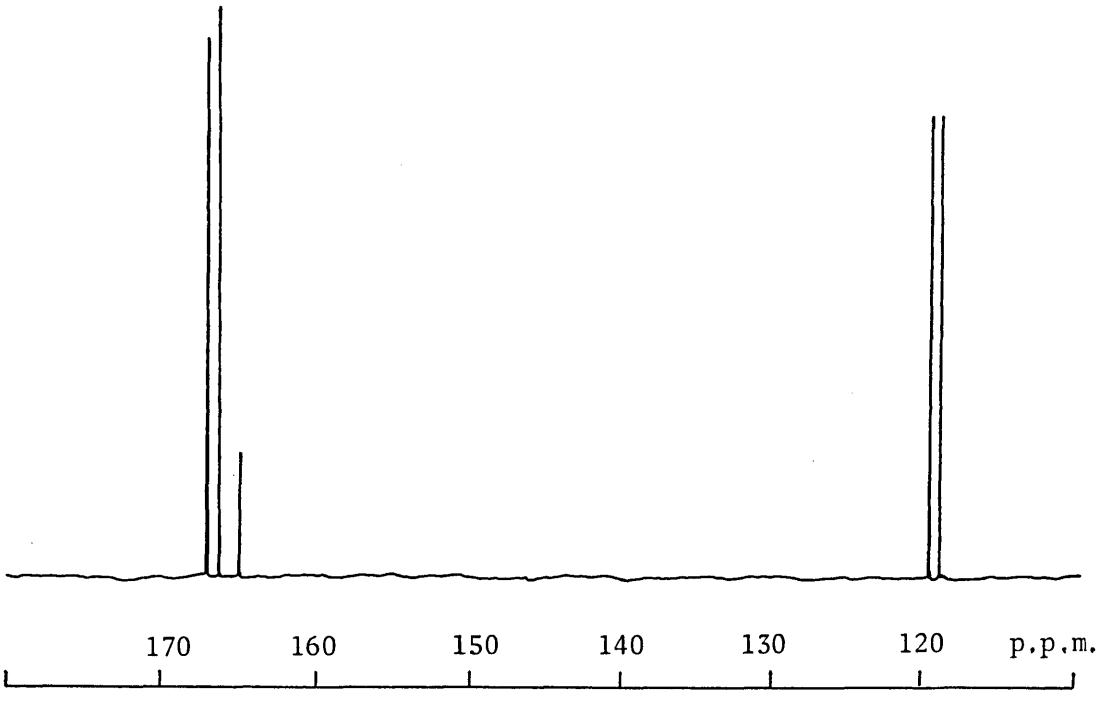


Figure 1.21 - ^{13}C N.M.R. spectrum of $K_3[Rh(cat)_3]$.

A strong doublet was observed at 167.5 and 167.3 p.p.m., a position typical of the carbonate/bicarbonate species.[110] Three other resonances remain, one occurring at much higher frequency, at 165.0 p.p.m., and of slightly less intensity. The other two peaks occur at 118.3 and 118.2 p.p.m., very close to the values recorded for the equivalent pairs C_3 and C_6, and C_4 and C_5, of the free catechol. The peak at higher frequency is therefore assigned to the C_1/C_2 resonance.

The only other recorded ^{13}C N.M.R. spectrum of a tris-(catecholato) species is that arising from $Os(cat)_3$,[19] as described above. The C_1/C_2 resonance was found at 171.5 p.p.m. in this complex. The difference in chemical shifts of the C_1/C_2 resonance between $Os(cat)_3$ and $K_3[Rh(cat)_3]$ is tentatively ascribed to the greater electron-withdrawing powers of the osmium (VI) ion, which has only two d electrons in its outer shell, as compared to the rhodium (III) ion, having six d electrons in its outer shell.

(b) oxo-catecholato complexes

(i) $K_2[OsO_2(cat)_2]$

The ^{13}C N.M.R. spectrum of this complex shows an increase in the frequency of the C_1/C_2 resonance to 167.7 p.p.m. This is a significantly smaller change than that observed for $Os(cat)_3$. Presumably weaker osmium-catecholato bonds result in $K_2[OsO_2(cat)_2]$ because of the strong π-donating ability of the oxo ligands, preventing as much electron density withdrawal from the catechol ring in this complex, as compared to that found in $Os(cat)_3$. The spectrum is shown in Figure 1.22.

(ii) cis-dioxo molybdenum (VI) and tungsten (VI) complexes

The complexes $K_2[MoO_2(cat)_2]$, $(NH_4)_2[Mo_2O_5(cat)_2]$ and $Na_2[W_2O_5(cat)_2]$ exhibit the least change in the resonance arising from the C_1/C_2 nuclei, on coordination. This is presumably due to the trans-influence of the cis-dioxo groups. In each of these complexes, each catecholato ligand has an oxo ligand in a position trans to it. The strong π-donating oxo ligands weaken the catecholato to molybdenum bonds relative to those found in the other complexes reported here, leading to a smaller shift in the C_1/C_2 resonance.

(iii) cis-$(NH_4)_2[MoO_2(4\text{-nitrocat})_2]$ versus trans-$K_2[OsO_2(4\text{-nitrocat})_2]$

The difference in the shifts of the resonance due to the C_1 and C_2 nuclei on formation of the cis-dioxo-molybdenum (VI) and trans-dioxo-osmium (VI) complexes, is again observed with the ligand 4-nitrocatechol (Figure 1.23).

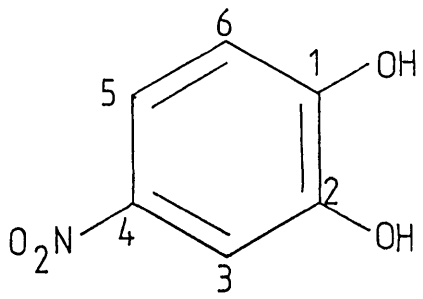


Figure 1.23 Labeling of carbon nuclei of 4-nitrocatechol

The spectrum of the free ligand shows separate positions for the resonances C_1 and C_2, due to the strong effect the nitro group has on the carbon in the position para to it (C_1). The resonance at 146.6 p.p.m. (see Table 1.17) is assigned to C_2 the usual position for a ^{13}C nucleus in this environment, as found for catechol. Since substituent effects on an aromatic ring have been found to be additive in ^{13}C N.M.R. spectroscopy, the effect of a nitro group on its para position (C_1) will be added to the effect bonding to the hydroxyl group has on the carbon, C_1, to result in a resonance at higher frequency- 154.4 p.p.m. in this instance. The resonance at 142.7 p.p.m. is assigned to C_4, due to the effect of the nitro group. The resonances due to C_3, C_5, and C_6 are found between 113 and 121 p.p.m.

On coordination of this ligand to form $(NH_4)_2[MoO_2(4\ nitrocat)_2]$ a new peak is observed at 165.5 p.p.m., and another at 157.4 p.p.m. These are assigned to C_1 and C_2 respectively, each having shifted approximately 11 p.p.m. to higher frequency. This is of the same order as that found on coordination of catechol in $K_2[MoO_2(cat)_2]$, and is observed separately for each carbon nucleus attached to the donor oxygen atom i.e. C_1 and C_2.

On coordination of 4-nitrocatechol to form trans-$K_2[OsO_2(4\text{-nitrocat})_2]$ new peaks are observed at 174.9 p.p.m. and 167.1 p.p.m. This is a shift of about 20 p.p.m., as found on coordination of catechol to form $K_2[OsO_2(cat)_2]$. In this spectrum, however, each resonance appears to have another very close to it, or coinciding with it. More than the number of resonances

expected for the 4-nitro-catecholato ligand are observed. This suggests the two ligands are not exactly equivalent within the complex, so that each of the coordinated ligands produces its own slightly different resonances. For this to be the case, the following arrangement is postulated (Figure 1.24):-

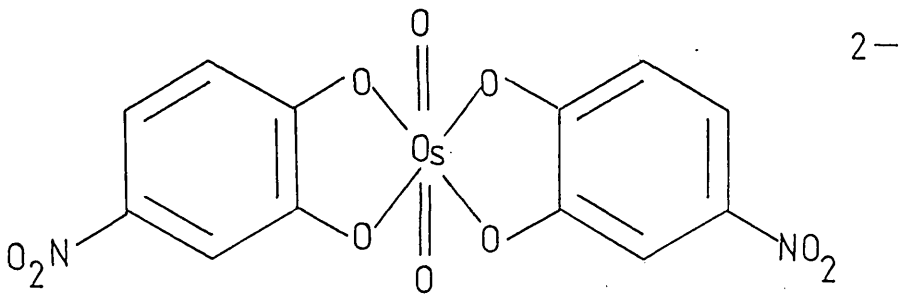


Figure 1.24 $K_2[OsO_2(4\text{-nitrocat})_2]$

(c) $Pt(PPh_3)_2(cat)$

This complex shows a greater shift in the C_1/C_2 catechol resonance on coordination, than was found for the cis-dioxo molybdenum and tungsten complexes. Presumably, despite the not so great electron-withdrawing power of the platinum (II) centre, electron density is easily removed from the catecholato ligand because of the ability of the phosphorous donor atoms to accept electron density back from the metal by overlap of its empty d-orbitals with the d-orbitals of the metal.[111]

(d) Spectra of reformulated molybdenum complexes

As may be noted from Table 1.16 little difference is observed between the spectra of $K_2[MoO_2(cat)_2]$ and $(NH_4)_2[Mo_2O_2(cat)_2]$. This technique is therefore expected to be of little use in the reformulation of these complexes, and indeed little difference is found between the spectra of the authentic complexes named above, and of "$K[MoO_2(OH)(cat)]$" or between $(NH_4)_2[MoO_2(C_6H_3O_2(OH))_2]$ and "$(NH_4)[MoO_2(OH)(C_6H_3O_2(OH)]$" The spectra of complexes reported as "$[MoO_3(cat)]^{2-}$" show no significant difference from those of $(NH_4)_2[Mo_2O_5(cat)_2]$ or $K_2[MoO_2(cat)_2]$. The pyridinium salts give spectra which are complicated by the cation resonances.

The differences between the spectra of free catechol and coordinated catechol are well illustrated in the ^{13}C N.M.R. spectrum of the complex analysed as $K_2[MoO_2(cat)_2]C_6H_4(OH)_2$, as shown in Figure 1.25. Six resonances are observed (as listed in Table 1.16). A peak at 158.7 p.p.m. is in the position expected for the C_1/C_2 resonance of the catecholato ligand in a cis-dioxo-molybdenum (VI) compound. A peak of approximately half the height of this resonance is found at 147.0 p.p.m. The remaining four peaks are observed at lower frequency, two of them showing significantly greater intensity than the other two. The peaks of greater intensity would appear to be due to the coordinated catechol nuclei C_3, C_4, C_5 and C_6; whilst those of lesser intensity are due to the same carbon nuclei of the free catechol molecule. This assignment is consistent with the small shifts to lower frequency which occur consistently for these resonances on coordination of catechol (as may be noted in Table 1.16). The reason for this effect

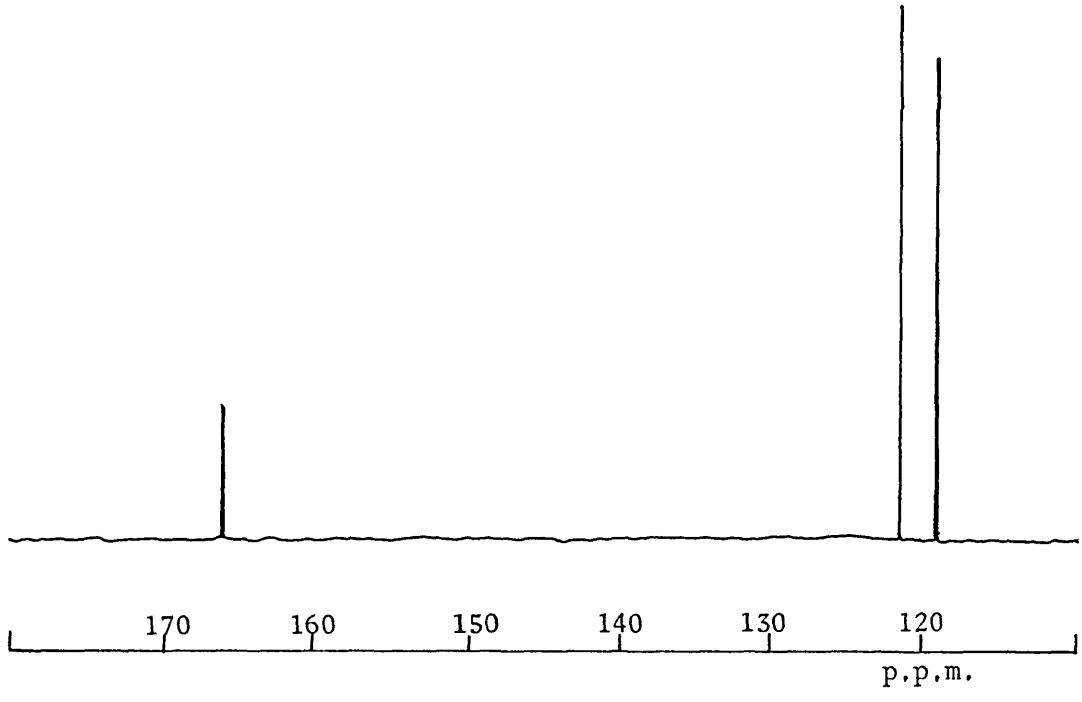


Figure 1.22 - ^{13}C N.M.R. spectrum of $K_2[OsO_2(cat)_2]$

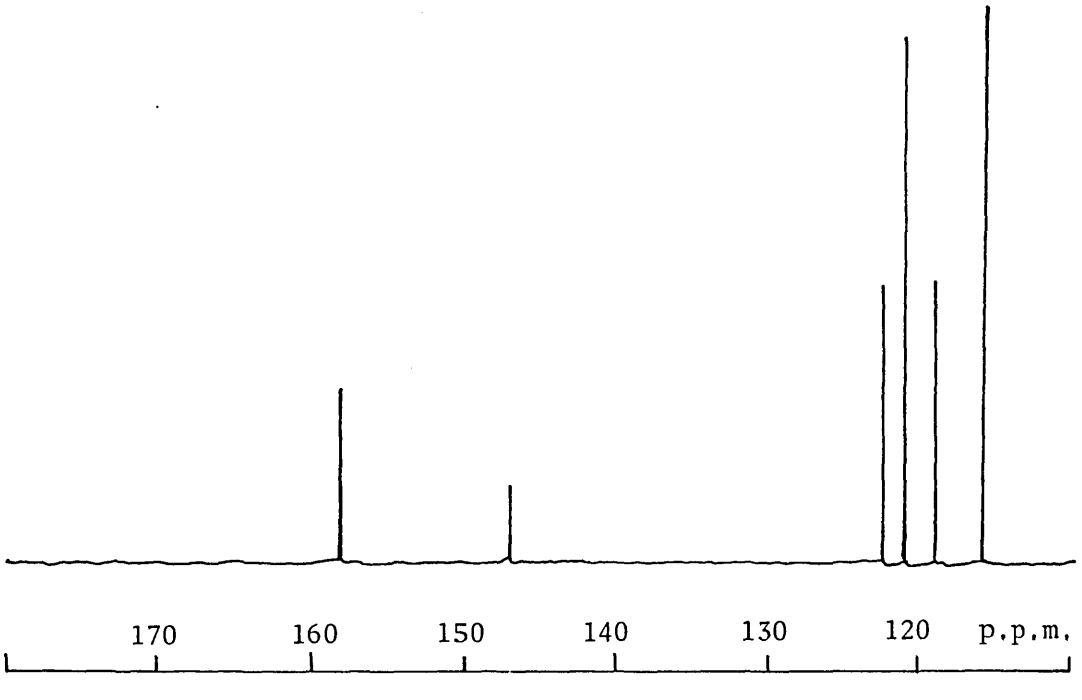


Figure 1.25 - ^{13}C N.M.R. spectrum of $K_2[MoO_2(cat)_2]$ $C_6H_4(OH)_2$

is not quite clear, but it seems likely it arises from some alteration of the ring currents of the aromatic ring upon coordination. The resonance at 147.0 p.p.m. is then assigned to the C_1 and C_2 nuclei of the catechol molecule of crystallisation. The peaks assigned to coordinated catechol all have significantly greater intensity than those assigned to free catechol, and this is consistent with the presence of two catecholato ligands, but only one catechol molecule of crystallisation within the complex. This technique could be used as the definitive method for identification of a catechol molecule of crystallisation.

(e) Benzoquinone vs. catecholato coordination

The 'H decoupled ^{13}C N.M.R. spectra of several free quinones were recorded i.e. 3,5-di-t-butyl-o-benzoquinone, tetrachloro-o-benzoquinone, and 9,10-phenanthrenequinone. These were compared with the spectra of the molybdenum (VI) complexes $[MoO(3,5\text{-DTBcat})_2]_2$, $[Mo(O_2C_6Cl_4)_3]_2$, and $Mo_2O_5(PSQ)_2$. As described earlier, the first two of these complexes were found to have catecholato coordination, the third was found to be a semiquinone complex, in which the paramagnetic ligands were coupled in such a way as to result in diamagnetism for the complex. It should be possible to identify benzoquinone, semiquinone, or catecholato type coordination by ^{13}C N.M.R. spectroscopy.

The resonances of these spectra are listed in Tables 1.18 and 1.19. As may be seen there is a major change in all resonances associated with the carbon rings on coordination of the benzoquinone ligands in the complexes $[Mo(O_2C_6Cl_4)_3]_2$ and $[MoO(3,5\text{-DTBcat})_2]_2$.

The spectrum of the free ligand tetrachloro-o-benzoquinone shows three peaks (as shown in Figure 1.27(a).). Those at 142.6 and 132.8 p.p.m. each show splitting due to the adjacent ^{35}Cl nucleus, and are therefore assigned to the nuclei, C_3, C_4, C_5, and C_6 as labelled in Figure 1.26.

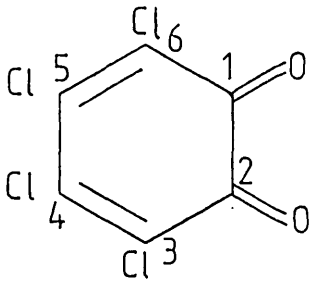


Figure 1.26. Labelling of carbon nuclei of $C_6Cl_4O_2$.

The resonance at 132.8 p.p.m. is possibly due to the C_3 and C_6 pair, by analogy with catechol. The third peak, at 169.5 p.p.m. is in the region typical of carbonyl carbon resonances.

On reaction of tetrachloro-o-benzoquinone to form $[Mo(O_2C_6Cl_4)_3]_2$, the resonances due to the carbons C_3, C_4, C_5 and C_6 are now found at lower frequency, having shifted between 12 and 19 p.p.m., as shown in Figure 1.27(b). The carbonyl resonance disappears, and a new peak is observed at 143.3 p.p.m. This position is typical of C_1/C_2 resonances in uncoordinated catechol compounds. It appears likely that the dimer has broken down in the solvent, d^6 acetone, and the observed spectrum is that of tetrachloro-catechol. Even if this is the case, it does, however, clearly show that the benzoquinone starting material has been reduced to the catecholato form.

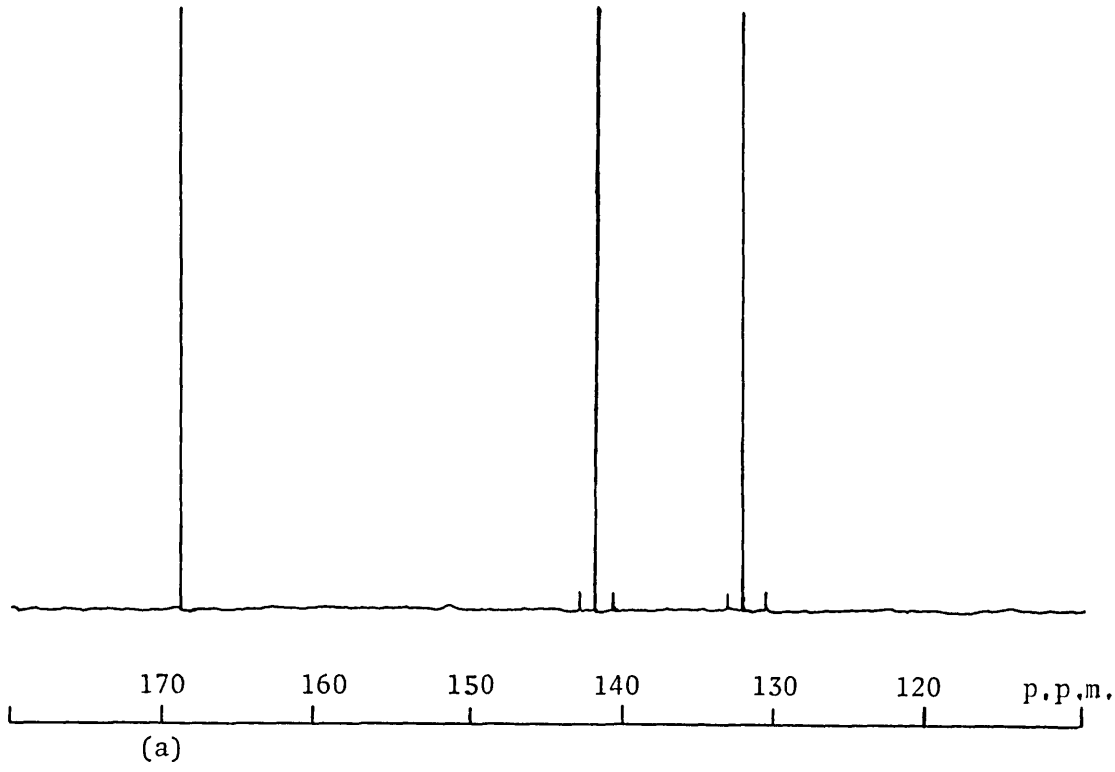
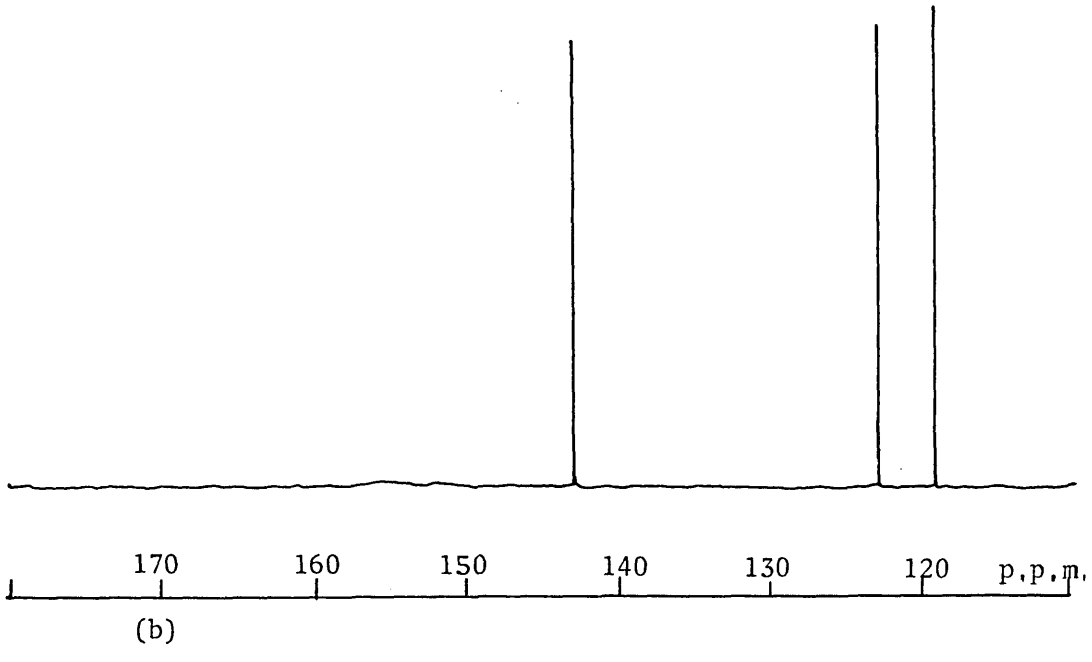


Figure 1.27 - ^{13}C N.M.R. spectra of $C_6Cl_4O_2$(a) and $Mo(O_2C_6Cl_4)_3$ (b).



The spectrum arising from 3,5-di-t-butyl-o-benzoquinone was recorded in d^6 acetone. The very strong resonances arising from the solvent peaks near 30 p.p.m. obscure any peaks that would be expected for the methyl carbons $C_{12} \rightarrow C_{14}$ and $C_8 \rightarrow C_{10}$ (as labelled in Figure 1.28).

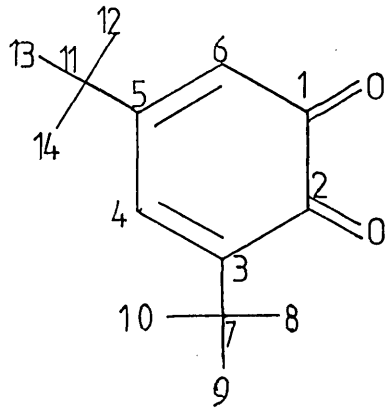


Figure 1.28 3,5-di-t-butyl-o-benzoquinone

Two peaks, at 36.4 and 35.9 p.p.m., are assigned to the carbon atoms C_7 and C_{11}, although it is difficult to distinguish one from the other. The two peaks at highest frequency, 181.6 and 181.0 are found in the region typical of carbonyl carbon resonances, and are assigned to C_1 and C_2. Of the other resonances, the two at 163.4 and 150.3 p.p.m. have significantly less intensity than the remaining two peaks,suggesting they arise from resonance of the nuclei C_3 and C_5. The resonances at 134.5 and 122.7 p.p.m. are then assigned to C_3 and C_6.

The complex $[MoO(3,5\text{-DTBcat})_2]_2$ exists as a dimer in the solid state and in solution of non-coordinating solvent, but forms $MoO(3,5\text{-DTBcat})_2(sol)$ in solvents such as acetone. The ^{13}C N.M.R. spectra of this complex in $CDCl_3$ and d^6 acetone reflect this behaviour.

Considering the $CDCl_3$ spectrum first, it is again apparent that significant changes have occurred on coordination. More peaks are observed than would be predicted for four equivalent ligands. This would be expected from the structure found by X-ray crystallography (as described earlier), when two chemically distinct ligands were found. This is reflected in the number of resonances observed. The carbonyl group resonances are no longer observed. Four new peaks are found between 152 and 158 p.p.m., the region we have found to be typical of the C_1 and C_2 resonances of the catecholato ligand. Four resonances between 148 and 135 p.p.m. are tentatively assigned to the tertiary carbon atom resonances of C_3 and C_5, whilst the peaks between 120 and 105 p.p.m., the region typical of aromatic carbon atoms with no substituents attached, are assigned to the C_4 and C_6 nuclei. Two doublets near 35 p.p.m.,are assigned to the C_7 and C_{11} nuclei of the tertiary-butyl groups, and four resonances of much greater intensity at slightly lower frequency are due to resonances of the CH_3 carbon nuclei of the t-butyl groups. The spectrum is complicated by resonances arising from the toluene molecule of crystallisation present in the complex, which occur between 120 and 130 p.p.m., with a CH_3 resonance in the region of the tertiary-butyl peaks.

The spectrum recorded in d^6 acetone was very weak, but it is evident that the same number of resonances is not observed as was the case for the $CDCl_3$ spectrum. The very large solvent peak obscures the region where the tertiary butyl resonances are expected. Peaks arising from toluene between 120 and 130 p.p.m. are again observed. No carbonyl resonances

can be identified, but neither can any resonances arising from C_1 and C_2 of a catecholato ligand be unequivocally identified. Peaks between 110 and 120 p.p.m. are assigned to C_4 and C_6.

It is therefore evident that the resonances typical of the benzoquinone, in particular the carbonyl carbon peak, change considerably on coordination in these two complexes. The new resonances observed coincide with the region typical of aromatic carbon resonances, and the C_1 and C_2 resonances of the catecholato ligand, clearly showing that this technique may be used to distinguish between the benzoquinone and catecholato modes of coordination.

(f) $Mo_2O_5(PSQ)_2$

Unfortunately, $Mo_2O_5(PSQ)_2$ was insufficiently soluble for a ^{13}C N.M.R. spectrum to be recorded in which all the peaks were clearly distinguishable from background noise.

5.3 Cyclohexanediol complexes

The ^{13}C N.M.R. spectrum of the complex $OsO_2(py)_2(O_2C_6H_{10})$ (where py = pyridine, $(C_6H_{10}O_2)^{2-}$ is the dianion of 1,2-cyclohexanediol) was recorded for comparison with catecholato complexes. The resonances recorded for the free ligand and for $OsO_2(py)_2(O_2C_6H_{10})$ are listed in Table 1.20.

The spectrum of trans-1,2-cyclohexanediol shows three peaks between 90 and 30 p.p.m. A mixture of cis and trans-1,2-cyclohexanediol shows six peaks presumably three arising from the cis and three from the trans-configuration of the molecule.

Trans-1,2-cyclohexanediol was used in the preparation of $OsO_2(py)_2(C_6H_{10}O_2)$. The spectrum recorded shows three peaks in the aromatic region, and three below 100 p.p.m. Those to lower frequency were assigned to the cyclohexanediolato ligand. The fact that only three resonances were observed indicates that cyclohexanediol is coordinated only in the trans-configuration. A shift of about 20 p.p.m. is observed in the peak at highest frequency of the cyclohexanediol resonances. This is presumably the resonance arising from the carbon nuclei attached to the oxygen atoms. The three peaks in the aromatic region are assigned to resonances of the coordinated pyridine molecules, and match well with reported positions.[105]

The complex $MoO_2(C_6H_{11}O_2)_2$ (when $(C_6H_{11}O_2)^-$ is the mono-deprotonated form of 1,2-cyclohexanediol) is insufficiently soluble for its ^{13}C N.M.R. spectrum to be recorded.

Table 1.16:- ^{13}C N.M.R. resonances for catechol and some catecholato complexes (p.p.m.)

Substance	C_1/C_2	C_4/C_5	C_3/C_6	Solvent
Catechol	146.6	123.6	118.9	H_2O
$K_3[Rh(cat)_3]$	165.0	118.4	118.2	H_2O
$Os(cat)_3$	171.5	124.0	117.1	a
$K_2[OsO_2(cat)_2]$	167.7	121.1	118.2	H_2O
$K_2[MoO_2(cat)_2]$	158.8	121.5	116.4	H_2O
$K_2[MoO_2(cat)_2]$ $C_6H_4(OH)_2$	b 158.7	121.4	116.3	H_2O
	c 147.0	124.0	119.4	
$(NH_4)_2[Mo_2O_5(cat)_2]$	157.1	122.4	117.2	H_2O
$Na_2[W_2O_5(cat)_2]$	158.3	121.9	117.4	H_2O
$Pt(PPh_3)_2(cat)$	163.0	115.9	115.3	$CDCl_3$

a. reference 19

b. coordinated catechol resonances

c. catechol of crystallisation resonances.

Table 1.17:- ^{13}C N.M.R. resonances of 4-nitrocatechol, and its complexes with cis-dioxomolybdenum (VI) and trans-dioxo-osmium (VI) (p.p.m.)

Nucleus	4-nitrocatechol	$(NH_4)_2[MoO_2(4\text{-nitrocat})_2]$	$K_2[OsO_2(4\text{-nitrocat})_2]$
C1	154.4	165.5	174.9
C2	146.6	157.4	167.1
C4	142.7	142.3	143.0/142.5
	120.4	120.7	121.0/121.4
C3,5,6	117.6	116.4	116.6
	113.8	112.2	112.8/113.0

carbon nuclei labelling as described in text

Table 1.18:- ^{13}C N.M.R. resonances of 3,5-di-t-butyl-o-benzoquinone and $[MoO(3,5\text{-}DTBcat)_2]_2$

Nucleus	3,5-di-t-butyl-o-benzoquinone	$[MoO(3,5\text{-}DTBcat)_2]_2$
C_1/C_2	181.6	157.2, 156.7
	181.0	154.4, 153.0
C_5/C_3	163.4	147.1, 139.4
	150.3	137.8, 135.6
	134.4	a
C_6/C_4	122.7	
C_7/C_{11}	36.4	35.4 35.8
	35.9	34.7 34.6
solvent	d^6 acetone	$CDCl_3$

a. These peaks could not be unequivocally assigned due to the presence of resonances due to the toluene molecule of crystallisation.

Table 1.19:- ^{13}C N.M.R. resonances of tetrachloro-o-benzoquinone and $[Mo(O_2C_6Cl_4)_3]_2$ (p.p.m.)

Nucleus	tetrachloro-o-benzoquinone	$[Mo(O_2C_6Cl_4)_3]_2$
C_1/C_2	169.5	143.3
C_4/C_5	142.6	123.0
C_6/C_3	132.8	120.0
solvent	d^6 acetone	d^6 acetone

Table 1.20:- ^{13}C N.M.R. resonances of 1,2-cyclohexanediol and $OsO_2(py)_2(O_2C_6H_{10})$

Nucleus	cis/trans $C_6H_{12}O_2$	$OsO_2(py)_2(O_2C_6H_{10})$
C_1/C_2	77.5	94.7
C_1/C_2	73.1	
	35.2	32.9
	31.8	
	26.4	
	23.7	
pyridine		149.6
carbon		140.3
nuclei		125.1
solvent	H_2O	$CDCl_3$

6. ELECTRON PARAMAGNETIC RESONANCE SPECTROSCOPY

E.P.R. has largely been used in investigations of quinone complexes to confirm the presence of a semiquinone ligand. Such a radical typically gives rise to an isotropic signal at $\underline{g}$ = 2.00,[6,53,55,114] with a width of approximately 10G.[7] Hyperfine splitting is sometimes observed from interaction with the ring protons.[48,115] or with the metal centre e.g. $V(O_2C_6Cl_4)_3$[46]- the ^{51}V coupling constant was reported to be 4.1G.

In this work we have made only limited use of E.P.R. spectroscopy using it primarily to confirm, where appropriate, the formulations postulated from consideration of other evidence.

The spectra were recorded in chloroform solutions at liquid nitrogen temperatures.

6.1 Tris-catecholato complexes

6.1.1 $(Ph_4P)_2[Ir(cat)_3]$

No distinguishable spectrum could be obtained for this complex at liquid nitrogen temperatures. Although some low spin $5d^5$ iridium spectra have been recorded at this temperature,[116,117] others needed a temperature as low as 22K.[118]

6.1.2 $(Ph_4P)_2[Re(cat)_3]$

No spectrum could be obtained for this complex at liquid nitrogen temperatures. This is consistent with reported spectra of rhenium (IV), which had to be recorded at liquid helium temperatures.[119]

6.1.3 $(Ph_4P)_3[Ru(cat)_3]$

The spectrum obtained from this complex is not very well defined, but three $\underline{g}$ values may be determined from it. The general shape is very similar to previously described spectra of low spin d^5 ruthenium complexes.[117]

The $\underline{g}$ values were calculated as 2.41, 2.19, and 1.98. These results are consistent with the formulation of this complex as having a ruthenium (III) centre.

6.2 $MoO_2(PSQ)_2$

The spectrum of this complex shows a sharp, almost isotropic peak with g value 2.00, as shown on Figure 1.29. This signal appears typical of an organic free radical spectrum,[7,47] and thus would appear to arise from the 9,10-phenanthrene-semiquinone radical. No hyperfine splitting is observed. The reported spectrum of 9,10-phenanthrenesemiquinone was said to show hyperfine splitting arising[120] from the hyperfine interaction with the protons of the aromatic rings. That spectrum was recorded in D.M.F. solution at ambient temperature. The total splitting was no more than 8 gauss. For this spectrum of $MoO_2(PSQ)_2$, the width of the g = 2.00 signal was 8G. Thus the observed signal is actually an envelope in which the hyperfine splitting due to interaction with the ring protons is unresolved.

A second, very broad feature may be identified in the spectrum of $MoO_2(PSQ)_2$, whose shape is characteristic of a d^1 ion, suggesting the presence of molybdenum (V). Only two g values were observed, at 3.20 and 2.07 , the third g value occurring below 1.32.

The semiquinone peak shows no evidence of any interaction with the metal ion. If the 9,10-phenanthrene-semiquinone ligand were directly attached to the molybdenum centre in this chloroform solution, then some interaction with the spin isotopes of molybdenum ($I=\frac{5}{2}$ Mo^{95} 16·7 Mo^{97} 9·4%) would be expected. It would therefore appear that the 9,10-phenanthrene-semiquinone ligand has become detached from the molybdenum centre in the chloroform solution. This type of behaviour was persistently observed when it was attempted to recrystallise this complex from chloroform. The green complex always resulted in orange crystals, found by infrared spectroscopy and elemental analysis to be 9,10-phenanthrenequinone. It is conceivable that the semiquinone ligand detaches from the metal centre in chloroform solution, giving rise to the signal typical of a free organic radical. However, the 9,10-phenanthrene-semiquinone appears to be oxidised to the benzoquinone form, as was shown from the recrystallisation attempts. This could possibly occur with concomitant reduction of the molybdenum (VI) metal centre, giving rise to the weak, broad signal tentatively assigned to the d^1 figure system of molybdenum (V).

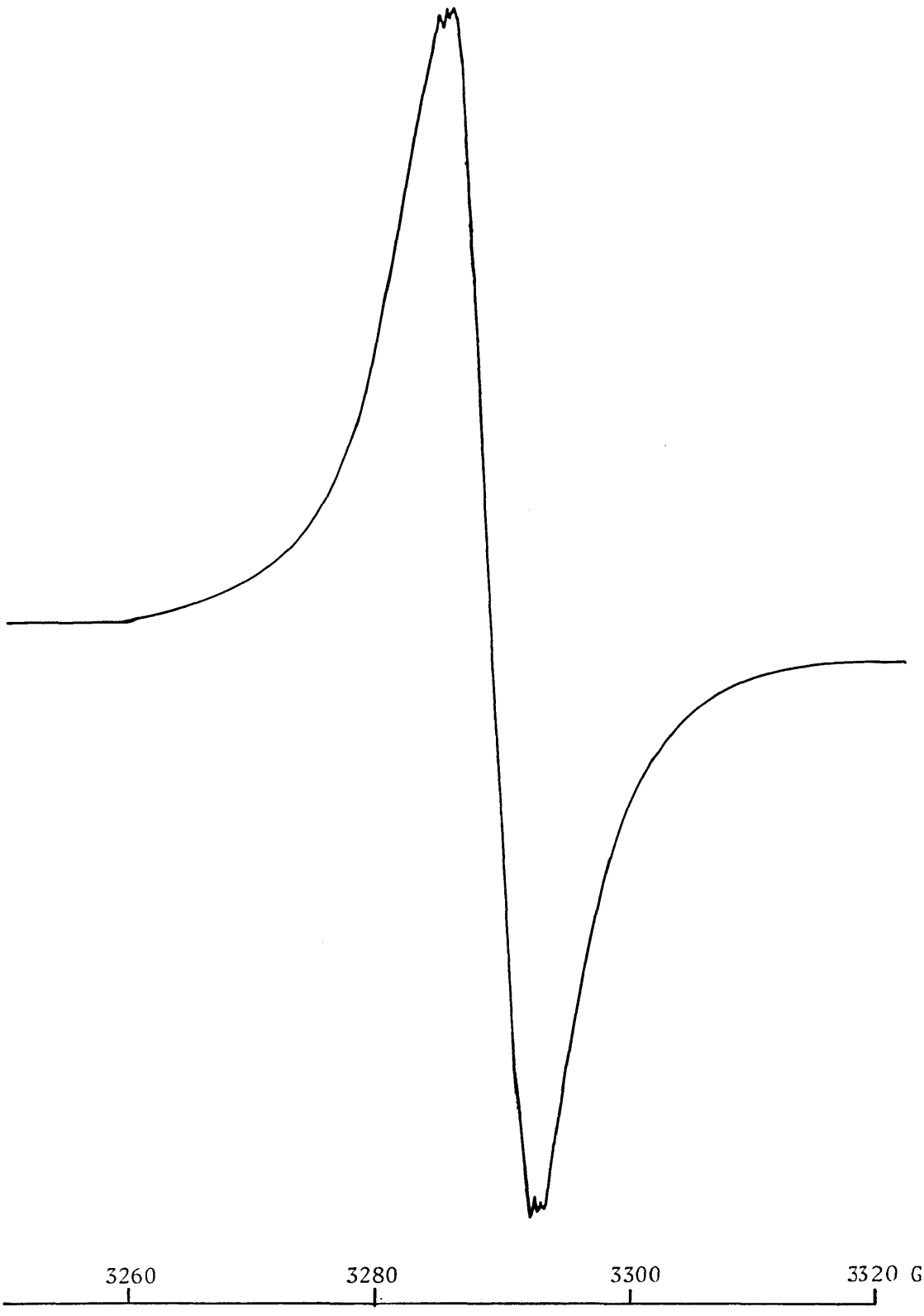


Figure 1.29 - Part of E.P.R. spectrum of $MoO_2(PSQ)_2$

7. ELECTROCHEMISTRY

As described earlier, catechol is a terminal member of the redox series catecholato ⇄ semiquinone ⇄ benzoquinone related by the transfer of one electron. This behaviour, together with the variety of oxidation states available in transition metals, makes the quinones and their complexes very interesting subjects for electrochemical investigations.[22]

7.1 Electrochemistry of the ligands

Several electrochemical studies of catechols and their related benzoquinones can be found in the literature, but they may not be compared with each other, due to the variety of conditions used.[51] The effects of media and acidity on the electron transfer thermodynamics of quinones are important in understanding their coordination chemistry with transition metals. The most comprehensive reference to date reports data for a number of catechols in a variety of aprotic solvents.[51]

Oxidation of a variety of catechols was found to lead to a single irreversible two electron peak at positive potentials, in each case.[51] The process was so rapid that individual steps of the electron-transfer process could not be distinguished within the limits of the techniques used. The overall reaction was oxidation of catechol followed by loss of two electrons to form the benzoquinone and two protons. A scheme was proposed for the multi-stepped oxidation of catechols (Scheme 1.1)

$$H_2cat \rightleftarrows H_2SQ^{+\cdot} + e^-$$
$$H_2SQ^{+\cdot} \rightleftarrows HSQ^{\cdot} + H^+ \qquad \text{Scheme 1.1}$$
$$HSQ^{\cdot} + HSQ^{\cdot} \rightleftarrows Q + H_2cat$$
$$HSQ^{\cdot} + H_2SQ^{+\cdot} \rightleftarrows HQ^+ + H_2cat$$
$$HQ^+ \rightleftarrows Q + H^+$$

After initial catechol oxidation the reverse scan showed a reduction peak arising from reduction of benzoquinone in the presence of strong acid, giving catechol as the overall product (equation 1.11)

$$Q + 2H^+ + 2e^- \rightarrow H_2cat. \qquad \text{Equation 1.11}$$

Reduction of catechols resulted in two irreversible peaks, the first arising from initial formation of the radical H_2cat^-, and its dissociation into the catechol mono-anion, $Hcat^-$, and molecular hydrogen; the second arising from reduction of H cat^- to the dianion and hydrogen (equations 1.12 and 1.13).

$$H_2cat + e^- \rightarrow \tfrac{1}{2} H_2 + Hcat^- \qquad \text{Equation 1.12}$$

$$H\ cat^- + e^- \rightarrow Hcat^{2-} \rightarrow \tfrac{1}{2} H_2 + cat^{2-} \qquad \text{Equation 1.13}$$

The overall reaction was equivalent to that found on addition of base to catechol, and the reduction potentials for catechol and catechol mono-anion, $Hcat^-$, correlate directly with their acidity. The more acidic the catechol proton, the more positive is the reduction potential. Substituent electron-withdrawing groups cause the catechol groups to become more acidic; [121] electron-donating groups have the opposite effect.

In aprotic solvents, the benzoquinones have been found to exhibit two reversible one-electron redox processes.[51,122] The first reduction is due to the benzoquinone-semiquinone couple, the second arising from the semiquinone-catecholato couple. As was the case for reduction of catechols, the nature of the ring substituents affects the reduction potentials observed, electron-withdrawing substituents leading to more positive potentials. Slightly different behaviour was observed for 3,5-di-t-butyl-o-benzoquinone, and this was ascribed to the strong basicity of the corresponding dianion.

7.2 Electrochemistry of quinone - transition metal complexes

7.2.1 Literature measurements

Several extensive studies have been undertaken on the electrochemical behaviour of various quinone complexes of first row transition metals [49,52,123,124,125] and molybdenum.[126,127]

The electrochemical behaviour of catechol appears to be slightly modified on coordination to a metal ion - one electron stepwise oxidation being observed, to form the semiquinone and benzoquinone. Reductive electrolysis of benzoquinones in the presence of divalent first row transition metal ions was shown to involve intramolecular electron transfer if the metal has available electrons to donate, as shown in equations[52] 1.14 and 1.15.

$$M^{II} + 2\ DTBQ \xrightarrow{2e^-} M^{II}(DTBSQ)_2 \xrightarrow{fast} M^{III}(DTBC)(DTBSQ)$$

$$\downarrow\ 1e^-$$

$$[M^{III}(DTBC)_2]^-$$

Equation 1.14

$$M^{II} + 3DTBQ \xrightarrow{3e^-} [M^{II}(DTBSQ)_3] \xrightarrow{-fast} [M^{III}(DTBC)_2]^- + DTBQ$$

$$\downarrow\ 1e^-$$

$$[M^{III}(DTBC)_2(DTBSQ)]^{2-}$$

Equation 1.15

In these cases the quinone is the electroactive substrate, and reduction of the ligand promotes oxidation of the metal ion.[52] This ability of quinones leads to the possibility of a redox series in which the ligand is reduced or oxidised in a number of steps, with the metal oxidation state remaining constant.

The only known example where the full range of this behaviour was shown is the neutral complex $Cr^{III}(SQ)_3$, as shown in equation 1.16.

$$Cr(BQ)_3^{3+} \overset{e^-}{\rightleftarrows} Cr(BQ)_2(SQ)^{2+} \overset{e^-}{\rightleftarrows} Cr(BQ)(SQ)_2^{+} \overset{e^-}{\rightleftarrows} Cr(SQ)_3$$

$$\overset{e^-}{\rightleftarrows} Cr(SQ)_2(cat)^{-} \overset{e^-}{\rightleftarrows} Cr(SQ)(cat)_2^{2-} \overset{e^-}{\rightleftarrows} Cr(cat)_3^{3-}$$

Equation 1.16

This behaviour was most clearly observed with the 9,10-phenanthrenequinone ligand. No such extensive a series is observed with any other metal and this is attributed to the kinetic stability of chromium (III)[62] complexes and the fact that the ligands are more tightly bound to the metal centre than is the case for other such complexes.[49,128]

7.2.2. Experimental data

The potentials found for catechol in this study do not always agree with those reported in the literature. For this reason, too much emphasis should not be put on the actual values of the potentials quoted for the redox processes, but the general behaviour and shapes of the cyclic voltammograms (C.V.'s) should rather be regarded as qualitative evidence for the presence of catechol or of some structural aspect of the complex.

The electrochemical data recorded in this investigation are listed in Table 1.21.

(a) Tris-catecholato complexes

(i) $(Ph_4P)_2[Ir(cat)_3]$

The initial oxidation run for this complex in acetonitrile shows a small peak at + 0.52V, followed by a strong,quite sharp peak, at +1.18V. The reverse scan has a reduction peak at +0.35V. The process is irreversible, and is typical of the oxidation of catechol to o-benzoquinone. Further investigation of the small peak at +0.52V, results in a quasi-reversible couple, with peak separation of 100mV (separation, $\Delta Ep = Ep^{ox} - Ep^{red} = 59/n$ mV for reversible reaction, where n = number of electrons transferred), and $E_{\frac{1}{2}} = 0.47V$[129] when the scan is reversed immediately after recording the oxidation peak. This oxidation process is tentatively assigned to one electron oxidation of catechol to form the semiquinone, and is then further oxidised to benzoquinone. The absence of any peak on the reverse scan after oxidation to the benzoquinone, corresponding to reduction of a semiquinone species indicates the iridium-semiquinone species is only transiently stable.

An initial reduction scan shows a weak peak at +0.54V; the product is oxidised on the reverse run at +0.39V. The ease of reduction suggests it may arise from formation of iridium (III), which is easily reoxidised to iridium (IV). The quasi-reversible nature of the reduction, and the ease with which it occurs is consistent with one electron reduction of the metal centre in a tris(catecholato) complex, where little structural change is involved.[127,126] Such reversible one electron transfers are found for tris(catecholato) complexes of chromium (III), iron (III), manganese (III)[94], and cerium (IV).[39]

(ii) $(Ph_4P)_2[Re(cat)_3]$

Investigation of this complex under similar conditions also resulted in the dominant oxidation peak, characteristic of formation of o-benzoquinone from catechol, at +1.19V, as shown in Figure 1.30. The product of this oxidation was reduced at +0.40V. Again these results indicate the presence of the catecholato ligand.

A further irreversible oxidation peak was observed at +1.70V, and is tentatively assigned to oxidation of rhenium (IV).

(iii) $(Ph_4P)_3[Ru(cat)_3]$

This complex also exhibits the typical oxidation of catechol to benzoquinone.

A reduction peak is observed at -0.66V, with the corresponding anodic peak at -0.38V. Reduction of catechol only results in a totally irreversible process, and we therefore tentatively suggest this process is due to reduction of ruthenium (III) to ruthenium (II). As described above, this is a typical electrochemical process for a tris(catecholato) complex, where the metal has a relatively stable lower oxidation state.

(b) $MoO_2(PSQ)_2$

For the purposes of comparison the cyclic voltammograms of the known complexes $Mo_2O_5(PSQ)_2$ and $RuCl_2(PPh_3)_2(C_{14}H_8O_2)$ ($C_{14}H_8O_2$ is 9,10-phenanthrenequinone bonded in the catechol mode) were also examined.

Oxidation of the complex $RuCl_2(PPh_3)_2(C_{14}H_8O_2)$ results in two almost reversible oxidations, with anodic peak potentials of +0.65V and +1.35V. This type of behaviour has also been reported for $Ru(CO)_2(PPh_3)_2(C_6Cl_4O_2)$, in which two reversible one electron transfer processes were recorded at +0.65V and +1.7V (in dichloromethane with $(C_4H_9)_4NPF_6$ as electrolyte).[130] Similar complexes with different metals only exhibit the first redox couple. In this case, for $RuCl_2(PPh_3)_2(C_{14}H_8O_2)$, by analogy with the reported complexes, the two oxidation peaks may be regarded as successive one-electron oxidations of coordinated 9,10-phenanthrenequinone (in the catecholato mode) to the semiquinone form, and then to the benzoquinone.

The well-characterised semiquinone complex, $Mo_2O_5(PSQ)_2$, exhibits an oxidation peak at +0.72V, the product of which was reduced at +0.42V on the reverse scan. The C.V.'s due to the quinone ligands tend to be much stronger and clearer than those observed for redox processes of the metal centres. The nature of the quasi-reversible oxidation leads to the suggestion that it arises from one electron oxidation of the 9,10-phenanthrenesemiquinone ligand to the benzoquinone. A subsequent weak peak due to an irreversible oxidation probably arises from electron transfer processes of the $Mo_2O_5^{2+}$ core. No evidence was found for consecutive oxidation of each of the 9,10-phenanthrenesemiquinone ligands, as was the case for $Cr(PSQ)_3$.

As expected, the new complex, $MoO_2(PSQ)_2$, behaves very similarly to $Mo_2O_5(PSQ)_2$. Oxidation is observed at +0.68V, with the reverse scan producing a cathodic peak at +0.35V. The product is stable, as shown by holding the pen for five minutes before recording the reverse scan:- the cathodic peak showed exactly the same position and height as observed for the peak recorded immediately. This behaviour again probably arises from one-electron oxidation of the semiquinone ligands to the benzoquinone, and once again, there is no evidence for the separate oxidation of the two ligands. The electrochemical behaviour of this complex therefore adds further evidence to its formulation as $MoO_2(PSQ)_2$, containing a semiquinone ligand.

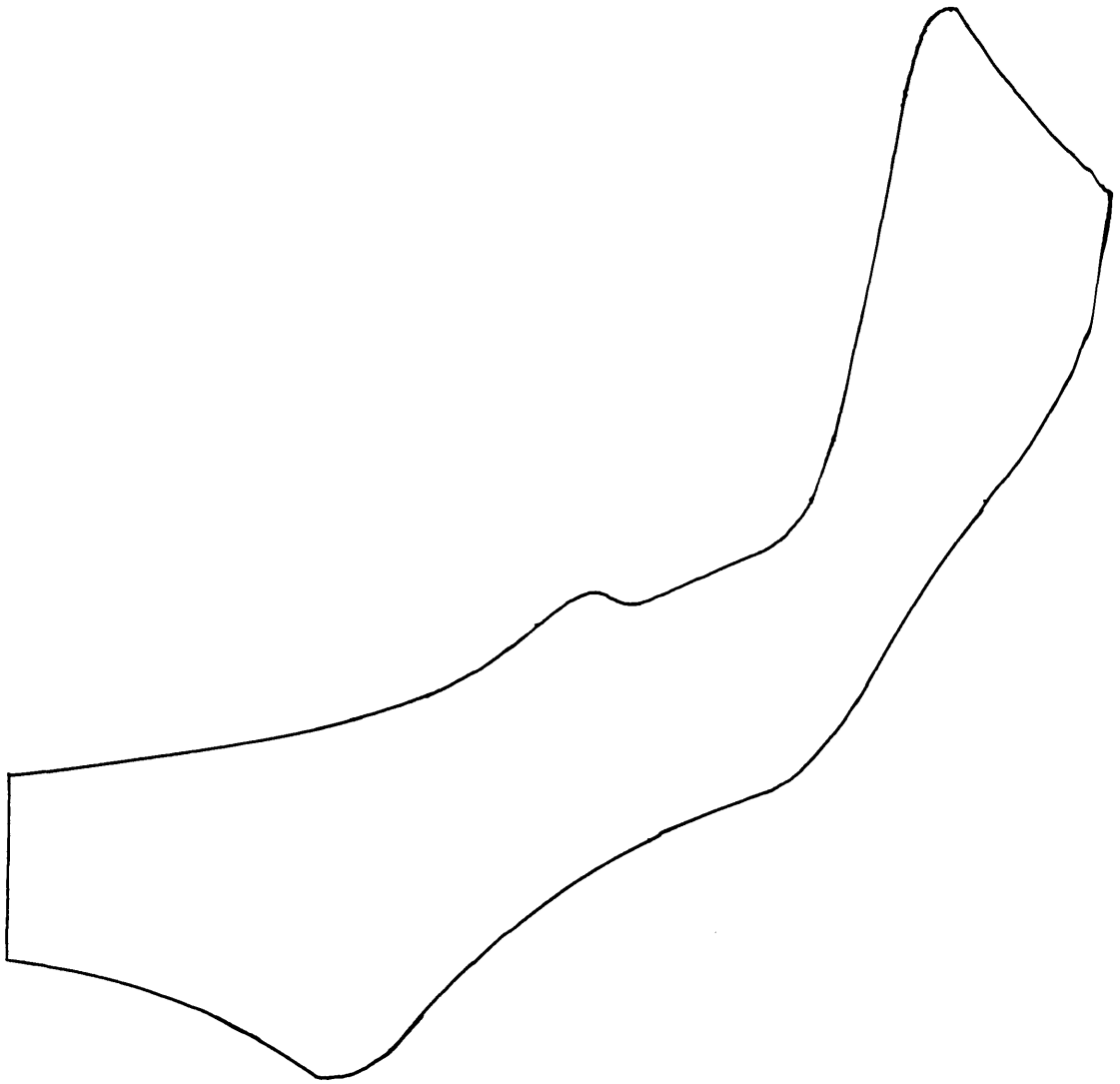


Figure 1.30 - Cyclic voltammogram of $(Ph_4P)_2[Re(cat)_3]$

Oxidation from OV (1cm = 100mV)

Table 1.21:- Electrochemical data

Complex	Ep^{ox}	Ep^{red}	Probable reaction
$(Ph_4P)_2[Ir(cat)_3]$	+0.52V		$cat^{2-} \rightarrow SQ^- + e^-$
	+1.18V		$SQ^- \rightarrow Q + e^-$
		+0.35V	$Q + 2e^- \rightarrow cat^{2-}$
	+0.52V		$Ir(IV) + e^- \rightarrow Ir(III)$
		+0.68V	$Ir(III) \rightarrow Ir(IV) + e^-$
$(Ph_4P)_2[Re(cat)_3]$	+1.22V		$cat^{2-} \rightarrow Q + 2e^-$
		+0.40V	$Q + 2e^- \rightarrow cat^{2-}$
	+1.69V		$Re(IV) \rightarrow Re$
$(Ph_4P)_3[Ru(cat)_3]$	+1.39V		$cat^{2-} \rightarrow Q + 2e^-$
		+0.36V	$Q + 2e^- \rightarrow cat^{2-}$
		-0.66V	$Ru(III) + e^- \rightarrow Ru(II)$
	-0.38V		$Ru(II) \rightarrow Ru(III) + e^-$
$RuCl_2(PPh_3)_2$ $(C_{14}H_8O_2)$	+0.64V		$cat^{2-} \rightarrow SQ^- + e^-$
		+0.42V	$SQ^- + e^- \rightarrow cat^{2-}$
	+1.35V		$SQ^- \rightarrow Q + e^-$
		+1.27V	$Q + e^- \rightarrow SQ^-$
$Mo_2O_5(PSQ)_2$	+0.72V		$SQ^- \rightarrow Q + e^-$
		+0.44	$Q + e^- \rightarrow SQ^-$
$MoO_2(PSQ)_2$	+0.68V		$SQ^- \rightarrow Q + e^-$
		+0.35V	$Q + e^- \rightarrow SQ^-$

Recorded in acetonitrile solutions, 1 - 5 m molar in sample, 100 m molar in electrolyte (tetrabutyl ammonium perchlorate), from +1.0V to -1.0V. All voltages are measured vs. saturated calomel electrode (S.C.E.).

Ep^{ox} is potential of oxidation peak

Ep^{red} is potential of reduction peak.

RESUME OF CHAPTER I

The preparation, vibrational, ^{1}H and ^{13}C N.M.R. and E.P.R. spectra, and electrochemical properties of a number of catecholato, substituted catecholato, semiquinone, 1,2-aminophenol, and cyclohexane-1.2-diolato complexes are reported.

The following new complexes have been prepared and studied by the above methods:- $(Ph_4P)_2[Ir(cat)_3]2H_2O$; $(Ph_4P)_2[Re(cat)_3]H_2O$; $(Ph_4P)_3[Ru(cat)_3]3H_2O$; $Na_2[W_2O_5(cat)_2]2H_2O$; $MoO_2(PSQ)_2$; $MoO_2(C_6H_6NO)_2$; $K_2[OsO_2(C_6H_5NO)_2]$. Improved preparations of $K_2[MoO_2(cat)_2]H_2O$, $K_2[MoO_2(cat)_2]C_6H_4(OH)_2$, and of $Mo_2O_5(PSQ)_2$ are described. The following complexes reported in the literature are reformulated (reformulations in parentheses):- (pyH) H $[MoO_3(cat)]1\frac{1}{2}H_2O$ ($(pyH)_2[Mo_2O_5(cat)_2]$); $K[MoO_2(OH)(cat)]$ ($K_2[Mo_2O_5(cat)_2]$), $(NH_4)[MoO_2(OH)(C_6H_4O_3)]$ ($(NH_4)_2[Mo_2O_5(C_6H_4O_3)_2]$.)

8. EXPERIMENTAL

The complexes were prepared as follows:-

8.1 Catecholato complexes

(a) Bis (tetraphenyl phosphonium) tris (catecholato) iridium (IV)

$(Ph_4P)_2[Ir(cat)_3]\ 2H_2O$

The method used was adapted from that described for $K_3[Cr(cat)_3]$[131] and $K_3[Fe(cat)_3]$.[12]

Method 1 Sodium hexachloroiridate, $Na_2[IrCl_6]$ (0.5g, 0.001 moles) and catechol (0.33g, 0.003 moles) were dissolved in water ($10cm^3$) and the red-brown solution degassed with nitrogen. Sodium hydroxide (0.4g, 0.01 moles) in water ($5cm^3$) was degassed and added anaerobically to the iridium (IV) solution. This immediately became a very dark green colour. It was left to stand for fifteen minutes. Tetraphenylphosphonium chloride (0.75g, 0.002 moles) in degassed water ($10cm^3$) was added under nitrogen. The solution was left to stand until a thick green precipitate formed. After standing for about two hours, the solid was filtered anaerobically. The product was washed with water, then dried under a nitrogen stream, then in a desiccator over concentrated sulphuric acid.

$[(C_6H_5)_4P]_2[Ir(C_6H_4O_2)_3]2\ H_2O$

Found:- C = 64.7, H = 4.4

$C_{66}H_{56}IrO_8P_2$ requires:- C = 64.4, H = 4.6%

Yield = 30%

Method 2 This complex was also prepared from iridium trichloride:-

Hydrated iridium chloride (0.1g, 0.0003 moles) was dissolved in water ($10cm^3$) by warming, and catechol (0.1g, 0.0003 moles) added. The green solution was degassed. Potassium hydroxide (0.2g, 0.004 moles) in degassed water ($5cm^3$) was added anaerobically to the iridium solution, which immediately turned red. No precipitate was observed after fifteen minutes, so tetraphenylphosphonium chloride (0.33g, 0.0009 moles) in degassed water ($5cm^3$) was added. A cloudiness with a fine flocculent precipitate was immediately observed. After standing for an hour, the precipitate was filtered off under nitrogen, and washed with a little degassed water. It was dried by passing nitrogen over it, then in a desiccator over concentrated sulphuric acid. The precipitate became green even before it was totally exposed to the air.

$[(C_6H_5)_4P]_2[Ir(C_6H_4O_2)_3]$ 3 H_2O

Found:- C = 63.6, H = 4.6%

$C_{66}H_{58}IrO_9P_2$ requires:- C = 63.5, H = 4.7%

Yield = 25%

b) Bis(tetraphenylphosphonium)tris(catecholato)rhenium (IV), $(Ph_4P)_2[Re(cat)_3]H_2O$

A similar method to that described for the iridium (IV) - catecholato complex was used. A solution of $K_2[ReCl_6]$ (0.02g, 0.0004 moles) and catechol (0.14g 0.0013 moles) in water ($5cm^3$) was degassed. Potassium hydroxide (0.3g, 0.005 moles) in degassed water ($5cm^3$) was added anaerobically. The light green solution immediately became very dark green.

After standing for fifteen minutes, no precipitate was observed, so tetraphenyl phosphonium chloride (0.49g, 0.0013 moles) in degassed water ($10cm^3$) was added under nitrogen. After standing in the refrigerator overnight the resulting purplish solid was filtered off under nitrogen, and washed with water. It was dried under the nitrogen stream and then in a de.siccator over concentrated sulphuric acid.

$[(C_6H_5)_4P]_2\ [Re(C_6H_4O_2)_3]\ H_2O$

Found:- C = 65.4, H = 4.5, P = 4.5%

$C_{66}H_{54}O_7P_2Re$ requires C = 65.7, H = 4.5, P = 5.1%

Yield = 20%

c) Tris (tetraphenylphosphonium)tris(catecholato)ruthenium(III) $(Ph_4P)_3[Ru(cat)_3]$

Tris (acetylacetonato) ruthenium (III), $Ru(acac)_3$, (0.102g, 0.00005 moles) was dissolved in methanol ($5cm^3$) and degassed. Potassium hydroxide (0.1g, 0.002 moles) dissolved in degassed water ($5cm^3$) was added anaerosically to a solution of catechol (0.02g, 0.00018 moles) in degassed methanol ($5cm^3$). This mixture was immediately added, under nitrogen, to the ruthenium solution. The dark red solution was stirred and warmed for an hour. Tetraphenylphosphonium chloride (0.056g, 0.00015 moles) in degassed water ($5cm^3$) was transferred to the reaction mixture under nitrogen. No colour change was seen, so the solution continued to be warmed and stirred. After standing overnight the resulting dark red solid was filtered off under nitrogen, and then dried in a de siccator over concentrated sulphuric acid, $[(C_6H_5)_4P]_3[Ru(C_6H_4O_2)_3]\ 3H_2O$

Found:- C = 72.3, H = 5.3, P = 6.7%

$C_{90}H_{78}O_9P_3Ru$ requires:- C = 72.2, H = 5.3, P = 6.2%

Yield = 35%

d) Bis (potassium) bis (catecholato) cis-dioxo-molybdenum (VI)

$K_2[MoO_2(cat)_2]H_2O$

The preparation of this complex is described in the literature,[44] but the following modification was found to be more satisfactory.

Molybdenum trioxide (0.7g, 0005 moles) was added to a solution of potassium hydroxide (0.55g, 0.01 moles) in water ($7.5cm^3$), and dissolved by gentle warming and stirring. This solution was filtered into a flask containing catechol (1.1g, 0.01 moles). A deep red solution formed immediately, as the solid dissolved. This solution was then heated gently and left to stand for several days. The red product was filtered off, washed with a little ethanol and diethyl ether and dried in a desiccator over concentrated sulphuric acid. It was recrystallised from water.

$K_2[MoO_2(C_6H_4O_2)_2]H_2O$

Found:- C = 32.7, H = 2.0

$C_{12}H_{10}K_2MoO_7$ requires:- C = 32.7, H = 2.3%

e) Bis (pyridinium) bis(catecholato) cis-dioxo molybdenum (VI)

$(C_5H_6N)_2[MoO_2(cat)_2]$

The literature procedure was followed.[43] Molybdenum trioxide (1.4g, 0.01 moles), catechol (2.2g, 0.02 moles) and pyridine were refluxed in water ($30cm^3$). After thirty minutes the solution was filtered hot, and left to stand. An orange-red crystalline product was soon observed. It was filtered off, washed with ethanol and diethyl ether, and dried in a desiccator.

$(C_5H_6N)_2[MoO_2(C_6H_4O_2)_2]$

Found:- C = 52.5, H = 4.0, N = 5.6

$C_{22}H_{20}MoN_2O_6$ requires:- C = 52.4, H = 4.0, N = 5.6%

f) Bis (ammonium) bis(catecholato)-μ-oxo-bis(cis-dioxo-molybdenum(VI)), $(NH_4)_2[Mo_2O_5(cat)_2]\ 2H_2O$

The method used was that described for "$NH_4H\ [MoO_3(cat)]\ 1\frac{1}{2}H_2O$".[43] This was subsequently found to be $(NH_4)_2[Mo_2O_5(cat)_2]$ by X-ray crystallographic studies.[69]

Ammonium molybdate (1.96g, 0.01 moles) was dissolved in water ($20cm^3$) by warming. The solution was filtered. Catechol (1.1g, 0.01 moles) in water ($10cm^3$) was added. Immediately the colourless solution became dark red. The solution was reduced by heating, until solid first started to appear, then it was left to cool. The resulting dark red solid was filtered off, washed with ethanol and diethyl ether, and dried in a desiccator.

$(NH_4)_2[Mo_2O_5(C_6H_4O_2)_2]\ 2H_2O$

Found:- C = 25.8, H = 3.6, N = 5.1

$C_{12}H_{20}Mo_2N_2O_{11}$ requires:- C = 25.7, H = 3.6, N = 5.0%

g) Bis (Potassium) bis(catecholato) -μ- oxo - bis (cis-dioxo-molybdenum(VI), $K_2[Mo_2O_5(cat)_2]$

The literature method for "$K[MoO_2(OH)(cat)]$"[44] was followed. Molybdenum trioxide (1.4g, 0.01 moles) and potassium hydroxide (0.6g, 0.01 moles) were dissolved by warming in water ($20cm^3$). The solution was filtered into a flask containing catechol (1.1g, 0.01 moles). The resulting dark orange-red solution was reduced slightly by heating and left to stand. The red-brown precipitate that formed was filtered off, washed with ethanol and diethyl ether, and dried in a desiccator.

Found:- C = 25.1, H = 1.7

$K[MoO_2(OH)(C_6H_4O_2)]$ requires:- C = 24.7, H = 1.4

$K_2[Mo_2O_5(C_6H_4O_2)_2]$ requires:- C = 25.5, H = 1.4%

h) Bis (pyridinium) bis (catecholato) μ - oxo - bis (cis - dioxo-molybdenum (VI)), $(pyH)_2[Mo_2O_5(cat)_2]$

The method used was that described in the literature for "(pyH) H $[MoO_3(cat)]$ $1\frac{1}{2}H_2O$"[43]

Molybdenum trioxide (1.4g, 0.01 moles), catechol (1.1g, 0.01 moles) and pyridine (1.6cm^3) were refluxed in water (50cm^3). After twenty minutes the solution was filtered hot and left to stand. The resulting orange-red precipitate was filtered off, washed with a little cold water, and dried in a de siccator over concentrated sulphuric acid.

Found:- C = 39.1, H = 3.1, N = 4.0

(pyH)H $[MoO_3(C_6H_4O_2)]$ requires:- C = 39.9, H = 2.7, N = 4.2

$(pyH)_2[Mo_2O_5(C_6H_4O_2)_2]$ requires:- C = 38.8, H = 3.0, N = 4.1%

i) Bis (ammonium) bis (pyrogallolato) cis-dioxo-molybdenum (VI), $(NH_4)_2[MoO_2(C_6H_4O_3)_2]$

The method described in the literature was used.[44] Ammonium molybdate (4.2g, 0.018 moles) was dissolved in water (15cm^3). Pyrogallol (6.0g, 0.05 moles) was added. The solution immediately became dark red-brown in colour. It was left to cool, then 35% ammonia (2.6cm^3) was added. The solution was heated, then left to stand. The resulting red-brown solid was filtered off, washed with a little cold water and dried in a de siccator over concentrated sulphuric acid.

$(NH_4)_2[MoO_2(C_6H_4O_3)_2]$

Found:- C = 34.5, H = 3.7, N = 6.6

$C_{12}H_{16}MoN_2O_2$ requires:- C = 35.0, H = 3.9, N = 6.8%

j) Bis (ammonium) bis (pyrogallolato) μ - oxo - bis (cis-dioxo molybdenum (VI)), $(NH_4)_2[Mo_2O_5(C_6H_4O_3)_2]2H_2O$

The literature method described for "(NH_4) $[MoO_2(OH)(C_6H_4O_3)]$" [44] was used. Pyrogallol (0.3g, 0.02 moles) was added to a solution of ammonium molybdate (4.2g, 0.02 moles) in water ($15cm^3$). The very dark solution was reduced slightly by heating. After standing for a day, the resulting product was filtered off, washed with ethanol and diethyl ether, and dried in a desiccator.

Found:- C = 24.5, H = 2.8, N = 4.3

(NH_4) $[MoO_2(OH)(C_6H_4O_3)]$ requires:- C = 25.1, H = 3.2, N = 4.9

$(NH_4)_2[Mo_2O_5(C_6H_4O_3)_2]$ requires C = 24.4, H = 3.0, N = 4.8%

k) Bis (potassium) bis(catecholato) cis dioxo-molybdenum (VI) with catechol of crystallisation, $K_2[MoO_2(cat)_2]C_6H_4(OH)_2H_2O$

The method for the preparation of this complex is described in the literature.[44] However, in this work, it was found more successful to use the method described for the formation of $K_2[MoO_2(cat)_2]$ [44] but using excess catechol.

Potassium hydroxide (1.4g, 0.025 moles) was added to a solution of ammonium molybdate (2.1g, 0.011 moles) in water ($10cm^3$), immediately giving an effervescence. The solution was heated for thirty minutes to expel ammonia, after which time it was filtered into a flask containing catechol (2.62g, 0.024 moles). The solution immediately became deep red in colour. It was heated until solid appeared on the surface. The solution was then left to stand, and the

resulting solid was filtered off, washed with a little water, and dried in a desiccator.

$K_2[MoO_2(C_6H_4O_2)_2]\ C_6H_4(OH)_2.H_2O$

Found:- C = 39.7, H = 2.8

$C_{18}H_{16}K_2MoO_9$ requires: C = 39.3, H = 2.9%

l) Bis (pyridinium) bis (catecholato) cis-dioxo-molybdenum (VI), with catechol of crystallisation, $(pyH)_2[MoO_2(cat)_2]C_6H_4(OH)_2$

The method used was that described in the literature for the preparation of "$2[MoO_2(cat)_2](pyH)_2.3C_6H_4(OH)_2.4H_2O$".[43]

Molybdenum trioxide (1.4g, 0.01 moles) catechol (5.5g, 0.05 moles) and pyridine ($8cm^3$) were refluxed in water ($50cm^3$). After thirty minutes the solution was filtered hot and left to stand. The orange-red crystalline precipitate was filtered off and washed with a little ethanol and diethyl ether. It was dried in a desiccator over concentrated sulphuric acid.

$(C_5H_6N)_2[MoO_2(C_6H_4O_2)_2]C_6H_4(OH)_2$

Found:- C = 54.2, H = 4.1, N = 4.6

$C_{28}H_{26}MoN_2O_8$ requires:- C = 54.7, H = 4.3, N = 4.6%

m) Bis (sodium) bis (catecholato)-μ-oxo-bis (cis-dioxo-tungsten (VI)) $Na_2[W_2O_5(cat)_2]2H_2O$

Sodium tungstate (0.29g, 0.001 moles) was dissolved in water ($10cm^3$). A solution of catechol (0.11g, 0.001 moles) in water ($5cm^3$) was added. The colourless solutions immediately became yellow-green on mixing.

The solution was reduced by heating, until solid was first seen to form, then it was left to stand. The resulting

yellow-green precipitate was filtered off, washed with ethanol and diethyl ether. It was dried in vacuo.

$Na_2[W_2O_5(C_6H_4O_2)_2]2H_2O$

Found:- C = 19.4, H = 1.9

$C_{12}H_{12}Na_2O_{11}W_2$ requires:- C = 19.3, H = 1.6%

8.2 Semiquinone Complexes

a) Bis (9,10-phenanthrenesemiquinonato) cis-dioxo-molybdenum (VI), $MoO_2(PSQ)_2$

The method used was a modification of that described for $Mo_2O_5(PSQ)_2$.[64]

Molybdenum hexacarbonyl, $Mo(CO)_6$, (0.5g, 0.002 moles) and 9,10-phenanthrenequinone (0.5g, 0.002 moles) were refluxed under nitrogen for three hours, in dichloromethane ($50cm^3$), whilst being irradiated with ultraviolet light. During this time, a dark green solid formed, and it was filtered off in air. It was dried in a desiccator.

$MoO_2(C_{14}H_8O_2)_2$

Found:- C = 61.8, H = 3.1

$C_{28}H_{16}MoO_6$ requires:- C = 61.8, H = 3.0%

Yield = 40%

All attempts at recrystallisation resulted in formation of orange crystals, found by infrared spectroscopy and elemental analyses to be the starting ligand, 9,10-phenanthrenequinone.

b) Bis (9,10-phenanthrenesemiquinonato) -μ-oxo-bis (cis-dioxo-molybdenum (VI)), $Mo_2O_5(PSQ)_2$

The literature method could not be successfully repeated; it described the reaction as taking place only "under the fluorescent lights of the laboratory" suggesting the reaction was photocatalysed. We therefore irradiated the reaction mixture of molybdenum hexacarbonyl (0.5g, 0.002 moles) and 9.10-phenanthrenequinone (0.5g, 0.002 moles) in dichloromethane ($50cm^3$) with ultra-violet light for one hour, whilst refluxing under nitrogen. The resulting green solid was filtered off in air, and dried in a de sicator.

$Mo_2O_5(C_{14}H_8O_2)_2.CH_2Cl_2$

Found:- C = 44.7, H = 2.4

$C_{29}Cl_2H_{18}Mo_2O_9$ requires:- C = 45.1, H = 2.4%

8.3 Ortho-amino phenol complexes

a) Bis (o-aminophenol) cis-dioxo-molybdenum (VI), $MoO_2(C_6H_6NO)_2$

Ammonium molybdate (0.45g, 0.0023 moles) was dissolved in water ($10cm^3$) and degassed. Ortho-aminophenol (0.5g, 0.0046 moles) dissolved in degassed water ($25cm^3$) was added anaerosically to the molybdenum (VI) solution. As the yellow o-aminophenol solution was added, the molybdenum solution became slightly orange. The mixed solutions were heated gently for a while, leading to formation of a green precipitate. This was filtered off under nitrogen, and washed

with water. The green-brown solid was dried in the air in a desiccator over concentrated sulphuric acid.

$MoO_2(C_6H_6NO)_2$

Found:- C = 42.0, H = 3.5, N = 8.2

$C_{12}H_{12}MoN_2O_4$ requires:- C = 41.9, H = 3.5, N = 8.1%

b) Bis (potassium) bis (o-aminophenol) trans-dioxo-osmium (VI)

$K_2[OsO_2(C_6H_5NO)_2]$

This new complex was prepared by a method similar to that described for the analogous complexes of catechol, $K_2[OsO_2(cat)_2]$.[19]

Potassium osmate, $K_2[OsO_2(OH)_4]$, (0.25g, 0.0007 moles) was dissolved in water ($10cm^3$) by stirring. Ortho-aminophenol (0.15g, 0.0014 moles) was dissolved in ethanol ($15cm^3$) by stirring and was added to the osmium solution. The purplish colour of the potassium osmate solution appeared to become very dark green, then very dark blue (although the depth of colour was so great it was difficult to identify exact colours). A very dark, fine precipitate formed gradually. It was filtered off, and washed with ethanol and diethyl ether, then dried in a desiccator.

$K_2[OsO_2(C_6H_5NO)_2]$

Found:- C = 27.7, H = 1.9, N = 5.2

$C_{12}H_{10}K_2N_2O_4Os$ requires:- C = 28.0, H = 2.0, N = 5.4%

The following complexes were prepared as described in the literature:-

$K_3[Fe(cat)_3]$,[12] $K_3[Cr(cat)_3]$,[131] $Cr(PSQ)_3$, $RuCl_2(PPh_3)_2(C_{14}H_8O_2)$,[32] $Mo_2(O_2C_6Cl_4)_6$,[71] $[MoO(3,5\text{-}DTBC)_2]_2$,[17] $Pt(PPh_3)_2(cat)$,[27] $[Co(en)_3][Rh(cat)_3]$,[11] $UO_2(cat).H_2O$,[41] $K_2[OsO_2(cat)_2]$,[19] $Pd(C_6H_6NO)_2$,[101] MoO_2(cyclohexanediol)$_2$,[132] OsO_2(pyridine)$_2$(cyclohexanediol).

Complexes of molybdenum (VI) and osmium (VI) with substituted catechols were prepared by using the appropriate method described above.

CHAPTER II COMPLEXES CONTAINING CATECHOLAMINES AS LIGANDS

Our work on catecholato complexes (Chapter I) prompted us to study the reactions of catecholamines, which contained the 1,2-dihydroxybenzene (catechol) group, with transition metals. For the sake of brevity, the trivial names for the five catecholamines studied here are used throughout.

1. INTRODUCTION

1.1 The catecholamines

(a) Nomenclature and structure

Biogenic amines possessing a 1,2-dihydroxyphenyl (catechol) nucleus are generally called catecholamines. They have an important physiological role as hormones and neurotransmitters. The three most important biologically are[133]:- adrenaline (epinephrine) or 4-(1-hydroxy)-2-(methylamino)-ethyl-1,2-benzenediol (I); noradrenaline (norepinephrine) or 4-(2-amino-1-hydroxethyl)-1,2-benzenediol (II); and dopamine (hydroxtyramine) or 4-(2-amino-ethyl)-1,2-benzenediol (III). The amino acid, Dopa, or 1,2-dihydroxyphenylalanine (IV), a precursor of dopamine, and the N-isopropyl derivative, isoproterenol (V) are also considered. The structures are shown in Figure 2.1.

The hydrochlorides of dopamine, noradrenaline and isoproterenol were used in this work, and they have the following type of structure (Figure 2.2).

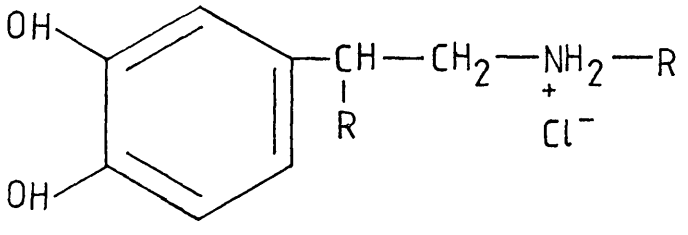
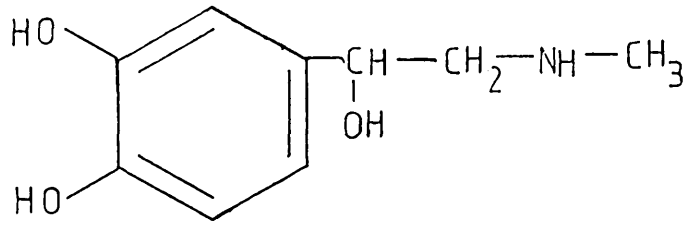
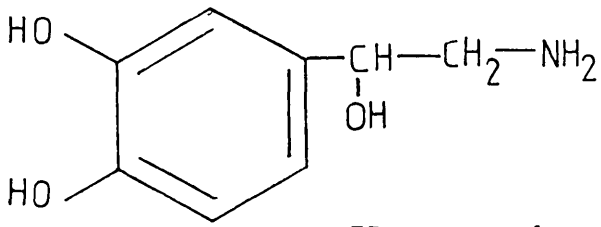


Figure 2.2:- Structure of hydrochoride salts of some catecholamines.

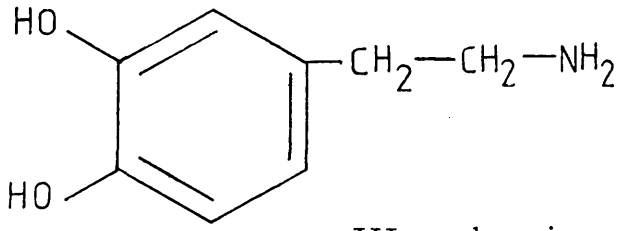
Figure 2.1 - Structures of the catecholamines.



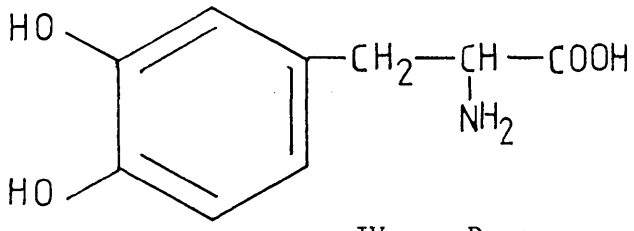
I adrenaline



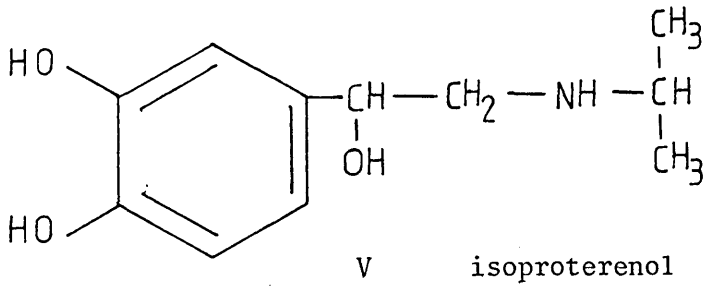
II noradrenaline



III dopamine



IV Dopa



V isoproterenol

The free ligands, adrenaline and Dopa are Zwitterions. In adrenaline[134] the proton of the meta-hydroxy group is transferred to the amino group, as shown in Figure 2.3.

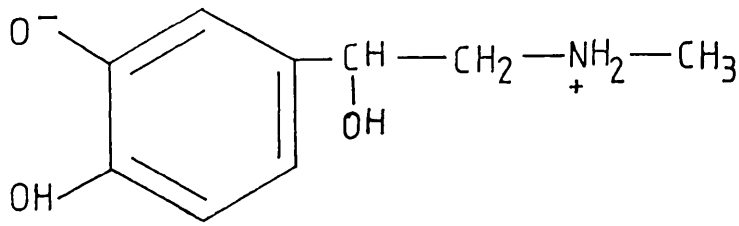


Figure 2.3 The Adrenaline Zwitterion

The amino-acid side chain of Dopa also forms a Zwitterion.[135]

(b) Biochemical function

The catecholamines dopamine, adrenaline and noradrenaline act as neurotransmitters in the brain and nervous system. Nervous impulses are transmitted electrochemically through the nerve cells or neurones. At the junction of two nerve cells, or where a nerve meets muscle, is the region called the synapse.[136] In this area the nervous impulse is transmitted using a specific set of chemical reactions involving certain key substances known as neurotransmitters. The neurotransmitter is stored in vesicles within the nerve cell, and it is only released in response to the correct electrochemical message. The neurotransmitter diffuses across the small gap between the nerve cells (the synapse) to the adjacent cell where it stimulates an electrical nerve impulse by interacting with receptors on the cell membrane surface.[137] There is some evidence to suggest that there are at least two receptor sites, A and B, with the possibility that the catecholamine may bind differently at each site.

Adrenaline and noradrenaline[138] also behave as typical hormones, secreted from the adrenal medulla,[139] then transported to the target organ through the bloodstream. Uptake of the hormone by the organ then regulates its metabolism.

Dopa acts as the precursor to dopamine in the biosynthesis of catecholamines.[140] Isoproterenol has been found in the adrenal glands of cats.[141]

Naturally occurring adrenaline, noradrenaline, and Dopa are all found in the laevo-rotatory form.[141]

Any abnormality in the behaviour of the catecholamines or the agents interacting with them can lead to very serious effects. Insufficient dopamine in a specific region of the brain has been identified as the cause of Parkinson's disease[102,103] and this is treated by dosing the patient with L-Dopa.[102,103] Schizophrenia,[144] aging,[145] epilepsy,[136,137] depression,[147,148] hypertension,[146] and breast cancer[149] have each been associated with catecholamine activity.

A number of catecholamines have also lately been found to possess antitumour activity,[150] and their importance to medicine seems likely only to increase as we learn more about their behaviour.

(c) Interactions of catecholamines with metals

These interactions are very important biologically. Copper (II) ions are known to participate in the hydroxylation of dopamine to form noradrenaline by the enzyme dopamine-β-hydroxylase[151] and, indeed, other copper (II) - containing enzymes catalyse oxidative transformations of certain catecholamines. Transport of Dopa across the blood-brain barrier is thought to be facilitated by chelation to copper (II) and zinc (II) ions.[146] The metals copper, magnesium, iron, and zinc appear consistently in certain

regions of high catecholamine concentration,[153,154,155,156,157] especially in the synaptic region of the nerve cells. It would seem likely that these metals are involved to some extent in the transport, storage and receptor site binding of catecholamines, particularly in conjunction with adenosine triphosphate (ATP), also found in high concentrations in these regions.

Noradrenaline and adrenaline have also been used as antihistamine agents.[158] It is thought that antihistaminic activity may involve competitive binding at a metal ion site. Any elucidation of the interactions of adrenaline and noradrenaline with metal ions would shed more light on this process.

(d) Histochemical location of catecholamines using the electron microscope

The location and identification of catecholamines for electron microscopic studies has led to the development of a number of techniques in which a heavy metal is used to stain the tissue of catecholamine-rich sites, to delineate different cell types. Before staining is carried out, some preparation of the cells is required. Fixation preserves the original structure of the cell.[159] Common fixatives are glutaraldehyde and osmium tetroxide, OsO_4, used in buffered aqueous solutions. Staining may be carried out during or after fixation, although staining is not always necessary after fixation by OsO_4. Although OsO_4 has long been used[160] in electron microscopic studies of biological tissue, little is known of its actual mode of action. Other common staining agents are uranyl acetate and lead citrate.

Identification of catecholamine-containing sites has been largely associated with OsO_4 treatment,[161,162,163] picking out the vesicles in the nerve cells. Since OsO_4 is known to stain a variety of biological compounds, there has been some debate as to which substances in the vesicle actually react with OsO_4, and in what manner. It seems that OsO_4 alone will react with phenols containing ortho-hydroxy groups, resulting in very stable chelate complexes, in which the catecholato unit is the coordinating moiety. The resulting Os(VI) species are much less reactive than those osmium esters formed by reaction of OsO_4 with olefins.[164] This enhanced stability may arise from conjugation with the aromatic ring, permitted by coordination through the phenolic oxygen atoms to osmium. This type of reaction may explain the enhanced contrast obtained with certain tissues where they are prefixed with o-dihydroxy phenolic species, such as tannic acid, before conventional fixation with OsO_4.[165,166,167,168]

1.2 Catecholamine Complexes with transition metals

The roles of OsO_4, uranyl acetate, and lead citrate as possible centres for catecholamine complex formation on staining of catecholamine-containing tissues, lead us to investigate complexes of these metals with the five catecholamines listed above. We review here the literature on catecholamine-metal complexes. Much of the data refer only to solutions, so structural results are sparse. Few complexes have been isolated. Most of the published work has concerned complexes of Dopa.

(a) Complexes with Dopa

The amino-acid Dopa (Figure 1.2 (IV)) has two potential chelating sites - being able to coordinate to a metal ion via the amino acid group (O,N) or through the catecholato site (O,O).

A number of solution studies have investigated the mode of chelation of Dopa with various transition metals at differing pH values. The Cu(II) - Dopa system has been most extensively studied. On the basis of potentiometric and spectrophotometric data, it was suggested that the mode of coordination was dependent on the pH of the reaction medium. Complexes were proposed have (O,N) chelation at lower pH,[152] (O,O) chelation at higher pH, and one at intermediate pH having a mixed mode of chelation i.e. one ligand bound via the (O,N) site, the other via the (O,O) site within the same molecule. A number of cyclic and open chain dimeric species were also proposed. Electron spin resonance studies in nonaqueous solution indicated that the Cu (II) ions were coordinated to Dopa at the amino acid site.[169] Two Cu (II) - Dopa complexes have been isolated,[170] confirming the theory that the different modes of chelation are favoured at different pH's. At pH 5, a blue-purple complex was isolated, sparingly soluble in water and methanol, but soluble in DMF and DMSO. It was studied by E.P.R. electronic and cyclic voltammetric techniques. It was concluded that the ligand was coordinated through the amino acid site (Figure 2.4) with trans-square planar coordination geometry.

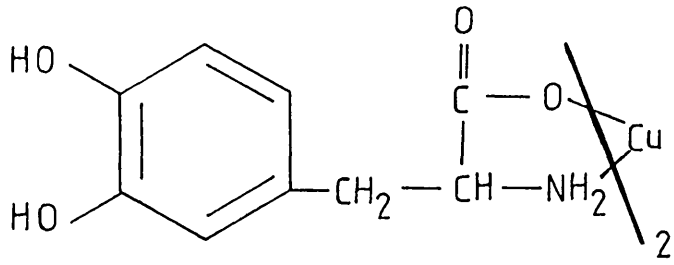


Figure 2.4 Cu(O,N-Dopa)

An olive-green, water soluble complex was isolated at pH 9.5. It was characterised by cyclic voltammetric, infra-red, and absorption spectra as $(NH_4)_2$[Cu (O,O-Dopa)$_2$]4 H_2O, with a square-planar CuO_4 coordination sphere. When this compound was redissolved in water, the pH was found to be 6.4, and the electronic spectrum indicated the presence of only one species. Thus, even below physiological pH, the (O,O) bound form is a viable species, although it is not formed exclusively when solutions of Cu(II) and Dopa are mixed in a 1:2 molar ratio at pH 7. Since neither the (O,O) nor the (O,N) complexes are exclusively formed at physiological pH, some mixed mode of bonding may occur.

Spectrophotometric and potentiometric studies of nickel (II) interactions with Dopa showed different behaviour from that of other transition metals studied.[171] Nickel (II) forms many complexes with amino acids. In a 2:1 molar mixture of Dopa and Ni(II) there is apparently no binding via the catechol moiety.[172]

However, Ni(II) does appear to form a mixed complex in solution; one ligand bound via the amino acid site, the other through the catechol moiety, within the same molecule.

Solution studies of the interactions of iron,[173] manganese[135] and the uranyl[171] group indicate these metals appear to have a greater affinity for the catecholato mode of bonding. A series of transition metals were found, by potentiometric and spectrophotometric studies, to bind to the amino acid chelation site of Dopa[174] in the pH range 3 - 7.

(b) Complexes with other catecholamines

Dopamine (Figure 2.1(III)) may coordinate to metal ions via the amine group, or chelate using the cis-hydroxy groups of the catechol moiety. The other catecholamines we have studied may also coordinate through their amine groups and the β-hydroxy groups (Figure 2.5).

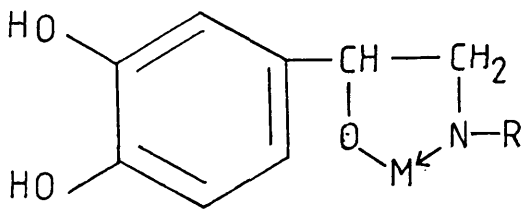


Figure 2.5:- Binding through the amine site of the catecholamine, Chelation between the amine nitrogen and a phenolic oxygen is stereochemically impossible.[175]

Again there have been a number of solution studies investigating the nature of the interactions between transition metals and these catecholamines. Copper (II) ions[151,158,174,175,176] were found to form catecholato complexes when mixed in a 1:2 molar ratio.

Various complexes appear to form with mixed modes of bonding.[158] Only in equimolar solutions where water otherwise occupies the co-ordination positions, does appreciable amine bonding occur to form polymeric species.[175]

In solutions where more stable complexes are formed with catecholamines a large number of species are expected to exist with varying degrees of protonation. The less stable complexes are more liable to hydrolysis, with precipitation of the resulting metal hydroxides taking place at a pH too low to allow formation of the 2:1 complexes. This was found for complexes of zinc (II), cadmium (II) and Pb(II).[174]

Complexes of dopamine and isoproterenol (Figure 2.1(V)) with copper (II), nickel (II) and cobalt (II) ions have been isolated.[177] They were characterised by elemental analysis and infrared spectroscopy, and studied by conductometric and spectrophotometric techniques.

The complexes were prepared by reflux of neutral solutions of the metal salt and the ligand in a 1:2 metal:ligand mole ratio. Results showed that co-ordination took place through the catechol moiety, but only one of the hydroxy groups is deprotonated (as shown in Figure 2.6).

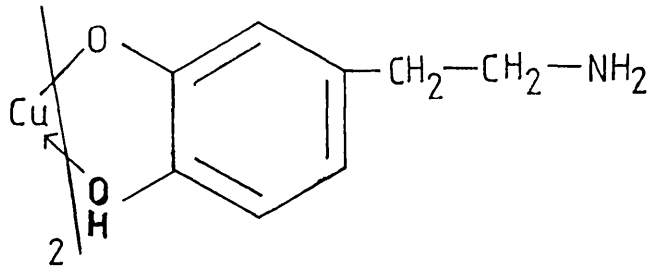


Figure 2.6 $Cu(dopamine)_2$

Complexes of the type $M(PPh_3)_2$(catecholamine),[150,178] (where M = Pd(II), Pt(II); catecholamine = dopamine, L-Dopa, L-noradrenaline, L-adrenaline, DL-isoproterenol, α-methyl dopa, D.L-dops and adrenalone) have been isolated by reaction of $M(PPh_3)_2Cl_2$ in alcoholic potassium hydroxide solution and a stoichiometric amount or slight excess of ligand, under anaerosic conditions. Characterisation by infrared and ^1H N.M.R. techniques indicated the ligand was bound via its two deprotonated cis-hydroxy groups i.e. in the catecholato mode.

Reaction of adrenaline with uranyl chloride or uranyl acetate[179] in methanol solution resulted in the isolated products UO_2(adrenaline) $Cl.2H_2O$ and UO_2(adrenaline)$(CH_3COO)2H_2O$ respectively. The stoichiometry of these complexes suggests that adrenaline is coordinated as a monoanion. However, the report does not discuss the infrared evidence in terms of which mode of binding is present in those complexes, but suggests it is via the catecholato site.

1.3 New catecholamine complexes

(a) Investigation of catecholamine interactions with osmium(VI) and uranium(VI)

Since OsO_4 is known to form very stable complexes with catechols, by analogy, it seems probable that it will bind with catecholamines via the catechol moiety to form osmium(VI) species. Complex formation may also occur with the other common electron microscopic stain uranyl acetate. These reactions were investigated with the aim of showing that these staining agents are indeed capable of reacting with catecholamines, and, therefore, are able to pick out these substances in biological tissue. Care must be taken, however, in reading too much into the investigation of model compounds. They can only provide a guideline to the possible reactions of the reagents involved, which may be radically altered under the actual conditions of tissue fixation and staining, e.g. the reaction of OsO_4 with lipids initially forms an osmium(VI) ester, as postulated from model compounds, but hydrolysis and reduction of these species by the fixing and staining processes result in the formation of osmium(IV) and osmium(III), as well as osmium(VI).

(b) Other metals as potential staining agents

A successful electron microscopic stain should be of relatively high atomic mass so that electron-scattering is enhanced and hence the contrast and resolution of the sample improved. A second criterion must be the ability of the stain to react easily with the substrate, and for a large proportion

of the resulting material to bind with the tissue. A stain should also preferably be selective, and able to pick out a given substance in the tissue without altering the morphology of the cell constituents.

The possibility that catecholamines would coordinate metals through their catechol moiety leads to the consideration of metals which form catecholato complexes, as possible staining agents. Almost all the transition metals form catecholato complexes, but for the purposes of electron-scattering, a metal of relatively high atomic number must be used, so the first row transition metals may be ruled out. Complexes which only form under anaerosic conditions must also be excluded because of the conditions required in fixing and staining of tissue. Only two metals meet these criteria - molybdenum and tungsten, both of which easily form catecholato complexes in neutral aqueous solution. We, therefore, look at the interactions of these catecholamine ligands with molybdenum and tungsten as a possible preliminary investigation in the development of a new electron microscopic stain.

Materials in sections 2-6

Very little work has been reported in the literature for these types of complex, so the following sections generally describe our own work on the new complexes prepared. Each section follows the general order:-

1) Spectra of the ligands
2) Spectra of the complexes:- a) Os(VI) complexes
   b) uranyl complexes
   c) molybdenum and tungsten complexes.

2. PREPARATION OF COMPLEXES

The ligands used were adrenaline, Dopa, and the hydrochlorides of noradrenaline, dopamine, and isoproterenol, as described above.

2.1 Osmium complexes

It has been previously shown that osmium tetroxide is easily reduced by catechol to osmium(VI),[10,67] and so, for convenience, we use trans - $K_2[Os^{VI}O_2(OH)_4]$ ("potassium osmate") as a source of osmium in these investigations. The reaction of potassium osmate with catechol in neutral aqueous solutions resulted in the formation of the catecholato complex, $K_2[OsO_2(cat)_2]$, but analogous products were not obtained using these catecholamine ligands under the same conditions. Either a red-brown polymeric substance resulted, or the solution became deep-blue on standing - a colour characteristic of the polymeric species $[OsO(cat)_2]_n$, reported to form on acidification of solutions of trans-dioxo-osmium(VI) - catecholato complexes. These products were not fully characterised. Reaction of the catecholamines with $K_2[OsO_2(OH)_4]$ in basic solutions under nitrogen (to prevent oxidation and polymerisation of the catecholamines at high pH) resulted in the characteristic deep red solutions of the complexes of the type $K_2[OsO_2(cat)_2]$, and the isolated products were indeed characterised as such, with each catecholamine ligand bound via its catechol moiety.

2.2 Uranyl complexes

Uranyl acetate was found to react in neutral aqueous solutions with each of the five catecholamine ligands to form insoluble brown products of the type $UO_2(cat^*).nH_2O$ analogous to the catecholato complex[41] (cat^* represents a catecholamine bound

in the catecholato mode).

Addition of a solution of the appropriate ligand to a basic solution of uranyl acetate under nitrogen led to initial formation of the brown amorphous solid, typical of $UO_2(cat).nH_2O$; but continued addition caused this solid to redissolve and a very dark brown solution resulted. The product was not easily isolated from this solution, but the system certainly merits further investigation, as it is possible that the complex formed on dissolution of $UO_2(cat)nH_2O$ is the salt $Na_2[UO_2(cat)_2]$, which may be extremely water soluble. A spectrophotometric investigation has reported the formation of a species $[UO_2(cat)_2]^{2-}$ [180] forming a higher pH than $UO_2(cat)$.

2.3 Molybdenum and tungsten complexes

Sodium molybdate and sodium tungstate, when reacted with the catecholamine ligands in neutral aqueous solutions, formed complexes of the type $Na_2[MO_2(cat)_2]$ (where M = Mo(VI), W(VI); cat. is catecholamine coordinated in the catecholato mode) as expected by analogy with $K_2[MoO_2(cat)_2]$ (see Chapter I), but only with the three ligands Dopa, noradrenaline hydrochloride, and isoproterenol hydrochloride. Reaction with dopamine hydrochloride, however, immediately resulted in formation of a precipitate, found to be insoluble in common solvents. These complexes were characterised as $MO_2(dopamine)_2$ (M = Mo(VI), W(VI), where dopamine is coordinated through the catechol moiety but in a monodeprotonated form)

A short investigation of the reactions between sodium tungstate or sodium molbydate and these ligands under acidic conditions was undertaken. The only product successfully isolated and characterised was the complex $Mo_2O_5(adrenaline)_2$, in which the adrenaline ligand coordinates via its amine group and the deprotonated hydroxy group of its aliphatic side-chain. Catechol itself is not a good ligand in acidic conditions,[12] and in this case, coordination is obviously preferable through the amine site. The analogous tungsten complex could not be prepared, since all reactions involving sodium tungstate under these conditions only produced a brown, amorphous solid, which appeared to contain no organic matter.

It would be of interest in further work to investigate the reactions between sodium molybdate or sodium tungstate with catecholamine ligands in basic conditions under nitrogen. We would expect the reactions with isoproterenol, noradrenaline, and Dopa to be the same, but it would seem probable that the higher pH would lead to double deprotonation of the catechol moiety of dopamine, resulting in the complex $Na_2[MO_2(dopamine)_2]$ (where M = Mo(VI), W(VI)- dopamine is coordinated in the catecholato mode). Since adrenaline is soluble in aqueous base it should also be possible to obtain the analogous complex with this ligand.

Reaction of sodium molybdate or sodium tungstate with the catecholamine ligands in 1:1 mole ratios may result in the products $Na_2[M_2O_5(cat^{*})_2]$, (M = Mo(VI), W(VI)- cat - catecholamine bound in the catecholato mode) by analogy with the catecholato complexes.

Where the hydrochloride salts of the ligands were used in the preparation of all of these complexes, no trace was found of chlorine in the product.

3. INFRARED AND RAMAN SPECTROSCOPY OF CATECHOLAMINE COMPLEXES

Catecholamine ligands have three possible modes of coordination to a metal ion as described above (p.160) Infrared spectroscopy is a major technique for the identification of the coordinating site of the molecule.

3.1 Spectra of the ligands

The significant peaks of the I.R. spectra of the free ligands used are listed in Table 2.1.

(a) Region 4000 - 1650cm^{-1}

Each of the free ligands has a strong, broad absorption in the region 3,500 - 3,000cm^{-1} due to the catechol OH stretching vibrations, ν(OH). The hydrochloride salts of dopamine, noradrenaline, and isoproterenol show a series of weak bands between 3,000 and 2,000cm^{-1} - a characteristic absorption pattern of hydrochlorides.[181] Similarly Dopa shows a set of weak absorptions in this region, typical of amino acids. Some of the spectra exhibit a weak peak at 3,050cm^{-1} due to the aromatic C-H stretch, ν(C-H). Isoproterenol and adrenaline have peaks that may be assigned to the CH_3 stretching vibrations near 2690 and 2860cm^{-1}. Peaks due to the CH_2, NH_2^+ and NH_3^+ absorptions of the various ligands cannot be positively identified due to the very large OH stretch absorption, and the number of weak absorptions occurring in this region.

Between 2,000cm^{-1} and 1650cm^{-1} are observed a series of weak absorptions characteristic of a substituted aromatic ring,

(b) Region 1650 - 1300cm^{-1}

Each of the ligands shows several sharp peaks due to the aromatic C-C stretches in this region.

Dopamine HCl, noradrenaline HCl, and Dopa all show a strong peak between 1660 and 1620cm^{-1} due to the NH_3^+ asymmetric deformation $\delta^{as}(NH_3^+)$. The symmetric deformation of this group is observed near 1320cm^{-1}. Isoproterenol HCl shows a peak at 1620cm^{-1} due to the NH_2^+ deformation, but any amine deformation of adrenaline could not be unequivocally assigned.

A CH_2 deformation, $\delta(CH_2)$, peak is found near 1460cm^{-1} in each of the ligands. Adrenaline and isoproterenol HCl also show deformations due to the CH_3 groups around 1370cm^{-1}. A peak in the region 1370 to 1320cm^{-1} present in each of the spectra is assigned to the catechol OH deformation frequency. Dopa also shows a large peak centred at 1570cm^{-1} due to the ionised carboxyl group.

(c) Region 1300–c 600cm^{-1}

This region consists mostly of peaks due to the C-H vibrations of the aromatic ring. Certain of these peaks are typical of 1,2,4-substitution (as listed in Table 2.1).

Near 1250cm^{-1} is the absorption due to the C-O stretch, coupled with some aromatic C-C stretching. This is present in the spectra of each of the ligands.

3.2 Spectra of the complexes

This section is concerned with the infrared and, in two cases, Raman spectra, of the new catecholamine complexes reported in this thesis.

Table 2.1:- Major peaks of the infra-red spectra of dopamine hydrochloride and adrenaline (cm^{-1})

Dopamine HCl	Adrenaline	Assignment
3340 sb	3330 sb	ν(OH)
1616 s		$\delta^{as}(NH_3^+)$
1600 s		
1585 s	1585	ν(C-C)
1520 m		
1500 s	1490	
1464 m	1460	$\delta(CH_2)$
	1420	
-	1370	
1338 m	1340 m	δ(OH)
	1325 m	δ(OH) 2° alcohol
1320 m		$\delta^{s}(NH_3^+)$
1287 s	1275 s	
1260 s	1255 s [b]	ν(C-O+C-C)
	1220 s	
1207 s	1220 w	δ(OH)+ (CH)
1190 s	1180 m	
1175 s	1155 m	
1147 s	1139 m	δ(CH) in plane
1082 m	1098 s	
	1080 m	
	1060 s	
1015 m	1026 s	
968 s	980 m	
	942 vs	
877 s	870 s	δ(CH) out of plane
816 s	810 s	
774 m	779 s	
750 s	740 w	
602 s	648 s	

Table 2.2:- Major peaks of the infra-red spectra of noradrenaline hydrochloride, isoproterenol hydrochloride and Dopa (cm^{-1})

Noradrenaline HCl	Isoproterenol HCl	Dopa	Assignment
3280 sb	3150 sb	3360 sb	ν(OH)
1630 s	1620 s	1658 s	$\delta(NH_2^+)$/ (NH_3^+)
1604 s	1605 vs		
		1575 s	$\delta^{as}(COO^-)$
1537 s	1575 m	1529 s	
1515 s	1534 vs	1500 s	ν(C-C)
1458 s	1460 vs	1458 s	$\delta(CH_2)$
		1405 s	$\delta^{S}(COO^-)$
	1380 s		$\delta(CH_3)$
1335 w	1355 m	1355 m	δ(OH)catechol
1320 w			$\delta^{S}(NH_3^+)$
1300 w	1315 w		δ(OH)2°alc.
1270 s	1294 s	1283 s	
1242 s	1245 s	1248 s	ν(C-O+C-C)
	1228 s	1229 m	
1202 w	1205 m	1205 m	δ(OH)+ (CH)
1167 m	1170 s	1163 m	
	1135 s	1135 w	
1114 m	1114 s	1122 s	δ(CH) in plane
1060 m	1054 s	1064 m	
1035 s	1040/1025s		
996 m	957 m	984 s	
945 m	942 s	946 s	
863 s	868 s	868 m	
827 s	819 s	823 s	δ(CH)out of plane
765 s	786 s	779 m	
745 s	740 s	732 s	
644 sb	645 sb	675 s	

(a) Changes in the spectra expected for the three postulated modes of coordination

(i) Catecholato coordination

We would expect the catechol OH stretching vibrations, ν(OH), near 3,500 - 2,000cm^{-1}, and the phenolic OH deformation, δ(OH), near 1350cm^{-1}, to disappear on complex formation. By analogy with the catecholato complexes described in Chapter I, this mode of coordination would also be expected to lead to an increase in intensity of the peak near 1250cm^{-1}, arising from the C-O stretch, coupled with some aromatic vibrations, ν(C-O + C-C). The aromatic stretching vibration, ν(C-C), near 1500cm^{-1} would shift to approximately 1485cm^{-1} with a concomitant increase in intensity.

This mode of coordination has been found for complexes of the type $M(PPh_3)_2$ (catecholamine),[150,178] where M = Pt(II), Pd(II) as described earlier. The I.R. spectra of these complexes were described as "typical of catechol coordination" with two characteristic bands, one between 1450 - 1480cm^{-1}, the other near 1250cm^{-1}. A weak absorption assigned to ν(N-H) at 3290cm^{-1} [178] was found, which was thought to be too high a value for coordinated amines.

(ii) Monodeprotonated catechol coordination

The catechol monoanion, described in Chapter I (p.45) is coordinated to the metal ion through one oxygen atom only. In this case, however, both oxygen atoms are postulated as coordinating to the metal centre, but only one of the phenolic protons is lost. This mode of coordination was reported for complexes of copper (II), cobalt (II) and nickel (II) with dopamine and isoproterenol.[177] The infrared spectra were

reported to show considerable changes in the characteristic frequencies of the OH groups in the complexes, and coordination was therefore assumed to take place through the catechol moiety. The infrared spectrum of the monodeprotonated cyclohexanediol complex, $MoO_2(C_6O_2H_{11})_2$, shows a loss of the strong ν(OH) peaks of the free ligand, despite the fact that only one of the hydroxyl protons is lost. This mode of coordination should still be distinguishable from the catecholato mode if the δ(OH) absorption can be identified.

(iii) Coordination through the amine group

This mode would cause fewer changes in the spectrum, as may be seen for the known complex Cu(O,N - Dopa)$_2$,[170] described earlier (p.158). The region 4,000 - 2,500cm^{-1} still shows the large broad peak due to the hydrogen-bonded catechol hydroxy groups. A peak at 1658cm^{-1} assigned to $\delta(NH_3^+)$ of the free ligand is no longer observed on complexation. A new peak at 1622cm^{-1} is presumably due to the NH_2 deformation, $\delta(NH_2)$, of the coordinated Dopa molecule. The broad peak centred at 1590cm^{-1} is assigned to the coordinated carboxyl group, which compares well with reported values of between 1580 - 1660cm^{-1}.[182]

(b) Osmium(VI) complexes with catecholamines

The significant peaks of these complexes are listed in Table 2.3. Each of the spectra shows a strong, sharp peak near 830cm^{-1}. Its position, intensity, and shape change little with variation in ligand. This band is almost

certainly due to the asymmetric stretching vibration of the trans-"osmyl" group. This mode, $\nu^{as}(OsO_2)$ is found at 830cm^{-1} in $K_2[OsO_2(cat)_2]$ species, and in many osmyl complexes, as described in Chapter I (p.60).

The presence of this osmyl grouping, the stoichiometry, elemental analyses and similarity in colour and general properties to the $[OsO_2(catecholato)_2]^{2-}$ [19] species suggest that coordination occurs in the catecholato mode. The general features of the infrared spectra bear this out.

No ν(OH) vibrations are observed between 3,500 and 3,000cm^{-1}. The OH deformation peak has also disappeared. The absorption at 1250cm^{-1}, ν(C-O + C-C) shows enhanced intensity on coordination, as does the aromatic ring absorption at 1490cm^{-1}. These data indicate the ligands are indeed bound in the catecholato mode.

The ligands used as their hydrochloride salts no longer show the characteristic hydrochloride absorption in the range 2,000 to 3,000cm^{-1}. Consistent with this is the change observed in the amine vibrations. For the primary amines (dopamine and noradrenaline), the NH_3^+ peaks disappear. A broad, strong peak near 1600cm^{-1} is assigned to a mixture of the absorptions due to the aromatic C-C stretch, NH_2 deformation, and deformation vibrations of lattice water. The NH_3^+ symmetric deformation peaks near 1320cm^{-1} disappear on coordination. Isoproterenol HCl loses its strong peak at 1620cm^{-1} due to NH_2^+ deformation. The NH vibrations due to the secondary amine are too weak for identification.

Table 2.3(a):- Major peaks of the infra-red spectra of complexes of the type $K_2[OsO_2(cat)_2]$ (cat = Dopa, isoproterenol, noradrenaline bound in the catecholato mode) (cm^{-1})

$K_2[OsO_2(nor)_2]$	$K_2[OsO_2(iso)_2]$	$K_2[OsO_2(Dopa)_2]$	Assignment
		1640 sb	$\delta(NH_3^+)/\delta(COO^-)$
1628 sb			$\delta(NH_2)$
1579 s	1580 s	1575 s	
1485 s	1487 s	1485 s	ν(C-C)
1440 m	1430 m	1432 m	$\delta(CH_2)$/ (C-C)
1260 s	1260 s	1260 s	ν(C-O+C-C)
1215 w		1210 w	
1160 w	1175 w	1174 m	
1120 m	1118 m	1110 w	δ(CH)in plane
1020 m	1020 m	1020 m	
870 m	980 w	970 w	
837 s	834 s	827 s	$\nu^{as}(OsO_2)$
805 s	810 s	810 s	δ(CH)out of plan
764 w	765 w	770 w	
645 m	640 m	630 w	
540 m	540 m	530 w	

where nor represents noradrenaline bound in the catecholato mode.

iso represents isoproterenol bound in the catecholato mode.

Table 2.3(b):- Major peaks of the infra-red spectra of complexes of the type $K_2[OsO_2(cat)_2]$ (cat = dopamine, adrenaline bound in the catecholato mode) (cm^{-1})

$K_2[OsO_2(dopamine)_2]$	$K_2[OsO_2(adrenaline)_2]$	Assignment
1630 sb	1630 sb	
1575 s		$\delta(NH_2)$
1490 S	1485 s	ν(C-C)
1460 w	1462 w	$\delta(CH_2)/\nu$(C-C)
1259 s	1260 s	ν(C-O+C-C)
1215 m	1216 m	
1163 w	1160 w	
1120 m	1118 m	δ(CH) in plane
1010 m	1020 m	
975 w	975 w	
833 s	835 s	$\nu^{as}(OsO_2)$
808 s	810 s	δ(CH) out of plane
766 w	770 w	
642 w	645 w	
555 w	543 w	

The osmium (VI)-Dopa complex shows a very broad band centred at 1610cm^{-1}, with a breadth of 120cm^{-1}. This is ascribed to overlap of the absorptions due to the NH_3^+ group, ionised carboxyl group, aromatic vibrations and H_2O deformations. It is concluded that Dopa still exists as the Zwitterion when coordinated. Whether adrenaline remains as the Zwitterion on coordination could not be decided from the spectra.

A slight change is observed in the positions of the aromatic C-H in-plane and out-of-plane vibrations on coordination. This may be expected if donation were through the catecholato moiety, coordination possibly affecting the vibrational frequencies of the aromatic ring.

(c) Uranyl complexes with catecholamines

The significant peaks of the I.R. spectra of these complexes are listed in Table 2.4.

The formula obtained from analysis and by analogy with the uranyl-catechol complex, UO_2(catecholamine)nH_2O, suggests a polymeric structure for these species. The infrared spectra obtained are of lower quality than those recorded for the osmium, molybdenum, and tungsten complexes, the peaks being broader and less well resolved. The general profiles, however, are similar to those found for the osmium complexes, suggesting that the catecholato mode of coordination is operative.

Table 2.4(a):- Major peaks of the infra-red spectra of complexes of the type $UO_2(cat^*)nH_2O$ (where cat^* = Dopa, isoproterenol, noradrenaline bound in the catecholato mode) (cm^{-1})

UO_2(nor)	UO_2(iso)	UO_2(Dopa)	Assignment
1598 s	1600 s	1604 s	$\delta(H_2O)/\delta(NH_3)$
1480 s	1490 s	1493 s	ν(C-C)
1428 w	1445 m	1427 m	
1264 s	1264 s	1256 s	ν(C-O+C-C)
1216 m	1213 w	1220 w	
1158 w	1157 m	1152 w	δ(CH) in plane
1119 m	1115 m	1120 m	
1040 w	1070 m	1061 w	
970 w	975 w	995 w	
903 vs	918 vs	915 vs	$\nu^{as}(UO_2)$
812 m	810 m	825 m	δ (CH)out of plane
622 m	624 m	621 m	
520 m	520 m	540 w	

where nor represents noradrenaline bound in the catecholato mode.

iso represents isproterenol bound in the catecholato mode.

Table 2.4(b):- Major peaks of the infra-red spectra of complexes of the type $UO_2(cat)n.H_2O$ (cat = dopamine, adrenaline bound in the catecholato mode) (cm^{-1})

UO_2(dopamine)	UO_2(adrenaline)	Assignment
1595 s	1600 s	$\delta(H_2O)\delta(NH_3)$
1485 s	1490 s	ν(C-C)
1420 m	1420 m	
1265 s	1260 vs	ν(C-O+C-C)
1224 m	1218 m	
1150 w	1165 m	
1123 m	1120 m	δ(CH) in plane
1020 w	1020 w	
965 w	975 w	
902 vs	903 vs	$\nu^{as}(UO_2)$
808 m	815 m	δ(CH) out of plane
620 m	625 m	
535 m	500 m	

In addition to the ligand peaks, a strong, broad peak just above 900cm^{-1} is seen in each of the complex spectra. This is assigned to the asymmetric stretching vibration of the uranyl group, $\nu^{as}(UO_2^{2+})$ as described in Chapter I (p. The position of this peak depends on the basicity of the equatorially coordinated groups. This may account for the difference in frequency between the $\nu^{as}(UO_2)$ in these complexes, and that of the catechol complex at 940cm^{-1}.

The presence of water is indicated by the broad absorptions in the region 3,500 - 3,000cm^{-1}, and the broadening of the peaks around 1600cm^{-1} on formation of the complexes, due to the H_2O deformation modes. Whether the water is present as lattice water,[184] or coordinated to the metal cannot be discerned from these spectra. However, a previous report[41] on $UO_2(cat)2H_2O$ suggested this complex contained coordinated water. This would seem likely for these complexes, so as to increase the coordination number around the metal. To allow for a coordination number of at least six (common for uranyl complexes) and to explain the insolubility of these complexes, a polymeric structure is postulated.

(d) Molybdenum (VI) and Tungsten (VI) - Catecholamine Complexes

(i) $Na_2[MoO_2(catecholamine)_2]nH_2O$ (M = Mo(VI), W(VI): catecholamine = noradrenaline, isoproterenol, Dopa.)

The major peaks of the molybdenum species are listed in Table 2.5, those for tungsten in Table 2.6.

The infrared spectra of these complexes are very similar to those of the complexes $K_2[OsO_2(catecholamine)_2]$. Of course, no band is now seen at $830cm^{-1}$, for $\nu^{as}(OsO_2)$, but two peaks are found between 900 and $800cm^{-1}$ not found in the free ligand spectra. These bands are typical of the stretching vibrations of the metal (VI) - cis-dioxo group, as described in Chapter I (p.60).

The Raman spectrum of $Na_2[MoO_2(noradrenaline)_2]$ supports the assignment of the stretching vibrations of the MoO_2^{2+} group. As described in Chapter I (p.60) the asymmetric stretching vibration, $\nu^{as}(MoO_2)$ is found to lower wave number than the symmetric stretch, $\nu^{s}(MoO_2)$, and appears with greater intensity in the infrared. The vibration, $\nu^{s}(MoO_2)$, has greater intensity in the Raman spectrum than does the asymmetric stretch. The Raman spectrum shows a strong peak at $897cm^{-1}$ with a weaker peak at $821cm^{-1}$. These peaks agree well with the infrared positions of $894cm^{-1}$ and $822cm^{-1}$. The I.R. and Raman spectra of $Na_2[MoO_2(noradrenaline)_2]$ are shown in Figures 2.7 and 2.8.

The ν(OH) bands of the ligand, found between 3,500 and $3,000cm^{-1}$ and the δ(OH) peak near $1350cm^{-1}$ disappear on coordination. The peak at $1260cm^{-1}$ due to ν(C-O + C—— C) shows enhanced intensity, as does the peak at $1490cm^{-1}$ due to the aromatic ring stretches. These changes are indicative of catecholato coordination. Other ligand vibrations follow the same pattern as that observed for the corresponding osmium (VI) complexes.

The positions of the cis - MoO_2^{2+} absorptions are found to the lower end of wavenumbers quoted for these vibrations (see Chapter I), but very close to the values observed for $K_2[MoO_2(cat)_2]$ (see p. 80) This adds further weight to the postulated catecholato coordination mode for these complexes.

(ii) $MO_2(dopamine)_2$ (M = Mo(VI), W(VI).)

The major peaks of these spectra are listed in Table 2.7, and the infrared spectrum of $MoO_2(dopamine)_2$ is shown in Figure 2.9. The expected salts, $Na_2[MO_2(dopamine)_2]$, are not found for this ligand, but insoluble, neutral species are obtained instead.

Two strong bands are observed in the spectra of these complexes, which are not found for the free ligands, at 880cm^{-1} and 818cm^{-1} for the molybdenum complex, and 896cm^{-1} and 820cm^{-1} for the tungsten complex. These bands suggest a cis-dioxo arrangement about the metal(VI) centres.

The Raman spectrum of $MoO_2(dopamine)_2$ confirms the assignment of the $\nu(MoO_2^{2+})$ absorptions, showing a strong band at 881cm^{-1} due to $\nu^s(MoO_2^{2+})$ and a weaker band at 820cm^{-1} due to $\nu^{as}(MoO_2^{2+})$, values very close to those observed in the infrared.

A different pattern of ligand absorptions, however, is observed compared to those found for the complexes $Na_2[MO_2(catecholamine)_2]$. The very large, broad ν(OH) peaks of the free ligand are no longer observed, but a broad, strong peak is seen near 3,050cm^{-1} in each complex. The peak thought to arise from the δ(OH) vibration is still observed at 1340cm^{-1}.

The change in the ν(OH) vibrations indicates coordination has taken place through the catechol moiety of dopamine, but the persistence of the ν(OH) peak suggests the catechol group is not fully deprotonated. The absorption at 3,050cm^{-1} is not found in the spectrum of the free ligand, nor in the spectra of the dopamine complexes of osmium and uranium. Its strength and broadness suggest it arises from an OH vibration, and it is possibly due to a coordinated OH group. This evidence leads us to postulate coordination mode (II) for this complex, where chelation occurs through the monodeprotonated catechol site, as shown in Figure 2.10.

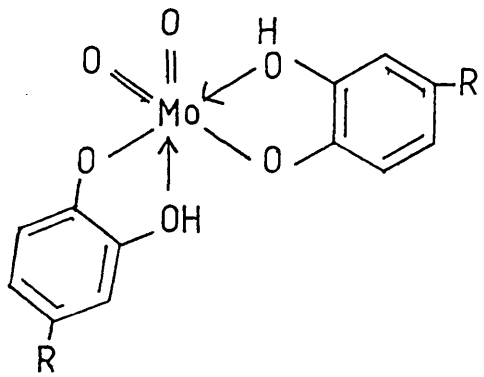


Figure 2.10 Postulated structure of MoO_2(dopamine)$_2$

To add further evidence to this formulation postulated for these two complexes, a sample of MoO_2(dopamine)$_2$ was prepared using dopamine HCl in D_2O solution. The infrared spectrum recorded for this deuteriated complex, shows a loss of the strong peak at 3,050cm^{-1} and the presence of a new, broad peak at 2270cm^{-1}. The groups likely to be deuteriated

are the OH groups or the amine group. Since no similar absorption to that at 3,050cm^{-1} is found in the dopamine HCl spectrum or for other dopamine complexes, it seems unlikely that this peak is due to amine vibrations. The calculated position of the ν(OD) absorption is 2225cm^{-1}. The discrepancy between this value and the value observed is an acceptable error as was found for the complex Fe(salen)(catH), with ν(OH) at 3380cm^{-1}, and Fe(salen)(catD), ν(OD) at 2520cm^{-1}, calculated position 2460cm^{-1}.[99]

The pattern of absorptions between 1,300 and 1,200cm^{-1} is consistent with the postulated coordination mode. Dopamine HCl shows two peaks, at 1,287 and 1,260cm^{-1}, the latter assigned to (C-O + C —— C). The peak at 1,287cm^{-1} has greater intensity. On coordination to molybdenum, a very strong peak is observed at 1,250cm^{-1}, assigned to ν(C-O + C —— C), typical of catecholato coordination. There is also a new peak at 1,268cm^{-1}. This peak is not found in other dopamine complexes, and it possibly corresponds to the absorption at 1,260cm^{-1} of the free ligand, and is tentatively assigned to ν(C-O + C —— C) of the protonated catechol oxygen.

Other changes in the ligand absorptions on coordination show the same trends as observed in the reported dopamine complexes of osmium and uranium.

(iii) Mo_2O_5(adrenaline)$_2$

The significant peaks of this complex are listed in Table 2.8.

The spectrum of this complex (shown in Figure 2.11) shows a number of strong peaks between 950 and 850cm^{-1}, not observed for the ligand. The number of peaks of similar intensity precludes

any definite assignment, but the pattern is typical of vibrations of the cis-dioxo-molybdenum(VI) moiety, mixed with ligand vibrations. Absorptions due to $\nu(MoO_2)$ are probably two of the three peaks at 928, 912 and 890cm^{-1}. These values are higher than those found for the mononuclear cis-dioxo-molybdenum(VI) complexes, $Na_2[MoO_2(catecholamine)_2]$ and $MoO_2(dopamine)_2$. This suggests the possibility of the presence of a $Mo_2O_5^{2+}$ core, which generally has $\nu(MoO_2)$ absorptions at slightly higher wavenumber and in a narrower range. This binuclear moiety, $Mo_2O_5^{2+}$, may exist with a linear oxygen bridge or a bent bridge between the two molybdenum atoms. The high number of bands of similar strength in this region leads to great difficulty in assigning any particular absorptions. However, by comparison with the spectra of the free ligand adrenaline, and with the adrenaline complexes of osmium and uranium, it appears that there is a new peak at 562cm^{-1}, of medium strength, possibly arising from the symmetric stretching vibration of a bent bridge. The corresponding asymmetric stretch would be expected to be near 750cm^{-1}, but the presence of several peaks in this region, precludes any definite assignment. A new, strong peak at 666cm^{-1} may arise from a vibration of the metal bridging bond of a ligand. This leads us to suggest the formula $Mo_2O_5(ligand)_2$, and the insolubility of the complex in water, however, and its elemental analyses, suggest the ligand has only one negative change.

No change is observed for this complex, as compared to the free ligand, in the region of the ν(OH) absorptions between 3,500 and 3,000cm^{-1}. This suggests that coordination does not take place through the catecholato moiety. The δ(OH) peak at 1340cm^{-1} is still present, and little change is seen in the position or shape of the ν(C-O + C-C) peak at 1275cm^{-1}, confirming this assumption. The aromatic ring stretching absorption at 1490cm^{-1} also shows no change on coordination.

The absorption of the free ligand at 1325cm^{-1} was assigned to the secondary alcohol deformation, but is no longer observed in the spectrum of this complex. This suggests coordination may occur through the deprotonated β-hydroxy group. We postulate formation of a five-membered chelate ring via the deprotonated β-hydroxy group, the secondary amine group, and the molybdenum(VI) centre. The suggested structure is shown in Figure 2.12.

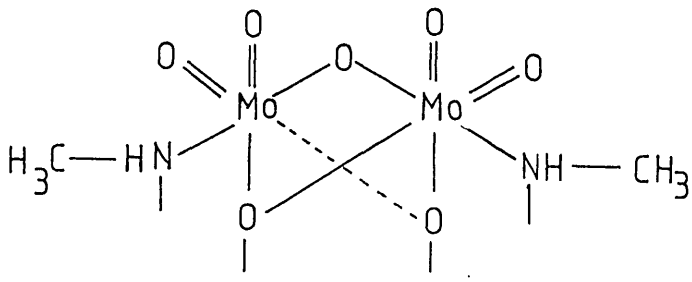


Table 2.5:- Major peaks of the infra-red spectra of complexes of the type $Na_2[MoO_2(cat)_2]$ (cat = Dopa, isoproterenol, noradrenaline bound in the catecholato mode) (cm^{-1})

$Na_2[MoO_2(nor)_2]$	$Na_2[MoO_2(iso)_2]$	$Na_2[(MoO_2(Dopa)_2]$	Assignment
		1620 sb	$\delta(NH_3^+)/\delta(COO^-)$
1595 mb	1590 w		$\delta(NH_2)/\delta(NH)$
1473 s	1485 s	1485 s	ν(C-C)
1429 m	1428 m	1418 m	$\delta(CH_2)/\nu$(C-C)
	1397 w		$\delta(CH_3)$
1346 w	1340 w	1345 w	
1250 vs	1270 vs	1270 s	ν(C-O+C-C)
1220 m	1220 m	1222 w	
1154 m	1156 w	1150 w	
1122 m	1120 w	1120 m	δ(CH) in plane
	1078 m		
1040 s	1045 w		
970 w	970 w	960 w	
893 vs	892 s	898 s	$\nu^s(MoO_2)$
858 vs	855 s	855 s	
817 vs	815 vs	825 vs	$\nu^{as}(MoO_2)$
775 m	765 w	760 w	δ(CH) out of plane
620 s	648 b	630 m	
510 mb	510 mb	530 w	

where nor represents noradrenaline bound in the catecholato mode.

iso represents isoproterenol bound in the catecholato mode.

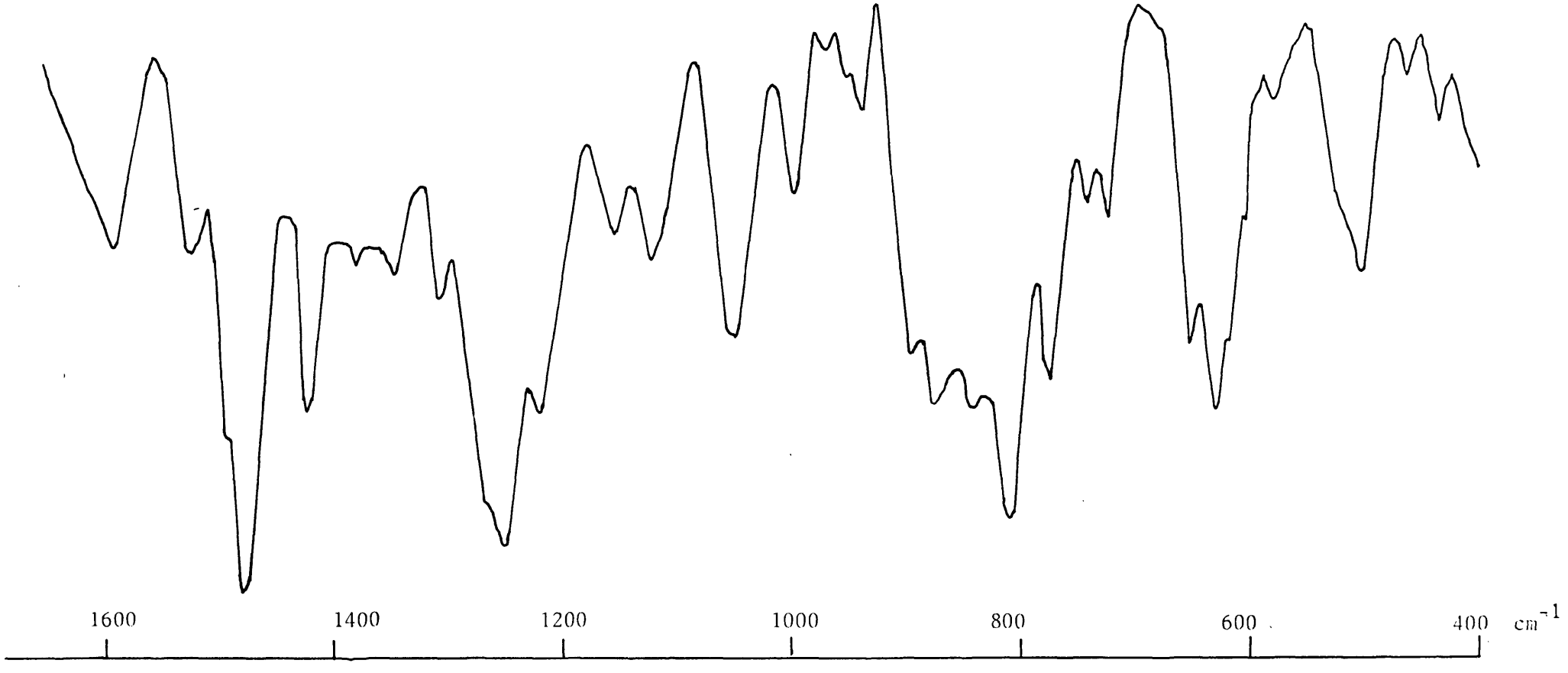


Figure 2.7 - Infra-red spectrum of $Na_2[MoO_2(noradrenaline)_2]$

Table 2.6:- Major peaks of the infra-red spectra of complexes of the type $Na_2[WO_2(cat)_2]$ (cat = Dopa, isoproterenol, noradrenaline, bound in the catecholato mode) (cm^{-1})

$Na_2[WO_2(nor)_2]$	$Na_2[WO_2(iso)_2]$	$Na_2[WO_2(Dopa)_2]$	Assignment
		1620 sb	$\delta(NH_3^+)/\delta^{as}(COO^-)$
1600 mb	1590 wb		$\delta(NH_2)/\delta(NH)$
1485 s	1490 s	1495 s	ν(C-C)
1430 m	1430 m	1430 m	$\delta(CH_2)$/ (C-C)
	1397 w		$\delta(CH_3)$
1345 w	1344 w	1340 w	
1250 s	1270 sb	1260 s	ν(C-O+C-C)
1220 m	1220 m	1212 m	
1152 m	1155 w	1145 w	
1120 m	1120 w	1120 m	
	1070 m		δ(CH) in plane
1040 m	1045 w		
940 w	970 w	963 w	
898 s	905 s	905 s	$\nu^s(WO_2)$
867 m	845 s	850 s	
810 vsb	818 vs	820 vs	$\nu^{as}(WO_2)$
772 m	762 w	760 w	δ(CH)out of plane
650/630 sb	650 sb	640 sb	
515 mb	520 mb	510 w	

where nor represents noradrenaline bound in the catecholato mode.

iso represents isoproterenol bound in the catecholato mode.

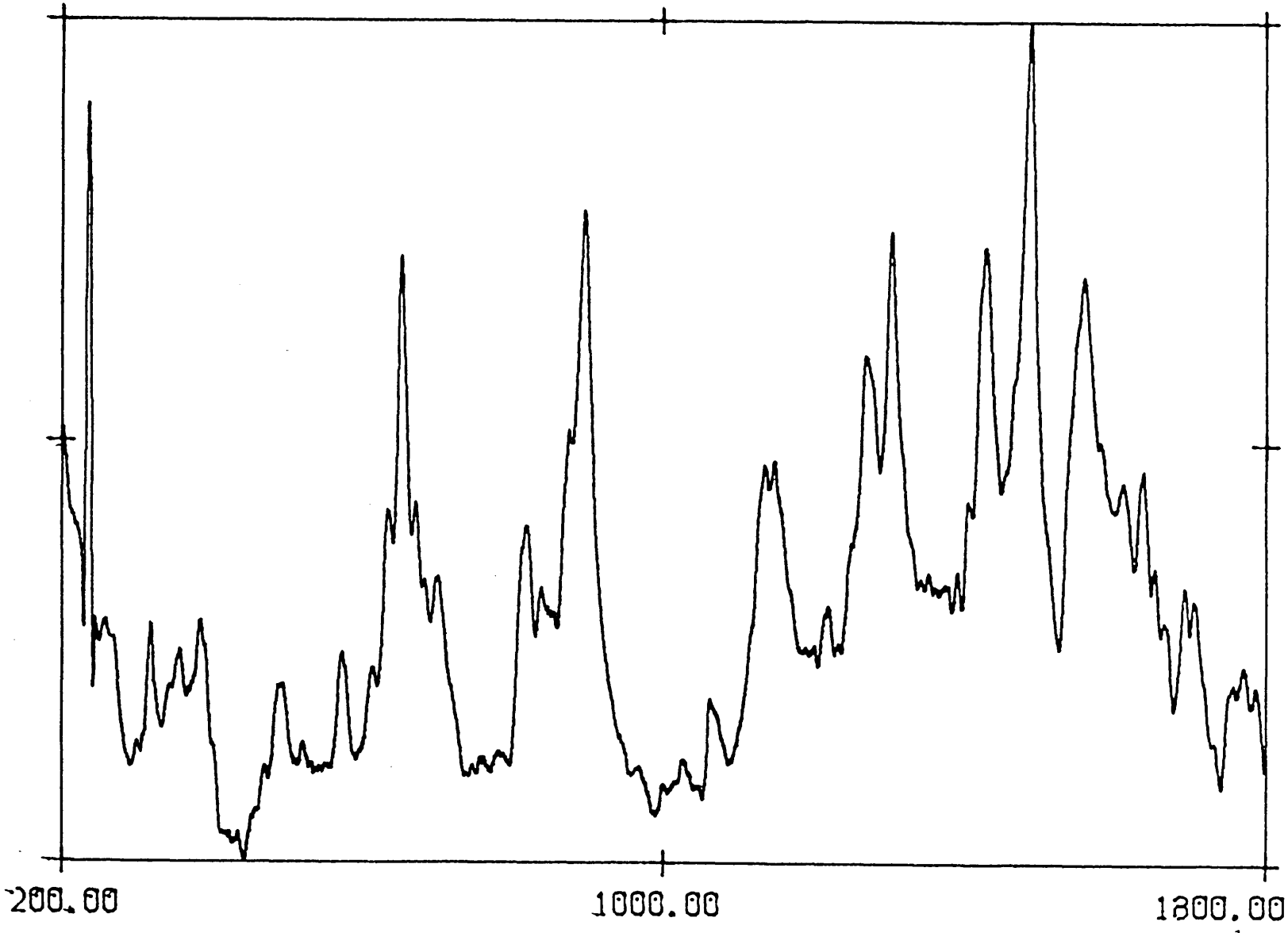


Figure 2.8 - Raman spectrum of $Na_2[MoO_2(noradrenaline)_2]$

Table 2.7:- Major peaks of the infra-red spectra of complexes of the type $MO_2(dopamine)_2$, (M = Mo(VI), W(VI)) (cm^{-1})

$MoO_2(dopamine)_2$	$WO_2(dopamine)_2$	Assignment
3050 sb	3030 sb	ν(OH)
1595 m	1600 s	$\delta(NH_2)$
1538 s	1550 s	
1486 vs	1490 vs	ν(C-C)
1462 s	1460 s	$\delta(CH_2)/\nu$(C-C)
1430 m	1428 m	
1337 w	1340 m	δ(OH)
1284 m	1290 s	
1268 s		ν(C-O+C-C)
1250 vs	1257 vs	ν(C-O+C-C)
1221 m	1222 s	
1151 m	1160 m	δ(CH) in plane
1136 m	1129 s	
1020 w	1022 m	
945 m	946 s	
880 vs	896 vs	$\nu^{s}(MO_2)$
838 s	862 m	
818 vs	820 vsb	$\nu^{as}(MO_2)$
767 m	769 m	δ(CH) out of plane
740 w	738 w	
652 s	650 vs	
642 s	645 vs	
632 s	632 s	
515 m	532 s	
500 m	515 s	

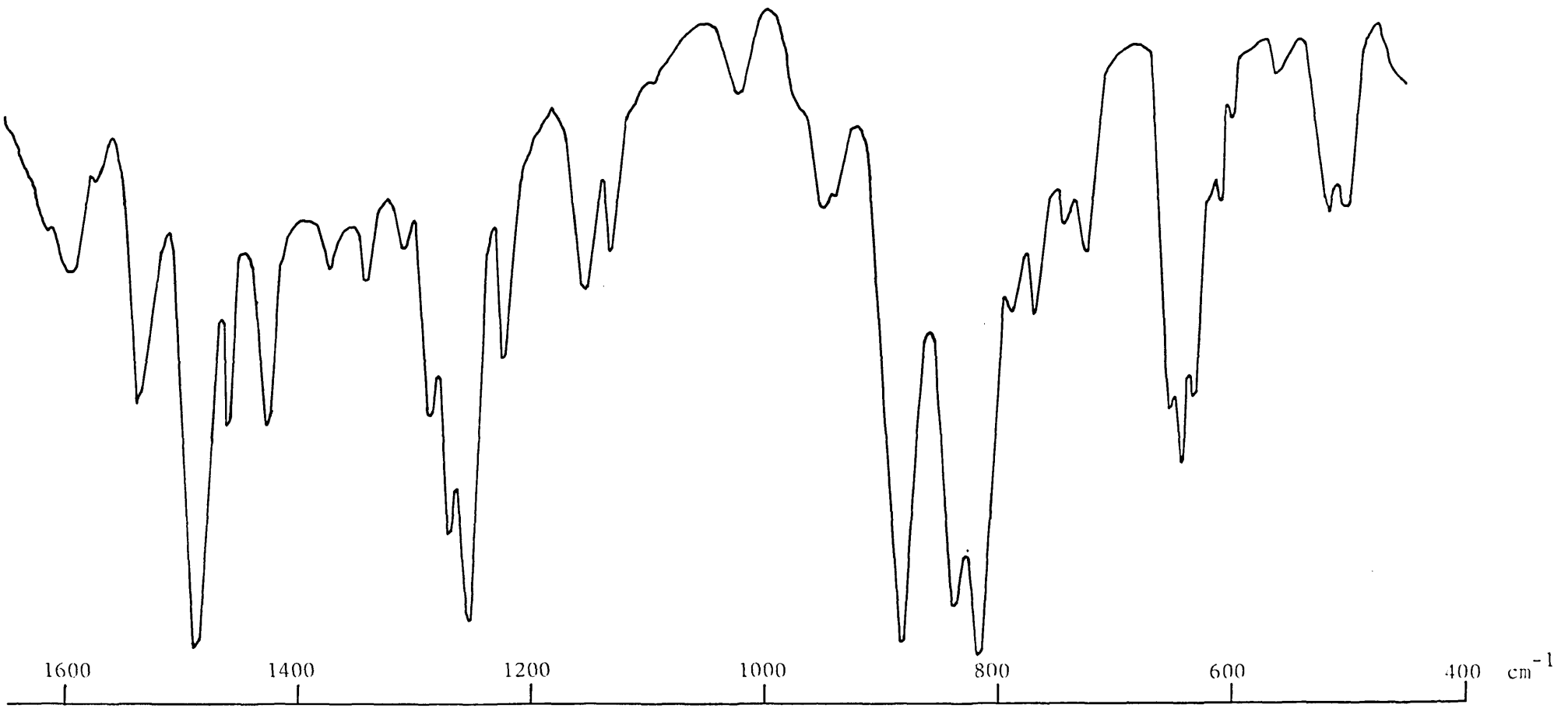


Figure 2.9 - Infra-red spectrum of $MoO_2(dopamine)_2$

Table 2.8:- Major peaks of the infra-red spectra of $Mo_2O_5(adrenaline)_2$ (cm^{-1})

$Mo_2O_5(adrenaline)_2$	Assignment
3490 ab	ν(OH)
3380 sb	
1642 w	
1618 w	
1603 s	
1490 s	ν(C-C)
1460 m	δ(CH_2)
1420 s	
1340 m	δ(OH)
1275 s	ν(C-O+C-C)
1210 m	
1167 m	
1124 m	δ(CH) in plane
1080 m	
1025 m	
928 vs	
912 vs	ν(MoO_2)
890 s	
876 vs	
865 sh	
838 m	δ(CH) out of plane
811 m	
771 m	
737 w	$\nu^{as}(M_2O)$
666 s	ν(Mo-Olb)
643 s	
595 w	
562 m	$\nu^{s}(M_2O)$
527 mb	

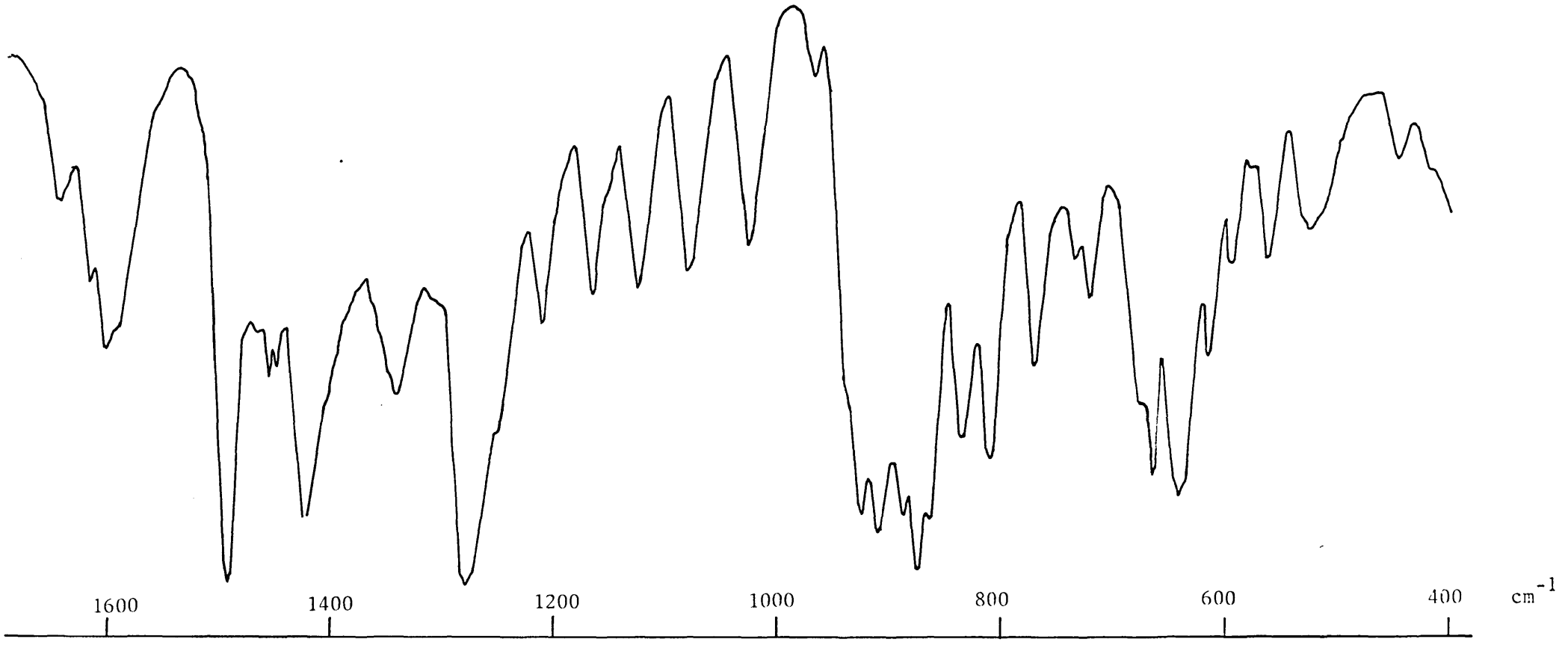


Figure 2.11 - Infra-red spectrum of $Mo_2O_5(adrenaline)_2$

4. ^{1}H NUCLEAR MAGNETIC RESONANCE SPECTROSCOPY

4.1 Spectra of the ligands

The spectra of dopamine HCl, noradrenaline HCl, and isoproterenol HCl were recorded in D_2O solutions. The ligands adrenaline and Dopa were too insoluble to allow measurement of their ^{1}H N.M.R. spectra. However, the spectrum of Dopa has been previously reported, as have the spectra of noradrenaline HCl, dopamine HCl and isoproterenol HCl, in different solvents.[85] The reported spectra agree well with our measurements and thus we can use the reported spectrum of Dopa for the purposes of comparison. The ligand resonances are listed in Table 2.9.

The resonances arising from the aromatic protons gave a typical ABC type pattern,[103] as labelled in Figure 2.13.

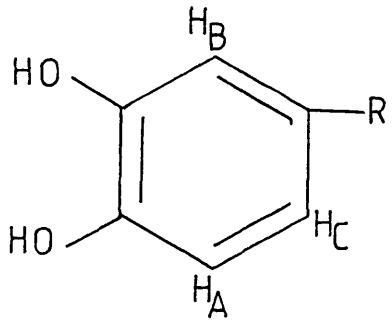


Figure 2.13 ABC protons of catecholamines

The aliphatic side chain resonances are observed at lower frequencies. No resonance due to the hydroxyl protons or the amine protons was observed in D_2O solution; due to rapid exchange with the solvent.

4.2 Spectra of the complexes

The uranyl-catecholamine complexes are insufficiently soluble to allow measurement of their ^{1}H N.M.R. spectra.

(a) Osmium(VI) catecholamine complexes

Due to the limited solubility of these complexes, the resonances arising from the aliphatic side chain of the ligands could not always be distinguished from the smaller peaks of the internal reference substance, D.S.S. The aromatic resonances, however, were more easily identified and are listed in Table 2.10.

On coordination to the "osmyl" group, the ABC pattern observed for the aromatic resonances of the free ligands, split into two separately distinguishable multiplets, in a pattern similar to that found for ABX splitting[103] (see Figure 2.14). The broader multiplet found at higher frequency (between 7.4 and 6.8 p.p.m.) corresponds approximately to the position of the aromatic resonances of the free ligand spectra (between 7.8 and 6.8 p.p.m.) and probably arises from the proton in the X position, as labelled in Figure 2.15.

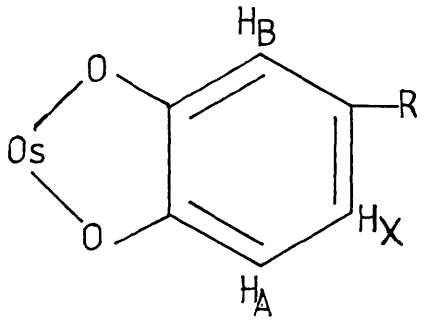


Figure 2.15. ABX protons of coordinated catecholamines

The second multiplet shows a shift to lower frequency of between 0.24 and 0.35 p.p.m. and is tentatively assigned to the resonances of the H_A and H_B protons. The adrenaline complex shows a similar pattern of aromatic resonances, although the difference in chemical shifts on coordination may not be measured.

The observed change in the pattern of resonances arising from the aromatic protons on coordination of the ligand suggests that coordination takes place through the aromatic end of the ligand, rather than through the aliphatic side chain. Indeed, an ABX pattern of resonances was reported for the ^1H N.M.R. spectra of osmium (VI) complexes of catechols substituted in the 4-position. The ^1H N.M.R. spectra of these osmium (VI) - catecholamine complexes, therefore, suggest catecholato coordination for the catecholamine ligands in complexes of the type $K_2[OsO_2(catecholamine)_2]$.

Although the ^1H N.M.R. spectra of complexes of the type $(PPh_3)_2Pt$(catecholamine) have been reported as typical of catecholato coordination, insufficient details were given to make any meaningful comparisons with these complexes.[150]

(b) Molybdenum (VI) - and tungsten (VI) - catecholamine complexes

The complexes $MoO_2(dopamine)_2$, $WO_2(dopamine)_2$, and $Mo_2O_5(adrenaline)_2$ are too insoluble for their ^1H N.M.R. spectra to be measured. The resonances arising from the complexes $Na_2[MO_2(catecholamine)_2]$, (where M = Mo(VI), W(VI) and catecholamine is Dopa, isoproterenol and noradrenaline) are listed in Table 2.11.

On coordination of the ligand to the molybdenum (VI) or tungsten (VI) centre there is little change in the observed pattern of aromatic resonances, but the position of the multiplet is shifted to lower frequency by up to 0.4 p.p.m. in each case. The aliphatic side-chain resonances show little change in position, and no change in pattern. This behaviour is very similar to that observed in the complexes $K_2[MoO_2(cat)_2]$ and $Na_2[W_2O_5(cat)_2]$ as described earlier. The aromatic resonances showed very little change on coordination, and only a slight shift in position to lower frequency. Thus this evidence lends further weight to the postulation of catecholato-type coordination for the catecholamine ligands in these complexes.

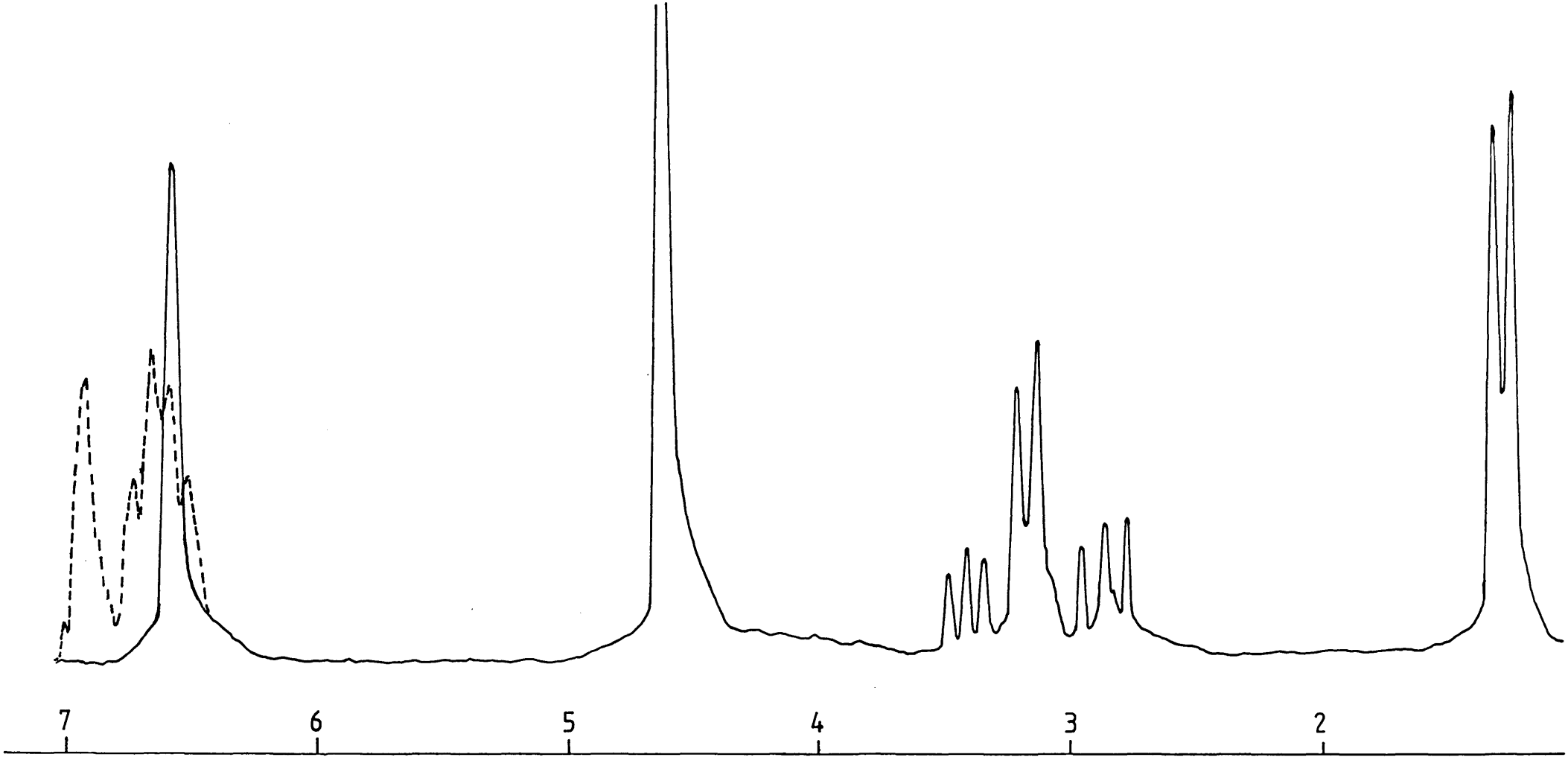


Figure 2.14 - ^{1}H N.M.R. spectrum of $K_2[OsO_2(isoproterenol)_2]$ (---) compared to $Na_2[MoO_2(isoproterenol)_2]$ (—) (p.p.m.)

Table 2.9:- ^{1}H N.M.R. resonances of the free catecholamines (p.p.m.)

Substance	Phenyl ring resonances	Aliphatic resonances
Dopamine HCl	6.85(m)	2.82, 2.92, 3.00 3.22, 3.29, 3.37 (4H, CH_2-CH_2)
Noradrenaline HCl	6.96(m)	3.28, 3.37 (3H, CH-CH_2)
Isoproterenol HCl	6.89(m)	1.35, 1.42(d)(6H-2CH_3) 3.61, 3.52, 3.53, 3.47(q) 3.31, 3.24(d) 3.00, 2.92, 2.82(q) (4H, -CH-CH_2-N-CH)
Dopa[a]	6.95(m)	4.5, 4.4, 4.3(t) 3.3, 3.2, 3.1 (3H, CH_2-CH)

[a] reference 185.

Table 2.10:- ^1H N.M.R. resonances of the aromatic protons of complexes of the type $K_2[OsO_2(cat^{*})_2]$.(p.p.m.)

Complex	Phenyl ring resonance H_C	H_A H_B
$K_2[OsO_2(dopamine)_2]$	6.80(m)	6.53(m)
$K_2[OsO_2(noradrenaline)_2]$		6.69(m)
$K_2[OsO_2(isoproterenol)_2]$	6.92(m)	6.65(m)
$K_2[OsO_2(Dopa)_2]$	7.37(m)	6.60(m)
$K_2[OsO_2(adrenaline)_2]$	6.93(m)	6.62(m)

Table 2.11:- ^1H N.M.R. resonances of complexes of the type $Na_2[MO_2(cat)_2]$ (M = Mo(VI), W(VI)) (p.p.m.)

Complex	Phenyl ring resonances	Aliphatic resonances
$Na_2[MoO_2(noradrenaline)_2]$	6.62(m)	3.17, 3.24 (3H,CH-CH_2)
$Na_2[WO_2(noradrenaline)_2]$	6.69(m)	3.08, 3.16 (3H,CH-CH_2)
$Na_2[MoO_2(isoproterenol)_2]$	6.63(s)	1.26, 1.33(d) (6H-2CH_3) 2.81, 2.90, 2.98(q) 3.15, 3.23(d). 3.37, 3.43, 3.52, 3.58(q) (4H,-CH-CH_2-N-CH)
$Na_2[WO_2(isoproterenol)_2]$	6.60(m)	1.27, 1.34(d)(6H-2CH_3) 2.78, 2.87, 2.97(q) 3.15, 3.22(d) 3.35, 3.43, 3.50,3.57(q) (4H,-CH-CH_2-N-CH)
$Na_2[MoO_2(Dopa)_2]$	6.47(m)	Not identified
$Na_2[WO_2(Dopa)_2]$	6.52(m)	

5. ^{13}C NUCLEAR MAGNETIC RESONANCE SPECTROSCOPY

5.1 Spectra of the Ligands

(a) Literature measurements

The spectra of the ligands dopamine,[186,187] noradrenaline[187] and adrenaline[187] have been reported, and the resonances assigned. They each showed a similar pattern of resonances, those due to the aliphatic side-chain occurring below 80 p.p.m., those arising from the aromatic carbon nuclei above 100 p.p.m.

(b) Experimental data

For the purposes of direct comparison with the spectra of the complexes, we have recorded the ^{1}H decoupled ^{13}C N.M.R. spectra of the ligands dopamine HCl, noradrenaline HCl, isoproterenol HCl and Dopa in aqueous solutions. Adrenaline is too insoluble to allow measurement of its spectrum. The resonances recorded for dopamine HCl and noradrenaline HCl matched well with the reported values,[186,187] and hence the assignments were made for the spectra of Dopa and isoproterenol HCl by comparison with the literature assignments for dopamine, noradrenaline and adrenaline. The resonances recorded, and their assignments are listed in Tables 2.12. The spectrum of Dopa is shown in Figure 2.16.

To confirm the identification of the resonances, the off-resonance decoupled spectrum of Dopa was recorded. For the purposes of convenient identification, the carbon nuclei of the Dopa molecule will be labelled as shown in Figure 2.17.

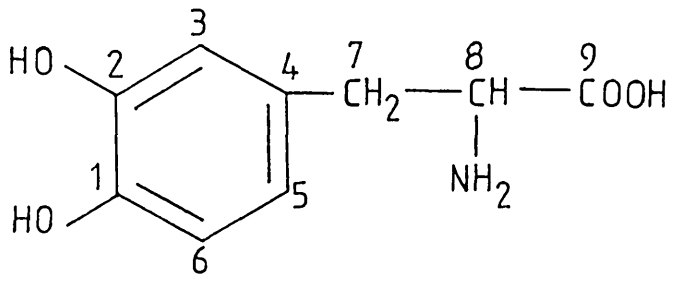


Figure 2.17. Labeling of carbon nuclei of Dopa.

In an off-resonance decoupled spectrum, a peak arising from any carbon nucleus would be expected to split into a number of lines related to the number of protons directly attached to that carbon nucleus i.e. one proton attached to a carbon nucleus results in a doublet, two protons in a triplet etc.

The resonance observed at highest frequency (as listed in Table 2.13) is found in the region characteristic of a carbon nucleus of a carbonyl group.[105] This appears as a singlet in the off-resonance decoupled spectrum, as expected, and is thus assigned to the nucleus C_9.

Six peaks are found between 150 and 110 p.p.m., the region typical of aromatic carbon nuclei resonances. Two peaks, at 147.0 and 146.0 p.p.m., show no splitting in the off-resonance decoupled spectrum. These two facts suggest that these peaks arise from two nuclei in similar environments, having no protons directly attached. By comparison with the ^1H-decoupled ^{13}C N.M.R. spectrum of catechol (described on page 104) they are assigned to nuclei C_1 and C_2.

A resonance of low intensity is found in the decoupled spectrum at 130.3 p.p.m. Its lack of splitting in the off-resonance decoupled spectrum suggests it is due to the quaternary carbon, C_4. The remaining three peaks in this aromatic region must arise from the nuclei C_3, C_5, and C_6. The resonances are all of approximately the same intensity, and each is split into a doublet in the off-resonance spectrum, due to attachment of each one to a single proton. The peak at 124.4 p.p.m. is to slightly higher frequency than the other two resonances, which are only separated from each other by approximately 0.5 p.p.m. By comparison with the catechol spectrum the peak at 124.4 p.p.m. is tentatively assigned to the nucleus C_5.

Below 80 p.p.m. there are two resonances arising from the aliphatic side-chain nuclei, C_7 and C_8. The peak at higher frequency is split into a doublet in the off-resonance decoupled spectrum, suggesting this resonating ^{13}C nucleus is attached to one proton, and is thus assigned to C_8.

Corroborating this is the splitting of the second peak (at 38.3 p.p.m.) into a triplet, in the off-resonance spectrum due to the interaction of two protons attached to the nucleus, C_7.

5.2 Spectra of the complexes

The osmium (VI) and uranyl-catecholamine complexes together with the molybdenum and tungsten complexes of dopamine, are too insoluble to allow their spectra to be recorded.

(a) Complexes of the type $Na_2[MO_2(catecholamine)_2]$

(M = Mo(VI),W(VI); catecholamine = Dopa, isoproterenol, noradrenaline)

The resonances of these complexes recorded in aqueous solutions are listed in Tables 2.12 and the spectrum of $Na_2[MoO_2(Dopa)_2]$ is shown in Figure 2.18. In each case, the resonances arising from the nuclei, C_1 and C_2, attached to the catechol hydroxy groups, appear to be shifted to higher frequency, compared to that found for the free ligand, by at least 10 p.p.m. This is the most significant change of the spectrum and is almost identical to that found in the ^1H decoupled ^{13}C N.M.R. spectrum of catechol, on coordination in the complexes $K_2[MoO_2(cat)_2]$ and $Na_2[W_2O_5(cat)_2]$; both shift to higher frequency by about 10 p.p.m.

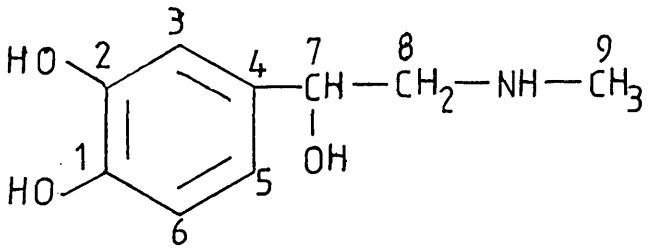
In each case a slight shift to lower frequency is consistently observed for the aromatic ring carbon nuclei C_3, C_4, C_5, and C_6, on coordination. This is comparable to the shift reported for the aryl carbon resonance of enterobactin [107] on coordination to gallium via the catecholato moieties, and is further evidence for coordination through the aromatic part of the catecholamine molecules.

Very little change is observed for the resonances due to the aliphatic side-chain. If coordination did occur through this side-chain, some change would be expected in the positions of these resonances, and little change would occur in the aromatic carbon resonances.

(b) Spectrum of the complex Mo_2O_5(adrenaline)$_2$

The ^1H decoupled ^{13}C N.M.R. spectrum of this complex was recorded in d^6 D.M.S.O. Because of the limited solubility of this complex in any solvent, not all the resonances could be clearly distinguished or unequivocally assigned. Two peaks, at 145.1 and 144.8 p.p.m., however, may be clearly observed, and the position compares well with the reported values[187] for the resonances of the nuclei C_1 and C_2 in uncoordinated adrenaline (as labelled in Figure 2.19). This suggests that the catecholato moiety remains uncoordinated in this complex.

FIG. 2.19



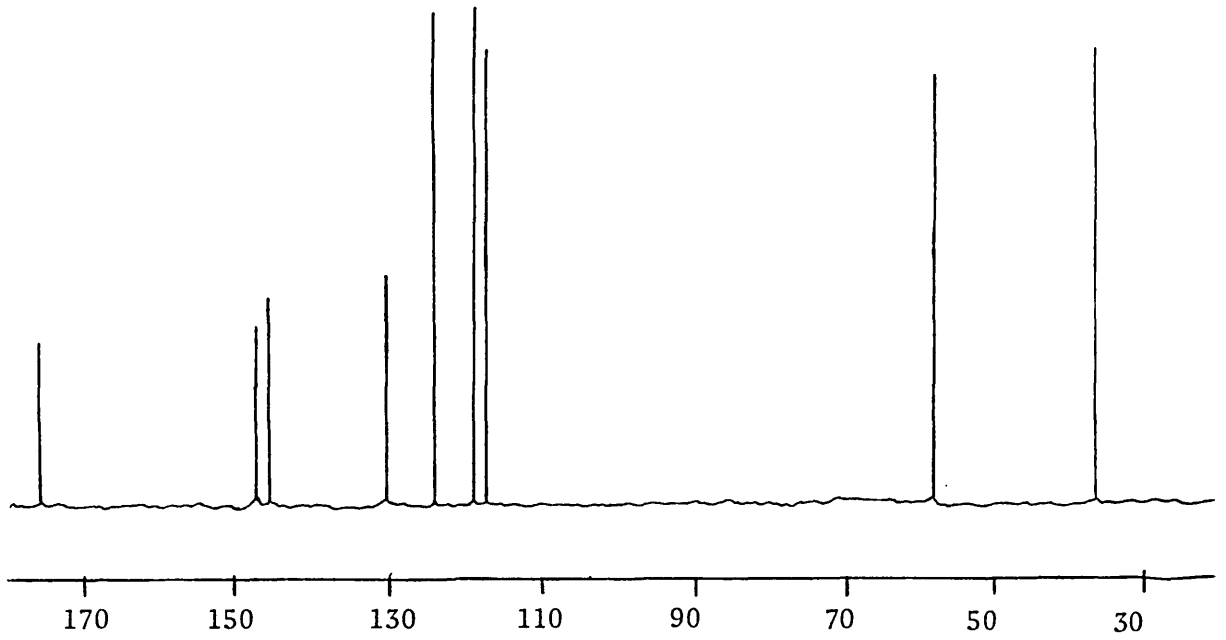


Figure 2.16 - ^{13}C N.M.R. spectrum of Dopa

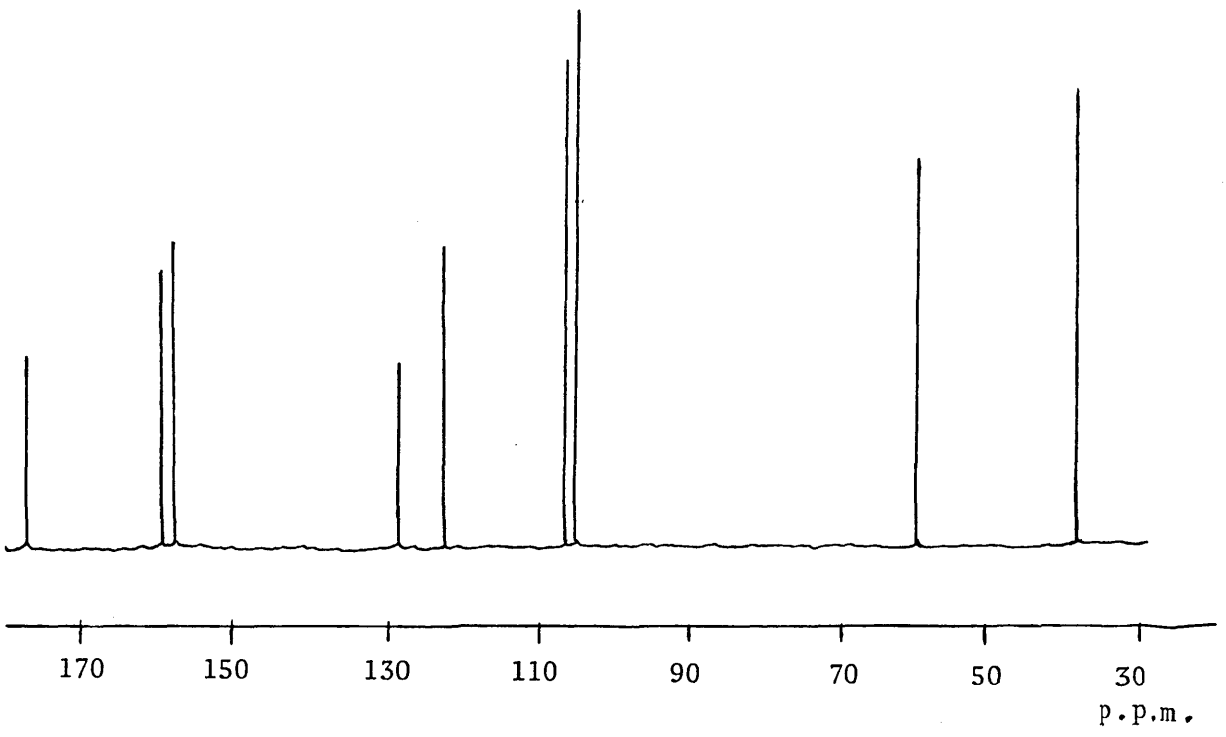


Figure 2.18 - ^{13}C N.M.R. spectrum of $Na_2[MoO_2(Dopa)_2]$

Table 2.12(a):- ^{13}C N.M.R. Resonances of Dopa, $Na_2[MoO_2(Dopa)_2]$ and $Na_2[WO_2(Dopa)_2]$ (p.p.m.)

Dopa	$Na_2[MoO_2(Dopa)_2]$	$Na_2[WO_2(Dopa)_2]$	Assignment
176.5	177.1	177.0	C_9
147.0	159.0	158.5	C_1/C_2
146.1	158.0	157.5	C_1/C_2
130.3	128.3	128.7	C_4
124.4	121.9	122.4	
119.7	117.0	118.0	$C_3/C_5/C_6$
119.3	116.1	117.1	
58.8	59.6	59.4	C_8
38.3	39.0	38.9	C_7

Carbon nuclei labelling as shown in Figure 2.17.

Table 2.12(b):- ^{13}C N.M.R. Resonances of Noradrenaline Hydrochloride, $Na_2[MoO_2(noradrenaline)_2]$ and $Na_2[WO_2(noradrenaline)_2]$ (p.p.m.)

Noradrenaline HCl	$Na_2[MoO_2(nor)_2]$	$Na_2[WO_2(nor)_2]$	Assignment
	158.1		
146.8	158.0	158.1	C_1/C_2
134.9		135.8	C_4
121.3	118.6	118.8	
119.3	115.5	116.6	$C_3/C_5/C_6$
116.8	113.2	114.6	
72.0	72.2	72.5	C_7
48.5	47.7	48.1	C_8

where nor represents noradrenaline bound in the catecholato mode.
Carbon nuclei labeling as shown in Figure 2.20.

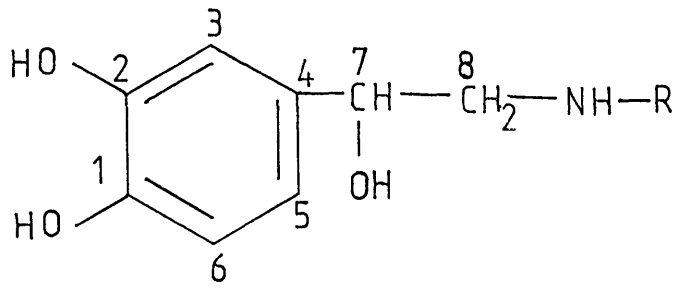
Table 2.12(c):- ^{13}C N.M.R. Resonances of Isoproterenol Hydrochloride, $Na_2[MoO_2(isoproterenol)_2]$ and $Na_2[WO_2(isoproterenol)_2]$ (p.p.m.)

Isoproterenol HCl	$Na_2[MoO_2(iso)_2]$	$Na_2[WO_2(iso)_2]$	Assignment
	158.1		
147.0	157.9	157.6	C_1/C_2
135.0	131.9	132.2	C_4
121.2	118.6		
119.1	115.4	116.4	$C_3/C_5/C_6$
116.6	113.2	114.3	
71.4	71.6	71.6	C_7
53.9	53.3	53.3	C_8/C_9
53.1	52.6	52.6	C_8/C_9
21.1	20.6	20.6	C_{10}/C_{11}
20.8	20.2	20.2	C_{10}/C_{11}

where iso represents isoproterenol bound in the catecholato mode.

Figure 2.20:- Carbon nuclei labeling for noradrenaline and isoproterenol.

a b



a R=H

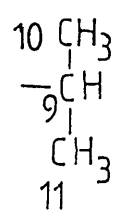
b R= 

Table 2.13:- ^{13}C N.M.R. resonances of the off resonance coherent decoupled spectrum of Dopa (p.p.m.)

Peak position	Assignment
176.5	C_9
146.9	C_1/C_2
146.1	C_1/C_2
130.3	C_4
124.8	C_5
123.9	C_5
120.1	
119.7	C_3/C_6
119.2	
118.7	
59.1	C_8
58.5	C_8
38.7	C_7
38.3	C_7
37.9	C_7

Carbon nuclei labeling as shown in Figure 2.17

6. ELECTROCHEMISTRY

As in the case of the catecholato complexes, this is not an extensive electrochemical investigation, but the technique is used to gain possible further knowledge of the types of complexes obtained with catecholamine ligands, by comparison to known catecholato complexes.

6.1 Literature measurements

The complex $K_2[MoO_2(cat)_2]$ has been extensively investigated electrochemically.[126,127] The system was found to be very sensitive to only slight changes in conditions; the medium which was found to give the best results was a pH 6.26 pyridine buffer. Two reversible reductions were observed; an initial one electron transfer, corresponding to the reduction of the metal centre to molybdenum (V) followed by a two-electron transfer to molybdenum (III). These products were found to have only transient stability, and this can lead to the occurrence of chemical reactions which give rise to different peaks in the cyclic voltammograms recorded. Uptake of two protons accompanies each electron-transfer step, replacing an oxo group, with a coordinated water molecule. The aquo groups are labile and may be replaced by a pyridine molecule, or undergo dimerisation (in the case of molybdenum (V)). The major processes are shown in equations 2.1 - 2.3.

$$[MoO_2(cat)_2]^{2-} + 2H^+ + 2e^- \rightleftarrows [MoO(H_2O)(cat)_2]^- \quad \text{Equation 2.1}$$

$$[MoO(H_2O)(cat)_2]^- + 2H^+ + 2e^- \rightleftarrows [Mo(H_2O)_2(cat)_2]^- \quad \text{Equation 2.2}$$

$$2[MoO(H_2O)(cat)_2]^- \rightarrow [Mo_2O_4(cat)_2(H_2O)_2]^{2-} + 2\,H_2cat \quad \text{Equation 2.3}$$

6.2 Experimental results

Since a pH 6.26 pyridine buffer was the most successful medium for investigation of $K_2[MoO_2(cat)_2]$ this medium is used here in the study of these catecholamine complexes.

(a) $K_2[OsO_2(catecholamine)_2]$ complexes

Dissolution of these complexes in the pyridine buffer solution (pH 6.7) immediately resulted in the deep blue colour characteristic of polymeric osmium (VI) - catecholato complexes, $[OsO(O_2R)_2]_n$ which forms in acidic media. Any cyclic voltammograms recorded would not then necessarily be those of the complex $K_2[OsO_2(catecholamine)_2]$.

(b) $UO_2(catecholamine)nH_2O$ complexes

These complexes are insoluble in the aqueous (or any other) medium.

(c) Catecholamine complexes of molybdenum(VI) and tungsten(VI)

The complexes $MoO_2(dopamine)_2$ and $WO_2(dopamine)_2$ are insufficiently soluble for any electrochemical investigation.

(i) $Na_2[MO_2(catecholamine)_2]$. (M = Mo(VI), W(VI); catecholamine = Dopa, isoproterenol, noradrenaline)

The purpose of this investigation is to compare the electrochemistry of the catecholamine complexes in aqueous media with the well-defined $[MoO_2(cat)_2]^{2-}$ system. However, although we can reproduce the general shape of the cyclic voltammograms for $[MoO_2(cat)_2]^{2-}$, and for each of the catecholamine complexes studied, in pyridine and phosphate buffers, the peak potentials measured are not consistent.

The results can, therefore, only be used to show qualitatively any similarity between the catecholamine complexes and the analogous catecholato complex.

These complexes each showed two quasi-reversible reductions. The cyclic voltammograns (C.V.'s) are very weak, so the peak positions and reversibility are confirmed by the more sensitive technique of differential polarography. A typical C.V. is shown in Figure 2.21.

Oxidation of $K_2[MoO_2(cat)_2]$ shows behaviour typical of the catecholato ligand (as described earlier, p.28) with the corresponding peak on the reverse scan due to reduction of the oxidation product, benzoquinone, back to catechol. This oxidation is also observed for these complexes, although the corresponding reduction peak is not always recorded. Such an oxidation would presumably occur whichever mode of coordination the catecholamine molecule has attained. The potential at which it occurs is no guide in this case because of the inconsistency of any measurements.

The reduction behaviour described is almost identical with that found for $[MoO_2(cat)_2]^{2-}$, with two reversible, or quasi-reversible, reductions, presumably arising from reduction to molybdenum(V) and molybdenum(III).

(ii) Mo_2O_5(adrenaline)$_2$

Within the limits of these experiments it would not be possible to differentiate between the proposed mode of coordination in this complex and the catecholato mode.

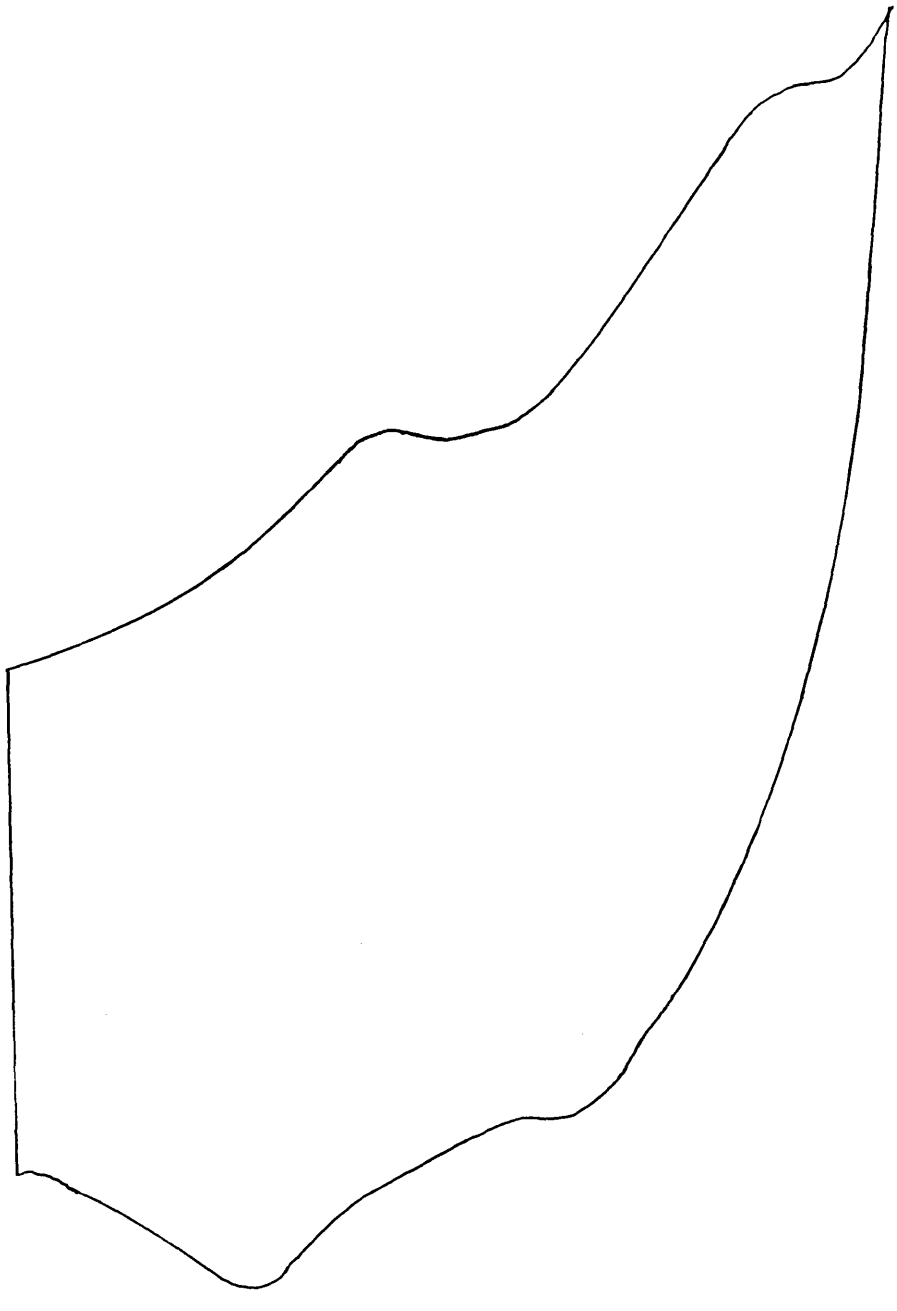


Figure 2.21 - Cyclic voltammogram of $Na_2[WO_2(isoproterenol)_2]$

Reduction from 0V. (1cm = 50 mV)

RESUME OF CHAPTER II

The preparation, vibrational, ^{1}H and ^{13}C N.M.R. spectra, and electrochemical properties of a number of new catecholamine complexes are reported.

Complexes of the five catecholamines, adrenaline, noradrenaline, dopamine, isoproterenol, and Dopa with osmium are prepared and studied by the above methods. It is suggested that they have the general formula $K_2[OsO_2(cat^*)_2]$, where cat^* represents the double deprotonated catecholamine, bound in the catecholato mode.

The same five catecholamines form complexes with the uranyl group, and have been studied by infrared spectroscopy. They are formulated as $UO_2(cat^*)nH_2O$, where cat^* represents the double deprotonated catecholamine, bound in the catecholato mode.

Complexes of the type $Na_2[MO_2(cat^*)_2]$ (where M = Mo(VI), W(VI) and cat^* is the double deprotonated catecholamine bound in the catecholato mode) are prepared with the ligands noradrenaline, isoproterenol and Dopa. Under the same conditions, the complex $MO_2(dopamine)_2$ forms (M = Mo(VI) where dopamine is postulated to be monodeprotonated and to coordinate through the catechol moiety),

Under acidic conditions, the complex $Mo_2O_5(adrenaline)_2$ has been isolated. The ligand is thought to coordinate through its aliphatic side-chain.

7. EXPERIMENTAL

The ligands dopamine hydrochloride, noradrenaline hydrochloride, isoproterenol hydrochloride, Dopa and adrenaline were obtained from the Aldrich Chemical Company.

7.1 Preparation of osmium (VI) - catecholamine complexes

The preparations were carried out under nitrogen, using degassed solvents.

A solution of potassium hydroxide (0.1g, 0.002 moles) in water ($5cm^3$) was added to a solution of potassium osmate, trans - $K_2[OsO_2(OH)_4]$,(0.2g, 0.0005 moles) in water ($10cm^3$). Addition of a solution of the hydrochloride ligand (0.001 moles) to the above solution followed immediately, to give the deep red colour characteristic of the trans-osmyl catecholato complexes, instantaneously.[19] The solution was immediately reduced on the rotary evaporator and the product recrystallised from a water-ethanol mixture, giving very dark red-brown solids.

In the preparation of the Dopa and adrenaline complexes the potassium hydroxide solution was added to a flask containing the ligand, so that the ligand completely dissolved.

Dipotassium trans-bis (dopamine) dioxo-osmium (VI) $K_2(OsO_2(C_8H_9NO_2)_2]$

Found:- C = 31.5, H = 3.0, N = 4.5

$C_{16}H_{18}K_2N_2O_6Os$ requires C = 31.9, H = 3.0, N = 4.7%

Yield = 50%

Dipotassium trans-bis(noradrenaline) dioxo-osmium (VI)

$K_2[OsO_2(C_8H_9NO_3)_2]$

Found:- C = 30.7, H = 2.5, N = 3.9;

$C_{16}H_{18}K_2N_2O_8Os$ requires C = 30.3, H = 2.8

N = 4.4%

Yield = 55%

Dipotassium trans-bis(isoproterenol) dioxo-osmium (VI)

$K_2[OsO_2(C_{11}H_{15}NO_3)_2]$

Found:- C = 37.5, H = 3.9, N = 3.7,

$C_{22}H_{30}K_2N_2O_8Os$ requires C = 37.1, H = 4.3, N = 3.9

Yield = 50%

Dipotassium trans-bis (Dopa) dioxo-osmium (VI)

$K_2[OsO_2(C_9H_9NO_4)_2]2H_2O$

Found:- C = 29.3, H = 2.6, N = 3.8;

$C_{18}H_{22}K_2N_2O_{12}Os$ requires C = 29.7, H = 3.0, N = 3.9

Yield = 50%

Dipotassium trans-bis (adrenaline) dioxo-osmium (VI)

$K_2[OsO_2(C_9H_{11}NO_3)_2]3H_2O$

Found:- C = 29.7, H = 2.9, N = 3.8;

$C_{18}H_{28}K_2N_2O_{11}Os$ requires C = 30.2, H = 3.9, N = 3.9%

Yield = 60%

The tetraphenylphosphonium salts were prepared by addition of an aqueous solution of tetraphenylphosphonium chloride to the deep red solution, in a mole ratio of 2:1 with the metal ion.

Bis[tetraphenylphosphonium]trans-bis (noradrenaline) dioxo-osmium (VI), $[(C_6H_5)_4P]_2[OsO_2(C_8H_9NO_3)_2]H_2O$

Found:- C = 61.9, H = 4.4, N = 2.6;

$C_{64}H_{60}N_2O_9OsP_2$ requires C = 61.3, H = 4.8, N = 2.2%

Yield = 70%

Bis[tetraphenylphosphonium]trans-bis (isoproterenol) dioxo-osmium (VI), $[(C_6H_5)_4P]_2[OsO_2(C_{11}H_{15}NO_3)_2]$

Found:- C = 64.5, H = 5.8, N = 2.4;

$C_{70}H_{70}N_2O_8OsP_2$ requires C = 63.7, H = 5.4, N = 2.1%

Yield = 70%

Bis[tetraphenylphosphonium]trans-bis (Dopa) dioxo-osmium (VI), $[(C_6H_5)_4P]_2[OsO_2(C_9H_9NO_4)_2]3H_2O$

Found:- C = 58.3, H = 4.3, N = 2.3;

$C_{66}H_{64}N_2O_{11}OsP_2$ requires C = 58.9, H = 4.8, N = 2.1%

Yield = 65%

Bis[tetraphenylphosphonium]trans-bis (adrenaline) dioxo-osmium(VI) $[(C_6H_5)_4P]_2[OsO_2(C_9H_{11}NO_3)_2]$

Found:- C = 62.3, H = 5.3, N = 2.6;

$C_{66}H_{62}N_2O_8OsP_2$ requires C = 62.8, H = 5.0, N = 2.2%

Yield = 65%

Bis (tetraphenylphosphonium) trans-bis(dopamine)dioxo-osmium(VI)

$[(C_6H_5)_4P]_2[OsO_2(C_8H_9NO_2)_2]2H_2O$

Found:- C = 61.6, H = 5.3, N = 2.8

$C_{64}H_{62}N_2O_8OsP_2$ requires C = 62.0, H = 5.0, N = 2.3%

Yield = 70%

7.2 Preparation of the uranyl-catecholamine complexes

The ligand hydrochloride (0.001 moles) in water ($5cm^3$) was added to a solution of uranyl acetate (0.14g, 0.00024 moles) in water ($10cm^3$). The solution immediately became dark brown and a flocculent brown precipitate soon formed. After standing a few hours the product was filtered off or separated by centrifugation. It was washed with ethanol and diethyl ether, and dried over concentrated sulphuric acid.

The ligands Dopa and adrenaline were much more difficult to dissolve than the hydrochlorides of the other ligands. Dopa (0.001 moles) was dissolved in water (approximately $25cm^3$) by warming and stirring. Adrenaline (0.001 moles) was stirred for a few hours in water ($100cm^3$) and the resulting solution was filtered into the uranyl acetate solution. Only a small amount of adrenaline would dissolve.

Mono (dopamine) trans-dioxo-uranium (VI), $UO_2(C_8H_9NO_2)H_2O$

Found:- C = 20.4, H = 2.4, N = 2.2

$C_8H_{11}NO_5U$ requires C = 20.7, H = 3.7, N = 2.7%

Mono (noradrenaline) trans-dioxo-uranium (VI), $UO_2(C_8H_9NO_3)H_2O$

Found:- C = 21.2, H = 2.0, N = 2.6;

$C_8H_{11}NO_6U$ requires C = 21.1, H = 2.4, N = 3.1%

Mono (isoproterenol) trans-dioxo-uranium (VI), $UO_2(C_{11}H_{15}NO_3)2H_2O$

Found:- C = 25.7, H = 3.0, N = 2.2;

$C_{11}H_{19}NO_7U$ requires C = 25.6, H = 3.7, N = 2.7%

Mono (Dopa) trans-dioxo-uranium (VI), $UO_2(C_9H_9NO_3)H_2O$

Found:- C = 22.8, H = 2.6, N = 2.9;

$C_9H_{11}NO_6U$ requires C = 22.4, H = 2.3, N = 2.9%

Mono (adrenaline) trans-dioxo-uranium (VI), $UO_2(C_9H_{11}NO_3)4H_2O$

Found:- C = 20.4, H = 2.4, N = 2.2

$C_9H_{19}NO_9U$ requires C = 20.7, H = 3.7, N = 2.7%

7.3 Preparation of Molybdenum (VI) and Tungsten (VI) - Catecholamine Complexes

(a) Complexes of the type, $Na_2[MO_2(cat)_2]$, (M = Mo(VI), W(VI), cat. represents noradrenaline, isoproterenol, and Dopa bound in the catecholato mode).

Sodium molybdate (0.16g, 0.00066 moles) in water ($10cm^3$) and a solution of the hydrochloride ligand (0.0013 moles) in water ($5cm^3$) were mixed. A deep red colour was immediately observed. No precipitate resulted after long standing, so the solid was isolated either by precipitation with ethanol or by reduction on the rotary evaporator. The dark red products were recrystallised from a water ethanol mixture.

Dopa was dissolved in water ($25cm^3$) by warming and stirring.

Disodium bis (noradrenaline)-cis-dioxo-molybdenum(VI), $Na_2[MoO_2(C_8H_9NO_3)_2]H_2O$

Found:- C = 36.3, H = 4.0, N = 5.4

$C_{16}H_{20}MoN_2Na_2O_9$ requires C = 36.5, H = 3.8, N = 5.3%

Yield = 50%

Disodium bis (isoproterenol)-cis-dioxo-molybdenum(VI),

$Na_2[MoO_2(C_{11}H_{15}NO_3)_2]H_2O$

Found:- C = 43.6, H = 5.5, N = 4.6

$C_{22}H_{32}MoN_2Na_2O_9$ requires C = 43.3, H = 5.3, N = 4.6%

Yield = 50%

Disodium bis-(Dopa) cis-dioxo-molybdenum (VI),

$Na_2[MoO_2(C_9H_9\ NO_4)_2]H_2O$

Found:- C = 36.5, H = 3.9, N = 4.4

$C_{18}H_{20}MoN_2Na_2O_{11}$ requires C = 37.00, H = 3.8, N = 4.8%

Yield = 50%

The analogous tungsten complexes were similarly prepared using sodium tungstate. Bright yellow solids resulted.

Disodium bis-(noradrenaline) cis-dioxo-tungsten (VI),

$Na_2[WO_2(C_8H_9NO_3)_2]H_2O$

Found:- C = 30.9, H = 3.3, N = 4.5;

$C_{16}H_{20}N_2Na_2O_9W$ requires C = 31.3, H = 3.3, W = 4.6%

Yield = 60%

Disodium bis-(isoproterenol) cis-dioxo-tungsten (VI)

$Na_2[WO_2(C_{11}H_{15}NO_3)_2]$

Found:- C = 38.2, H = 4.9, N = 4.0;

$C_{22}H_{30}N_2Na_2O_8W$ requires C = 38.7, H = 4.7, N = 4.1%

Yield = 50%

Disodium bis-(Dopa) cis-dioxo-tungsten (VI),

$Na_2[WO_2(C_9H_9\ NO_4)_2]2H_2O$

Found:- C = 31.0, H = 2.9, N = 3.6;

$C_{18}H_{22}N_2Na_2O_{12}W$ requires C = 31.4, H = 2.9, N = 3.6%

Yield = 60%

The tetraphenylphosphonium salts of the isoproterenol complexes were prepared by addition of an aqueous solution of tetraphenylphosphonium chloride (in a 2:1 ratio of chloride to metal) to the solution resulting from mixing of the ligand solution with that of sodium molybdate or sodium tungstate.

Bis (tetraphenylphosphonium)- bis (isoproterenol) cis-dioxo-molybdenum (VI), $[(C_6H_5)_4P]_2[MoO_2(C_{11}H_{15}NO_3)_2]H_2O$.

Found:- C = 68.1, H = 5.9, N = 2.2, P = 5.6;

$C_{70}H_{72}MoN_2O_9P_2$ requires:- C = 67.6, H = 5.8, N = 2.3 P = 5.0%

Bis (tetraphenylphosphonium)- bis (isoproterenol) cis-dioxo-tungsten (VI), $[(C_6H_5)_4P]_2[WO_2(C_{11}H_{15}NO_3)_2]2H_2O$

Found:- C = 62.8, H = 5.9, N = 2.4, P = 5.1

$C_{70}H_{74}N_2O_{10}P_2W$ requires:- C = 62.3, H = 5.5, N = 2.0, P = 4.6%

(b) Molybdenum (VI) and Tungsten (VI) - Dopamine Complexes

(i) Sodium molybdate (0.16g, 0.00066 moles) in water (10cm^3) and dopamine hydrochloride (0.25g, 0.0013 moles) in water (5cm^3) were mixed. An orange precipitate formed immediately. It was filtered off, washed with ethanol and diethyl ether, and dried over concentrated sulphuric acid.

Bis (dopamine) cis-dioxo-molybdenum(VI), $MoO_2(C_8H_{10}NO_2)_2H_2O$

Found:- C = 42.9, H = 4.5, N = 6.3

$C_{16}H_{22}MoO_7N_2$ requires C = 42.7, H = 4.9, N = 6.2%

Yield = 100%

The tungsten complex was prepared similarly, using sodium tungstate. A bright yellow precipitate immediately formed.

Bis (dopamine) cis-dioxo-tungsten (VI), $WO_2(C_8H_{10}NO_2)_2$

Found:- C = 34.9, H = 3.8, N = 5.5;

$C_{16}H_{20}N_2O_6W$ requires C = 34.8, H = 3.7, N = 5.1%

Yield = 100%

(ii) Deuteriated MoO_2(dopamine)$_2$

Dopamine hydrochloride was dissolved in D_2O and shaken for ten minutes. Sodium molybdate in D_2O was added to the ligand solution. The orange precipitate that immediately resulted was filtered off, and dried, without washing, on the filter pump.

(c) Mo_2O_5(adrenaline)$_2$

Adrenaline (0.26g, 0.0013 moles) was dissolved in dilute hydrochloric acid (10cm^3), and added to a solution of sodium molybdate (0.16g, 0.00066 moles) in water (10cm^3). A deep red colour was observed immediately. After 45 minutes a fine precipitate formed. It was filtered off after standing overnight. The deep red product was washed with ethanol and diethyl ether, then dried over concentrated sulphuric acid.

Bis (adrenaline)-μ-oxo bis(cis-dioxo-molybdenum (VI))

$Mo_2O_5(C_9H_{12}NO_3)_2H_2O$

Found:- C = 32.9, H = 3.9, N = 4.3;

$C_{18}H_{26}Mo_2N_2O_{12}$ requires C = 33.0, H = 4.0, N = 4.3%

7.4 Preparation of Copper(II)-Dopa Complex

Cu(O,N-Dopa)$_2$ was prepared as reported in the literature.[145]

CHAPTER III TROPOLONE AND THE TROPOLONATO LIGAND

Our work on the chelating oxygen donor ligands of catechol and catecholamines described earlier has led us to investigate complexes of the tropolonato ligand. Like catechol tropolone also functions as an aromatic 0,0 chelating ligand, when the hydroxyl proton is removed. Tropolone has been found to have an inhibitory effect on the enzyme catechol-o-methyltransferase,[141] (concerned with the inactivation of circulating catecholamines) and dopamine-β-hydroxylase, the enzyme responsible for converting dopamine to noradrenaline.[188] Although there have been many reports of tropolonato complexes of the first row transition elements,[189–193] lanthanides and actinides,[189,194] very little has been done with the platinum group metals, or with molybdenum and tungsten. We have prepared and characterised a number of new tropolonato complexes, and studied them by ^{1}H, and ^{13}C N.M.R., E.P.R., infrared and Raman spectroscopy, electrochemistry, mass spectrometry and, in one case, X-ray crystallography.

1. INTRODUCTION

1.1 Tropolone

Tropolone ($C_7H_6O_2$,2-hydroxy-2,3,6 - cycloheptatrien-1-one) is a non-benzenoid aromatic compound, X-ray crystallographic studies have shown the compound to be dimeric in the solid state.[195,196] Shimonouchi and Sasada[195] suggested a bifurcated hydrogen bond; the hydroxyl group proton bonding to one carbonyl group intramolecularly and to another carbonyl group intermolecularly as shown in Figure 3.1.

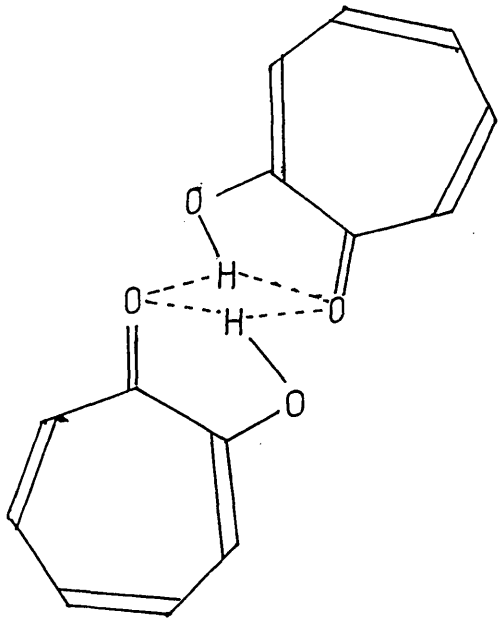


Figure 3.1 The tropolone dimer.

The aromaticity of the compound is indicated by the bond distances as shown in Figure 3.1. The bond lengths, excepting the bond C_1 - C_2 have values very close to that of a typical aromatic value (1.392Å),[196] although C_4 - C_6 is significantly shorter than the others.[197]

This was said to indicate that the averaging effect on the bond lengths due to the electron-attracting carbonyl group may not be exerted on the distant-part of the seven-membered carbon ring.[195] The C_1 - C_2 length approaches that of a single bond distance between two sp^2 hybridised carbon atoms (1.48Å).[118]

The molecule is essentially planar. The C_1 - O_1 length is shorter than the C_2 - O_2 distances, indicating that O_2 is the hydroxyl group oxygen. This was confirmed by the location of the proton.

The structure of tropolone may be explained by assuming it is a resonance hybrid of the three canonical forms shown in Figure 3.2.[195]

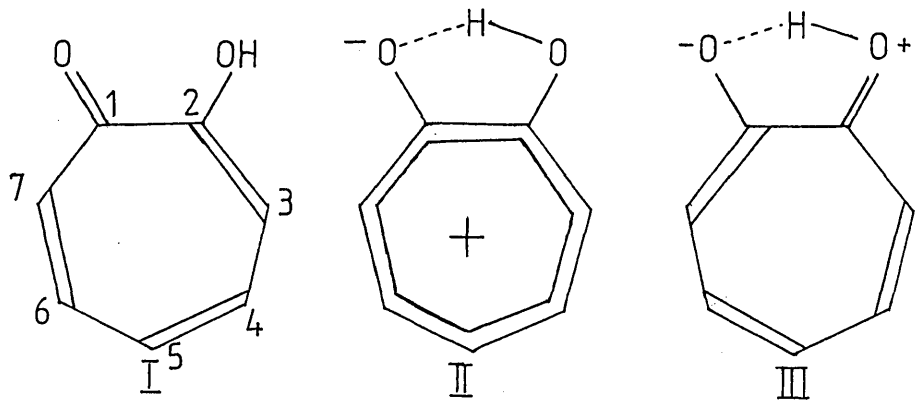


Figure 3.2 Canonical forms of tropolone.

The C - C - O angles, which give some indication of the polarisation of the carbonyl group, are found to be 124.2°, compatible with significant carbonyl polarisation, as in form III. Polarisation of the carbonyl group is significantly enhanced by the hydrogen bonding at the carbonyl oxygen atom.

An X-ray crystallographic investigation of sodium tropolonate (structural parameters listed in Table 3.3) has shown that the seven-membered carbon ring has much less variation of bond length than was found to be the case for tropolone. The C-O bond lengths were found to have approximately equal length in sodium tropolonate (1.27Å),[203] but the distance was found to be significantly longer than the other carbon-carbon distances, its length being very close to the value typical of a carbon-carbon single bond (1.48Å).[198]

The crystal structure of tropolone hydrochloride, on the other hand, revealed a regular heptagon of carbon atoms, the mean C-C distance being 1.40Å.[202] The C-O bonds again,have very similar lengths (1.40 and 1.42Å), being significantly longer than the C-O distances found for tropolone or sodium tropolonate. Lattice packing is very similar to that found for ionic crystals of the sodium chloride type. Tropolone hydrochloride was concluded to have the structure shown in Figure 3.3, with a net positive charge distributed over the whole carbon ring.

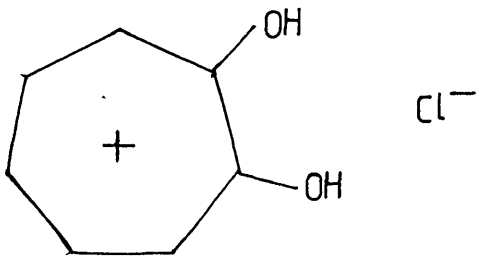


Figure 3.3 Tropolone Hydrochloride

Similar behaviour was found in the X-ray crystallographic study of $B(trop)_2Br.H_2O$.[204]

To explain this behaviour two possible modes of delocalisation of electron density through the tropolonato ligand have been proposed (Figure 3.4). For mode I, delocalisation involves only the peripheral atoms, including the oxygen atoms, but not the bond C_1 - C_2. The C-O bonds then have substantial double bond character, leading to bond distances similar to those found for the acetylacetonate complexes (1.27 - 1.29Å), and the C_1 - C_2 length would be approximately that of a Csp^2 - Csp^2 single bond. (1.48 - 1.51Å)[204]

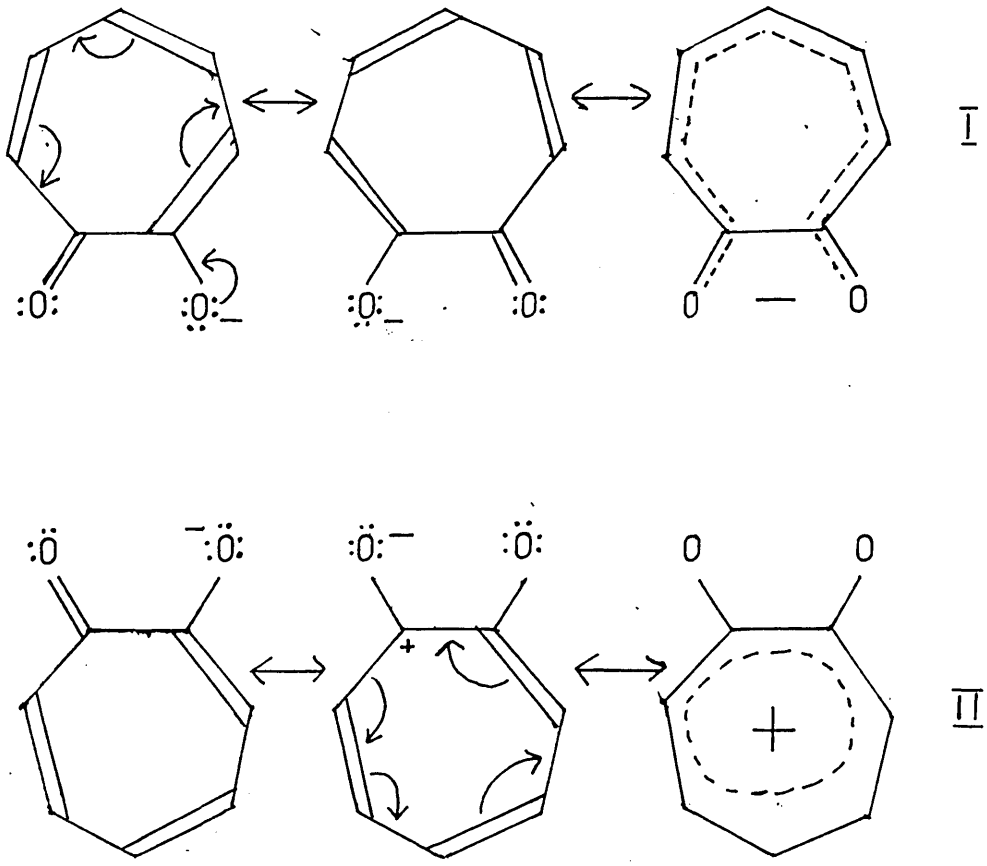


Figure 3.4 Modes of delocalisation of the tropolonato ligand

For mode II, the C-O bonds are not included in the delocalisation while the C_1 and C_2 atoms are involved. The two C-O lengths are now longer (1.343Å for the boron complex) and only slightly shorter than the length found for catechol (1.385Å). The carbon-carbon bond distances would be expected to be all of approximately equal length.

These different modes of delocalisation were thought to be influenced by the affinity of the coordinating ion for oxygen. Boron and the proton in tropolone HCl are both good acids towards oxygen, as compared to the more electropositive metals, and mode II is then stabilised.[204]

A perusal of the relevant literature soon elicits the information that Mode I is preferred in transition metal-tropolonato complexes. The tropolonato ligand may be observed to show a remarkable degree of inflexibility in its structure, as studied by X-ray crystallography. The bonding parameters of the tropolonato ligand hardly vary,[205] whatever the coordination number, metal ion radii, or metal ion electronic configuration in the complex. As may be ascertained from the tables of crystallographic data listed below, the ligand bite distance (defined as the distance between the two ligating oxygen atoms of one ligand) falls consistently within the narrow range of 2.40Å - 2.60Å. The bond between the two carbon atoms, C_1 - C_2, has a bond length which is always significantly greater (about 0.07Å) than any of the other bonds of the carbon ring. Its value is just a little less

than the value that has been suggested as typical of the length of a bond between two trigonally hybridised carbon atoms, leading to the conclusion that this bond is not involved to any great extent in the π electron delocalisation of the ligand.[200,201,206,207] Conjugation appears to be virtually complete around the periphery of the tropolone ring and includes the oxygen atoms.[206,208] The C-C bond lengths of this part of the ligand are very near to the typical aromatic value of 1.394Å. Increasing strength of the complexing bonds generally appears to be accompanied by a modest lengthening of the C-O bonds, and some shortening of the C_1 - C_2 bond.[198,209,210] Several reports noted a sequential decrease of the C-C bond lengths proceeding from the carbon atoms vicinal to the oxygen atoms to the central carbon atom, C_5.[198,205] Only part of this sequential decrease was considered to be real,[205] but it would seem feasible that the C_2 - C_3(C_1-C_7) distance is longer than the C_3-C_4(C_7-C_6) and C_4-C_5(C_6-C_5) sets, which are equivalent.

These factors are almost identical to the structure of the tropolonato anion described for sodium tropolonate.[206]

Distortions of the ligand from planarity have been reported, and are generally ascribed to constraints of lattice packing.[201,205]

The nature of the tropolonato ligand, in particular its compact planar conformation, low overall charge, and small, rigid ligand bite, leads to it being a very suitable ligand for the formation of complexes of high coordination number, especially with suitably large and highly charged cations.[189,190,194,198]

1.3 Transition-metal tropolonato complexes

(a) Occurence

There are many instances of bis(tropolonato) complexes with divalent metals.[110] Tropolonato complexes have been reported for all the first row transition metals.[193-198] The bis(tropolonato) complexes of the divalent metals between manganese and nickel, inclusive, were found to behave differently from the simple four-coordinate, mononuclear species, such as $Cu(trop)_2$. They have lower volatility and much less solubility. It was postulated that these complexes had polynuclear structures, in which the metal coordination number was greater than four, achieved by sharing oxygen atoms of the chelated tropolonato complexes.[190] This was subsequently found to be correct, as described below (for bridging tropolonato complexes).[200,201]

The most common tropolonato complexes are the tris(tropolonato) complexes which are discussed separately below.

Of the platinum metals, the complexes $Rh(trop)_3$[189] and $Pd(trop)_2$[190] have been well characterised. The preparation of $Ru(trop)_3$[211] involved complicated separation techniques, unusual in the formation of most tropolonato complexes. The only reported iridium complex appears to be $[Ir(all)_2(trop)]$,[212] where all is the π-allyl ligand.

The complex $[MoO(trop)_2Cl]$ has been reported.[189] The only tungsten-tropolonato complex mentioned is the substituted complex $[W(CO)_2(trop)(\eta^3\text{-allyl})Cl]^-$,[213] which was reported to be prepared from $[W(CO)_4(trop)]^-$.

Many complexes with the lanthanides and actinides have been reported.[189,190,215,216,217] Tris(tropolonato) and tetrakis(tropolonato) complexes were the most common formulations, but several uranyl-tropolonato[218-222] complexes have also been reported. The ability of the tropolonato ligand to form complexes of high coordination numbers, described above, has led to the preparation of ten-coordinate complexes in the pentakis(tropolonato) complexes of thorium(IV),[194,214,223] uranium(IV),[194,223] uranium(V),[224,225] and protactinium(V).[224,225]

(b) Preparation of Tropolonato Complexes

Tropolonato complexes are generally prepared by mixing an aqueous solution of a salt of the metal in the required oxidation state, with a solution of tropolone, usually in a polar solvent, in a stoichiometric ratio. Some form of pH control is often used e.g. sodium acetate solution, and gentle heating may be required. The tropolonato complex usually precipitates from the reaction mixture. Complexes with higher coordination numbers are usually prepared from the appropriate lower coordinate complex with sodium or lithium tropolonate, e.g. reaction of $U(trop)_4$ and Li(trop) to form $Li[U(trop)_5]$.[194]

(c) Tris(tropolonato) complexes

X-ray crystallographic studies have been undertaken on a number of these complexes; their significant structural parameters are listed in Table 3.1. The rigid nature of the tropolonato ligand leads to considerable distortion from octahedral coordination of the oxygen atoms about the metal ion,

The closely related acetylacetonato(acac) ligands are more flexible and can undergo rotations and foldings. Ligand interactions in acetylacetonato complexes can therefore be kept to a minimum by varying the ligand bite. The inflexible tropolonato ligand does not appear to be able to undergo any distortions itself,[226] so ligand interactions are minimised by distortion of the oxygen atom arrangement about the metal ion. The "MO_6"(M = metal ion) coordination polyhedron is twisted away from octahedral (or trigonal antiprismatic) coordination, towards trigonal prismatic coordination.

In complexes where the ligands do not control stereochemistry, it has been shown that, for most metal ions, ligand field stabilisation energy (L.F.S.E.) of a trigonal prismatic complex is less than that for octahedral coordination.[226] Exceptions are predicted for ions with d^0, d^1, low spin d^2, high spin d^5 and d^{10} electronic configurations, where there is no stereochemical preference. Further studies have concluded that the stereochemistry is affected by the nature of the donor atoms, the availability of d electrons in the metal, interactions between the ligands and the ligand bite.[205] A small ligand bite seems to favour trigonal prismatic coordination.

A measure of the degree of distortion of a six-coordinate complex from the ideal octahedral or trigonal prismatic geometry is the projected twist angle, ϕ.[205] This angle is defined by the projection of the metal ligand vectors on a plane

normal to the C_3 or pseudo-C_3 axis, as shown in Figure 3.5. The angle ϕ is 60^o for the trigonal antiprism, 0^o for trigonal prismatic coordination.

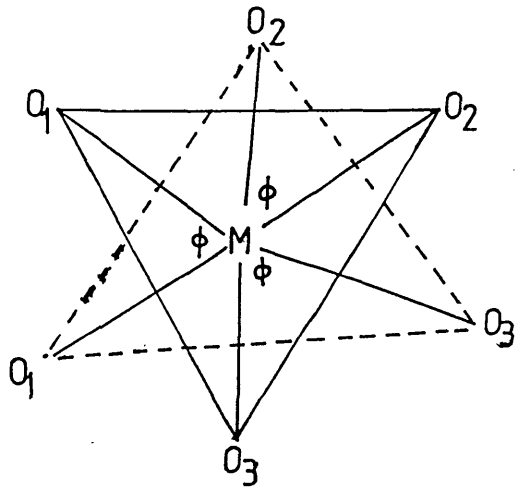


Figure 3.5:- Definition of the twist angle ϕ

Another such parameter is the compression ratio. This is a measure of the departure from a regular octahedral arrangement of the ligating atoms.[205]

These effects are clearly seen in $Al(trop)_3$,[205] where the short ligand bite of tropolone would lead to an untenable compression ratio for the trigonal antiprism, so that the resulting structure is found to be midway between the two extremes, with $\phi = 48^o$.

The complex $Sc(trop)_3$ was found to have a twist angle of 33^o. Since scandium(III) has a d^o electronic configuration, no L.F.S.E. considerations affect the structure of the complex. The observed configuration is a result of a balance between inter- and intra-molecular contacts.

In this molecule, although trigonal prismatic stereochemistry was shown to be stable on geometric grounds, in the crystalline lattice,intermolecular compressive forces tend to distort the molecule towards trigonal antiprismatic coordination. A diagram showing the significant bond lengths of this tris(tropolonato) complex is shown in Figure 3.6.[226]

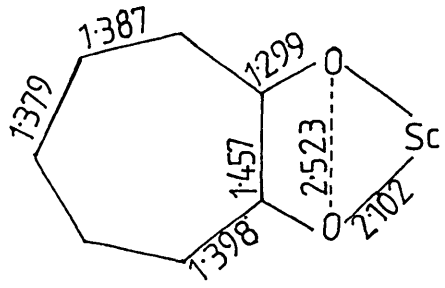


Figure 3.6:- Bond lengths of $Sc(trop)_3$

For the complexes $Co(trop)_3$ and $Mn(trop)_3$, the L.F.S.E.'s arising from the cobalt(III) and manganese(III) ions, having electronic configurations d^6 and d^4 respectively, must be considered. The twist angles are much closer to that of ideal trigonal antiprismatic coordination (60^o).

An interesting variation in structure was observed for $Mn(trop)_3$.[208] Within each unit cell, there were found to be two crystallographically independent molecules, of which one has tetragonally distorted $Mn-O_6$ geometry, the other shows orthorhombic $Mn-O_6$ distortion. This effect may be due to a weak intermolecular coupling through the tropolonato ligands.

Stereochemical non-rigidity has been reported for some tropolonato complexes in solution.[214] Tris-chelate complexes of general type $M(A-B)_3$,[227] containing three unsymmetrical bidentate ligands, may undergo intramolecular processes of isomerisation (cis-trans) or racemisation ($\Lambda \rightarrow \Delta$). Temperature - dependent ^1H nuclear magnetic resonance studies of complexes with isopropyl- and isopropenyl tropolone have been carried out, particularly with aluminium and cobalt(III).[211,214,227] The stereochemically non-rigid behaviour of $Co(R\text{-}trop)_3$, (where R-trop is α-isopropyltropolone or α-isopropenyltropolone) is unprecedented among cobalt(III) complexes. Rearrangement rates frequently exhibit a significant dependence on the nature of the chelating ligand, and on the size and electronic configuration of the coordinating metal ion. It would appear that twist angles considerably less than 60^o can lead to stereochemical non-rigidity using the trigonal twist mechanism. This does not explain the exceptional behaviour of $Co(R\text{-}trop)_3$, however.

The tris(tropolonato) complexes of many of the lanthanides were found to be insoluble in most solvents,[190] in distinct contrast to other reported tris(tropolonato) complexes, such as $Fe(trop)_3$, which are soluble in such media as ethanol and chloroform. Their infra-red spectra also exhibited a peak at $1590cm^{-1}$, found only for the insoluble and polymeric cobalt(II) and nickel(II) tropolonates, believed to be characteristic of "polymeric" metal tropolonates.[189] This behaviour was explained by assuming polynuclear structures $[Ln(trop)_3]_n$ with $n>1$, linked by sharing some of the chelated tropolonato oxygen atoms (to give three coordinate oxygens - as described for bridging tropolonates below). This is in line with the tendency of rare earth chelates not to be satisfied with any coordination number less than seven.[189] This behaviour manifests itself in the lanthanide tris(acetylacetonato) complexes which are often solvated, and easily add strong bidentate bases, such as o-phenanthroline, resulting in eight coordination.

Polynuclear complexes are postulated for all the lanthanide tris(tropolonato) complexes from lanthanum ($4\ f^0$) to the holmium ($4\ f^{10}$) ion. Complexes of the smaller ions erbium to lutetium ($4f^{11}$ - $4f^{14}$) were found to be mononuclear.[189]

(d) Tetrakis-tropolonato complexes

Tetrakis complexes of the tropolonato ligand occur mainly with the early transition metals, the lanthanides and actinides.

The tris(tropolonato) complexes of scandium, yttrium and the rare earth trivalent ions react with sodium tropolonate to form sodium salts of the respective metal tetrakis(tropolonato) anions, $Na[M(trop)_4]$.[189] The X-ray crystal structure of the acid dimer of tetrakis(tropolonato) scandium (III), $HSc(trop)_4$, has been reported[229,230] (X-ray data are listed in Table 3.2). It was found to have a coordination polyhedron of eight oxygen atoms about the scandium ion, arranged as an irregular bicapped trigonal prism distorted towards a dodecahedron. The compound is a hydrogen-bonded dimer.

The metals zirconium, hafnium and thorium, of Group IV of the periodic table all form tetrakis (tropolonato) complexes of the type $M(trop)_4$.[189] The structures of $Hf(trop)_4$[232] and $Zr(trop)_4$[231] were found to be slightly distorted dodecahedra. Unlike the smaller hafnium and zirconium ions, thorium (IV) has shown an ability to expand its coordination sphere,[190] as found in the X-ray crystallographic study of $Th(trop)_4DMF$.[198] This complex was shown to contain DMF in the inner coordination sphere achieving nine coordination and the coordination polyhedron about the metal was described as a monocapped square antiprism.

The cationic complexes $[Nb(trop)_4]^+$ [189] and $[Ta(trop)_4]^+$ were reported to be easily prepared, and the structure of the niobium complex has been determined by X-ray studies. The "NbO_8" coordination polyhedron was found to be an irregular bicapped trigonal prism, distorted towards a dodecahedron. This complex was found to have unexpectedly small O,...,O interligand distances (2.432Å). The counter-ion of the complex studied

in the X-ray crystallographic report of $[Nb(trop)_4]_2$ $[O(H...Cl)_3]CH_3CN$ was found to contain the H_3O^+ cation hydrogen-bonded to the three chloride ions placed at the base of a flattened trigonal prism.[189]

(e) The bridging tropolonato ligand

The tropolonato ligand has been found, by X-ray crystallographic studies, to act in a bridging role in two complexes. The relevant data are listed in Table 3.3.

The complex $[Ni(trop)_2H_2O]_2$ was found to be a centrosymmetric dimer,[200] in which each nickel(II) atom has six oxygen atoms arranged around it in a distorted octahedral manner. Two distinct types of tropolonato ligand were identified:- one ligand only chelates to a nickel atom, the other type chelates to one nickel atom, and bonds to the second metal atom of the dimer via a bridging oxygen atom. Six coordination is completed by bonding to a water molecule. The different bond lengths found for the metal to oxygen distances of the bridge were thought to be due to geometrical requirements of the small rigid ligand bite, rather than to any inherent weakness in the bridging bond.

The cobalt(II) tropolonato complex was found to exist as a tetramer $Co_4(trop)_8(H_2O)_2$, containing two distinct cobalt(II) sites. One type of cobalt ion achieves six coordination with five tropolonato oxygens and one water molecule, the other cobalt site is coordinated by tropolonato oxygen atoms only.

Two of the eight tropolonato ligands chelate to one metal centre only, the remaining tropolonato ligands chelate to one cobalt atom, and have one trigonal oxygen atom bridging to another cobalt centre. The bridging ligands were found to have longer Co-O chelating distances, than was the case for the ligands which chelate only. The bond lengthening was explained by an electron delocalisation mechanism. The π electron system of the carbon ring, acting as a source of electron density enhances the ability of the tropolonato oxygen atoms to bind to more than one metal. Each of the cobalt atoms has a distorted octahedral arrangement of oxygen atoms around it.

The structural stability of these two bridged tropolonato hydrates (no such stable acetylacetonato complexes exist) was ascribed to the compact nature of the tropolonato ligands, facilitating efficient lattice-packing, and so allowing hydrogen-bonding to take place between the water molecules and tropolonato oxygen atoms of adjacent molecules.

In the following sections we present our experimental results, using the following general order:-

1) Spectrum of the ligand
2) Spectra of sodium tropolonate and tropolonato complexes
   - 2.1 Literature measurements
   - 2.2 Experimental results
     - (a) <u>tris</u>-tropolonato complexes
     - (b) oxo-tropolonato complexes
     - (c) $[(PPh_3)_2Pt(trop)][BPh_4]$

Table 3.1:- Significant bond lengths (Å) and the twist angles for tris(tropolonato) complexes studied by X-ray crystallography.

Complex	M-O	O---O[a]	C-O	C_1-C_2	C-C(ave)[b]	ϕ[c]	ref
Al(trop)$_3$	1.888	2.490	1.291	1.450	1.384	48	205
Sc(trop)$_3$	2.102	2.523	1.299	1.457	1.388	33	226
Mn(trop)$_3$[d]	2.00	2.548	1.294	1.454	1.40	49	208
Fe(trop)$_3$	2.008	2.522	1.294	1.463	1.387	40	206
Co(trop)$_3$	1.884	2.546	1.298	1.451	1.385	55	227

a. ligand bite distance

b. average C-C length in carbon ring, excluding C_1-C_2.

c. projected twist angle in degrees

d. average values of the two different Mn(trop)$_3$ molecules.

Table 3.2:- Significant bond lengths (Å) for tetrakis (tropolonato) complexes studied by X-ray crystallography

Complex	M-O	O--O[a]	C-O	C_1-C_2	C-C(ave)[b]	Ref
$HSc(trop)_4$	2.214	2.505	1.284	1.465	1.386	229,230
$Zr(trop)_4$	2.180	2.493	1.303	1.44	1.378	231
$Hf(trop)_4DMF$	2.183	2.575	1.286	1.464	1.403	232
$[Nb(trop)_4]_2[O(HCl)_3]CH_3CN$	2.086	2.432	1.300	1.408	1.384	209
$Th(trop)_4DMF$	2.457	2.541	1.277	1.471	1.392	198

a - ligand bite distance

b - average C-C length of carbon ring, excluding C_1-C_2

Table 3.3:- Bond lengths (Å) for tropolone and some complexes containing the tropolonato ligand.

Compound	M-O	O---O	C-O	C_1-C_2	C-C
Tropolone[195]	-	-	1.261	1.454	1.38
Na(trop)[203]	2.4-2.6	2.650	1.284	1.470	1.40
TropHCl[202]		-	1.41	1.42	1.40
$B(trop)_2Br.H_2O$[204]	1.472	-	1.335	1.409	1.388
$(Trop)_3SnCl$[233]	2.129	2.548	1.287	1.453	1.399
$(Trop)_3SnOH$[233]	2.146	2.538	1.285	1.458	1.384
$(CH_3)_2Tl(trop)$[234]	2.47	2.61	1.23	1.51	1.40
$[Co_4(trop)_8(H_2O)_2]$[201]	2.074	2.578	1.273	1.478	1.402
$[Ni(trop)_2(H_2O)]$[200]	2.024	2.583	1.279	1.486	1.398
$Cu(trop)_2$[207,235]	1.91	2.557	1.30	1.44	1.40
$Rh(CO)(PPh_3)(trop)$[210]	2.058	-	1.291	1.461	1.40
$(\eta^5\text{-}C_5H_5)Zr(trop)$ CH_2Cl_2[237]	-	-	1.28	1.46	1.39
$UO_2(trop)_2(pyridine)$[218]	2.38	2.52	1.30	1.47	1.41

2. PREPARATION OF COMPLEXES

As noted earlier, the tropolonato anion, as a ligand, behaves in a similar manner to the β-diketonate in e.g. acetylacetonate. The method of preparation of tropolonato complexes often reflects this similarity; the techniques used for the preparation of acetylacetonato (acac) complexes may sometimes be successfully adapted for analogous tropolonato complexes, e.g. $Cr(trop)_3$[191] was prepared using the method described for $Cr(acac)_3$. In this study, the method of preparation of $Os(acac)_3$[238] was successfully used to prepare the new complex $Os(trop)_3$.

The new tris (tropolonato) complex, $Ir(trop)_3$, was prepared by using the method described in the literature for $Rh(trop)_3$[189] i.e. using sodium acetate to maintain a suitable pH during the reaction.

Both the new tris(tropolonato) complexes have solubilities similar to previously reported tris(tropolonato) metal (III) complexes, chloroform being the most useful solvent.[189]

The literature method for the preparation of $Ru(trop)_3$ involved separation of the end product by complicated chromatographic techniques,[211] in contrast to other tris (tropolonato) complexes which may be isolated fairly easily. We attempted to find a simple method for the preparation of $Ru(trop)_3$, by using conditions similar to those described for $Rh(trop)_3$ and $Ir(trop)_3$. Unfortunately this method could not always be repeated.

Although the methods used for the preparation of acetylacetonato complexes are often successfully adapted for tropolonato complexes, this was not the case where platinum (II) is concerned. No identifiable product could be obtained when the method described for the preparation of $Pt(acac)_2$ [239] (where the acac ligand is O-bonded) was adapted for tropolone.

Tropolone, being a potential bidentate, aromatic, oxygen donor ligand, might behave in a similar way to catechol. Several new complexes were prepared by adapting the preparation for the analogous catecholato complex to conditions conducive to the formation of a tropolonato complex. Thus, addition of tropolone to a neutral solution of ammonium molybdate immediately produced a precipitate of the new complex, $MoO_2(trop)_2$. The equivalent reaction using sodium tungstate, however, resulted in the formation of $W_2O_5(trop)_2$. Addition of tropolone to a neutral solution of <u>trans</u>-$K_2[OsO_2(OH)_4]$ brought about the immediate formation of the $OsO_2(trop)_2$. Whereas $W_2O_5(trop)_2$ was insoluble in water and common organic solvents $MoO_2(trop)_2$ showed slight solubility in dimethyl sulphoxide, and $OsO_2(trop)_2$ was only slightly soluble in chloroform and dimethyl sulphoxide.

Tropolone was used instead of catechol, in the reaction of $Pt(PPh_3)_2O_2$ to form $Pt(PPh_3)_2(cat)$.[27] Precipitation in the presence of sodium tetraphenylboronate brought down the complex $[Pt(PPh_3)_2(trop)][BPh_4]$.

3. INFRA-RED AND RAMAN SPECTROSCOPY

3.1 Spectra of the parent tropolone

The infra-red and Raman spectra of tropolone have been reported and are listed in Table 3.4.[240,241]

In the infra-red, tropolone has been reported to show several peaks in the region 4,000 - 3,000cm^{-1}, arising from stretching vibrations of the tropolone OH group, ν(OH).[242,243] In the solid state, the strongest bond was found at 3,208cm^{-1}, and this was assigned to ν(OH) of hydrogen-bonded tropolone. Another distinct band was found at 3540cm^{-1}, and this was ascribed to the OH stretch of tropolone molecules in which no hydrogen-bonding occurs i.e. for the conformation shown in Figure 3.7.[242]

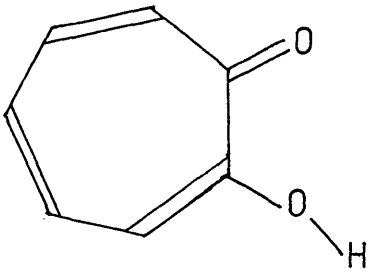


Figure 3.7:- Non-hydrogen bonded tropolone.

No peak was observed for tropolone in the region typical of ketone ν(C=0) vibrations (1720 - 1650cm^{-1})[244] and this has been ascribed to the fact that conjugation of the carbonyl group with the partially delocalised bonds of the carbon ring causes a lowering of ν(C=0). The two very strong peaks found

at 1615 and 1555cm^{-1} in the infra-red have been assigned to coupled stretching vibrations of the carbon ring. ν(C-C) together with the C-O stretch, ν(C-O).[245] Investigation by Ikegami[245] of the infra-red spectrum of tropolone recorded in deuterosulphuric acid found a significant decrease in intensity of the 1555cm^{-1} band as compared to the normal spectrum. The absorption having the greater ν(C-C) contribution would be expected to be more sensitive to protonation, or deuteriation, in this case. Thus, it was concluded that the 1555cm^{-1} peak was largely due to ν(C-O), with a small contribution from the C-C ring stretches, whilst the 1615cm^{-1} absorption was ascribed largely to ν(C-C), with only a small contribution from ν(C-O). This assignment was confirmed by the ^{18}O isotopic substitution experiments of Junge.[247]

Further deuteriation studies led to the tentative assignments of the strong band at 1490cm^{-1} and the peak at 1267cm^{-1} as arising in some part from deformations of the C-O-H group, δ(COH).[240] Ikegami did not assign the strong peaks occurring between 1300 and 1400cm^{-1}.[240] The ^{18}O-isotopic substitution techniques used by Junge, however, led to the assignment of these peaks as arising from vibration of the C=O band.[247]

The remainder of the tropolone spectrum was attributed to vibrations of the carbon ring, and deformations of the C-H bonds.[241]

Table 3.4:- Major peaks of the infra-red and Raman spectra of tropolone (cm^{-1})

Infra-red	Raman[a]	Assignment
3530 wb		
3260 mb	3229	ν(OH)
1615 vs	1618	ν(C-C)
1555 s	1559	ν(C-C+C-O)
1490 s	1490	δ(COH)
1475 s	1473	ν(C-C)
1444 s		
1425 m	1418	δ(CH) in plane
1355 w		
1312 m		
1308 m	1304	ν(C-O)
1265 s	1265	δ(CH)
1250 s	1239	δ(COH)
1210 m	1211	δ(CH)
1048 w	1049	ν(C-C)
960 w	957	ν(C-C)
920 w		
875 m		δ(CH) out of plane
860 m		
	828	
740 m	744	
	719	δ(COH) out of plane
715 s		
675 m	678	skeletal
654 w		deformations
551 w		
440 s	439	

[a]reference 241, recorded in CCl_4 solution.

In the Raman spectrum[241] the strongest peak was reported to be that arising from the C=C in-plane stretching vibration near 1470cm^{-1}. The vibrations due to the C-O-H group, generally strong in the infra-red, were found to be weaker in the Raman.

3.2 The tropolonato ion

The spectrum of sodium tropolonate in theory may be regarded as that which would arise from the free tropolonato anion. In practice, however, this was not found to be quite the case. In a study of the metal-ligand stretching frequencies, ν(M-O) of non-transition metal tropolonates, the ν(M-O) values assigned were found to be rather high, at 545 and 469cm^{-1}, for the supposed ionic metal-ligand bonding.[248] This has been confirmed by the X-ray crystallographic study of sodium tropolonate, which found that the distance between each sodium ion and any one of its six oxygen neighbours, was between 2.37 and 2.60Å, i.e. shorter than expected for purely ionic bonding.

The prominent peaks of the infra-red spectrum of sodium tropolonate as recorded in this work are listed in Table 3.5, and its spectrum shown in Figure 3.8.

In this investigation we find that the ν(OH) absorptions of tropolone, between 3,000 and 4,000cm^{-1}, are no longer observed for sodium tropolonate, as expected. The peaks at 1615cm^{-1} and 1555cm^{-1} for tropolone are now shifted to lower frequency, the 1555cm^{-1} being most affected.

Table 3.5:- Major peaks of the infra-red spectra of sodium tropolonate (cm^{-1})

Sodium tropolonate	Assignment
1585 s	ν(C-C)
1514 s	ν(C-C+C-O)
1439 s	
1405/1392 s	
1363 m	ν(C-O)
1360 m	
1230 s	
1215 s	δ(CH) in plane
1209 s	
973 m	
891 m	
885 m	δ(C-H) out of plane
870 w	
725 s	
716 s	
589 m	
535 m	ν(M-O)
460 m	ν(M-O)

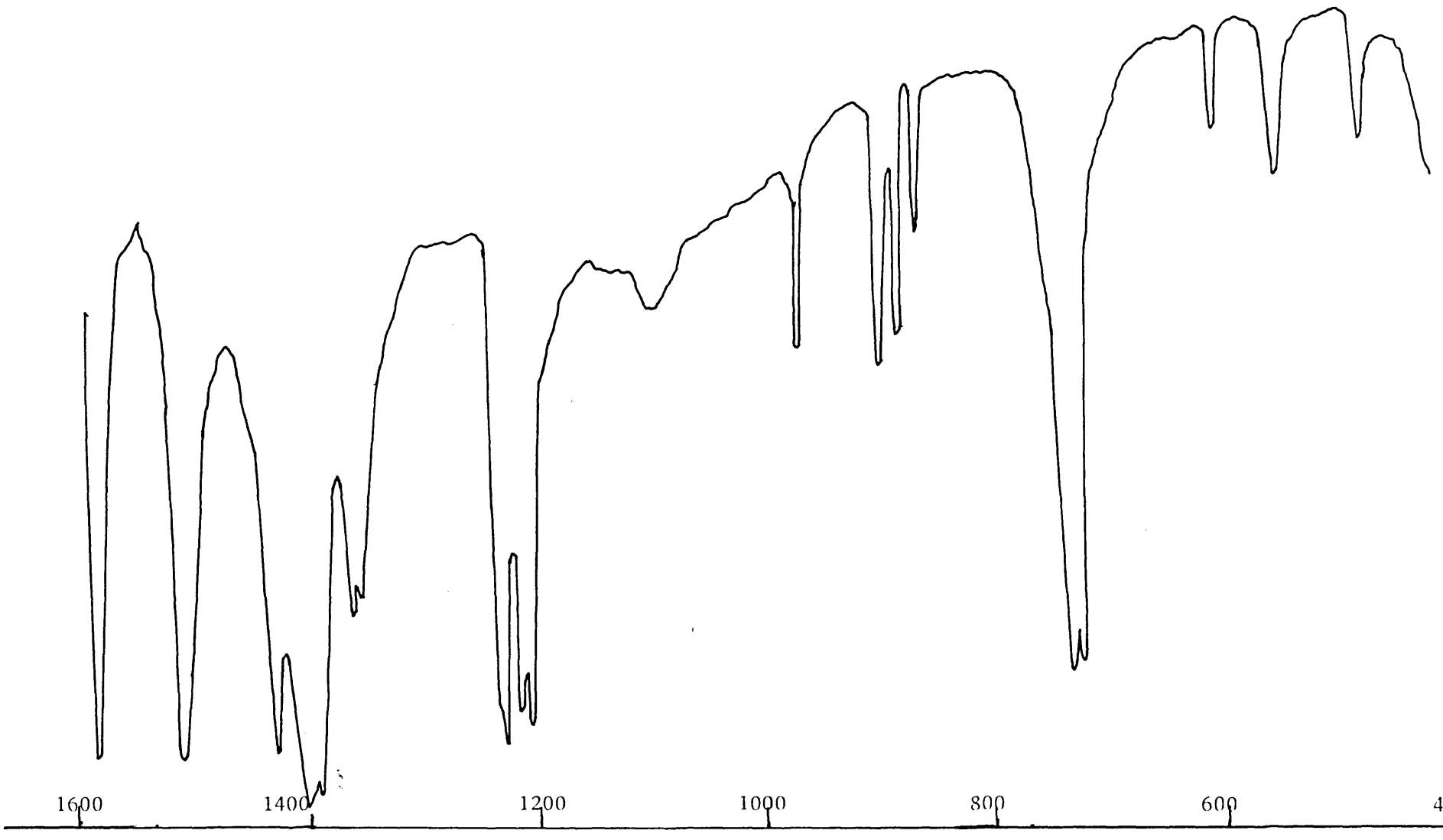


Figure 3.8 - Infra-red spectrum of sodium tropolonate.

No peak at 1490cm^{-1} is observed for sodium tropolonate, adding further weight to the assignment of this absorption as due to δ(COH). The doublet at 1312 and 1308cm^{-1} of the tropolone spectrum, now occurs at 1363/1360cm^{-1}. This, again, suggests the assignment of these peaks as arising mainly from ν(CO) is correct, since only those absorptions connected with the carbonyl or hydroxyl groups would be expected to show significant change on deprotonation of tropolone. The shift to higher frequency of ν(CO) is representative of the increased double bond character of the C-O (hydroxyl group) bond on going from tropolone to the tropolonato anion, as found by X-ray crystallography. The pattern of peaks between 1300 and 1200cm^{-1} is also subject to change.

This is consistent with the assignment of at least one of these bands as arising from some vibration of the C-O-H group of the free ligand.

The remainder of the spectrum, assigned to C-C vibrations and C-H deformations shows a number of small changes, none of which is of much diagnostic value.

3.3 Tropolonato transition-metal complexes

3.3.1 Literature measurements

The infra-red spectra of many transition metal[191,249,250,251] and rare earth[215,216] tropolonato complexes have been reported, with particular regard to the ν(M-O) bands, and their relationship with the crystal field stabilisation energy of the complex.

All the complexes studied showed similar band patterns above $750cm^{-1}$.[191] Complexes of the type $M^{II}(trop)_2$ had no absorptions exhibiting metal sensitivity above $750cm^{-1}$; for the $M^{III}(trop)_3$ complexes, peaks in the region 1300 - $1360cm^{-1}$ were found to vary with the metal, their frequencies being roughly in an inverse order to that found for the crystal field stabilisation energies (C.F.S.E.'s). For $Cu(trop)_2$ ^{18}O-labelling caused a significant shift in the peak at $1347cm^{-1}$, which was subsequently assigned to ν(Cu-O). This value is considerably lower than that found for ν(C-O) in $Cu(acac)_2$, and this is in line with structural determinations on $Cu(trop)_2$ and $Cu(acac)_2$, which revealed a significantly greater C-O bond distance for $Cu(trop)_2$.[191]

From these reports and our own observations we conclude that the following changes may be taken as indicative of coordination of the tropolonato anion:-

(1) disappearance of the ν(OH) absorptions.

(2) the two peaks most characteristic of tropolone, at 1615 and $1555cm^{-1}$, shift to lower wave-number, and show enhanced intensity.

(3) the peaks between 1300 and $1380cm^{-1}$, are shifted to higher frequency, as observed for sodium tropolonate, but,in complexes of tropolone, they have considerably greater intensity, and a slight broadening is often found, so that the doublet of sodium tropolonate disappears, and one very large peak is observed. If this behaviour is compared to the situation described

earlier for catecholato complexes, it may be considered to be analogous to the major change found in the catechol spectrum on complexation i.e. the enhancement of intensity found for the peak near 1250cm^{-1}, assigned to the ν(C-O + C-O) vibration. This is further evidence for these peaks of the tropolone spectrum arising from ν(C-O). The difference in behaviour of these peaks for sodium tropolonate and tropolonato complexes is indicative of the different types of bonding present between the metal and the ligand.

(4) The absorptions between 1300 and 1200cm^{-1} show a change of pattern.

3.3.2 Experimental Results

(a) Tris (tropolonato) complexes

The new complexes Os(trop)$_3$ and Ir(trop)$_3$ show absorptions in a pattern typical of previously reported tris(tropolonato) metal (III) complexes.[191,249] The spectrum of Ir(trop)$_3$ is very similar to that of Rh(trop)$_3$, as is Os(trop)$_3$ to Ru(trop)$_3$. The major peaks of these spectra are listed in Table 3.6 and the spectrum of Ir(trop)$_3$ is shown in Figure 3.9.

Unequivocal assignment of the metal-oxygen stretching bands is very difficult due to the large number of peaks in the region below 750cm^{-1}. Many of the ν(M-O) vibrations are expected to be coupled with ring deformations, as is the case for most β-diketones.[183]

Table 3.6:- Major infra-red absorptions of some tris (tropolonato) complexes (cm^{-1})

$Rh(trop)_3$	$Ir(trop)_3$	$Ru(trop)_3$	$Os(trop)_3$	Assignment
1586 s	1592 s	1586 vs	1592 vs	ν(C-C)
1510 s	1516 s	1507 vs	1519 vs	ν(C-O)+ ν(C-C)
1434 s	1446 s	1443 s	1438 vs	
1378 s	1380 m	1380 m	1380 s	
1330 br.s	1339 br.s	1338 s	1350 br.s	ν(C-O)
1260 m	1265 m	1260 m	1262 m	
1230 w	1228 m	1230 m	1220 m	δ(C-H)
1210 m	1217 m	1217 s	1212 m	
972 m	973 w	970 w	970 w	ν(C-C)+δ(C-H)
880 s	881 m	878 s	878 m	
723 s	740 s	760 m	754 m	ring deformation
715 s	730 s	724 vs	727 s	
660 s	666 m	649 m	625 w	skeletal vibrations
583 s	592 m	634 m	-	and ν(M-O)
433 m	560 m	570 s	569 m	

vs = very strong w = weak intensity

s = strong br = broad

m = medium

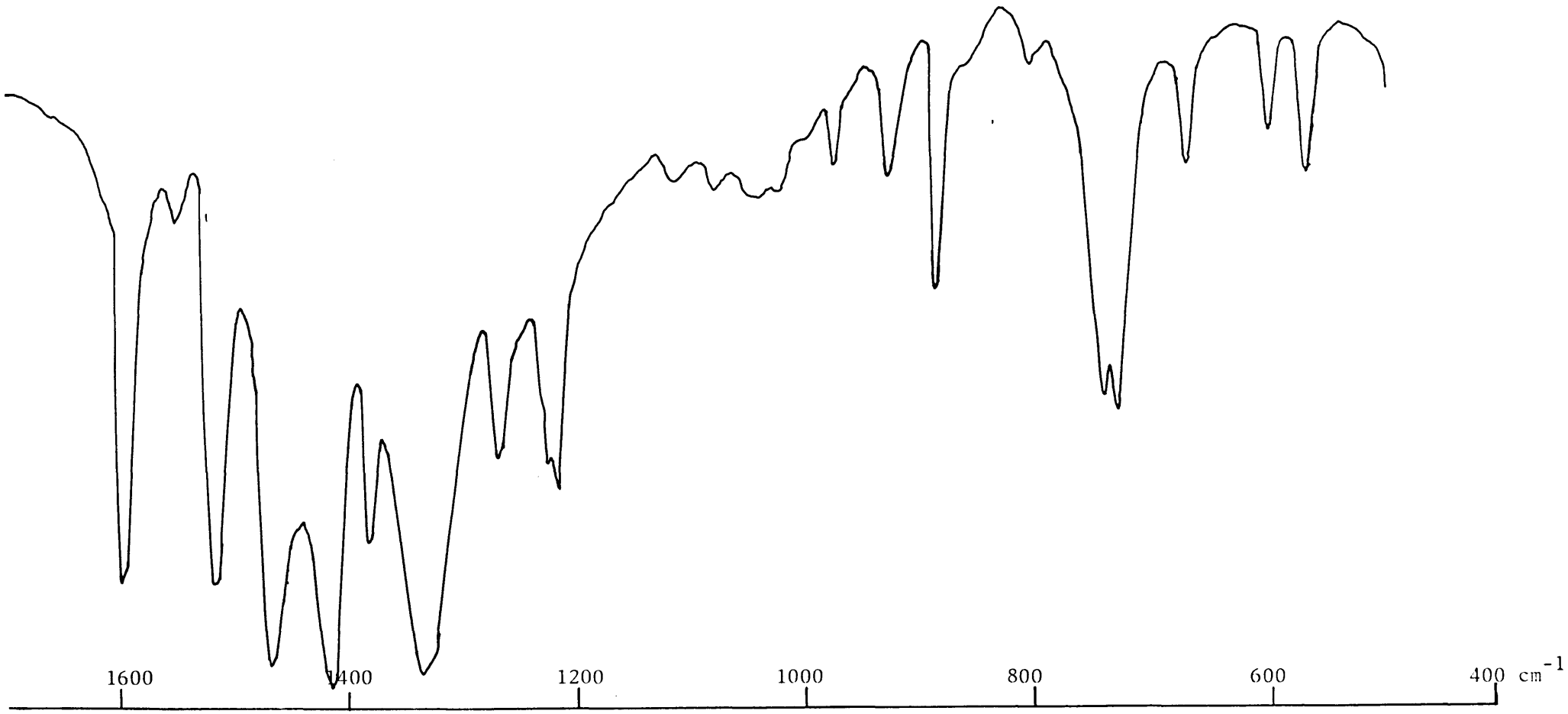


Figure 3.9 - Infra-red spectrum of $Ir(trop)_3$

(b) Oxo-tropolonato complexes

(i) $MoO_2(trop)_2$

The significant peaks of the infra-red spectrum of this complex are listed in Table 3.7. The ligand absorptions present are similar to those found for other tropolonato complexes.

Two strong peaks are also observed at 930 and 898cm^{-1}, not found for sodium tropolonate, or in the free ligand spectrum. These peaks are typical of the stretching vibrations of the cis-dioxomolybdenum(VI) group, $\nu(MoO_2)$, as described earlier. The frequencies observed here for $\nu(MoO_2)$ are very close to those found for $MoO_2(acac)_2$, reported to be 933 and 904cm^{-1}.[252]

The Raman spectrum of $MoO_2(trop)_2$ shows a very strong peak at 931cm^{-1}, with a weaker peak at 900cm^{-1}, which are not present in the free ligand spectrum. They are therefore assigned to $\nu(MoO_2)$, confirming the assignments made for the infra-red (as shown in Figure 3.10).

Two strong peaks at 570 and 554cm^{-1} are tentatively assigned to the stretching vibrations of the molybdenum-tropolonato oxygen bonds ν(Mo-O1) by comparison with the assignments made for $MoO_2(acac)_2$ found at 576 and 550cm^{-1}.[252] The Raman spectrum of $MoO_2(trop)_2$ also exhibits two peaks at 552 and 570cm^{-1}, which would be expected for these vibrations.

An additional ligand peak was observed at 1575cm^{-1} in the infra-red spectrum. This absorption has been reported for other tropolonato complexes, and has been described as typical of "polymeric" tropolonato complexes, where a tropolonato ligand may be bound to more than one metal centre, via a trigonally bound oxygen atom, as described above. The peak is thought to arise from a further vibration of the carbon ring.

(ii) $W_2O_5(trop)_2$

This complex similarly shows two strong bands in its infra-red spectrum, as listed in Table 3.7, not observed for sodium tropolonate or tropolone, at 940 and 902cm^{-1}. These are assigned to stretching vibrations of the cis-dioxotungsten (VI) group. In this case, however, the frequencies of these absorptions do not tally as closely with those found for $WO_2(acac)_2$,[252] as is the case for the molybdenum complex ($WO_2(acac)_2\nu^s(WO_2)$, 954cm^{-1}; $\nu^{as}(WO_2)$ 908cm^{-1}). A peak closely coinciding with a ligand band to form a doublet at 740cm^{-1} is tentatively assigned to the asymmetric stretching vibration of a bent tungsten-oxygen-tungsten bridge, $\nu^{as}(WOW)$. This leads us to postulate the structure $W_2O_5(trop)_2$, by analogy with the catecholato complex, $Na_2[W_2O_5(cat)_2]$. The suggested $(W_2O_5)^{2+}$ grouping helps to explain the observed differences between the $\nu(WO_2)$ vibrations for the tungsten (VI) - tropolonato complex and $WO_2(acac)_2$.

From this evidence, and by analogy with the catecholato complex, the following structure is postulated (Figure 3.11):-

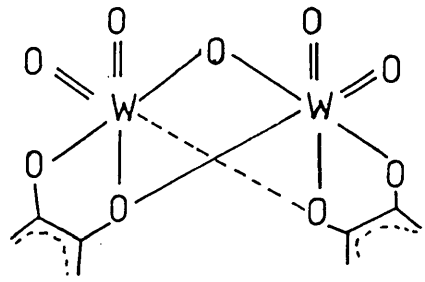


Figure 3.11:- Postulated structure of $W_2O_5(trop)_2$.

A strong, very broad band at 640cm^{-1} is tentatively assigned to vibrations of the ligand bridging bonds. This is commonly observed in molybdenum(VI) complexes,[86] as described in Chapter I. The ability of the tropolonato ligand to form such a bridge has been confirmed by the structural studies of $[Ni(trop)_2H_2O]_2$[200] and $[Co_4(trop)_8(H_2O)_2]$, described earlier in this chapter.

This complex also has a peak at 1590cm^{-1}, assigned in carbon ring vibrations of "polymeric" tropolonato complexes.

Absorptions at 563 and 550cm^{-1} are tentatively assigned to vibrations of the non-bridging tungsten to ligand oxygen bonds, although one of these absorptions may arise from the symmetric stretch of the W-O-W bridge, as reported for other complexes of such a system.[81,84]

(iii) $OsO_2(trop)_2$

The spectrum of the osmium(VI) tropolonato complex shows a strong, sharp peak at 845cm^{-1} as listed in Table 3.7 which is not observed for tropolone or sodium tropolonate, and is typical of the asymmetric stretch of the trans-"osmyl" group, O = Os = O.[82] The Raman spectrum of this complex has a very strong peak at 884cm^{-1}, and this is characteristic of the symmetric stretching vibration, $\nu^s(OsO_2)$, of the trans-osmyl group (no such peak is found in the Raman spectrum of tropolone or $Ir(trop)_3$). Due to the symmetry of the group, neither of the stretching vibrations is active in both the Raman and the infra-red, as described in Chapter I. The spectra are shown in Figure 3.12.

A peak found at 604cm^{-1} in the infra-red spectrum of this complex is tentatively assigned to a stretching vibration of the osmium-tropolonato oxygen bond (typical range 300-650cm^{-1}).[19]

The ligand absorptions show a pattern similar to other tropolonato complexes.

The vibrations described here lead to the following structure as that most probable for $OsO_2(trop)_2$ (Figure 3.13).

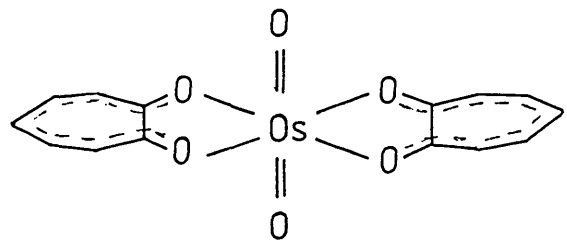


Figure 3.13:- Postulated structure of $OsO_2(trop)_2$

(c) $[Pt(PPh_3)_2(trop)](BPh_4)$

This spectrum is necessarily very complex due to the many peaks of the triphenylphosphine spectrum; the most distinctive are those found at 1581, 1430, 1089, 740 and 690cm^{-1}. These absorptions are all observed in the spectrum of this complex, confirming the presence of triphenylphosphine. Many of the absorptions found in the sodium tetraphenylboronate spectrum coincide with those observed for triphenylphosphine. The slightly different arrangement of peaks at 745 and 713cm^{-1} is of little use for identification in the spectrum of the complex, since the region 750 to 690cm^{-1} is very complicated.

A peak at 604cm^{-1}, however, is observed for the tetraphenylboronate anion, but not for triphenylphosphine. This peak is also found in the spectrum of the platinum complex, giving evidence for the presence of the anion.

The spectrum of the complex also exhibits the strong absorptions characteristic of tropolonato coordination with peaks at 1603 and 1531cm^{-1}, 1340cm^{-1}, and a group of peaks between 1245 and 1218cm^{-1}. The tropolonato ligand also usually absorbs near 720cm^{-1}. The complex region 750 to 690cm^{-1} consists of peaks arising from triphenylphosphine, the tetraphenylboronate anion and the tropolonato ligand.

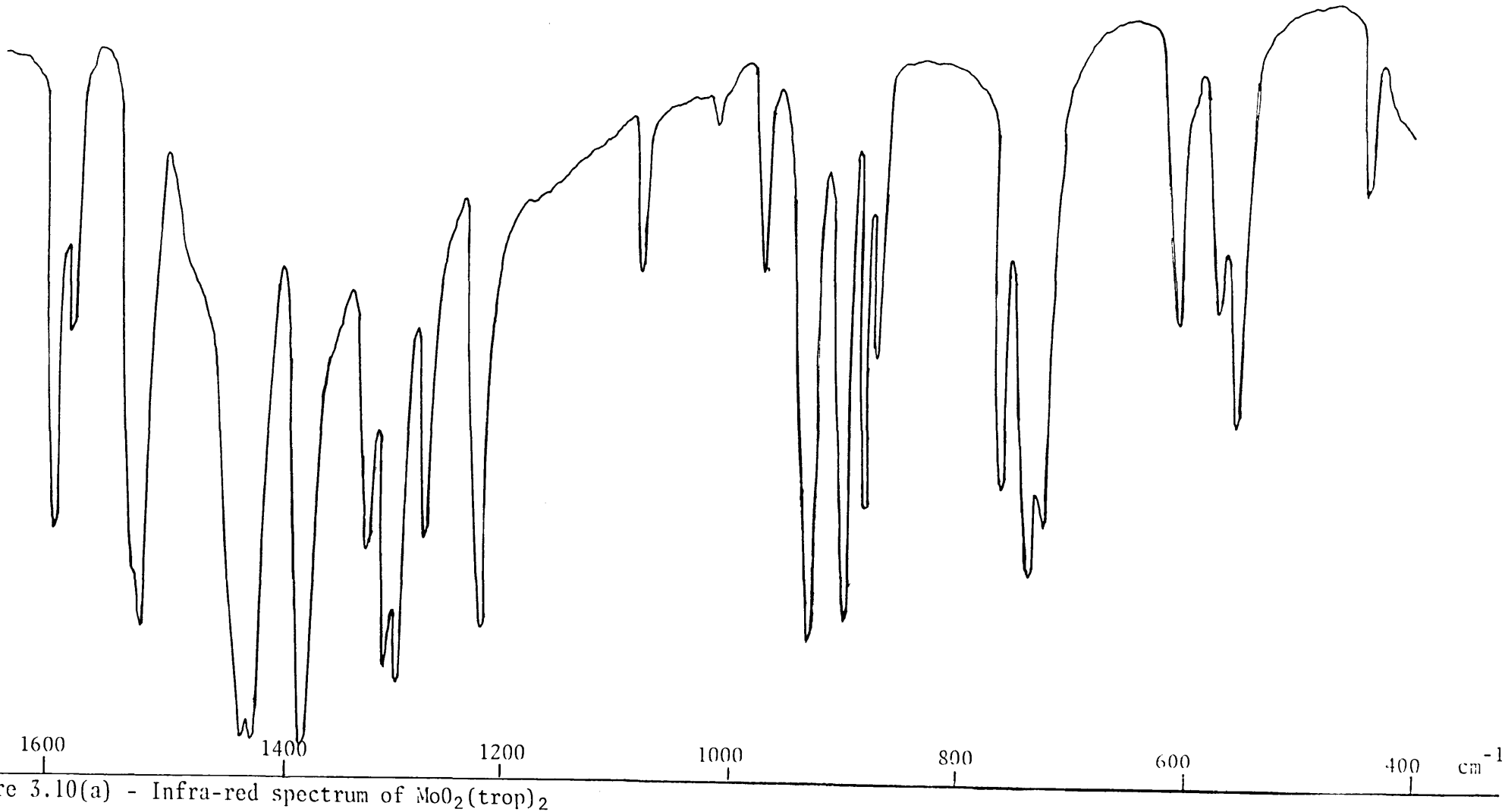


Figure 3.10(a) - Infra-red spectrum of $MoO_2(trop)_2$

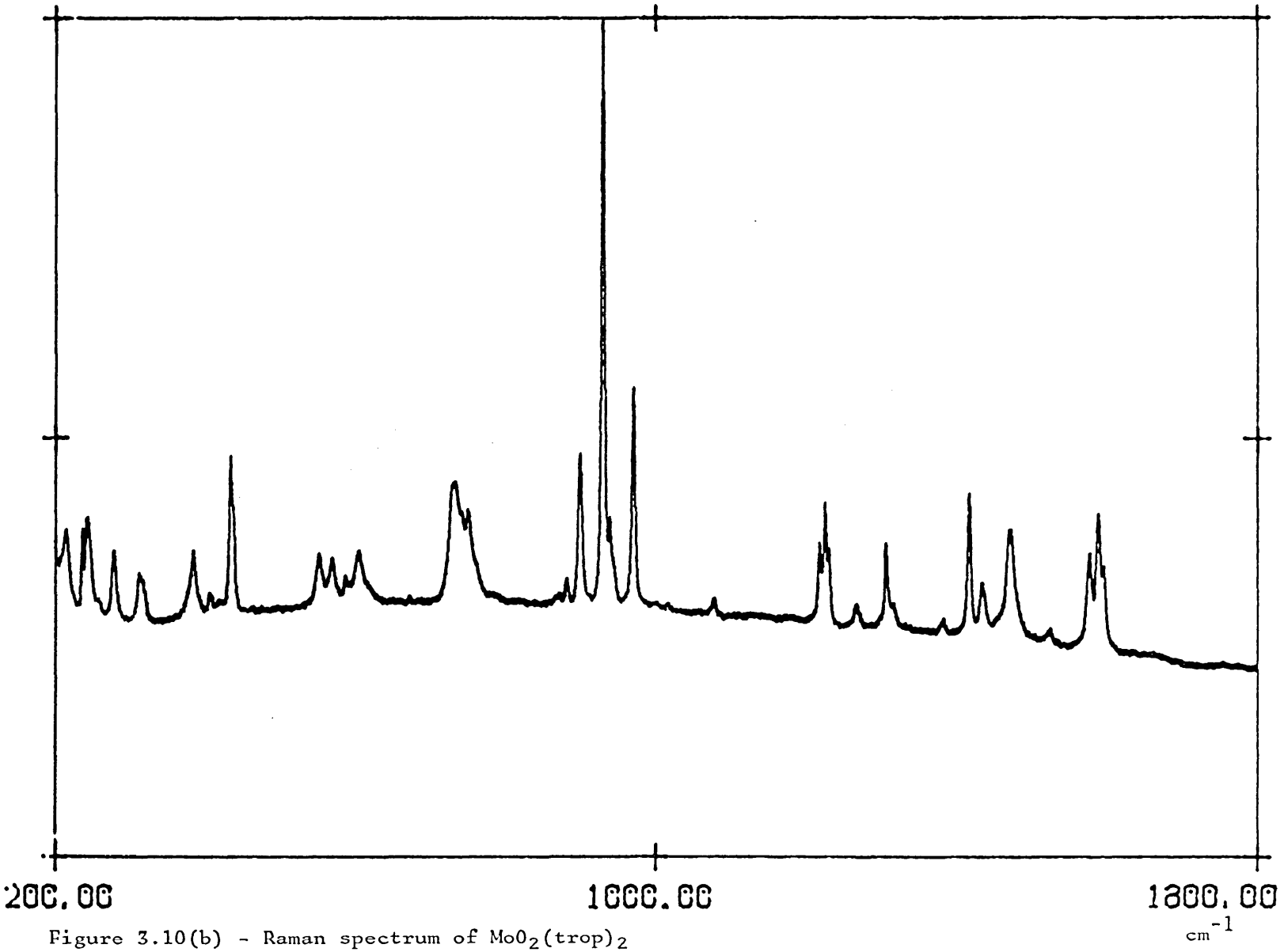


Figure 3.10(b) - Raman spectrum of $MoO_2(trop)_2$

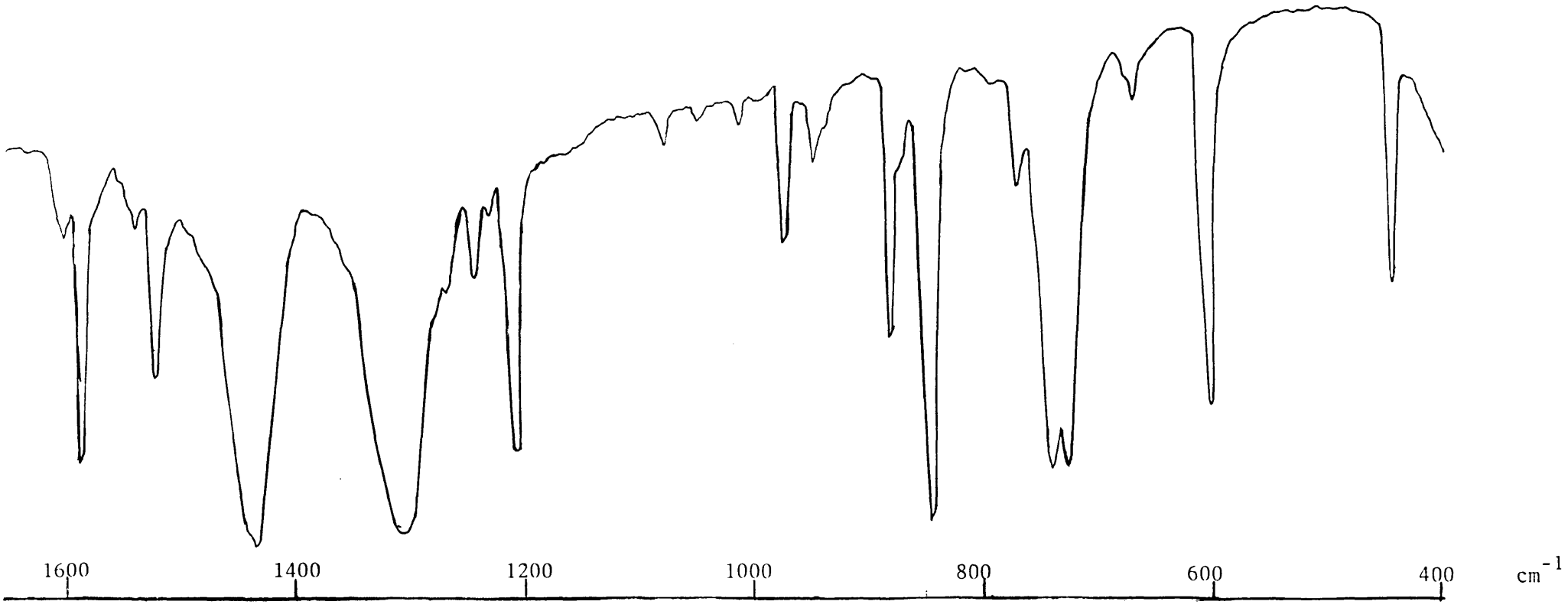


Figure 3.12(a) - Infra-red spectrum of $OsO_2(trop)_2$

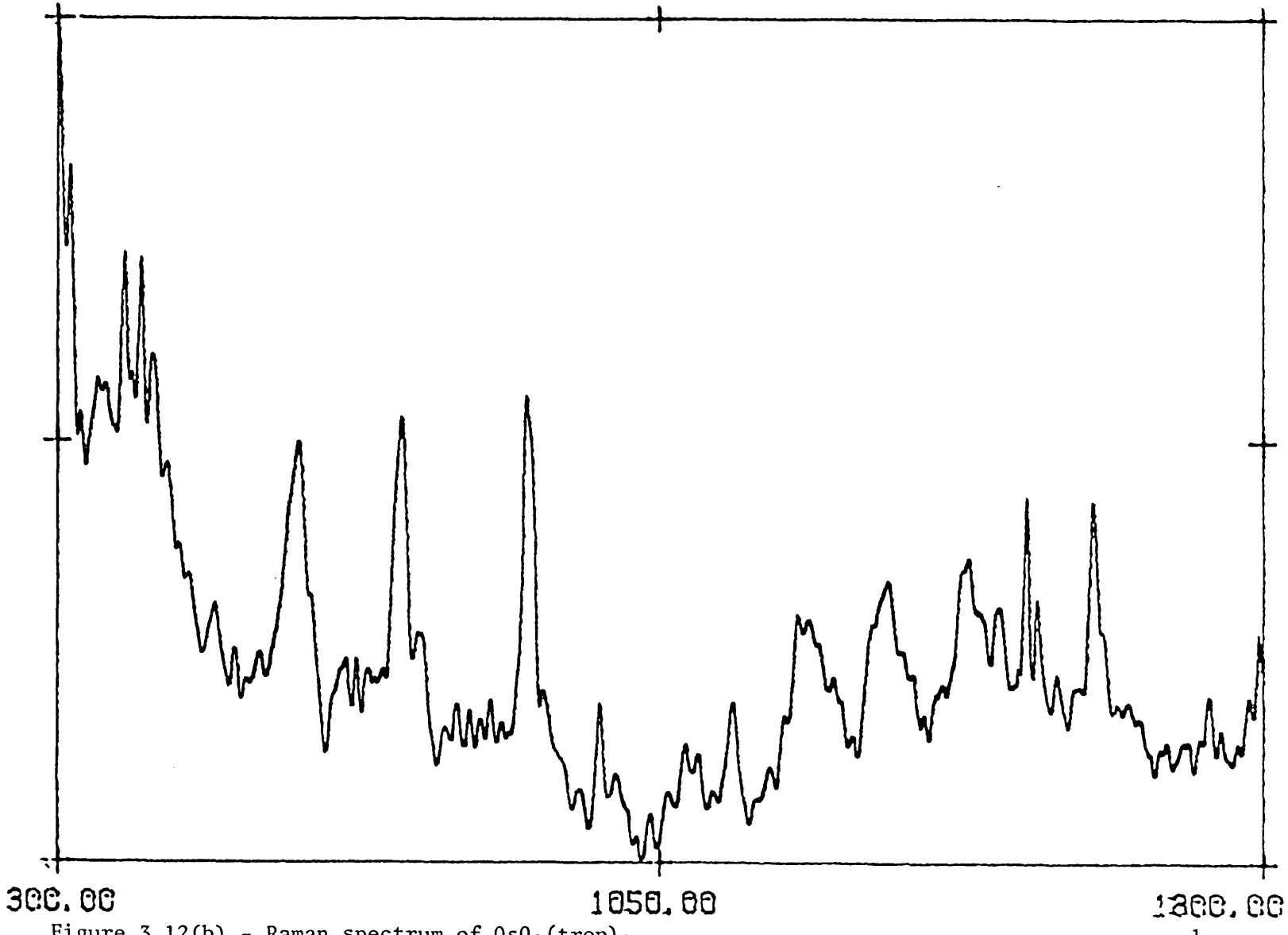


Figure 3.12(b) - Raman spectrum of $OsO_2(trop)_2$

Table 3.7:- Major infra-red absorptions of $MoO_2(trop)_2$, $W_2O_5(trop)_2$, and $OsO_2(trop)_2$ (cm^{-1})

$OsO_2(trop)_2$	$MoO_2(trop)_2$	$W_2O_5(trop)_2$	Assignment
1590 s	1593 s	1600 s	ν(C-C)
	1575 m	1590 m	
1522 s	1520 s	1530 s	ν(C-O) + ν(C-C)
1440 s	1435 s	1438 s	
1310 sbr	1315 s	1360 s	ν(C-O)
	1302 s	1310 m	
	1292 s	1298 m	ν(C-C)
	1267 s	1268 m	+δ(C-H)
		1230 s	
1209	1218 s	1216 m	
972 w	966 m	968 w	
	931 vs	940 vs	$\nu^{s}(MO_2)$
	900 vs	902 vs	$\nu^{as}(MO_2)$
881 s	878 s	880 vs	ν(C-C) + δ(C-H)
	868 s	860 s	
845 vs			$\nu^{as}(OsO_2)$
770 w	757 s	758 s	
740 s	736 s	740 sd	ring deformation/ ν^{as}(W-O-W)
730 s	723 s	725 s	
		640 sbr	ν(W-O(trop)-W)
604 s	604 s	615 s	
	570 m	563 m	skeletal vibrations and ν(M-O)
	554 s	556 w	
442 m			

vs = very strong
s = strong
m = medium
w = weak intensity
br = broad
d = doublet

4. ^{1}H NUCLEAR MAGNETIC RESONANCE SPECTRSCOPY

4.1 Spectrum of tropolone

The ^{1}H N.M.R. spectrum of the free ligand, tropolone, in $CDCl_3$, shows a complex multiplet, ranging from 6.87 to 7.55 p.p.m., as shown in Figure 3.14. In d^6 acetone solution, we found that each peak of the multiplet ranging between 6.91 and 7.74 p.p.m. had greater breadth than was the case for the spectrum recorded in $CDCl_3$. No single peak could be unequivocally assigned to the hydroxyl proton.

4.2 Spectrum of sodium tropolonate

The spectrum of sodium tropolonate was recorded in D_2O. It showed a broad multiplet between 6.5 and 7.5 p.p.m. as shown in Figure 3.15.

4.3 Spectra of troplonato complexes

4.3.1 Literature measurements

Few ^{1}H N.M.R. studies have been reported for tropolonato complexes, although several studies have been undertaken concerning intramolecular rearrangements of tris (isopropyltropolonato) complexes.[214,227] The mixed ligand complexes bis(π-ally) tropolonato rhodium and bis(π-allyl)tropolonato iridium[212] both showed complex multiplets between 6.7 and 7.4 p.p.m. attributable to the tropolonato ligand, and a series of complexes of the type Rh(trop)(diolefin)[253] gave rise to a multiplet between 7.0 and 7.5 p.p.m. arising from the tropolonato ring protons. An investigation of the ^{1}H N.M.R. spectra of 4-t-butyltropolone and its palladium(II) complex, Pd(4-t-butyltrop)$_2$,

showed that little change occurs in the tropolonato resonances on coordination.[251] The complex $[Re(CO)_3(trop)]_2$ ($C_4H_{10}O_2$) was reported to have tropolonato resonances centred at 7.5 p.p.m.[254]

4.3.2 Experimental results

The resonances recorded for tropolone, sodium tropolonate, and tropolonato complexes are listed in Table 3.8.

The spectra of the complexes, when recorded in $CDCl_3$, also showed a multiplet in a similar position, and only of slightly different shape from that found for tropolone in the same solvent. This is consistent with the behaviour reported in the literature, and is well exhibited with $Ir(trop)_3$ as shown in Figure 3.16.

The spectra recorded in d^6D.M.S.O. show broader multiplets than those observed from $CDCl_3$ solutions. This is also the case, as noted above, for tropolone in another coordinating solvent, d^6 acetone. A comparison of the spectrum of $Rh(trop)_3$ in $CDCl_3$ and d^6D.M.S.O. was made. The $CDCl_3$ spectrum shows one sharp peak at 7.20 p.p.m., with some barely distinguishable peaks just to higher frequency of it. The spectrum recorded in d^6D.M.S.O. shows more peaks, each of which is broader than the strong peak of the $CDCl_3$ spectrum. The strongest peak of the d^6D.M.S.O. spectrum is found at 7.48 p.p.m. The spectrum of $UO_2(trop)_2$D.M.S.O. also shows a well-spaced multiplet with the strongest peak at 7.45 p.p.m. The new complex $MoO_2(trop)_2$ shows a very similar pattern for tropolone ring resonances (see Figure 3.17).

The new complex $[(PPh_3)_2Pt(trop)](BPh_4)$ shows two multiplets in the region of interest, one centred at 7.20 p.p.m., the other at 7.54 p.p.m. These are assigned to overlap of the multiplets arising from the tropolonato ring protons, and protons of the phenyl rings.

Insofar as any trend in the shift of peak positions on coordination can be distinguished, it appears that the resonances of the complexes recorded in d^6D.M.S.O. i.e. of $MoO_2(trop)_2$, $UO_2(trop)_2$.D.M.S.O. and $Rh(trop)_3$, occur at higher frequency than is found for the tropolone spectrum recorded in d^6 acetone (taking the strongest peak as indicator). If this shift is real, and not simply due to solvent effects, it occurs in the opposite direction to that found for the catecholato and catecholamine complexes described earlier. In these cases the shift occurring in the resonances of the aromatic ring protons on coordination, was described in the literature as arising from the electron-withdrawing effect of the metal ion in the complex, causing decreased electron density in the aromatic ring. This led to greater deshielding of the ring protons so that they resonate to lower frequency. In this case, however, the tropolonato anion experiences increased electron delocalisation in the seven-membered ring, as compared to the free ligand. We tentatively suggest that, if this shift is indeed real, then it may arise from the increased delocalisation of the tropolonato ring causing greater deshielding for the ring protons.

No meaningful comparison may be made between the tropolonato anion in sodium tropolonate and in the transition metal complexes, due to their varying solubilities in different solvents.

Table 3.8:- ^{1}H N.M.R. Resonances of tropolone, sodium tropolonate and some tropolonato complexes.

Substance	Resonances	Strongest Peak	Solvent
Tropolone	6.87-7.55(m)	7.22	$CDCl_3$
	6.91-7.74(m)	7.27	d^6acetone
Na(trop)	6.39-7.45(m)	7.14	D_2O
$Pd(trop)_2$	7.23-7.33(m)	7.23	$CDCl_3$
$Rh(trop)_3$	7.20-7.40(m)	7.20	$CDCl_3$
	7.05-7.68(m)	7.45	d^6D.M.S.O.
$Ir(trop)_3$	7.16-7.32(m)	7.16	$CDCl_3$
$OsO_2(trop)_2$		7.07	$CDCl_3$
$MoO_2(trop)_2$	7.50-8.06(m)	7.72	d^6D.M.S.O.
$UO_2(trop)_2$D.M.S.O.	7.09-7.81(m)	7.45	d^6D.M.S.O.
$[Pt(PPh_3)_2(trop)](BPh_4)$	7.45(m)/7.20(m)		$CDCl_3$

resonances recorded as δ(p.p.m.) from T.M.S.(δ= 0).

m = multiplet

Figure 3.14 - ^{1}H N.M.R. spectrum of tropolone

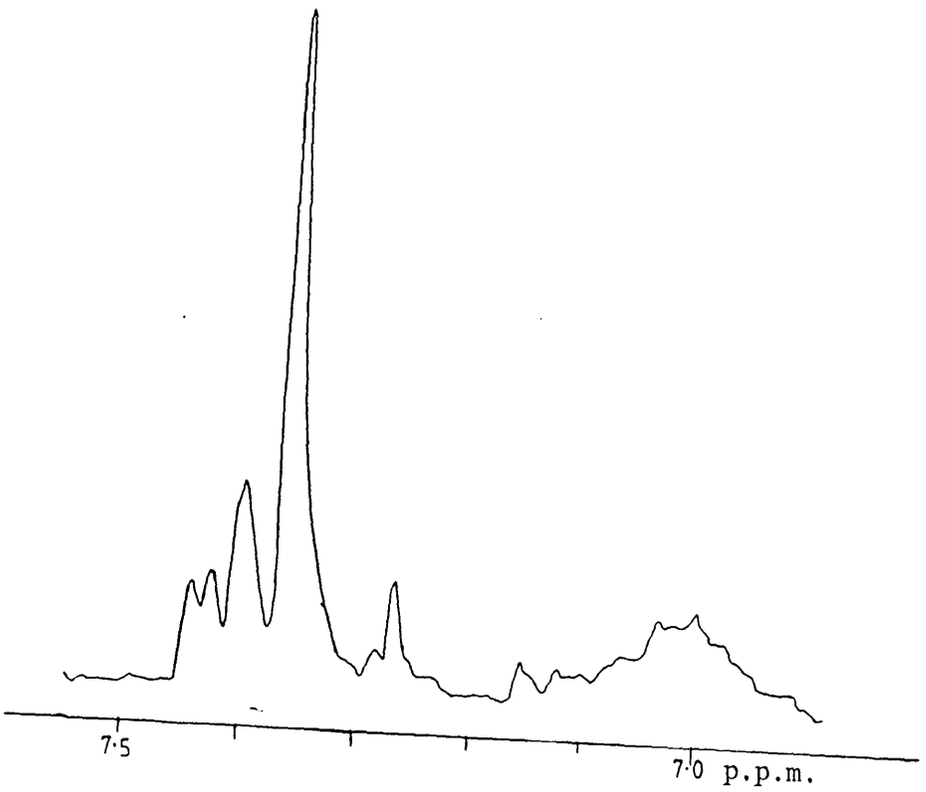


Figure 3.15 - ^{1}H N.M.R. spectrum of Na(trop).

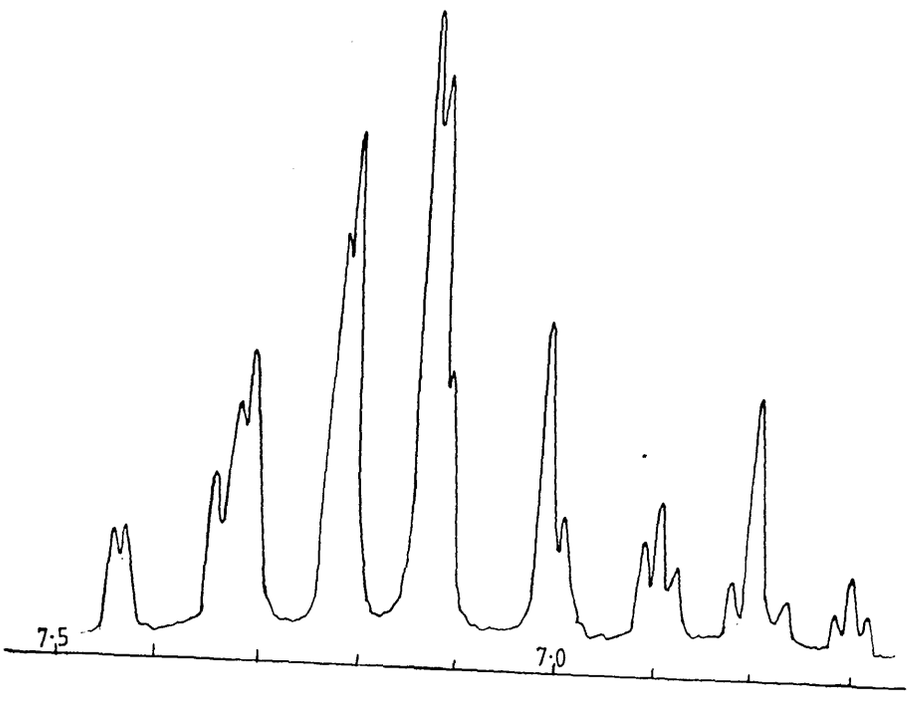


Figure 3.16 - ^{1}H N.M.R. spectrum of $Ir(trop)_3$

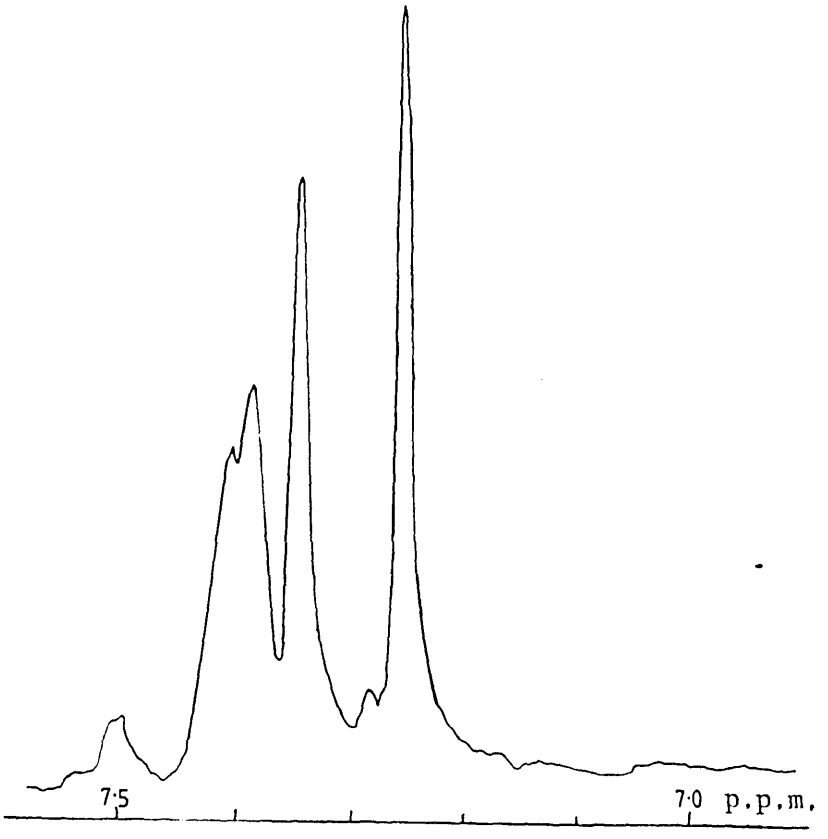
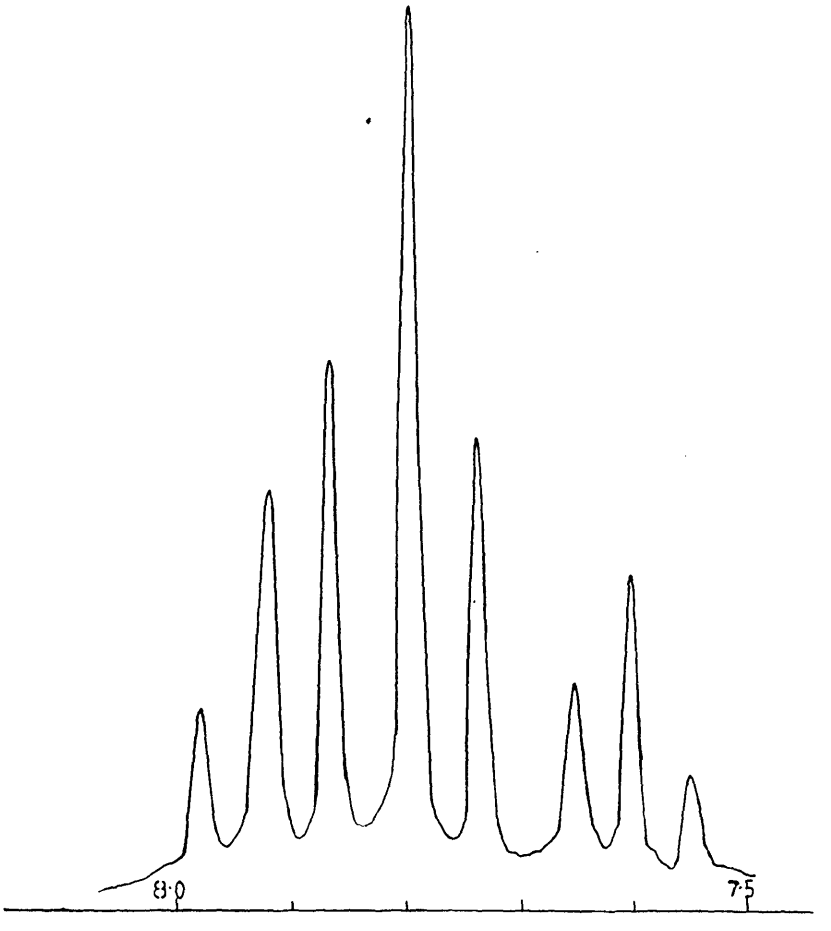


Figure 3.17 - ^{1}H N.M.R. spectrum of $MoO_2(trop)_2$



5. ^{13}C NUCLEAR MAGNETIC RESONANCE SPECTROSCOPY

5.1 Spectrum of the free ligand, tropolone

The resonances recorded for this ligand in aqueous solution are listed in Table 3.9.

The ^{1}H-decoupled ^{13}C N.M.R. spectrum shows four resonances, indicating the presence of four different carbon environments. The peak at highest frequency (171.90 p.p.m.) is found in the region typical of a carbon atom attached to oxygen.[103] It is therefore assigned to carbon atoms C_1 and C_2, as labelled in Figure 3.18.

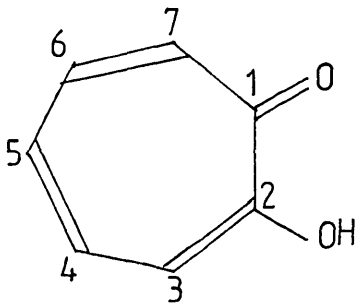


Figure 3.18 Labeling of carbon nuclei of tropolone.

The occurrence of only one peak in this region leads us to conclude that these two carbon atoms are equivalent on the N.M.R. time scale. This is in agreement with previous postulations that the hydroxylic proton is symmetrically located between the two oxygen atoms on a time-average basis.[199] The suggested resonance structures are shown in Figure 3.19.

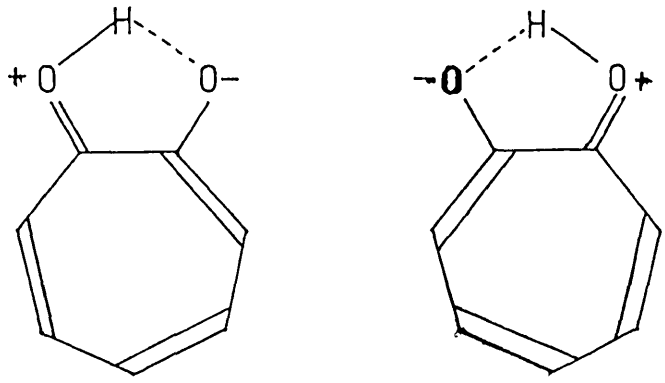


Figure 3.19 :- Resonance Structures of tropolone.

Although in the solid state, X-ray crystallographic studies have shown the solid to exist as an intermolecularly hydrogen-bonded dimer, ebullioscopic and cryoscopic measurements gave no evidence for the existence of a dimer[199] in the liquid or gaseous states. In solution, therefore, it may be assumed that the molecule exists as a monomer, with the suggested intramolecular hydrogen-bond. The proton may be considered to oscillate between the two oxygen atoms at such a rate that, on the N.M.R. time scale, the two oxygen atoms, and therefore the carbon nuclei, C_1 and C_2, are chemically equivalent. This would also lead to an apparent "smearing-out" of the single and double bonds of the carbon ring, leading to equivalence for the carbon atom pairs C_7 and C_3, and C_6 and C_4, with a unique nucleus at C_5. These would lead to three further peaks, as observed.

These assignments are confirmed by the off-resonance decoupled spectrum of tropolone. A degree of ^{13}C - ^{1}H coupling will now be observed for any ^{13}C nucleus attached to a proton as shown in Figure 3.20. The peak at highest frequency

(171.9 p.p.m.) shows no splitting, consistent with its assignment as arising from nuclei C_1 and C_2. The other three peaks all split into doublets, as expected for the ring carbon atoms, each being attached to one hydrogen atom. The intensities of the peaks, although not directly proportional to the number of carbon atoms giving rise to them because of the Nuclear Overhauser effect, do give some indication of the numbers of equivalent nuclei involved. The doublet centred at 128.1 p.p.m. is of significantly less intensity than the other peaks, and is therefore assigned to the unique nucleus, C_5. The other two peaks arising from the pairs C_3 and C_7, and C_4 and C_6, cannot be unequivocally assigned to either of these pairs of nuclei.

A subsequent report in the literature on the ^{13}C N.M.R. spectrum of liquid and solid tropolone, found that the spectrum of liquid tropolone gave rise to four resonances, due to the time-averaging proton-exchange process.[255] The solid spectrum did not display this averaging behaviour; each individual carbon-type was identified in a single resonance. This led to the conclusion that the rate of proton exchange in the solid state was determined by the reorientation of the molecule in the lattice, involving an energetically unfavourable rotation to restore proper lattice packing.

5.2 Spectrum of sodium tropolonate

The spectrum of sodium tropolonate, recorded in aqueous solution, may be considered as the spectrum of the free tropolonato anion. The major difference between this and the spectrum of tropolone is seen to be the shift to higher frequency by 14 p.p.m. of the resonance due to C_1/C_2 as shown in Figure 3.21. The peak tentatively assigned as arising from C_5 is now found to lower frequency, whilst the resonance at 123.8 p.p.m. in the tropolone spectrum has shifted to 128.1 p.p.m.

5.3 Spectra of tropolonato complexes

No ^{13}C N.M.R. spectra of any tropolonato complexes have been reported in the literature.

The resonances recorded for the diamagnetic complexes of the tropolonato anion are listed in Table 3.9. The peak arising from the unique nucleus C_5 was taken to be that with least intensity.

The tropolonato complexes show very similar changes in their ^{13}C N.M.R. spectra from that of the free ligand, as did sodium tropolonate. Again there is a shift to higher frequency of between 10 and 20 p.p.m. of the C_1/C_2 resonance as compared to the spectrum of free tropolone. Of the ring resonances, the peak near 138 p.p.m. for tropolone varies only a little for the spectra of the complexes. The peak at 123.8 p.p.m. of the free ligand, however, shows a shift to higher frequency on coordination. Although small (3-4 p.p.m.) the shift is consistently observed and is therefore of some significance. The resonance arising from the C_5 nucleus,

shows a shift to lower frequency of approximately 3 p.p.m. for sodium tropolonate, but does not show any consistent variation in the spectra of the tropolonato complexes. A typical example is the spectrum of $Ir(trop)_3$ shown in Figure 3.22.

The ^{13}C N.M.R. spectra of complexes of ligand which coordinate through a benzene ring, such as catechol and catecholamines, show a shift of ring carbon resonances to lower frequency on coordination. This is in the opposite direction from that observed for the shift in the 123.8 p.p.m. resonance of the tropolone, although the magnitude of the shifts is of the same order (3-4 p.p.m.). On formation of the tropolonato anion, X-ray crystallographic studies have found (as described earlier) that the variation in bond lengths found within the tropolone ring disappear, consistent with a greater degree of electron delocalisation over the ring. Although, in solution, the ^{13}C N.M.R. of tropolone does not see the bond alternation, because of rapid exchange of the hydroxylic proton, on formation of the tropolonato anion the increased aromaticity of the anion over free tropolone would tend to lead to increased ring currents being induced in the carbon ring under the influence of an applied field. This would lead to greater deshielding of all or some of the tropolonato carbon nuclei, as compared to free tropolone, and the resonances would then be expected to occur to higher frequency. The shift is of the size expected for ring current effects. This theory is offered as a tentative explanation for the observed changes in the resonances of the carbon nuclei.

The spectrum of $MoO_2(trop)_2$ is of particular interest since it is the only one in which two resonances assigned to C_1 and C_2 may be observed separately, indicating they have different chemical environments within the molecule. The spectrum is shown in Figure 3.23. This behaviour was not observed for $K_2[MoO_2(cat)_2]$, and this is possibly due to the greater flexibility of the tropolonato ligands in being able to vary its degree of electron delocalisation, as compared to benzene rings. This may allow the tropolonato ligand to vary its bond lengths in response to the trans influence of the oxo ligands. This may well lead to inequivalence of the two carbon nuclei C_1 and C_2. This is discussed in greater detail in the section describing the X-ray crystallographic investigation of $MoO_2(trop)_2$ (Chapter III, section 9).

The ^{13}C N.M.R. spectrum of $[Pt(PPh_3)_2(trop)](BPh_4)$ is very complicated due to the many resonances arising from the carbon nuclei of the phenyl rings overlapping with some of the tropolonato resonances. Not all the peaks can be satisfactorily assigned, but one resonance occurs at a frequency above that of the rest of the spectrum, and is assigned to the C_1/C_2 resonance of the tropolonato ligand.

Table 3.9:- $^{13}C - \{^{1}H\}$ - N.M.R. resonances of tropolone, sodium tropolonate and tropolonato complexes.

Substance	C_1/C_2	C_3/C_7 and C_4/C_6		C_5	Solvent
Tropolone	172.4	137.6	123.8	128.1	$CDCl_3$
	172.4	138.4	124.3	128.9	d^6acetone
Na(trop)	184.7	139.9	128.1	125.5	H_2O
$Pd(trop)_2$	186.7	137.1	127.4	128.9	$CDCl_3$
$Rh(trop)_3$	187.9	136.8	128.6	128.0	$CDCl_3$
$Ir(trop)_3$	188.6	134.8	129.0	129.6	$CDCl_3$
$MoO_2(trop)_2$	192.3	141.3	128.0	132.8	d^6D.M.S.O.
	177.6				
$UO_2(trop)_2$D.M.S.O.	187.2	139.5	127.4	127.0	d^6D.M.S.O.
$[Pt(PPh_3)_2(trop)](BPh_4)$	183.6				$CDCl_3$

resonances recorded as δ(p.p.m.) to higher frequency of T.M.S. (δ= o)

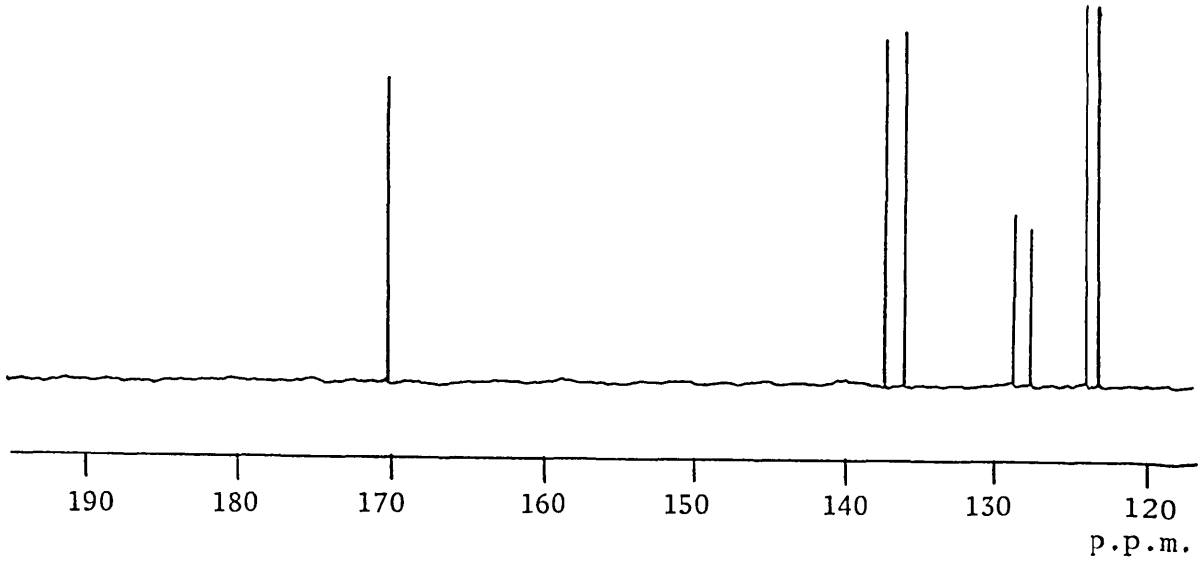


Figure 3.20 - Off resonance coherent decoupled ^{13}C N.M.R. spectrum of tropolone.

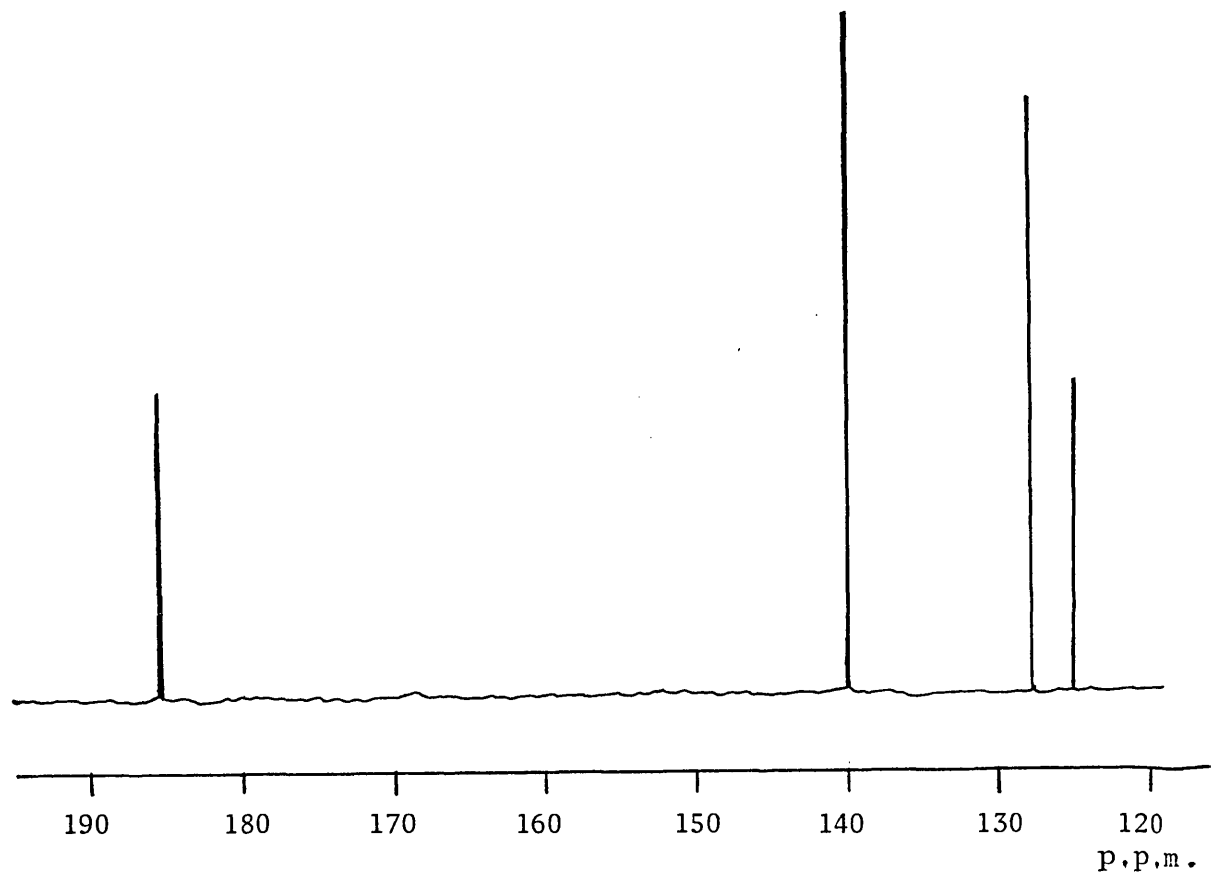


Figure 3.21 - ^{13}C N.M.R. spectrum of sodium tropolonate

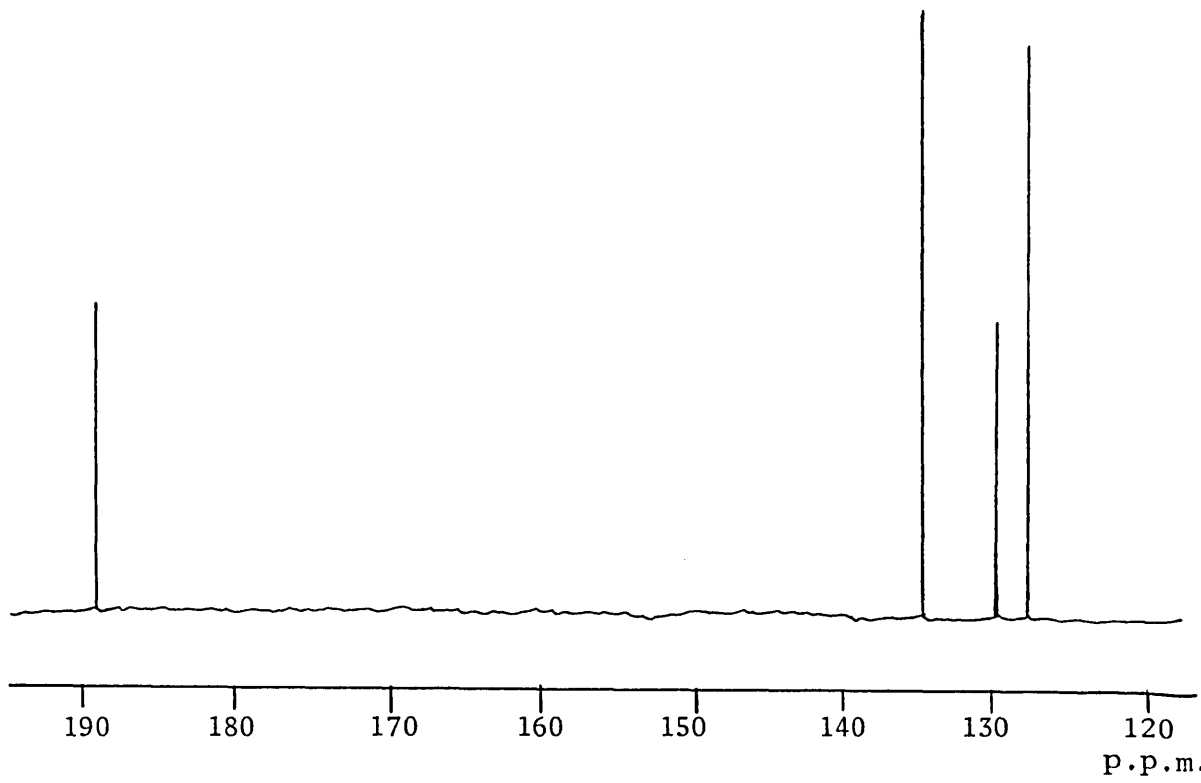


Figure 3.22 - ^{13}C N.M.R. spectrum of $Ir(trop)_3$

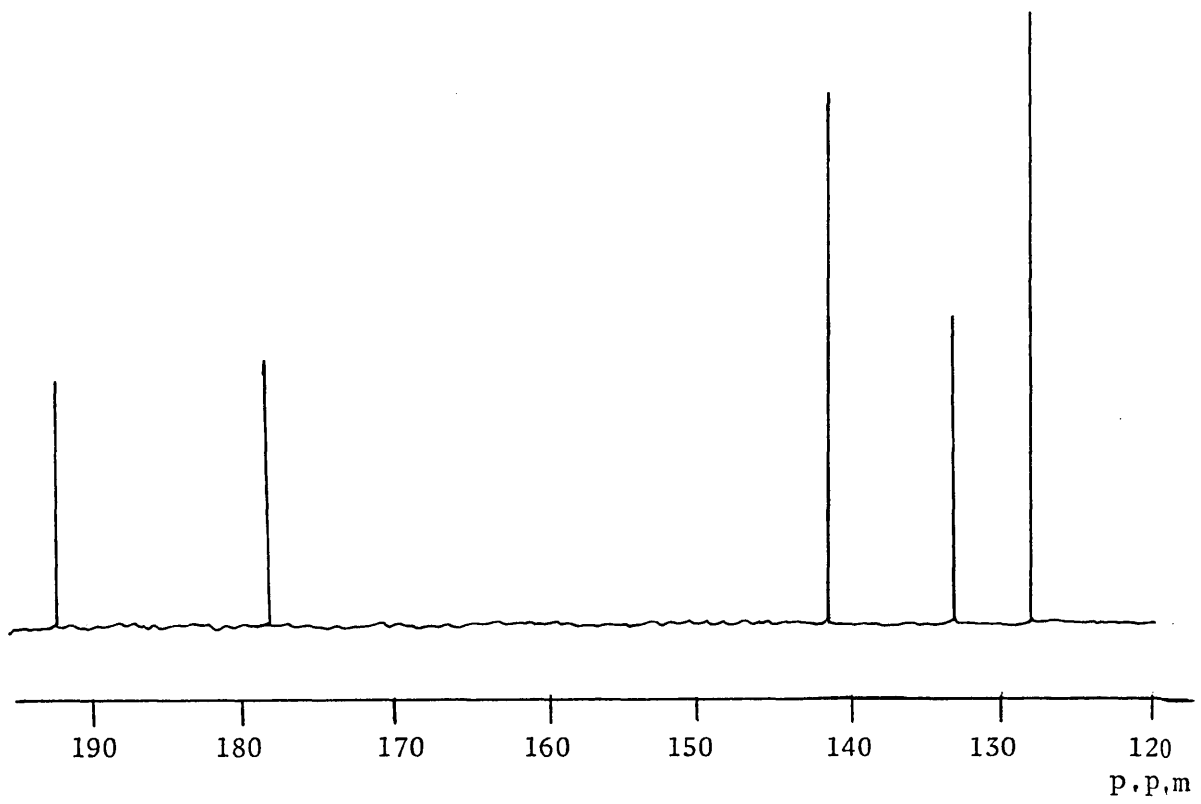


Figure 3.23 - ^{13}C N.M.R. spectrum of $MoO_2(trop)_2$

6. ELECTRON PARAMAGNETIC RESONANCE SPECTROSCOPY

As for the catecholato complexes, E.P.R. spectroscopy is only used in this work to seek further evidence in support of the postulated structure of any paramagnetic complex. Of the new tropolonato complexes reported here, only $Os(trop)_3$ is paramagnetic, having a $5d^5$ electronic configuration. The E.P.R. spectrum of this complex was recorded at liquid nitrogen temperature in chloroform solution.

Despite the presence of impurities the spectrum does show a signal consistent with a low spin d^5 metal ion, with g values of 2.34, 2.21, and 2.11. The second major signal of the spectrum has g values of 8.12 and 4.22, very close to those reported for $Fe(trop)_3$.[256] in chloroform (g = 8.11 and 4.42) with a high spin d^5 electronic configuration. Samples of $Os(trop)_3$ were indeed sometimes found to have $Fe(trop)_3$ as impurity.

Thus the E.P.R. spectrum does give a signal which may arise from a low spin d^5 metal ion, but due to the presence of other signals this cannot be unequivocally assigned to $Os(trop)_3$, although it appears likely that the signal does arise from this complex.

7. ELECTROCHEMISTRY

Little electrochemical data on transition metal tropolonato complexes are reported in the literature.

Cyclic voltammograms were recorded for all the new tropolonato complexes, and many of the known complexes, at 1-5 x 10^{-3} M concentrations in a 0.1M solution of tetrabutylammonium perchlorate in acetonitrile and in dimethyl sulphoxide. However, no reversible or sharply defined irreversible patterns were observed.

8. MASS SPECTROSCOPY OF TROPOLONATO COMPLEXES

8.1 Literature measurements

A number of main group and first row transition metal tropolonato complexes have been investigated by mass spectrometry. The main decomposition pathways were found to involve loss of tropolone radicals and CO molecules. The loss of carbon monoxide led to the formation of cyclopentadienyl metal ions, showing the ability of such metals to form complexes with unsaturated hydrocarbon ligands.

The tris(tropolonato) metal(III) complexes[257] investigated each showed the molecular ion $[M(trop)_3]^{+\bullet}$. This was found to fragment exclusively by loss of a ligand radical, $trop^{\circ}$, to give the even-electron ion $[M(trop)_2]^{+}$, which was often the most abundant ion. Subsequent fragmentation was found to depend on the nature of the metal, in particular its oxidation state characteristics and its ability to form complexes with unsaturated hydrocarbon ligands. Metals which could easily under-go reduction (M = Cr, Fe, Ga, In), showed successive loss of odd electron species from even-electron ions to give $[M(trop)]^{+}$ and $[M]^{+}$, showing reduction of the metal. The complexes of aluminium(III) and scandium(III) did not follow this path, due to the high stability of the +3 oxidation state for these metals - very low abundances for $[M(trop)]^{+}$ and no $[M]^{+}$ peaks were recorded.

8.2 Experimental results

The mass spectra of the tris(tropolonato) complexes $Ru(trop)_3$, $Os(trop)_3$, $Rh(trop)_3$ and $Ir(trop)_3$ were recorded. Not all the peaks can be clearly identified from the background noise, but the spectra are good enough to show the molecular ion and hence confirm the molecular weight of the complex. The major peaks arising from metal-containing ions and their tentative assignments are listed in Tables 3.10 and 3.11.

Each spectrum shows a peak corresponding to the molecular ion $[M(trop)_3]^{+\cdot}$, which confirms the postulated molecular weight of each complex. This may be seen in the mass spectrum of $Ir(trop)_3$ shown in Figure 3.24. The spectra show peaks in a pattern expected from the relative abundances found for the isotopes of the metal concerned. The peak of the molecular ion for $Os(trop)_3$ has considerably less abundance than is found for the molecular ions of the other spectra. Two groups of peaks are observed in the spectrum of $Os(trop)_3$ at a value of m/e 16 and 14 units, respectively, lower than the positions found for the molecular ion. This possibly reflects the relative instability of $[Os(trop)_3]^{+\cdot}$, and it breaks down to give metal-containing fragments, stable enough to be recorded, before formation of the stable ion $[Os(trop)_2]^{+}$.

Each spectrum shows a peak of quite large abundance, corresponding to $[M(trop)_2]^{+}$. This ion was found to be typical of tris(tropolonato) metal(III) complexes. After this, however, the complex $Ru(trop)_3$ appears to show different behaviour from that found for the other three complexes. We will first discuss

the spectra of $Rh(trop)_3$, $Os(trop)_3$, and $Ir(trop)_3$. In the spectra of these complexes, the ion $[M(trop)_2]^+$ breaks down by loss of carbon monoxide molecules to result in the cyclopentadienyl metal ion $[M(C_5H_5)_2]^+$. The spectrum of $Rh(trop)_3$ shows stepwise elimination of CO molecules to arrive at $[M(C_5H_5)_2]^+$; that of $Os(trop)_3$ does not exhibit a peak due to $[M(trop)_2\text{-}3CO]^+$ whilst $Ir(trop)_3$ has only a weak peak for $[M(trop)_2\text{-}2CO]^+$ and no peaks for the ions resulting from loss of one and of three CO molecules. A peak of higher abundance is found for $[M(C_5H_5)_2]^+$. This formulation is confirmed by the fragmentation pattern found below the m/e value for $[M(C_5H_5)_2]^+$.[259] The spectra of $Fe(trop)_3$ and $Cr(trop)_3$ were reported to show the ion $[M(C_5H_5)]^+$, its subsequent decomposition leading to the bare metal ions. However, the case is different for second and third row transition metal ions in this type of complex. Here the partial fragmentation of the ligands with stepwise elimination of acetylene becomes more important, in particular, the ion $[M(C_8H_8)]^+$, arising from loss of one acetylene molecule from $[M(C_5H_5)_2]^+$, shows a reasonably strong abundance. This pattern may be seen in the spectra recorded here. No peak is found for any of the complexes corresponding to the metal ion $[M]^+$, reflecting the stability of the +3 oxidation state for these metals. This behaviour was also reported for the complexes $M(acac)_3$, where M = Os(III), Rh(III), Ir(III).[260]

The spectrum of $Ru(trop)_3$ shows a group of peaks near m/e 465, corresponding to the molecular ion, $[Ru(trop)_3]^{+\cdot}$ The number of peaks corresponds to the several isotopes of ruthenium (Ru^{96} 5.51%, Ru^{99} 12.72%, Ru^{100} 12.62%, Ru^{101} 17.07%, Ru^{102} 31.63%, Ru^{104} 18.58%). A group of peaks in the same pattern is observed near m/e 344, corresponding to the ion $[Ru(trop)_2]^{+}$ This ion then breaks down by loss of acetylene and cyclopentadienyl fragments, leading to a peak at m/e 212, presumably arising from $[Ru(CO)_4]^{+}$ Indeed this has been reported in the fragmentation of $Ru_3(CO)_{12}$.[259] It would appear that the ruthenium-carbon monoxide bonds are more stable under these conditions than the ruthenium-cyclo-pentadienyl bonds, leading to the expulsion of cyclopentadienyl fragments. No evidence is found for any $[Ru(C_5H_5)_x]^{+}$ species, nor for $[Ru(trop)]^{+}$ or $[Ru]^{+}$. The peaks to lower m/e than 212, are weaker and not so clearly distinguished from the background, so any further fragmentation is difficult to identify.

Each of the mass spectra of these four complexes shows a large number of peaks in the lower m/e part of the spectrum. Clearly distinguished are those at m/e 122, due to tropolone, and others at m/e 94, 66, and 39. These match with those reported in the literature as the most abundant peaks of the non-metal containing fragments.[257]

Table 3.10:- Assignment of major peaks (m/e) of the mass spectra of $Rh(trop)_3$ and $Ir(trop)_3$

Ion	$Rh(trop)_3$	$Ir(trop)_3$
$[M(trop)_3]^{+\cdot}$	466	556
$[M(trop)_2]^+$	345	435
$[M(trop)_2]^+-CO$	317	-
$[M(trop)_2]^+-2CO$	289	379
		377
$[M(trop)_2]^+-3CO$	261	-
$[M(trop)_2]^+-4CO$	233	323
$[M(C_5H_5)_2]^+-C_2H_2$		294
$[M(C_5H_5)_2]^+-2C_2H_2$		271
$[M(C_5H_5)]^+$		258

Table 3.11:- Assignment of major peaks (m/e) of the mass spectra of $Ru(trop)_3$ and $Os(trop)_3$

Ion	$Ru(trop)_3$	$Os(trop)_3$
$[M(trop)_3]^{+\cdot}$	465	555
$[M(trop)_2]^+$	344	434
$[M(trop)_2]^+-CO$	-	404
$[M(trop)_2]^+-2CO$	-	378
$[M(trop)_2]^+-3CO$	-	-
$[M(trop)_2]^+-4CO$	-	322
$[M(C_5H_5)_2]^+-C_2H_2$	-	296
$[M(C_5H_5)_2]^+-2C_2H_2$	-	270
$[M(C_5H_5)]^+$	-	-
$[M(trop)_2]^+-C_2H_2$	318	-
$[M(trop)_2]^+-C_5H_5$	278	-
$[M(trop)_2]^+-2C_5H_5$	212	-

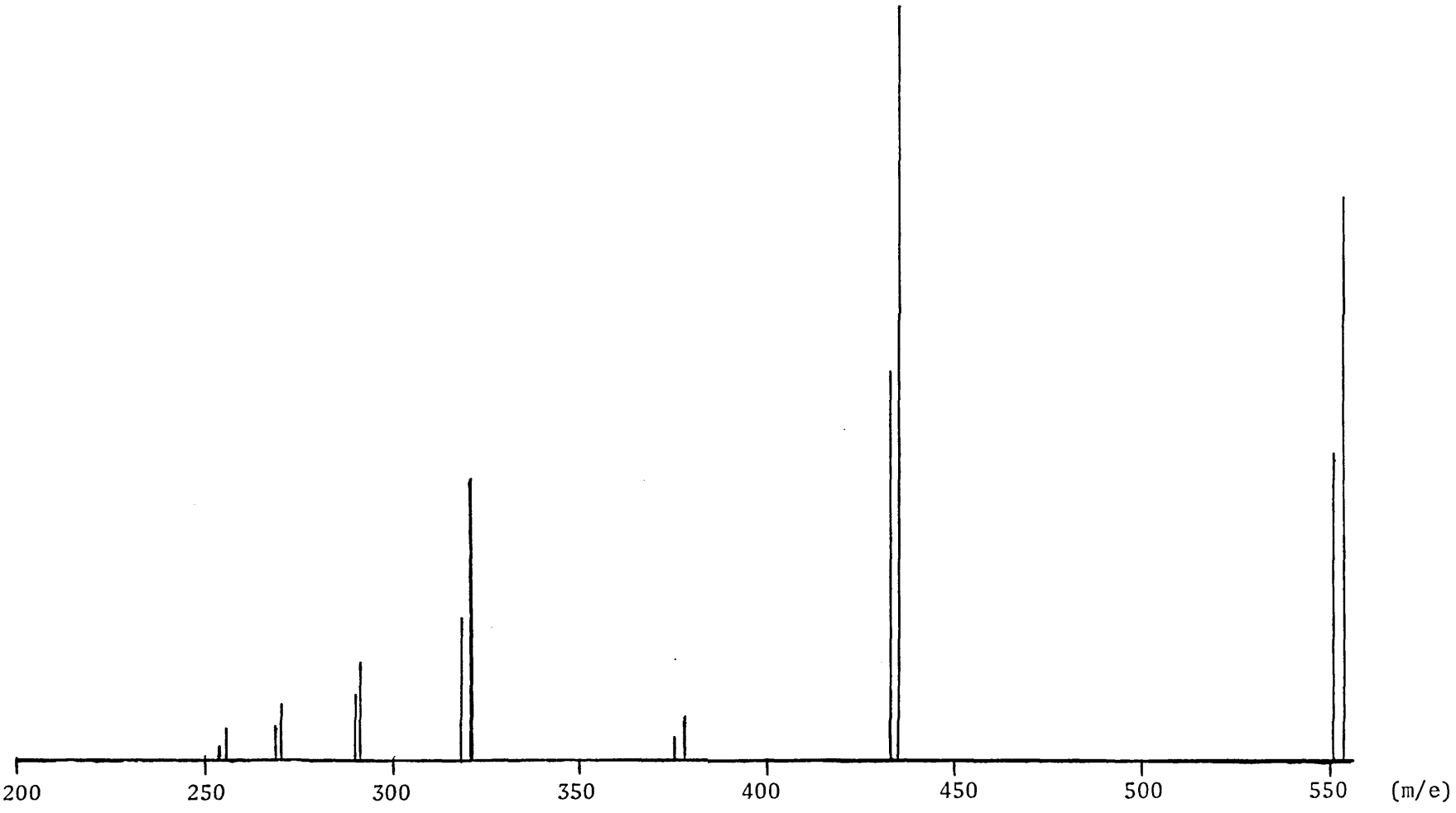


Figure 3.24 - Mass spectrum of $Ir(trop)_3$

9. CRYSTAL STRUCTURE OF $MoO_2(trop)_2$

The yellow crystals were grown by cooling a hot dimethyl sulphoxide solution of the complex. They were found to have space group C2/C, with cell dimensions a = 15.485(3), b = 13.583(3) c = 14.211(3) and β = 117.74(2)°. The R factor was found to be 3.33%.

The X-ray crystallographic study, carried out by Dr. Andrzej Skapski, Imperial College, confirms the structure of this complex deduced from spectroscopic evidence. The bond lengths and bond angles are listed in Tables 3.12 and 3.13 respectively, and the structure is shown in Figure 3.25.

The coordination geometry about the molybdenum centre is distorted octahedral, with the oxo ligands in mutually cis positions, with the remaining coordination sites occupied by the oxygen atoms of the tropolonato ligands. The molybdenum to terminal oxygen bond lengths are within the range expected for a molybdenum(VI) atom double bonded to an oxo ligand (1.68 - 1.73Å).[260] The two Mo-O(trop) bonds opposite to the oxo ligands are significantly longer than the other two Mo-O(trop) oxygen bonds. This is attributed to the trans-influence of the oxo ligands. Trans-lengthening of bonds opposite oxo ligands in molybdenum(VI) compounds is well documented.[68] The Mo-O length is of the same order (2.00Å) as that found for the molybdenum(VI) to ligand oxygen bonds in catecholato complexes. The complex $K_2[MoO_2(cat)_2]$ was also reported to show lengthening of the Mo-O(cat) bond in

the trans position to the oxo ligand,[68] but in this report the errors were so large that this difference is not necessarily significant. Other, more accurate, structural studies of catecholato complexes containing oxo ligands generally involve binuclear complexes of the type $[Mo_2O_5(cat)_2]^{2-}$. Any lengthening of the Mo-O(cat) bond in these complexes may involve factors arising from the bridging behaviour of the catecholato ligand, so no direct comparison may be made with this complex, concerning the trans-lengthening effect of the oxo ligands.

The carbon-oxygen bonds, C_{12} - O_{12} and C_{21} - O_{21} have lengths similar to those reported previously (see Tables 3.1, 3.2 and 3.3). The other two C - O bonds, C_{22} - O_{22} and C_{11} - O_{11}, are significantly longer. A previous study has noted that the X-ray crystallographic data suggest that increasing strength of the metal - O(trop)bond is generally accompanied by a modest lengthening of the C - O bonds.[209] This is consistent with the pattern observed here. The Mo-O(trop) bonds trans to the (Mo-O_{21} and Mo-O_{12}) are longer and, therefore, weaker than the other Mo-O(trop) bonds (Mo-O_{22},Mo-O_{12}). The C - O bonds adjacent to these longer Mo-O(trop) bonds (C_{21} - O_{21}, C_{12} - O_{12}) are shorter than the other two C - O bonds (C_{11} - O_{11}, C_{22} - O_{22}) reflecting the difference in strength of the Mo-O(trop) bonds.

No definite alternation of bond lengths is found around the carbon ring, indicating electron delocalisation as found for other tropolonato complexes. The bonds C_1 - C_2 are significantly longer than the others, in each ring

having values close to that typical of a single bond between two trigonally hybridised carbon atoms (1.48Å).[201] Previously reported structural studies of tropolonato complexes[205,228] have found that there is generally a sequential decrease of bond lengths of the carbon ring starting from the carbon atoms vicinal to oxygen and ending with the central C_5 atom. For the complex $MoO_2(trop)_2$, however, the bonds C_{12}-C_{13}, and its equivalent in the second ring C_{21}-C_{27} are longer than expected (at 1.410 and 1.404Å) whilst the other two bonds vicinal to the oxygen atoms, C_{22}-C_{23} and C_{11}-C_{17}, are shorter than expected (at 1.368 and 1.367Å). These differences in the bond lengths are again attributed to the effect of the oxo ligands i.e. they lead to a longer Mo-O(trop) bond than expected, a shorter C-O bond, followed by a longer C-C bond, adjacent to the C-O bond (i.e. the bonds C_{12}-C_{13} and C_{21}-C_{27}). This behaviour has not been previously reported in tropolonato complexes.

This type of "knock-on" effect from the presence of the oxo ligands was not observed in the catecholato complex $K_2[MoO_2(cat)_2]$. However, as noted above, the standard deviations of this determination were too large for any meaningful correlations to be made. It does not seem likely, however, that such an effect would be seen in the aromatic ring of catechol as that found for tropolone. The tropolone ring is a system in which the degree of electron delocalisation has been shown to vary. Thus it would possibly be able to respond in a more flexible manner to outside influence, such as <u>trans</u> oxo ligands, than would a catecholato ring.

These effects help to explain the ^{13}C N.M.R. spectrum recorded for MoO_2-(trop)$_2$. Two different environments are observed for the two carbon nuclei of the tropolonato ligands attached to the oxygen atoms in the N.M.R. spectrum. It is now obvious that the carbon atoms with the shorter C - O bonds (C_{12} - O_{12} and C_{21} - O_{21}) will have the greater degree of carbonyl character and will presumably resonate at higher frequency.

The values of the internal angles of the carbon ring are a consequence of the differences observed in the bond lengths.[205]

The C - H bonds are found to be 0.94Å, very close to the suggested optimal C - H distance.[229]

The bite angle is found to be the same for both rings at 73.2(0.1)°, and the bite distance is 2.510Å°, within the narrow range of values found for other tropolonato complexes, (see Tables 3.1, 3.2, and 3.3). The tropolonato ligands show a small deviation from planarity, with a slight twist of the ligand. This presumably arises from the tendency of tropolonato complexes to distortion in the solid state as a result of packing forces. This was ascribed to the small bite of the tropolonato ligand which contributes to loose packing of the ligand in the lattice.[198,229]

Figure 3.25 - Structure of $MoO_2(trop)_2$ found by X-ray crystallography

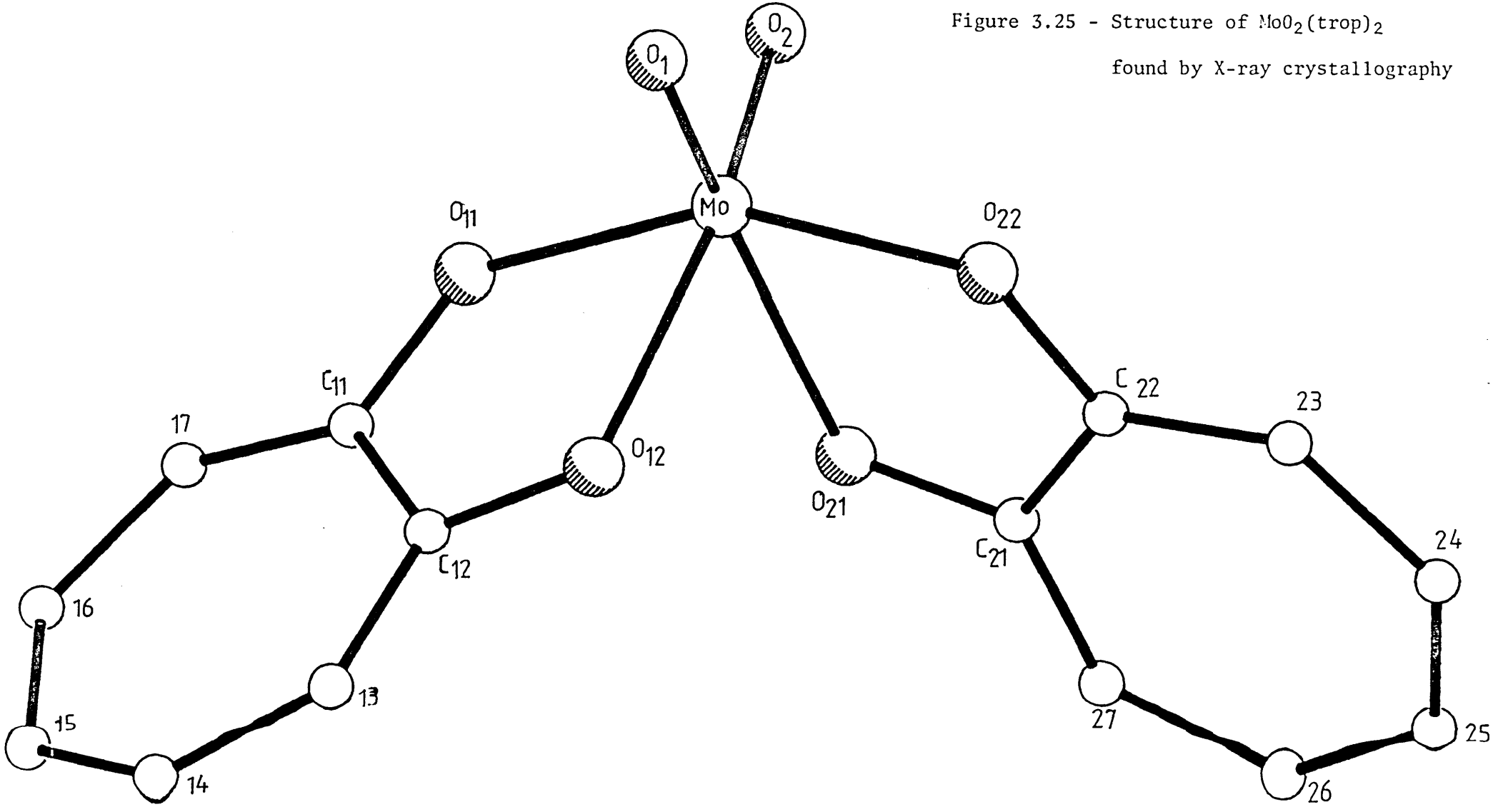


Table 3.12:- Bond lengths (Å) with standard deviations for $MoO_2(trop)_2$

Mo-O_1	1.689(0.004)	C_{11}-C_{12}	1.444(0.007)
Mo-O_2	1.699(0.004)	C_{12}-C_{13}	1.410(0.007)
		C_{13}-C_{14}	1.376(0.008)
Mo-O_{11}	2.005(0.003)	C_{14}-C_{15}	1.372(0.008)
Mo-O_{12}	2.169(0.003)	C_{15}-C_{16}	1.373(0.008)
Mo-O_{21}	2.186(0.004)	C_{16}-C_{17}	1.394(0.007)
Mo-O_{22}	2.018(0.003)	C_{17}-C_{11}	1.367(0.007)
O_{11}-C_{11}	1.321(0.006)	C_{21}-C_{22}	1.451(0.008)
O_{12}-C_{12}	1.277(0.006)	C_{22}-C_{23}	1.368(0.007)
O_{22}-C_{22}	1.322(0.006)	C_{23}-C_{24}	1.394(0.008)
O_{21}-C_{21}	1.281(0.006)	C_{24}-C_{25}	1.357(0.010)
		C_{25}-C_{26}	1.389(0.010)
[a]O_{11}...O_{21}	2.491	C_{26}-C_{27}	1.362(0.009)
[a]O_{21}...O_{22}	2.510	C_{27}-C_{21}	1.404(0.009)

[a]bite distance for tropolonato ligand.

Table 3.13:- Bond angles(degrees) for $MoO_2(trop)_2$

O_1-Mo-O_{11}	103.7(0.2)	C_{13}-C_{12}-O_{12}	119.9(0.5)
O_1-Mo-O_{12}	93.5(0.2)	C_{11}-C_{12}-O_{12}	114.7(0.4)
O_1-Mo-O_{21}	161.6(0.2)	C_{11}-C_{12}-O_{13}	125.5(0.5)
O_1-Mo-O_{22}	89.9(0.2)	C_{12}-C_{13}-C_{14}	129.3(0.5)
O_1-Mo-O_2	103.4(0.2)	C_{13}-C_{14}-C_{15}	130.7(0.5)
O_2-Mo-O_{11}	91.4(0.2)	C_{14}-C_{15}-C_{16}	127.3(0.5)
O_2-Mo-O_{12}	159.5(0.2)	C_{15}-C_{16}-C_{17}	129.2(0.5)
O_2-Mo-O_{21}	88.6(0.2)	C_{16}-C_{17}-C_{11}	129.8(0.5)
O_2-Mo-O_{22}	106.3(0.2)	C_{17}-C_{11}-C_{12}	128.3(0.5)
[a]O_{11}-Mo-O_{12}	73.2(0.1)		
[a]O_{21}-Mo-O_{22}	73.2(0.1)	C_{23}-C_{22}-O_{22}	118.4(0.5)
O_{11}-Mo-O_{21}	89.7(0.1)	C_{21}-C_{22}-O_{22}	113.7(0.4)
O_{12}-Mo-O_{21}	78.1(0.2)	C_{21}-C_{22}-C_{23}	127.9(0.5)
O_{11}-Mo-O_{22}	154.7(0.1)	C_{22}-C_{23}-C_{24}	129.9(0.5)
O_{12}-Mo-O_{22}	84.9(0.1)	C_{23}-C_{24}-C_{25}	129.4(0.5)
C_{11}-O_{11}-Mo	122.2(0.3)	C_{24}-C_{25}-C_{26}	127.2(0.6)
C_{12}-O_{12}-Mo	117.0(0.3)	C_{25}-C_{26}-C_{27}	130.3(0.6)
C_{21}-O_{21}-Mo	117.0(0.3)	C_{26}-C_{27}-C_{21}	129.9(0.6)
C_{22}-O_{22}-Mo	121.8(0.3)	C_{27}-C_{21}-C_{22}	125.1(0.5)

[a]bite angles for the tropolonato ligand.

RESUME OF CHAPTER III

In this chapter we have reported the preparation of a number of new tropolonato complexes, using methods adapted from preparations of acetylacetonato and catecholato complexes. The new complexes were characterised by vibrational, ^{1}H and ^{13}C N.M.R. and E.P.R. spectroscopy, mass spectrometry, and, in the case of $MoO_2(trop)_2$, X-ray crystallography. The following new complexes were identified:- $Ir(trop)_3$, $Os(trop)_3$, $OsO_2(trop)_2$, $MoO_2(trop)_2$, $W_2O_5(trop)_2$, and $[Pt(PPh_3)_2(trop)](BPh_4)$.

10. EXPERIMENTAL

The new tropolonato complexes described in this thesis are prepared as follows:-

10.1 Tris-tropolonato complexes

(a) Tris (tropolonato) iridium (III), $Ir(trop)_3$

Sodium acetate trihydrate (0.19g, 0.0014 moles) was dissolved in water ($10cm^3$). Hydrated iridium trichloride (0.12g, 0.00033 moles) was added and the solution warmed to give a dark green solution. Tropolone (0.25g, 0.001 moles) was added, with stirring. As the solid tropolone dissolved, the solution became brick red in colour. It was warmed and stirred for a few hours. After cooling, the oily precipitate was filtered off and washed with water, ethanol, and diethyl ether. The resulting red powder was dried over concentrated sulphuric acid.

$Ir(C_7H_5O_2)_3$

Found:- C = 45.0, H = 2.9

$C_{21}H_{15}IrO_6$ requires C = 45.4, H = 2.7%

Yield = 40%

(b) Tris (tropolonato) osmium (III), $Os(trop)_3$

The general method used was that described for the preparation of $Os(acac)_3$.[238]

Silver powder (1.1g, 0.01 moles) in water ($50cm^3$) with 36% hydrochloric acid ($10cm^3$), was degassed with nitrogen for thirty minutes. $Na_2[OsCl_6]$ (4.5g, 0.01 moles) was added, and the reddish solution was stirred under nitrogen overnight. To the resulting pale yellow-green solution,

potassium bicarbonate (0.6g, 0.006 moles) was added, causing much effervescence. This was followed by addition of tropolone (3.67g, 0.03 moles). The solution was boiled for fifteen minutes. Further potassium bicarbonate (0.4g, 0.004 moles) was then added to the resulting very dark solution, causing further effervescence. The solution was heated gently for two hours. After cooling, the solution was extracted twice with chloroform, and the chloroform solution washed twice with 2% aqueous sodium hydroxide solution. The resulting red chloroform solution was reduced on the rotary evaporator. The red-brown solid was recrystallised from ethanol.

$Os(C_7H_5O_2)_3$

Found:- C = 45.4, H = 3.0

$C_{21}H_{15}O_6Os$ requires C = 45.6, H = 2.7%

10.2 Oxo-tropolonato complexes

(a) Bis (tropolonato) cis-dioxomolybdenum (VI), $MoO_2(trop)_2$

Tropolone (0.25g, 0.002 moles) in ethanol (5cm^3) was added to a solution of ammonium molybdate (0.19g, 0.001 moles) in water (10cm^3). A light yellow precipitate immediately formed. After standing for thirty minutes it was filtered off, washed with water, ethanol, and diethyl ether. It was dried under vacuum.

$MoO_2(C_7H_5O_2)_2$

Found:- C = 44.9, H = 2.7

$C_{14}H_{10}MoO_6$ requires C = 45.4, H = 2.7%

Yield = 70%

(b) Bis (tropolonato)-μ-oxo-bis (cis-dioxotungsten (VI)]

$W_2O_5(trop)_2$

Tropolone (0.25g, 0.002 moles) in ethanol ($5cm^3$) was added to a solution of sodium tungstate (0.29g, 0.001 moles) in water ($10cm^3$). A pale yellow colour was seen immediately on mixing. After standing for two hours, the resulting pale yellow solid was filtered off, washed with water and ethanol, and diethyl ether, and dried under vacuum. (The solid may be obtained more quickly by precipitation with ethanol, after mixing of the two reactant solutions).

$W_2O_5(C_7H_5O_2)_2$

Found:- C = 24.7, H = 1.7

$C_{14}H_{10}O_9W_2$ requires:- C = 24.4, H = 1.5%

Yield = 60%

(c) Bis (tropolonato) trans-dioxo-osmium (VI), $OsO_2(trop)_2$

Potassium osmate, trans-$K_2[OsO_2(OH)_4]$ (0.37g,0.001 moles) was dissolved in water ($30cm^3$) by stirring. Tropolone (0.25g, 0.002 moles) in ethanol ($5cm^3$) was added. Immediately a mustard coloured precipitate came down. It was filtered off after standing for thirty minutes, washed with water, ethanol, and diethyl ether, and dried under vacuum.

$OsO_2(C_7H_5O_2)_2$

Found:- C = 36.7, H = 2.3

$C_{14}H_{10}O_6Os$ requires C = 36.2, H = 2.2%

Yield = 90%

10.3 Mono (tropolonato) bis (triphenylphosphine) platinum (II) tetraphenylboronate $[Pt(PPh_3)_2(trop)](BPh_4)$

This complex was prepared using the method described for $Pt(PPh_3)_2(cat)$.[27] i.e. via the intermediates $Pt(PPh_3)_4$ and $Pt(PPh_3)_2O_2$.

All manipulations were carried out under nitrogen, and all solvents were degassed before use.

Triphenylphosphine (0.6g, 0.002 moles) was dissolved in ethanol ($8cm^3$) by shaking and warming in a water bath at 60^oC. Potassium hydroxide (0.1g, 0.002 moles) in 80% aqueous ethanol ($3cm^3$) was added. To this was added $K_2[PtCl_4]$ (0.2g, 0.0005 moles) in water ($2cm^3$) over a twenty minute period. During this time the solution was kept at 60^oC and was stirred continuously. On completion of the $K_2[PtCl_4]$ addition, the solution was allowed to cool, and the resulting solid, $Pt(PPh_3)_4$, was filtered off. It was washed twice with ethanol, and dried almost to completeness on the vacuum line.

The $Pt(PPh_3)_4$ was dissolved in toluene (approx. $10cm^3$). Oxygen was bubbled through this solution for two hours; the yellow colour gradually deepened to become the orange characteristic of $Pt(PPh_3)_2O_2$.

Tropolone (0.06g, 0.0005 moles) in ethanol (5cm^3) was added slowly, with stirring, to the platinum solution, kept in an ice/water bath. The solution became yellow and was left to stir for one hour. No precipitate resulted so sodium tetraphenylboronate (0.17g, 0.0005 moles) in ethanol (8cm^3) was added to the clear yellow solution. A pale yellow precipitate formed immediately. It was filtered off, washed with ethanol and diethyl ether and left to dry under nitrogen. The solid was stable in air.

$[Pt(P(C_6H_5)_3)_2(C_7H_5O_2)][B(C_6H_5)_4]$

Found:- C = 68.9, H = 5.2, P = 5.0

$BC_{67}H_{55}O_2P_2Pt$ requires C = 69.4, H = 4.8, P = 5.3%

Yield = 50%

10.4 The following complexes were prepared by the methods reported in the literature:-

$Rh(trop)_3$[189] $Fe(trop)_3$[199] $Cr(trop)_3$[191] $La(trop)_3$[189]
$Ce(trop)_3$[189] $Ce(trop)_4$[189] $Cu(trop)_2$[190] $Mn(trop)_2$[190]
$[Co_4(trop)_8(H_2O)_2]$[190] $[Ni(trop)_2H_2O]_2$[190] $Pd(trop)_2$[190]
$UO_2(trop)_2MeOH$[218]

Sodium tropolonate was prepared as described by Sasada and Nitta.[203]

The preparation of $Ru(trop)_3$ was attempted by adapting the method used for $Ir(trop)_3$ and $Rh(trop)_3$. It was successful only once and could not be repeated.

$Ru(C_7H_5O_2)_3$

Found:- C = 54.0 H = 3.6

$C_{21}H_{15}O_6Ru$ requires C = 54.3, H = 3.3%

REFERENCES

1. Plinii Secundi "Historiae Naturalis Libri" XXXIV Section 126, A.D.76
2. Robert Boyle, "Short Memoirs for the Natural Experimental History of Mineral Waters" Smith, London 1684
3. S. Tennant Phil.Trans. 1804 94, 419
4. Cortlandt G. Pierpoint and Hartley H.Downs Inorg. Chem. 1977 16 2970
5. Philip J. Delmon Wine for all seasons 1978 5, 93
6. Stephen L. Kessel, R.M.Emberson, P.G. Debrunner and David N. Hendrickson, Inorg.Chem., 1980 19, 1170
7. John P. Wilshire, Luis Leon, Paula Bosserman and Donald T. Sawyer. J.Amer.Chem.Soc., 1979 101 3379
8. Keith D. Magers, Cecil G.Smith and Donald T. Sawyer, Inorg. Chem. 1978 17 515
9. Stephen E.Jones, Der-Hang Chin and Donald T. Sawyer, Inorg. Chem. 1981 20 4257
10. Robert C. Hider, A. Rahim Mohd-Nor, Jack Silver, Ian E.G. Morrison and Lovat V.C. Rees, J.C.S. Dalton Trans 1981 609
11. James V. McArdle, Stephen R. Sofen, Stephen R. Cooper and Kenneth N. Raymond. Inorg.Chem. 1978 17 3075
12. Kenneth N. Raymond, Stephen S. Isied, Leo D. Brown, Frank R. Fronczek and J. Hunter Nibert J.Amer.Chem.Soc. 1976 98 1767

13. Wesley R. Harris, Kenneth N. Raymond and Frederick L. Weitl. J.Amer.Chem.Soc. 1981 103 2667

14. Alex Ardeef, Stephen R. Sofen, Thomas L. Bregante and Kenneth N. Raymond. J.Amer.Chem.Soc. 1978 100 5362

15. John K. Hourie and Donald T. Sawyer. Inorg.Chem. 1976 15 1892

16. Meng-Chay-Lim and Donald T. Sawyer. Inorg.Chem. 1982 21 2839

17. Robert M. Buchanan and Cortlandt G. Pierpoint. Inorg.Chem. 1979 18 1616

18. Cortlandt G. Pierpoint and Robert M. Buchanan. Inorg.Chem. 1982 21 652

19. Alastair J. Nielson and William P. Griffith. J.C.S. Dalton Trans 1978 1501

20. D.R. Eaton. Inorg.Chem. 1964 3 1268.

21. Stephen R. Sofen, David C. Ware, Stephen R. Cooper and Kenneth N. Raymond. Inorg.Chem. 1979 18 234

22. William B. Shorthill, Robert M.Buchanan, Cortlandt G. Pierpoint, Mauro Ghedini and Giuliano Dolcetti Inorg.Chem. 1980 19 1803

23. Cortlandt G. Pierpoint and Robert M. Buchanan. Coord.Chem. Revs. 1981 38 45

24. Freimund Rohrscheid, Alan L. Balch and R.H. Holm. Inorg.Chem. 1966 5 1542

25. Kenneth Kustin, Sung-Tsuen Lui, Claudio Nicolini and David L. Toppen. J.Amer.Chem.Soc. 1974 96 7410

26. Stephen R. Cooper, Yun Bai Koh and Kenneth N. Raymond. J.Amer.Chem.Soc. 1982 104 5092

27. Shigeaki Muto, Kazuaki Tasaka and Yoshio Kamiya. Bull Chem.Soc.Jap. 1977 50 2493

28. S. Cenini, R. Ugo and G.La Monica. J.Chem.Soc(A) 1971 416

29. Joan S. Valentine and Donald Valentine Jr. J.Amer.Chem.Soc. 1970 92 5795

30. Y.S. Sohn and A.L. Balch. J.Amer.Chem.Soc. 1971 93 1290

31. Y.S. Sohn and A.L. Balch. J.Amer.Chem.Soc. 1972 94 1144

32. Tamal Y. Girgis, Y.S. Sohn and Alan L. Balch. Inorg.Chem. 1975 14 2327

33. G.La Monica, G. Navazio, R. Sandin and S. Cenini. J. Organomet Chem. 1971 30 C31.

34. Mauro Ghedini, Gianfranco Denti and Giuliano Dolcetti. Inorg.Chem. 1978 17 2157

35. G.La Monica, G. Navazio and P. Sandini. J.Organomet Chem. 1971 31 89.

36. Mauro Ghedini, Giuliano Dolcetti, Bruno Giovannitti and Gianfranco Denti. Inorg.Chem. 1977 16 1725.

37. Bruno Giovannitti, Ottavio Gandolfi, Mauro Ghedini and Giuliano Dolcetti. J. Organomet Chem. 1977 129 207

38. Alan L. Balch. J.Amer.Chem.Soc. 1973 95 2723

39. Stephen R. Sofen, Stephen R. Cooper and Kenneth N. Raymond, Inorg.Chem. 1979 18 1611

40. Stephen R. Sofen, Kamal Abu-Dari, Derek P. Freyburg and Kenneth N. Raymond. J.Amer.Chem.Soc. 1978 100 7882

41. Bong-Il Kim, Chie Miyake, Shosuka Imoto. J.Inorg.Nucl.Chem. 1974 36 2015

42. G.P. Haight Jr. and Vasken Paragamian. Anal.Chem. 1960 32 642.

43. R.F. Weinland and Fritz Gaisser. Z.Anorg.Chem. 1919 103 231

44. R.F. Weinland, Adolf Babel, Karl Gross, and Hermann Mai. Z.Anorg.Chem. 1926 150 177.

45. Debabrata Sen and Prujadaranjan Ray. J.Ind.Chem.Soc. 1953 30 253.

46. Douglas J. Gordon and Richard F. Fenske Inorg.Chem. 1982 21 2907.

47. Cortlandt G. Pierpoint and Hartley H. Downs. Inorg.Chem. 1975 14 343.

48. Robert M. Buchanan and Cortlandt G. Pierpoint J.Amer.Chem.Soc. 1980 102 4951.

49. Hartley H. Downs, Robert M. Buchanan and Cortlandt G. Pierpoint, Inorg.Chem. 1979 18 1736.

50. Judith Ann R. Hartman, Bruce M. Foxman and Stephen R. Cooper. J.C.S.Chem.Comm. 1982 583

51. Martin D. Stallings, Mark M. Morrison and Donald T. Sawyer. Inorg.Chem. 1981 20 2655.

52. Stephen E. Jones, Luis E. Leon and Donald T. Sawyer. Inorg.Chem. 1982 21 3692.

53. Marion E. Cass, David L. Greene, Robert M. Buchanan, and Cortlandt G. Pierpoint. J.Amer.Chem.Soc. 1983 105 2680.

54. Alan L. Balch. J.Amer.Chem.Soc. 1973 95 2723.

55. R.M. Buchanan, H.H. Downs, W.B. Shorthill, C.G. Pierpoint, S.L. Kessel and D.N. Hendrickson. J.Amer.Chem.Soc. 1978 100 4318.

56. G.A. Razuvaev, V.K. Cherkasov and G.A. Abakumov J.Organomet Chem. 1978 160 361.

57. G.A.Razuvaev, I.A. Teplova, K.G. Shalnova, and G.A. Abakumov. J. Organomet Chem. 1978 157 353.

58. G.A. Razuvaev, G.A. Abakumov, I.A. Teplova, K.G. Shalnova and V.K. Cherkasov. Inorg.Chim.Acta 1981 53 L267.

59. Joseph Knox and Helen Reid Innes. J.Chem.Soc. 1914 1451.

60. Paul J. Crowley and Helmut A. Haendler. Inorg.Chem. 1962 1 904.

61. Cortlandt G. Pierpoint and Robert M. Buchanan. J.Amer.Chem.Soc. 1975 97 6450.

62. Robert M. Buchanan, Stephen L. Kessel, Hartley H. Downs, Cortlandt G. Pierpoint and David N. Hendrickson. J.Amer.Chem.Soc. 1978 100 7894.

63. Michael W. Lynch, Robert M. Buchanan, Cortlandt G. Pierpoint and David N. Hendrickson. Inorg.Chem. 1981 20 1038.

64. Cortlandt G. Pierpoint and Robert M. Buchanan. J.Amer.Chem.Soc. 1975 97 4912.

65. Robert M. Buchanan, Brian J. Fitzgerald and Cortlandt G. Pierpoint. Inorg.Chem. 1979 18 3439.

66. Der-Hang Chin, Donald T. Sawyer, William P. Schaefer and Charles J. Simmons. Inorg.Chem. 1983 22 752.

67. Michael B. Hursthouse, Thelma Fram, Lucy New, William P. Griffith and Alastair J. Nielson. Trans.Met.Chem. 1978 3 255.

68. V.V. Tkachev and L.O. Atovmyan. Koord.Khim. 1975 1 845

69. L.O. Atovmyan, V.V.Tkachev and T.G. Shishova. Dokl.Akad.Nauk.SSSR. 1972 205 609

70. V.V. Tkachev and L.O. Atovmyan. Koord.Khim 1976 2 110

71. Cortlandt G. Pierpoint and Hartley H. Downs. J.Amer.Chem.Soc. 1975 97 2123.

72. Robert H. Heistand II, A.Lawrence Roe and Lawrence Que Jr. Inorg.Chem. 1982 21 676.

73. Cortlandt G. Pierpoint, James D. Ekstrand, Derek P. Freyburg and Kenneth N. Raymond. Inorg.Chem. 1979 18 108.

74. Cortlandt G. Pierpoint and Hartley H. Downs. J.Amer.Chem.Soc. 1976 98 4834.

75. C.J. Brown. Acta Cryst 1966 21 170.

76. Randall B. Lauffer, Robert H. Heistand II and Lawrence Que Jr. Inorg.Chem. 1983 22 50.

77. Bryan F. Anderson, David A. Buckingham, Glen B. Robertson, John Webb, Keith S. Murray and Paul E. Clark. Nature 1976 262 722.

78. Pablo Espinet, Pamela M.Bailey and Peter M. Maitlis. J.C.S.Dalton Trans. 1979 1542.

79. Kazi A. Azam, Antony J. Deeming, Richard E. Kimber and Padmaja R. Shukla. J.C.S. Dalton Trans. 1976 1853.

80. W.P. Griffith and T.D. Wickins. J.Chem.Soc.(A) 1968 400

81. W.P. Griffith. J.Chem.Soc.(A) 1969 211.

82. W.P. Griffith and R. Rossetti. J.C.S. Dalton Trans. 1972 1449.

83. R.M. Wing and K.P. Callahan. Inorg.Chem. 1969 8 871.

84. D.J. Hewkin and W.P. Griffith. J.Chem.Soc.(A) 1966 472.

85. F.A. Cotton and R.M. Wing. Inorg.Chem. 1965 4 867.

86. Carolyn Knobler, Bruce R. Penfold, Ward T. Robinson, Cuthbert J. Wilkins and Shim Hian Yong. J.C.S. Dalton Trans. 1980 248.

87. A. Hidalgo and Clara Otero. Spec.Acta 1960 16 528.

88. Herman A. Szymanski "Interpreted Infrared Spectra" Volume 3, p.23. Plenum Press, New York 1967.

89. M.M. Davies. Trans.Farad.Soc. 1938 34 1427.

90. Mansel M. Davies. J.Chem.Phys. 1940 8 577.

91. Dennis G. Brown and W. Leo Johnson Z.Naturforsch. 1979 34b 712.

92. Y. Itoh, M. Nakahara and Y. Kondo. Nippon Kagaku Zasshi 1971 92 227.

93. R.P. Henry, P.C.H. Mitchell and J.E. Prue. J.Chem.Soc.(A) 1971 3392.

94. Keith D. Magers, Cecil G. Smith and Donald T. Sawyer, Inorg.Chem. 1980 19 492.

95. Peter A. Wicklund and Dennis G. Brown. Inorg.Chem. 1976 15 396.

96. Lawrence Que Jr. and Robert H. Heistand. J.Amer.Chem.Soc. 1979 101 2219.

97. Lawrence Que Jr. and Robert M.Epstein. Biochem. 1981 20 2545.

98. Simon Salama, John D. Stang, J.B. Neilands and G. Thomas. Biochem. 1978 17 3781.

99. Robert H. Heistand II, Randall B. Lauffer, Erol Fikrig and Lawrence Que Jr. J.Amer.Chem.Soc. 1982 104 2789.

100. N.S. Gill, R.H. Nuttall, D.E. Scaife and D.W.A. Sharp. J.Inorg.Nucl.Chem. 1961 18 79.

101. George W. Watt and John F. Knifton. Inorg.Chem. 1968 7 1443.

102. Ichiro Yamaguchi and Naohiro Hayakawa. Bull.Chem.Soc.Jap. 1960 33 1128.

103. J.A. Pople, W.G. Scheider and H.J. Bernstein. "High Resolution Nuclear Magnetic Resonance". McGraw-Hill 1959.

104. John C. Schug and Joseph C. Deck. J.Chem.Phys. 1962 37 2618.

105. George C. Levy, Robert L. Lichter and Gordon L. Nelson. "^{13}C Nuclear Magnetic Resonance" John Wiley and Sons, New York, 1980.

106. LeRoy F. Johnson and William C. Jankowski. "^{13}C N.MR. Spectra" Wiley Interscience, New York 1972.

107. M. Llinas, D.M. Wilson and J.B. Neilands. Biochem. 1973 12 3836.

108. Wolfgang Buchner and Wolfdieter A. Schenk. Inorg.Chem. 1984 23 132.

109. Alan Carington and Andrew D. McLachlan. "Introduction to Magnetic Resonance" Harper and Row, New York 1967.

110. A.P. West. PhD. thesis University of London 1983.

111. F.A. Cotton and G. Wilkinson "Advanced Inorganic Chemistry" Wiley Interscience, New York 1972.

112. T. Bundgaard and H.J. Jakobsen. Acta Chem.Scand. 1972 26 2548

113. George C. Levy. "Topics in Carbon-13 N.M.R. Spectroscopy" Volume 3. Wiley Interscience New York 1979.

114. Antonio Araneo, Giorgio Mercati, Franca Morazzoni, and Tommaso Napoletano. Inorg.Chem. 1977 16 1196.

115. Christopher C. Felix and Roger C. Sealy J.Amer.Chem.Soc. 1982 104 1555.

116. Brian Harrison, Norman Logan and J. Barrie Raynor J.C.S. Chem.Comm. 1974 202.

117. A. Hudson and M.J. Kennedy. J.Chem.Soc.(A) 1969 1116.

118. J.H.E. Griffiths and J. Owen. Proc.Roy.Soc. 1954 96.

119. H.H. Pieper and K. Schwochau. J.Chem.Phys. 1975 63 4716.

120. Ronald Dehl and George K. Fraenkel. J.Chem.Phys. 1963 39 1793.

121. R. Glicksman. J.Electrochem.Soc. 1961 108 1.

122. M.E. Peover. J.Chem.Soc. 1962 4540.

123. Paula J. Bosserman and Donald T. Sawyer. Inorg.Chem. 1982 21 1545.

124. Stephen E. Jones, Der Hang-Chin and Donald T. Sawyer. Inorg.Chem. 1981 20 4257.

125. Subhash Harmalker, Stephen E. Jones and Donald T. Sawyer. Inorg.Chem. 1983 22 2790.

126. Lynn M. Charney and Franklin A. Schultz. Inorg.Chem. 1980 19 1527.

127. Lynn M. Charney, Harry O. Finklea and Franklin A. Schultz Inorg.Chem. 1982 21 549.

128. Douglas J. Gordon and Richard F. Fenske Inorg.Chem. 1982 21 2916.

129. Dennis H. Evans, Kathleen M. O'Connell, Ralph A. Petersen and Michael J. Kelly. J.Chem.Ed. 1983 60 290.

130. Alan L. Balch. J.Amer.Chem.Soc. 1973 95 2723.

131. Stephan S. Isied, Gilbert Kuo and Kenneth N. Raymond. J.Amer.Chem.Soc. 1976 98 1763.

132. R.A. Sheldon. Recueil. 1973 92 367.

133. Merck Index of Organic Compounds.

134. A.M. Andersen. Acta Chem.Scand. 1975 B29 239.

135. R. Bruce Martin. J.Phys.Chem. 1971 76 2657.

136. Rainer Fried. J. Chem.Ed. 1968 45 322.

137. Stephen Turner Chem.in Brit. 1978 14 603.

138. A.M. Andersen. Acta.Chem.Scand. 1975 B29 871.

139. Toshiharu Nagatsu "Biochemistry of Catecholamines - the biochemical method" University Park Press 1973.

140. E.J.W. Barrington "An Introduction to General and Comparative Endocrinology."

141. D.J. Triggle "Chemical Aspects of the Autonomic Nervous System" Academic Press, London, 1965.

142. Helen W. Richter and Walter H. Waddell J.Amer.Chem.Soc. 1983 105 5434.

143. D.B. Calne and M. Sandler Nature 1970 226 21

144. Donald J. Reis, Robert A. Ross and Tong Hyub Joh. Brain Res. 1977 136 465.

145. B. Nystrom, L.Olson and U.Ungerstedt.
Science 1972 176 925.

146. C. Victor Fazakerley, Peter W. Linder, Ralph G. Torrington and M. Robert W. Wright. J.C.S. Dalton Trans. 1979 1872.

147. A. Randrup, C. Braestrap, I. Munkvad, R. Fog, J. Scheel-Kniger and M. Nielsen. Brain.Res. 1977 127 373

148. M.J. Perlow, C.C.Chiueh, C.Raymond Lake and R.J. Wyatt.
Brain.Res. 1980 186 469.

149. Beatrice Eckstein, Kenneth Shaw and Gerald Stern.
The Lancet. 1973 1 431.

150. Ottavio Gandolfi and Jochanan Blum. Inorg.Chim.Acta.
1983 80 103.

151. Tamas Kiss and Arthur Gergely. Inorg.Chim.Acta. 1979 36 31

152. A. Gergely and T.Kiss. Inorg.Chim.Acta. 1976 16 51

153. K.S.Rajan, J.M. Davis and R.W. Colburn.
J.Neurochem. 1971 18 345.

154. Robert W. Colburn and James W. Maas. Nature 1965 208 37.

155. James W. Maas and Robert W. Colburn. Nature 1965 208 41.

156. W.H. Harrison, Walter W. Whisler and S. Ko.
J.Biol.Chem. 1967 242 1660.

157. K.S.Rajan and J.M. Davis. J.Inorg.Nucl.Chem. 1976 38 897.

158. R.F. Jameson and W.F.S. Neillie. J.Inorg.Nucl.Chem.
1965 27 2623.

159. R.W. Rollins. Imperial College dissertation. 1980.

160. David L. White, S.B. Andrews, J.W. Faller and Russell
J. Barnett. Biochem.Biophys.Acta. 1976 436 577.

161. M. Kimuli. Brain Res. 1976 112 156.

162. J.T. Polishock. Brain Res. 1976 114 379.

163. Ryo Tanceka, Hisatera Asaga and Minoru Takeda. Brain Res. 1976 115 273.

164. Alastair J. Nielson and William P. Griffith. J.Histochem.Cytochem. 1978 26 138.

165. Floyd E. Bloom. J.Histochem.Cytochem. 1973 21 333

166. Roger C. Wagner. J.Ultrastruct.Res. 1976 57 132.

167. Malcolm R. Wood and Melwin J. Cohen. Brain Res. 1980 194 613.

168. L.G. Tilney, J. Bryan, D.J. Bush, K. Fujiwara, M.S. Mooseker, D.B. Murphy and D.H. Snyder. J.Cell Biol. 1973 59 267.

169. S.G. Carr, T.D. Smith and J.R. Pilbrow. J.Chem.Soc.(A) 1971 2569.

170. Whei-Lu Kwik, Evelyn Purdy and Edward I. Stiefel. J.Amer.Chem.Soc. 1974 96 1638.

171. J.E. Gorton and R.F. Jameson. J.C.S.Dalton Trans. 1972 310

172. Arthur Gergely, Tamas Kiss and Gyorgy Deak. Inorg.Chim.Acta. 1979 36 113.

173. Edoardo Mentasti, Ezio Pelizzetti and Guido Saini. J.Inorg.Nucl.Chem. 1976 38 785.

174. Branka Grgas-Kuznar, V.L. Simeon and O.A. Weber. J.Inorg.Nucl.Chem. 1974 36 2151.

175. Robert K. Boggess and R.Bruce Martin. J.Amer.Chem.Soc. 1975 97 3076.

176. A.C. Andrews, T.D. Lyons and T.D.O'Brien. J.Chem.Soc. 1962 1776

177. B.L. Vijayvargiya, P.B. Chakrawanti and H.N. Sharma. J.Ind.Chem.Soc. 1980 57 471.

178. Ottavio Gandolfi, Giuliano Dolcetti, Mauro Ghedini and Michael Cais. Inorg.Chem. 1980 19 1785.

179. A. Marzotto and L. Galzigna. Congr.Naz.Chim.Inorg. (Atti) 13th 1980 160.

180. S. Ya. Shnaiderman and E.V. Galinker. Russ.J.Inorg.Chem. 1962 7 142.

181. L.J. Bellamy. "The infra-red spectra of complex molecules" Methuen, London 1958.

182. Ottavio Gandolfi, Giuliano Dolcetti and Mauro Ghedini. Trans.Met.Chem. 1980 5 149.

183. David M. Adams "Metal-ligand and related vibrations" Arnold 1967.

184. K. Nakamoto "Infra-red Spectra of Inorganic and Coordination Compounds", Wiley-Interscience, New York, 1970.

185. The Aldrich Library of N.M.R. Spectra.

186. Adolfo Lai, Mauro Monduzzi, Guiseppe Saba. Adv.in Mol. Relaxation and Interaction Processes. 1980 18 221.

187. Adolfo Lai, Mauro Monduzzi, Guiseppe Saba. J.C.S. Faraday Trans. 1981 2 227.

188. M. Goldstein, E. Lauber and M.R. McKereghan. Biochem.Pharmacol. 1964 13 1103.

189. E.L. Muetterties and C.M. Wright. J.Amer.Chem.Soc. 1965 87 4706.

190. E.L. Muetterties, H. Roesky and C.M. Wright. J.Amer.Chem.Soc. 1966 88 4856.

191. L.G. Hulett and D.A. Thornton. Spec.Acta. 1971 27A 2089.

192. Dennis J. Olszanski, Thomas J. Anderson, Melvin A. Neuman and Gordon A. Melson. Inorg.Nucl.Chem.Letts. 1974 10 137.

193. T.S. Davis, J.P. Fackler and M.J. Weeks. Inorg.Chem. 1968 7 1994.

194. E.L. Muetterties. J.Amer.Chem.Soc. 1966 88 305.

195. Hirotaka Shimanouchi and Yoshio Sasada. Acta Cryst. 1973 B29 81.

196. Hirotaka Shimanouchi and Yoshio Sasada. Tet.Letts. 1970 28 2421.

197. David Ginsberg (Ed) "Non-benzenoid aromatic compounds" "Tropones and Tropolones" by Tetsuo Nozoe. Wi ey 1959.

198. V.W. Day and J.L. Hoard. J.Amer.Chem.Soc. 1970 92

199. J.W. Cook, A.R. Gibb, R.A. Raphael and A.R. Somerville. J.Chem.Soc. 1951 503.

200. Roger J. Irving, Michael L. Post and David C. Povey. J.C.S.Dalton Trans. 1973 697.

201. Roger J. Irving, Michael L. Post and Roy W. Baker. J.C.S. Dalton Trans. 1975 1898.

202. Yoshio Sasada, Kenji Osaki and Isamu Nitta. Acta Cryst. 1954 7 113.

203. Yoshio Sasada and Isamu Nitta. Acta Cryst. 1956 9 205.

204. Anastas Karipides and James Graf. Inorg.Nucl.Chem.Letts. 1972 8 161.

205. E.L. Muetterties and L.J. Guggenberger. J.Amer.Chem.Soc. 1972 94 8046.

206. T.A. Hamor and D.J. Watkin. J.C.S.Chem.Comm. 1969 440.

207. Jan-Eric Berg, Anne-Marie Pilotti, Anne-Charlotte Söderholm and Bengt Karlsson. Acta Cryst. 1978 B34 3071.

208. A. Avdeef, J.A. Costamanga and J.P. Fackler Jr. Inorg.Chem. 1974 13 1854.

209. Alan R. Davis and Frederick W.B. Einstein. Inorg.Chem. 1975 14 3030.

210. J.G. Leipoldt, L.D.C.Bok, S.S. Basson and H. Meyer. Inorg.Chim.Acta 1980 42 105.

211. S.S. Eaton, G.R. Eaton, R.H. Holm and E.L. Muetterties. J.Amer.Chem.Soc. 1973 95 1116.

212. Michael Green and Graham J. Parker. J.C.S. Dalton Trans. 1974 333.

213. G. Doyle. J.Organomet-Chem. 1977 132 243.

214. E.L. Muetterties and C.W. Alegranti. J.Amer.Chem.Soc. 1969 91 4420

215. L.G. Hulett and D.A. Thornton. Chimia 1972 26 72.

216. L.G. Hulett and D.A. Thornton J.Mol.Struct. 1972 13 115.

217. D. Brown and C.E.F. Rickard J.Chem.Soc.(A) 1970 3373

218. Sandro Degetto, Gianpaolo Marangoni, Gabriella Bombieri, Eleonora Forsellini, Livio Baracco and Rodolfo Gazioni. J.C.S. Dalton Trans. 1974 1933.

219. Sandro Degetto, Livio Baracco, Gianpaolo Marangoni and Eloisa Celon. J.C.S. Dalton Trans. 1976 1645.

220. D.L. Plymale and W.H. Smith. J.Inorg.Nucl.Chem. 1968 30 2267.

221. D.L. Plymale and W.H. Smith. J.Inorg.Nucl.Chem. 1969 31 233.

222. G. Bombieri, S.Degetto, G. Marangoni, R. Graziani and E. Forsellini. Inorg.Nucl.Chem.Letts 1973 9 233

223. J. Selbin and J.D. Ortego. J.Inorg.Nucl.Chem. 1968 30 313.

224. Kenneth W. Bagnall, Akshya M. Bhandari, David Brown, Philip E. Lidster and Brian Whittaker. J.C.S. Dalton Trans. 1975 1249.

225. A.M.Bhandari and D.K. Kulkani. Current Sci. 1979 48 577.

226. Thomas J. Anderson, Melvin A. Neuman and Gordon A. Melson. Inorg.Chem. 1974 13 158.

227. S.S. Eaton, J.R. Hutchison, R.H. Holm and E.L. Muetterties. J.Amer.Chem.Soc. 1972 94 6411.

228. David M. Doddrell, M. Robin Bendall,Peter C. Healy, Graham Smith, Colin H.L. Kennard, Colin L. Raston and Allan H. White. Aust.J.Chem. 1979 32 1219.

229. Alan R. Davis and Frederick W.B. Einstein. Inorg.Chem. 1974 13 1880.

230. Thomas J. Anderson, Melvin A. Neuman and Gordon A. Melson. Inorg.Chem. 1974 13 1884.

231. Alan R. Davis and Frederick W.B. Einstein. Acta Cryst. 1978 B34 2110.

232. D. Tranqui, A. Tissier, J. Laugier, and P. Boyer. Acta Cryst. 1977 B33 392.

233. J.J. Park, D.M. Collins and J.L. Hoard. J.Amer.Chem.Soc. 1970 92 3636.

234. Yeh Mei Chow and Doyle Britton. Acta Cryst. 1975 B31 1929

235. J. Monteath Robertson. J.Chem.Soc. 1951 1222.

236. W.H. Macintyre, J.M. Robertson and R.F. Zahrobsky. Proc.Roy.Soc. Series A. 1966 289 161.

237. Mary McPartlin and J.D. Matthews. J.Organomet Chem. 1976 104 C20.

238. F.P. Dwyer and A. Sargeson. J.Amer.Chem.Soc. 1955 77 1285.

239. John P. Fuckler Jr. Progr.Inorg.Chem. 1966 7 361

240. Yusaku Ikegami. Bull.Chem.Soc.Jap. 1961 34 94

241. Yusaku Ikegami Bull.Chem.Soc.Jap. 1963 36 1118.

242. Yusaku Ikegami. Bull.Chem.Soc.Jap. 1961 34 91.

243. H.P. Koch. J.Chem.Soc. 1951 512.

244. G.P. Scott and D.S. Tarbell. J.Amer.Chem.Soc. 1950 72 240.

245. Yusaku Ikegami. Bull.Chem.Soc.Jap. 1962 35 972.

246. Haruo Hosoya and Sabura Nagakura. Bull.Chem.Soc.Jap. 1966 39 1414.

247. H. Junge Spec.Acta 1968 24A 1957.

248. L.G. Hulett and D.A. Thornton. J.Inorg.Nucl.Chem. 1973 35 2661.

249. L.G. Hulett and D.A. Thornton. Spec.Acta 1973 294 757

250. Bennett Hutchinson, David Eversdyk and Suzanne Olbricht. Spect.Acta 1974 30A 1605

251. Klaus Dietrich and Hans Musso. Angew.Chem. (Int.Ed.) 1975 14 358.

252. B. Soptrajanov, A. Nikolavski and I. Petrov. Spec.Acta 1968 24A 1617.

253. Mauricio Valderrama and Horacio Rafart. Trans.Met.Chem. 1981 6 221.

254. G. Doyle. Inorg.Chem. 1975 14 2008.

255. Nikolaus M. Szeverenyi, Ad Bax. and Garg E. Maciel. J.Amer.Chem.Soc. 1983 105 2579.

256. C.W. Ainscough, Andrew M. Brodie and Jeffrey E. Plowman. Inorg.Chem. 1980 19 3655.

257. J. Charalambous. Inorg.Chim.Acta 1976 18 241.

258. L. Grotjahn and P. Kruger. Org.Mass Spec. 1977 12 727.

259. J. Charalambous "Mass Spectrometry of Metal Compounds", Butterworths, London. 1975.

260. C.G. Macdonald and J.S. Shainon. Aust.J.Chem. 1966 19 1545.

261. F.A. Cotton. J.Less Common Metals. 1974 36 13.

Appendix:- Instrumentation

Infra-red spectra were recorded using Nujol and Voltalef mulls on KBr discs using a Perkin-Elner 683 infra-red spectrometer.

Raman spectra were recorded using a Spex Ramalog V triple Monochromator Spectrometer. Data was collected using a Spex Datamate computer controller. The samples were run as pressed KBr pellets spun at 5,000 rpm, and the red line at 647.1 nm of a coherent model 52 Krypton Ion laser was used.

^{1}H N.M.R. spectra were recorded on a Perkin-Elmer R32 (90MHz) spectrometer and a Jeol FX904 (90MHz) spectrometer.

^{13}C N.M.R. spectra were recorded on a Jeol FX904 (90MHz) Spectrometer and on a Bruker WM-250(250 MHz) spectrometer. The spectra were decoupled from the proton resonances unless off-resonance coherent decoupling was used (as stated in the text).

E.P.R. spectra were recorded on an E.P.R. Varian E12 instrument (X-band). The samples were run in chloroform solutions at liquid nitrogen temperatures using a finger Dewar.

Electrochemical measurements were carried out using a glassy-carbon working electrode, platinum auxiliary electrode and saturated calomel electrode as the reference. The electrolyte used was tetrabutyl-ammonium perchlorate in organic solvents.

Microanalyses and mass spectra were carried out by the Chemistry Department of Imperial College.